Title
Biochemical Characterization of Two Members of the Protein Arginine Methyltransferase Family, PRMT7 and PRMT9

Author
Hadjikyriacou, Androulla

Publication Date
2017

Peer reviewed|Thesis/dissertation

UNIVERSITY OF CALIFORNIA

Los Angeles

Biochemical Characterization of Two Members of the Protein Arginine Methyltransferase Family, PRMT7 and PRMT9

A dissertation submitted in partial satisfaction of the requirements for the degree of Doctor of Philosophy in Biochemistry and Molecular Biology

by

Androulla Hadjikyriacou

2017

ABSTRACT OF THE DISSERTATION

Biochemical Characterization of Two Members of the Protein Arginine Methyltransferase Family, PRMT7 and PRMT9

by

Androulla Hadjikyriacou

Doctor of Philosophy in Biochemistry and Molecular Biology

University of California, Los Angeles, 2017

Professor Steven G. Clarke, Chair

Protein arginine methylation is an important posttranslational modification in eukaryotes, shown to be involved in the regulation of transcription, the splicing machinery, signaling, and DNA repair. Mammalian protein arginine methyltransferases (PRMT) include a family of nine enzymes that transfer methyl groups onto the omega nitrogen atoms of the guanidino groups of arginine residues, producing monomethylarginine only (MMA, type III), symmetric dimethylarginine (SDMA) and MMA (Type II), or asymmetric dimethylarginine (ADMA) and MMA (Type I). While the other PRMTs have been extensively studied, the roles and activities of two members of this family, PRMT7 and PRMT9, had been less well investigated. Both PRMT7 and PRMT9 are distinguished from other family members with having two methyltransferase-

like domains and having acidic residues in an otherwise well-conserved "double-E" substrate-binding motif. My work confirms PRMT7 as the only type III enzyme in the group, with an unusual low temperature optimum for activity and preference for basic residues in an RXR sequence for methylation. I found that mutations of the acidic residues in the double-E motif result in a loss of the specific RXR substrate recognition motif and the appearance of a RG specificity motif typical of many of the other PRMTs. The physiological substrate(s) of PRMT7 remain to be determined, although I found that histone H2B is an effective *in vitro* substrate. PRMT9, on the other hand, had no reported activity, until I was able to show in a pulldown experiment using HeLa cells that it was associated with two RNA splicing factors. I was able to determine by amino acid analysis that PRMT9 is very specific for methylating the RNA splicing factor SF3B2. This PRMT9-dependent modification reaction produces both MMA and SDMA and thus makes PRMT9 the second example of a type II enzyme in mammals. I found that the position of the methylated arginine residue in SF3B2 is important for PRMT9 recognition, and that the acidic residues in the substrate-binding motif also play an important role in substrate recognition. In addition, mutagenesis studies in the active site cavity of the PRMT7 and PRMT9 enzymes uncovered conserved residues in the substrate binding double-E loop that are important for substrate recognition and residues in the conserved THW motif that are responsible for conferring the methylation activity type. Lastly, I examined the orthologous PRMT7 and PRMT9 enzymes in the nematode *Caenorhabditis elegans.* I found that the *C. elegans* PRMT-7 has a distinct substrate preference from the mammalian ortholog, while *C. elegans* PRMT-9 appears to be biochemically indistinguishable from its human ortholog.

The dissertation of Androulla Hadjikyriacou is approved.

Jorge Z. Torres

Siavash Kurdistani

Steven G. Clarke, Committee Chair

University of California, Los Angeles

2017

Dedication

I would like to dedicate my dissertation to my amazing parents (Savvas and Domniki), my grandmother, Androulla, boyfriend (Qais), and friends for their outstanding and priceless love and support throughout my graduate career.

To my parents, especially my dad, for inspiring me to pursue my dreams and being my role model for pursuing a career and an advanced degree in science, and seeing that you can be a successful scientist and stick to your goals. To my mom, for always being there and answering my calls at 3 am east coast time to talk. To my parents, for their sacrifices and moving to the United States with two small children, to give us better opportunities and education.

My grandmother, with whom I share a beautiful name, has always given me love and support, and gave me hope and wisdom to achieve my dreams in science that she was unable to.

To my boyfriend Qais, who has helped me with anything and everything throughout my time at UCLA, for always being there for me through the tough times and stress.

To all my friends who helped me get through the rough times of stress and anxiety that come with grad school. To Megan, who was always there for me to vent and give me advice.

To all the amazing people I have met at UCLA and connected with, and have supported me and worked together for various causes. I am grateful to have met and worked with such great and talented people.

To my high school calculus teacher Mr. Bramson, who believed in my abilities and knowledge, supported me and saw my potential as a mathematician and scientist.

To all the educators making a difference and those who push forward the importance of science education and communication. To those inspiring the future generation of scientists.

Thank you.

TABLE OF CONTENTS

LIST OF FIGURES

LIST OF TABLES

ACKNOWLEDGEMENTS

I would like to sincerely thank Dr. Steven Clarke for his amazing mentorship during my time at UCLA. He has been a great advisor, someone who I always felt comfortable talking to and asking for advice, whether it is work or life, and I am lucky to have been mentored by someone so genuine, smart, and sincere. I couldn't have asked for a better advisor and friend. I would also like to thank Dr. Jonathan Lowenson, who has always happily helped me whenever I needed advice or had difficulties with experiments. I would like to also thank former and present lab members who I have interacted with and made the lab environment enjoyable, and always being helpful and talking about science. I would like to particularly thank Dr. Alexander Patananan, who has been a great friend and colleague, always willing to answer questions and helping me during his time in the lab and afterwards. He also trained me in *C. elegans* culture techniques, and I am thankful for his guidance. In addition, I would like to thank Dr. Qais Al-Hadid for his help and advice on experiments. I would like to thank all of my collaborators for their help and insight on my projects, as well as my committee members, Dr. Cathy Clarke, Dr. Jorge Torres, Dr. Siavash Kurdistani, and Dr. Wohlschlegel, for their time and guidance.

Part of the work in this dissertation was supported by a Ruth L. Kirschstein National Research Service Award, particularly Chapters 3-7. The UCLA Dissertation Year Fellowship supported the work in Chapters 8 and 9.

Chapter 3 of this dissertation is a reprint of the publication entitled “Mammalian Protein Arginine Methyltransferase 7 (PRMT7) Specifically Targets RXR Sites in Lysine- and Arginine-rich Regions” in the *Journal of Biological Chemistry* (volume 288, pages 37010-37025). I would like to acknowledge the first author You Feng and the co-authors Ranjan Maity, Julian P.

Whitelegge, Ziwei Li, Cecilia Zurita-Lopez, Qais Al-Hadid, Amander T. Clark, Mark T. Bedford, Jean-Yves Masson, and Steven G. Clarke.

Chapter 4 of this dissertation is a reprint of the publication entitled "Substrate Specificity of Human Protein Arginine Methyltransferase 7 (PRMT7) – The Importance of Acidic Residues in the Double E Loop" in the *Journal of Biological Chemistry* (volume 289, pages 32604-32616). I would like to acknowledge the first author You Feng and corresponding author, Steven G. Clarke.

Chapter 5 of this dissertation is a reprint of the publication entitled "PRMT9 is a Type II methyltransferases that methylates the splicing factor SAP145" in *Nature Communications* (6:6428). I would like to acknowledge the first author Yanzhong Yang, and the co-authors Zheng Xia, Sitaram Gayatri, Daehoon Kim, Cecilia Zurita-Lopez, Ryan Kelly, Ailan Guo, Wei Li, Steven G. Clarke, and Mark T. Bedford.

Chapter 6 of this dissertation is a reprint of the publication entitled "Unique Features of Human Protein Arginine Methyltransferase 9 (PRMT9) and Its Substrate RNA Splicing Factor SF3B2" in the *Journal of Biological Chemistry* (volume 290, pages 16723-16743). I would like to acknowledge the co-authors Yanzhong Yang, Alexsandra Espejo, Mark T. Bedford, and Steven G. Clarke. In addition, I would like to acknowledge Ankur Golkar, Xiaoyu Xia, and Jorge Z. Torres for their generous help and resources for mammalian PRMT9 expression and microscopy.

Chapter 7 of this dissertation is a reprint of the publication entitled "Protein Arginine Methyltransferase Product Specificity Is Mediated by Distinct Active-site Architectures" in the *Journal of Biological Chemistry* (volume 291, pages 18299-18308). I would like to acknowledge

the first author, Kanishk Jain, and the co-authors Rebeccah A. Warmack, Erik W. Debler, Peter Stavropoulos, and Steven G. Clarke.

Chapter 8 of this dissertation is a reprint of the publication entitled "*Caenorhabditis elegans* PRMT-7 and PRMT-9 Are Evolutionarily Conserved Protein Arginine Methyltransferases with Distinct Substrate Specificities," in the ACS journal *Biochemistry*. I would like to thank corresponding author Steven G. Clarke.

Chapter 9 of this dissertation is manuscript entitled "Isoaspartyl Damage of Histone H2B and PRMT7 Methylation." I would like to thank my undergraduate student who helped with this project and experiments, Anuj "Sunny" Chhabra and Steven G. Clarke.

VITA

EDUCATION

University of California, Los Angeles, CA
Biochemistry and Molecular Biology PhD Program 2011 – Expected 2017

University of Massachusetts Amherst, MA
B.S. Biochemistry and Molecular Biology, *Summa cum laude* 2007 – 2011

RESEARCH EXPERIENCE

University of California, Los Angeles (Los Angeles, CA) August 2011 – June 2017
Graduate Student Researcher – Dr. Steven G. Clarke Lab, Department of Chemistry and Biochemistry

Sanofi Genzyme (Framingham, MA) May 2010 – August 2010
Intern – Morgenbesser Group, Department of Molecular Immunology/Oncology

University of Massachusetts Amherst (Amherst, MA) August 2007 – May 2011
Undergraduate Student Researcher – Dr. Jennifer Normanly Lab, Department of Biochemistry and Molecular Biology

PUBLICATIONS

(1) Hadjikyriacou, A. and Clarke, S.G. (2017). "Distinct Substrate Specificity and Conservation of Invertebrate Protein Arginine Methyltransferases." *Biochemistry,* 10.1021/acs.biochem.7b00283
(2) Jain, K., Warmack, R.A., Debler, E.W., Hadjikyriacou, A., Stavropoulos, P., and Clarke, S.G. (2016). "Protein Arginine Methyltransferase Product Specificity is Mediated by Distinct Active-site Architectures." *Journal of Biological Chemistry*, 291(35): 18299-308.
(3) Hadjikyriacou, A., Yang, Y., Espejo, A., Bedford, M.T., and Clarke, S.G. (2015). "Unique Features of Human Protein Arginine Methyltransferase 9 (PRMT9) and its Substrate RNA Splicing Factor SF3B2." *Journal of Biological Chemistry* 290(27): 16723-43.
(4) Yang, Y., Hadjikyriacou, A., Xia, Z., Gayatri, S., Kim, D., Zurita-Lopez, C., Kelly, R., Guo, A., Li, W., Clarke, S.G., and Bedford, M.T. (2015). "PRMT9 is a Type II methyltransferase that methylates the splicing factor SAP145." *Nature Communications,* 6:6428.
(5) Feng, Y., Hadjikyriacou, A., and Clarke, S.G. (2014). "Substrate Specificity of Human Protein Arginine Methyltransferase 7 (PRMT7): The Importance of Acidic Residues in the Double E Loop." *Journal of Biological Chemistry* 289(47), 32604-16.
(6) Feng, Y., Maity, R., Whitelegge, J.P., Hadjikyriacou, A., Li, Z., Zurita-Lopez, C., Al-Hadid, Q., Clarke, A.T., Bedford, M.T., Masson, J., and Clarke, S.G. (2013). "Mammalian Protein Arginine Methyltransferase 7 (PRMT7) Specifically Targets R-X-R

Sites in Lysine and Arginine-Rich Regions." *Journal of Biological Chemistry* 288(52), 37010-25.

HONORS AND AWARDS

- Roberts A. Smith Research Award for Research Excellence, UCLA Department of Chemistry and Biochemistry (December 2016)
- Dissertation Year Fellowship, UCLA Graduate Division (July 2016 – June 2017)
- Daniel E. Atkinson and Charles A. West Excellence in Biochemistry Dissertation Award, UCLA Department of Chemistry and Biochemistry (June 2016)
- Best Poster Award, FASEB Biological Methylation in Health and Disease 2016, Lisbon, Portugal (June 2016)
- Travel Award, FASEB Biological Methylation in Health and Disease 2016, Lisbon, Portugal (June 2016)
- ASBMB Student-Led Symposium Coordinator and Travel Award, San Diego, CA (April 2016)
- AG Leventis Foundation Graduate Fellowship, (September 2015)
- Trainee, UCLA Cellular and Molecular Biology Training Program, Ruth L. Kirschstein NIH National Research Service Award (April 2013 – March 2016)
- Genzyme University of Massachusetts Scholarship (May 2010)
- AG Leventis Undergraduate Scholarship (August 2008 – May 2011)
- University Scholars Award, University of Massachusetts Amherst, Amherst, MA (August 2007 – May 2011)
- John and Abigail Adams Scholarship University of Massachusetts Amherst, Amherst, MA (August 2007 – May 2011)
- Dean's List, University of Massachusetts Amherst, Amherst, MA (August 2007 – May 2011)

SELECTED PRESENTATIONS

(1) Biochemical Characterization of the Substrate Specificity of Two Unique Members of the Human Protein Arginine Methyltransferase Family, PRMT7 and PRMT9. *Seaborg Symposium*, UCLA, Los Angeles, CA, November 2016. (Poster)
(2) Biochemical Characterization of the Substrate Specificity of Two Unique Members of the Human Protein Arginine Methyltransferase Family, PRMT7 and PRMT9. *FASEB Biological Methylation in Health and Disease*, Lisbon, Portugal, June 2016. (Poster)
(3) A Novel Protein Arginine Methyltransferase Involved in mRNA Splicing. *Molecular Biology Institute Retreat,* Lake Arrowhead, CA, April 2016. (Oral and Poster)
(4) Biochemical Characterization of the Substrate Specificity of Two Unique Members of the Human Protein Arginine Methyltransferase Family, PRMT7 and PRMT9. *Amer Soc for Biochem and Mol Bio*, San Diego, CA, April 2016. (Poster)
(5) Biochemical Characterization of the Substrate Specificity of Two Unique Members of the Human Protein Arginine Methyltransferase Family, PRMT7 and PRMT9. *Protein Society*, Barcelona, Spain, July 2015. (Poster)
(6) PRMT9 Catalyzes Sequence-Dependent Symmetric Demethylation of SF3B2 to Regulate Alternative Splicing. *Amer Soc for Biochem and Mol Bio*, Boston, MA, March 2015. (Poster)

CHAPTER 1

Plan of the Dissertation

The focus of this dissertation is the biochemical characterization of two members of the protein arginine methyltransferases family, PRMT7 and PRMT9. The work done in this dissertation examines their activity type, the identification of their physiological substrates, and their substrate-motif specificity; additionally, this dissertation investigates the role of the enzyme and the role of the modification on the cellular processes and machinery.

Chapter 2 is a brief overview of protein arginine methylation, including previous knowledge in the field on PRMT7 and PRMT9, a discussion of protein arginine methylation in various organisms, including the nematode *Caenorhabditis elegans,* and a discussion of the role of protein arginine methylation in diseases such as cancer.

In Chapters 3 and 4, I focused on the characterization of mammalian PRMT7. Chapter 3 establishes the characteristics of mammalian PRMT7, providing further evidence for the production of monomethylarginine (MMA) only, as well as describing the substrate methylation motif. Using *in vitro* methylation assays and highly sensitive cation exchange chromatography methods, I worked with a postdoctoral fellow in the laboratory, Dr. You Feng, to determine that the enzyme highly prefers a basic-rich motif found in histone H2B. In collaboration with the laboratory of Professor Julian Whitelegge, we were able to use proteomics methods to reveal novel post-translational modification sites on intact histone H2B and within H2B and H4 peptides. This work demonstrated that PRMT7 has a unique preference for methylating arginine residues in lysine- and arginine-rich regions, particularly those in which arginines are separated by one residue, in an RXR motif.

Chapter 4 focused on mutagenesis studies to identify key residues that are implicated in the enzyme's substrate preference for arginine residues in basic-rich regions. Along with Dr. You Feng, we performed site directed mutagenesis on the two acidic residues found in the

substrate-binding double E loop that were shown to be important in modulating the substrate preference from basic rich regions to RG-rich motifs. This work additionally further confirmed the type III MMA activity of the enzyme, and showed that the enzyme has a remarkably low temperature optimum and a sensitive salt tolerance. Both of these properties result in a low activity of the enzyme under standard physiological conditions for mammalian cells. This work, in conjunction with Chapter 3, lays a biochemical foundation for the further characterization and identification of the physiological substrates of PRMT7 in the cell.

In Chapters 5 and 6, I present studies to identify and characterize the novel enzyme PRMT9. In Chapter 5, I collaborated with the laboratory of Dr. Mark Bedford at the MD Anderson Cancer Center in Smithville, Texas to identify the activity type and physiological substrate of the enzyme. Dr. Yanzhong Yang, then a postdoctoral fellow in the Bedford lab, and I worked together to show that PRMT9 is expressed in a complex with two splicing factors, SF3B2 and SF3B4, in two different cell types. In addition, we showed that PRMT9 symmetrically dimethylates a fragment of SF3B2 on an arginine residue flanked by two lysines. We tackled this problem in two ways: Dr. Yang used western blots and pull down assays to show the symmetric dimethylarginine (SDMA) modification on SF3B2, and I used *in vitro* methylation assays along with amino acid analysis by cation exchange chromatography and thin layer chromatography. These biochemical experiments confirmed the presence of the SDMA and Dr. Yang was able to show that the knockdown of PRMT9 modulated alternative splicing events. In addition, we demonstrated that the methylation of SF3B2 recruited the Spinal Motor Neuron (SMN) protein to allow for the correct assembly of spliceosomal subunits through the use of western blots.

In Chapter 6, I did site-directed mutagenesis studies on PRMT9 and its substrate SF3B2, showing that it is unique among the enzymes in the PRMT family and that it has a very specific and narrow substrate preference. I showed that the residues surrounding and the position of the methylatable arginine are important for the substrate recognition and subsequent methylation, and the single acidic residue in the substrate binding double E loop was crucial for activity. In addition, Dr. Alexsandra Espejo, from the Bedford lab, grew PRMT5 conditional knockdown cells, in which I was able to further analyze and quantify the endogenous amounts of methylated arginine species, using an optimized HPLC-based fluorometer assay. With these studies, we were able to show that PRMT9 is not redundant with PRMT5, the major and only other SDMA forming enzyme in the PRMT family.

In Chapter 7, I participated in a project to examine the residues responsible for the product specificity for the PRMT enzymes. My labmates, Kanishk Jain and Rebeccah Warmack, in collaboration with Dr. Erik Debler and Dr. Peter Stavropoulos from Rockefeller University, tested various point mutations in the *T. brucei* PRMT7 ortholog. In previous work they had done, they showed that a single mutation of a glutamate that is terminal in the substrate binding double E loop allowed for the production of asymmetric dimethylarginine (ADMA), instead of just MMA (1). In this chapter, Jain and Warmack showed that another mutant that contained two point mutations, one in the double E loop and one in the conserved THW motif, could now produce SDMA when reacted with a peptide containing MMA. My work showed that a similar point mutation in the THW loop of human PRMT9, which was shown to produce both SDMA and MMA, abolished the SDMA forming ability of the enzyme, making it a more robust enzyme that can only form MMA. These findings led to a model that rationalizes the control of methylation product specificity according to the size and architecture of the active site.

In Chapter 8, I characterized the PRMT orthologs PRMT-7 and PRMT-9 in the nematode *C. elegans*. I was interested to find that *C. elegans* contained orthologs of PRMT-1, PRMT-5, PRMT-7 and PRMT-9, yet lacked the rest of the PRMT family members. *C. elegans* PRMT-9 was initially identified as PRMT-3, although it is most closely related to PRMT9, with only 24% sequence identity and 40% similarity to its human counterpart. *C. elegans* PRMT-7, on the other hand, seems to have a more divergent history; it has 32% sequence identity and 47% similarity to the human enzyme. Previous work had been done to determine the structure of *C. elegans* PRMT-7, but no enzyme activity was reported (2, 3). A small type III MMA activity was determined for PRMT-9 (2) on histone H2A, but this enzyme was not further characterized in the literature. I requested and received the expression plasmids for both PRMT-7 and PRMT-9 from Dr. Akiyoshi Fukamizu at the University of Tsukuba in Tsukuba, Japan (2), and was able to express and purify these proteins. I hypothesized that these two enzymes would have a similar role and activity as their human orthologs. Through *in vitro* methylation assays and amino acid analysis, I showed that PRMT-7 was able to only produce MMA, and had a similar yet broader substrate specificity than the human ortholog. I additionally showed that PRMT-9 also produced SDMA and MMA, much like its human ortholog, on the orthologous splicing factor in *C. elegans*. I also performed RNAi studies to knockdown these proteins in *C. elegans* but did not find any noticeable phenotypes. This work was important as it showed that while these proteins are conserved from mammals to nematodes, they have slightly different roles and specificities, especially in regards to PRMT-7.

In Chapter 9, I examined the role of isoaspartyl damage on histone H2B and methylation by PRMT7. There is evidence for isoaspartyl damage on an aspartyl residue of the histone tail of histone H2B, a few residues away from the arginine residues that are preferentially methylated

by PRMT7 (4, 5). Working with an undergraduate student, Anuj (Sunny) Chhabra, we received isoaspartyl-containing H2B peptides from the Dr. Mark Mamula lab at Yale University and the Dr. Dana Aswad lab at UC Irvine. After using a base labile assay to determine the peptides did contain an isoaspartyl residue, we then set up *in vitro* methylation reactions to look at the effect of an isoaspartyl residue on the recognition and methylation of those arginine residues. In addition, we aged histone H2B peptide that our lab had that also contained an aspartate residue, checked for isoaspartyl damage via the base labile assay, and again tested with *in vitro* methylation reactions to check for methylation activity. We determined that the presence of an isoaspartyl residue affected the activity of the enzyme on the H2B peptide.

In Chapter 10, I discuss my ideas and goals for the future of these projects, and what can be further done or explored to increase our understanding of the roles of these enzymes.

REFERENCES

1. Debler, E. W., Jain, K., Warmack, R. A., Feng, Y., Clarke, S. G., and Blobel, G. (2016) A glutamate / aspartate switch controls product specificity in a protein arginine methyltransferase. *Proc. Natl. Acad. Sci.* **113**, 2068–2073
2. Takahashi, Y., Daitoku, H., Yokoyama, A., Nakayama, K., Kim, J.-D., and Fukamizu, A. (2011) The C. elegans PRMT-3 possesses a type III protein arginine methyltransferase activity. *J. Recept. Signal Transduct. Res.* **31**, 168–172
3. Hasegawa, M., Toma-Fukai, S., Kim, J. D., Fukamizu, A., and Shimizu, T. (2014) Protein arginine methyltransferase 7 has a novel homodimer-like structure formed by tandem repeats. *FEBS Lett.* **588**, 1942–1948
4. Doyle, H. A., Aswad, D. W., and Mamula, M. J. (2013) Autoimmunity to isomerized histone H2B in systemic lupus erythematosus. *Autoimmunity*. **46**, 6–13
5. Qin, Z., Zhu, J. X., and Aswad, D. W. (2015) The D-isoAsp-25 variant of histone H2B is highly enriched in active chromatin: potential role in the regulation of gene expression? *Amino Acids*. 10.1007/s00726-015-2140-9

CHAPTER 2

Protein Arginine Methylation and Scope of the Thesis

Protein Arginine Methylation

Protein arginine methyltransferases (PRMTs) are a family of seven beta-strand enzymes that recognize and methylate the terminal guanidino moieties of arginine residues. These methyltransferases transfer a methyl group from the donor *S*-adenosyl-L-methionine (AdoMet) onto their respective substrates. The enzymes methylate in various "types"; all PRMTs can monomethylate arginine residues – PRMT7 is the only enzyme that is limited to monomethylation (type III); the rest of the PRMTs can dimethylate, either on the same guanidino group, producing asymmetric dimethylarginine (ADMA; type I; PRMT1, -2, -3, -4, -6, and -8), or on opposite guanidino groups to generate symmetric dimethylarginine (SDMA; type II; PRMT5 and -9). The work presented in this dissertation shows evidence for PRMT9 as the second symmetrically dimethylating enzyme (Chapters 5 and 6). My work also showed that PRMT7 only produces MMA (Chapters 3 and 4), with acidic residues in the substrate-binding motif important for conferring its substrate specificity.

The members of the PRMT family contain conserved motifs, including Motif I and Post Motif I, Motif II, Post Motif II (the substrate-binding "double E" loop), Motif III and the THW loop. Motif I and Post Motif I contains conserved residues to bind AdoMet; Motif II is followed by the substrate-binding double E loop. This double E loop contains conserved glutamate residues flanking eight additional residues in a loop, and this substrate-binding motif coordinates and binds the methylatable substrate. The THW loop contains conserved Thr-His-Trp residues in the type I enzymes, and differs slightly in the type II and type III enzymes. The work shown in Chapter 7 shows that residues in the THW loop are important for contributing to the methylation type of the enzyme, as a mutation of a single cysteine in the loop of human PRMT9 allows the enzyme to only produce MMA, where as a combination of mutations of the central THW loop

residue along with one of the terminal glutamates of the double E loop allowed the *T. brucei* PRMT7 to produce SDMA. Other work (1) showed that a single mutation of one of the glutamate residues of the double E loop in *T. brucei* PRMT7 also changed the methylation type to producing only ADMA.

Previous Studies on PRMT7 and PRMT9

PRMT7 and PRMT9 are two members of the protein arginine methyltransferases family whose roles have been more elusive and harder to uncover than most of the other enzymes. Previous literature incorrectly classified PRMT7 as an enzyme producing SDMA (2) and although this was apparently supported by other work linking SDMA histone methylation marks to PRMT7 activity (3, 4), it now appears that such linkage may be due to an indirect effect (5). The field has also been confused by PRMT9 nomenclature used to designate two separate gene products, one encoded on human chromosome 4 that is homologous to other members of the PRMT family (6), and a separate gene on chromosome 2 (FBXO11) (7), that does not encode a homolog of the PRMT family but rather a ubiquitin ligase (8). Much of the confusion in this area has resulted from using FLAG-tags to purify putative PRMTs from mammalian cells. These tagged proteins are often isolated using the monoclonal M2 antibody that has been shown to recognize PRMT5 even in the absence of FLAG-tag (9–11). Thus, FLAG-tagged PRMT7 and FBX011 proteins will be contaminated with PRMT5, producing the SDMA products detected in these studies (2, 7). My work was not able to detect the presence of any SDMA activity with bacterially purified PRMT7 under conditions that would detect 0.2% of methylation activity (10–13) (Chapters 3 and 4). In this thesis, I studied the protein that was encoded by the gene located on chromosome 4q31, whose PRMT9 designation is now the standard of the HUGO Gene

Nomenclature Committee (14, 15) (Chapters 5 and 6). This gene product bears a close resemblance to PRMT7 and PRMT5, and is well conserved across vertebrates and invertebrates (16). My work in Chapters 5 (15) and 6 (14) biochemically characterizes this protein in its ability to produce SDMA and MMA and to define its only substrate discovered thus far, the SF3B2 splicing factor.

There is evidence that suggests crosstalk of PRMT7 with other PRMTs, in particular in the modification of histones H2A and H4. For example, studies have found increased histone H4R3 SDMA at loci of specific genes with the overexpression of PRMT7 (17). In addition, the amount of SDMA at that same mark was decreased in mammalian cells in which PRMT7 was knocked down (3, 18, 19). Even though *in vitro* we have no evidence of PRMT7 generating SDMA, its expression level in the cell seems to indirectly affect the SDMA marks on histones.

Protein Arginine Methylation in Various Organisms

Protein arginine methylation is a conserved modification, with the major PRMTs responsible for ADMA and SDMA (PRMT1 and PRMT5) having orthologs from the kingdoms of fungi to animalia. It has been generally accepted in the literature that bacteria and archaea do not contain protein arginine methyltransferases (20). There are no published reports of identified or characterized arginine methyltransferases in prokaryotes, but in Chapter 8, I report on BLAST searches that identified potential orthologs in *Rhizobium leguminosarum*, *Streptococcus pneumoniae, Geobacter sulfurreducens,* and *Pseudanabaena sp.* Biochemical studies need to be done to characterize these potential orthologs, especially to determine if they are indeed protein arginine methyltransferases. However, it is clear that orthologs of PRMT1, PRMT3 and PRMT5 exist in unicellular eukaryotes, like yeasts, molds, amoebae, and protozoa (21). In addition, a

PRMT7 ortholog has been identified in the parasitic protozoan *T. brucei*, and it harbors a type III MMA methyltransferase activity (22, 23).

Many of the other PRMTs in the mammalian family of enzymes (PRMT2, 3, 4, 6, 7, 8, and 9) contain orthologs in vertebrate and invertebrate organisms, from mammals (humans), birds (*G. gallus*), reptiles (*A. carolinensis*), amphibians (*X. laevis*), zebrafish (*D. rerio*), fruit flies (*D. melanogaster*), nematodes (*C. elegans*), chordates (*C. intestinalis, B. floridae*), and cnidarians (*N. vectensis*) (24). Almost all of the organisms contain the major PRMT family members PRMT1 and PRMT5, and depending on the organism and the evolutionary rate, higher organisms contain more of the additional PRMT enzymes that have evolved (24). PRMT orthologs have also been identified in plants such as *A. thaliana* and *Z. mays*. The major PRMT orthologous enzymes (PRMT1 and PRMT5) have been characterized in fungi such as yeast (*S. cerevisiae, S. pombe*). However, these fungi lack orthologs of all of the other mammalian PRMTs including PRMT7 and PRMT9. Based on the work by Wang and Li (2012) (24), it seems that PRMT1 and PRMT5 have an early eukaryotic ancestor, and based on the sequence identity and presence of PRMT1 in almost all of these organisms, it seems to have evolved much more slowly and plays a very important role. The role of other PRMTs seem to be more specific and have evolved more specialized functions in higher organisms.

Caenorhabditis elegans and Protein Arginine Methylation

Chapter 8 describes PRMT orthologs in the nematode *Caenorhabditis elegans. C. elegans* provides an advantageous model system, and what we learn biochemically from this nematode we can potentially apply to the mammalian system. Previous work has identified PRMT1, PRMT5, PRMT7 and PRMT9 orthologs in worms, along with small fragments that

were named PRMT4 and PRMT6 (25). However, these fragments have not been shown to have any activity or further homology to PRMT enzymes when subjected to a BLAST search. I attempted to conduct studies to determine phenotypes or additional substrates using siRNA methods in nematodes for PRMT-7 and PRMT-9, both of which were inconclusive; I searched for detectable physical phenotypes, such as embryonic lethality and growth defects. In previous studies (25), no phenotypes were seen when worms were treated with siRNA and irradiated with gamma-radiation. The lack of noticeable phenotypes could indicate potential compensation by the other PRMT enzymes.

Protein Arginine Methylation, Disease and Cancer

The deregulation of protein arginine methylation can be involved in cancer and other diseases (26–28). Since many of the PRMTs methylate histone tails, "reader" proteins, such as Tudor domain containing proteins, can recognize many of these methyl marks and can activate or repress transcription (26, 27). In many cases, overexpression of PRMTs leads to cancer; for example, PRMT1 is overexpressed in breast, prostate, lung, colon and bladder cancer, as well as leukemia (26, 28). PRMT2 is overexpressed in breast cancers that have ERα positive status, and PRMT3 is also shown to have higher levels of activity in breast cancer tumors (27) as well as probable post-transcriptional regulation by tumor suppressor protein DAL-1/4.1B *in vitro* and *in vivo* (29). PRMT4 (also known as CARM1) is overexpressed in breast, prostate, and colorectal cancers, while PRMT5 has been shown to be overexpressed or have an increase in activity in gastric, colorectal and lung cancers as well as in lymphomas and leukemias (26–28). PRMT7 has been shown to be involved in breast cancer metastasis as well as in the epithelial-to-mesenchymal transition (EMT) (26, 30). So far, a disease role for PRMT9 *in vivo* has yet to be

determined, but our work in Chapter 4 shows PRMT9 involvement in the regulation of alternative splicing through the methylation of splicing factors and the recruitment of the SMN protein.

The deregulation of protein arginine methylation is also involved in a wide variety of diseases, such as metabolic diseases, neurodegenerative diseases, and aging (27). For example, it has been shown that Alzheimer's disease associated neuronal death is facilitated by PRMT5, and inhibitors of these enzymes could potentially act as therapeutics (31). PRMTs have also shown to be involved in the regulation of the senescence of cells and premature aging, as was shown with $PRMT7^{-/-}$ mice, whose cells underwent cell-cycle arrest and premature cellular senescence (19). In addition, my work in Chapter 9 indicates a potential role and crosstalk of PRMT7 in response to isoaspartyl damage on histone H2B tail. Thus, the study of protein arginine methylation by the family of protein arginine methyltransferases plays a very important role in health and disease, and what we learn *in vivo* and *in vitro* can aid in future disease research and inhibitor development.

REFERENCES

1. Debler, E. W., Jain, K., Warmack, R. A., Feng, Y., Clarke, S. G., and Blobel, G. (2016) A glutamate / aspartate switch controls product specificity in a protein arginine methyltransferase. *Proc. Natl. Acad. Sci.* **113**, 2068–2073
2. Lee, J. H., Cook, J. R., Yang, Z. H., Mirochnitchenko, O., Gunderson, S. I., Felix, A. M., Herth, N., Hoffmann, R., and Pestka, S. (2005) PRMT7, a new protein arginine methyltransferase that synthesizes symmetric dimethylarginine. *J. Biol. Chem.* **280**, 3656–3664
3. Karkhanis, V., Wang, L., Tae, S., Hu, Y. J., Imbalzano, A. N., and Sif, S. (2012) Protein arginine methyltransferase 7 regulates cellular response to DNA damage by methylating promoter histones H2A and H4 of the polymerase δ catalytic subunit gene, POLD1. *J. Biol. Chem.* **287**, 29801–29814
4. Jelinic, P., Stehle, J. C., and Shaw, P. (2006) The Testis-Specific Factor CTCFL Cooperates with the Protein Methyltransferase PRMT7 in H19 Imprinting Control Region Methylation. *PLoS Biol.* **4**, 1910–1922
5. Hadjikyriacou, A., and Clarke, S. G. (2017) Caenorhabditis elegans PRMT-7 and PRMT-9 Are Evolutionarily Conserved Protein Arginine Methyltransferases with Distinct Substrate Specificities. *Biochemistry*. 10.1021/acs.biochem.7b00283
6. Lee, J., Sayegh, J., Daniel, J., Clarke, S., and Bedford, M. T. (2005) PRMT8, a new membrane-bound tissue-specific member of the protein arginine methyltransferase family. *J. Biol. Chem.* **280**, 32890–32896
7. Cook, J. R., Lee, J. H., Yang, Z. H., Krause, C. D., Herth, N., Hoffmann, R., and Pestka, S. (2006) FBXO11/PRMT9, a new protein arginine methyltransferase, symmetrically

dimethylates arginine residues. *Biochem. Biophys. Res. Commun.* **342**, 472–481

8. Díaz, V. M., and de Herreros, A. G. (2016) F-box proteins: Keeping the epithelial-to-mesenchymal transition (EMT) in check. *Semin. Cancer Biol.* **36**, 71–79
9. Nishioka, K., and Reinberg, D. (2003) Methods and tips for the purification of human histone methyltransferases. *Methods*. **31**, 49–58
10. Feng, Y., Maity, R., Whitelegge, J. P., Hadjikyriacou, A., Li, Z., Zurita-Lopez, C., Al-Hadid, Q., Clark, A. T., Bedford, M. T., Masson, J. Y., and Clarke, S. G. (2013) Mammalian Protein Arginine Methyltransferase 7 (PRMT7) Specifically Targets RXR Sites in Lysine- and Arginine-rich Regions. *J. Biol. Chem.* **288**, 37010–37025
11. Zurita-Lopez, C. I., Sandberg, T., Kelly, R., and Clarke, S. G. (2012) Human Protein Arginine Methyltransferase 7 (PRMT7) Is a Type III Enzyme Forming -NG-Monomethylated Arginine Residues. *J. Biol. Chem.* **287**, 7859–7870
12. Feng, Y., Hadjikyriacou, A., and Clarke, S. G. (2014) Substrate Specificity of Human Protein Arginine Methyltransferase 7 (PRMT7) - The importance of acidic residues in the double E loop. *J. Biol. Chem.* **289**, 32604–32616
13. Miranda, T. B., Miranda, M., Frankel, A., and Clarke, S. (2004) PRMT7 is a member of the protein arginine methyltransferase family with a distinct substrate specificity. *J. Biol. Chem.* **279**, 22902–22907
14. Hadjikyriacou, A., Yang, Y., Espejo, A., Bedford, M. T., and Clarke, S. G. (2015) Unique Features of Human Protein Arginine Methyltransferase 9 (PRMT9) and Its Substrate RNA Splicing Factor SF3B2. *J. Biol. Chem.* **290**, 16723–16743
15. Yang, Y., Hadjikyriacou, A., Xia, Z., Gayatri, S., Kim, D., Zurita-Lopez, C., Kelly, R., Guo, A., Li, W., Clarke, S. G., and Bedford, M. T. (2015) PRMT9 is a Type II

methyltransferase that methylates the splicing factor SAP145. *Nat. Commun.* 10.1038/ncomms7428

16. Wang, Y., Wang, J., Chen, C., Chen, Y., and Li, C. (2015) Molecular Phylogenetics and Evolution A novel BLAST-Based Relative Distance (BBRD) method can effectively group members of protein arginine methyltransferases and suggest their evolutionary relationship. *Mol. Phylogenet. Evol.* **84**, 101–111

17. Ying, Z., Mei, M., Zhang, P., Liu, C., He, H., Gao, F., and Bao, S. (2015) Histone Arginine Methylation by PRMT7 Controls Germinal Center Formation via Regulating Bcl6 Transcription. *J. Immunol.* **195**, 1538–47

18. Dhar, S. S., Lee, S. H., Kan, P. Y., Voigt, P., Ma, L., Shi, X., Reinberg, D., and Lee, M. G. (2012) Trans-tail regulation of MLL4-catalyzed H3K4 methylation by H4R3 symmetric dimethylation is mediated by a tandem PHD of MLL4. *Genes Dev.* **26**, 2749–2762

19. Blanc, R. S., Vogel, G., Chen, T., Crist, C., and Richard, S. (2016) PRMT7 Preserves Satellite Cell Regenerative Capacity. *Cell Rep.* **14**, 1528–1539

20. Gary, J. D., and Clarke, S. G. (1998) RNA and Protein Interactions Modulated by Protein Arginine Methylation. *Prog. Nucleic Acid Res. Mol. Biol.* **61**, 9752719

21. Bachand, F. (2007) Protein arginine methyltransferases: From unicellular eukaryotes to humans. *Eukaryot. Cell*. **6**, 889–898

22. Fisk, J. C., Sayegh, J., Zurita-Lopez, C., Menon, S., Presnyak, V., Clarke, S. G., and Read, L. K. (2009) A type III protein arginine methyltransferase from the protozoan parasite Trypanosoma brucei. *J. Biol. Chem.* **284**, 11590–11600

23. Wang, C., Zhu, Y., Caceres, T. B., Liu, L., Peng, J., Wang, J., Chen, J., Chen, X., Zhang, Z., Zuo, X., Gong, Q., Teng, M., Hevel, J. M., Wu, J., and Shi, Y. (2014) Structural

Determinants for the Strict Monomethylation Activity by Trypanosoma brucei Protein Arginine Methyltransferase 7. *Structure*. **22**, 756–768

24. Wang, Y. C., and Li, C. (2012) Evolutionarily conserved protein arginine methyltransferases in non-mammalian animal systems. *FEBS J.* **279**, 932–945

25. Yang, M., Sun, J., Sun, X., Shen, Q., Gao, Z., and Yang, C. (2009) Caenorhabditis elegans protein arginine methyltransferase PRMT-5 negatively regulates DNA damage-induced apoptosis. *PLoS Genet.* 10.1371/journal.pgen.1000514

26. Yang, Y., and Bedford, M. T. (2013) Protein arginine methyltransferases and cancer. *Nat. Rev. Cancer*. **13**, 37–50

27. Blanc, R. S., and phane Richard, S. (2017) Arginine Methylation: The Coming of Age. *Mol. Cell*. **65**, 8–24

28. Fuhrmann, J., Clancy, K. W., and Thompson, P. R. (2015) Chemical Biology of Protein Arginine Modifications in Epigenetic Regulation. *Chem. Rev.* **115**, 5413–5461

29. Singh, V., Miranda, T. B., Jiang, W., Frankel, A., Roemer, M. E., Robb, V. a, Gutmann, D. H., Herschman, H. R., Clarke, S., and Newsham, I. F. (2004) DAL-1/4.1B tumor suppressor interacts with protein arginine N-methyltransferase 3 (PRMT3) and inhibits its ability to methylate substrates in vitro and in vivo. *Oncogene*. **23**, 7761–7771

30. Yao, R., Jiang, H., Ma, Y., Wang, L., Wang, L., Du, J., Hou, P., Gao, Y., Zhao, L., Wang, G., Zhang, Y., Liu, D. X., Huang, B., and Lu, J. (2014) PRMT7 induces epithelial-to-mesenchymal transition and promotes metastasis in breast cancer. *Cancer Res.* **74**, 5656–5667

31. Quan, X., Yue, W., Luo, Y., Cao, J., Wang, H., Wang, Y., and Lu, Z. (2015) The protein arginine methyltransferase PRMT5 regulates A??-induced toxicity in human cells and

Caenorhabditis elegans models of Alzheimer's disease. *J. Neurochem.* **134**, 969–977

CHAPTER 3

Mammalian Protein Arginine Methyltransferase 7 (PRMT7) Specifically Targets RXR Sites in Lysine- and Arginine-rich Regions

Mammalian Protein Arginine Methyltransferase 7 (PRMT7) Specifically Targets *R*X*R* Sites in Lysine- and Arginine-rich Regions*

Received for publication, October 7, 2013, and in revised form, November 1, 2013 Published, JBC Papers in Press, November 18, 2013, DOI 10.1074/jbc.M113.525345

You Feng[‡], Ranjan Maity[§], Julian P. Whitelegge[¶], Andrea Hadjikyriacou[‡], Ziwei Li[‖], Cecilia Zurita-Lopez[‡], Qais Al-Hadid[‡], Amander T. Clark[‖], Mark T. Bedford[**], Jean-Yves Masson[§], and Steven G. Clarke[‡1]

From the Departments of [‡]Chemistry and Biochemistry and [‖]Molecular, Cellular, and Developmental Biology, Molecular Biology Institute, UCLA, Los Angeles, California 90095, the [§]Genome Stability Laboratory, Laval University Cancer Research Center, Hôtel-Dieu de Québec Research Center, Québec G1R 2J6, Canada, the [¶]Pasarow Mass Spectrometry Laboratory, NPI-Semel Institute for Neuroscience and Human Behavior UCLA, Los Angeles, California 90095, and the [**]Department of Molecular Carcinogenesis, University of Texas MD Anderson Cancer Center, Smithville, Texas 78957

Background: Protein arginine methyltransferase 7 (PRMT7) is associated with various functions and diseases, but its substrate specificity is poorly defined.
Results: Insect cell-expressed PRMT7 forms ω-monomethylarginine residues at basic R*X*R sequences in peptides and histone H2B.
Conclusion: PRMT7 is a type III PRMT with a unique substrate specificity.
Significance: Novel post-translational modification sites generated by PRMT7 may regulate biological function.

The mammalian protein arginine methyltransferase 7 (PRMT7) has been implicated in roles of transcriptional regulation, DNA damage repair, RNA splicing, cell differentiation, and metastasis. However, the type of reaction that it catalyzes and its substrate specificity remain controversial. In this study, we purified a recombinant mouse PRMT7 expressed in insect cells that demonstrates a robust methyltransferase activity. Using a variety of substrates, we demonstrate that the enzyme only catalyzes the formation of ω-monomethylarginine residues, and we confirm its activity as the prototype type III protein arginine methyltransferase. This enzyme is active on all recombinant human core histones, but histone H2B is a highly preferred substrate. Analysis of the specific methylation sites within intact histone H2B and within H2B and H4 peptides revealed novel post-translational modification sites and a unique specificity of PRMT7 for methylating arginine residues in lysine- and arginine-rich regions. We demonstrate that a prominent substrate recognition motif consists of a pair of arginine residues separated by one residue (R*X*R motif). These findings will significantly accelerate substrate profile analysis, biological function study, and inhibitor discovery for PRMT7.

Post-translational modifications dramatically increase the diversity of proteins in the cell and substantially contribute to epigenetic regulation and the control of cellular processes (1). One of the major groups of enzymes that catalyze these reactions in eukaryotic cells are protein arginine methyltransferases (PRMTs)[2] that transfer methyl groups from the methyl donor, *S*-adenosyl-*L*-methionine (AdoMet), to specific arginine residues on protein substrates (Fig. 1). In mammals, a group of nine sequence-related PRMTs have been characterized (2, 3). PRMT1, -2, -3, -4, -6, and -8 catalyze the formation of ω-N^G-monomethylarginine (MMA) and ω-N^G, N^G-asymmetric dimethylarginine (ADMA) and are classified as type I PRMTs. PRMT5 catalyzes the formation of MMA and ω-N^G, N'^G-symmetric dimethylarginine (SDMA) and is defined as a type II PRMT. More recently, PRMT7 has emerged as a type III PRMT that produces only MMA in its substrates (4, 5). In humans and mice, PRMT7 is a 692-amino acid protein with an ancestral duplication of the catalytic domains, both of which are required for its activity (4). PRMT7, when expressed as a GFP fusion protein, shows a predominantly cytoplasmic distribution (6).

The physiological roles of PRMT7 have been associated with broad cellular processes in mammalian cells (3, 7). It has been indicated that PRMT7 may play a role in Sm protein methylation and small nuclear ribonucleoprotein biogenesis (8). PRMT7 knockdown up-regulates the expression of genes involved in DNA repair, including ALKBH5, APEX2, POLD1, and POLD2 (9). It has also been suggested that PRMT7 plays a role in pluripotency state maintenance in undifferentiated embryonic stem cells and germ cells (10) and antagonizes MLL4-mediated differentiation (11). Interestingly, PRMT7 has been associated with cellular sensitivity to a number of drugs.

* This work was supported, in whole or in part, by National Institutes of Health Grants GM026020 (to S. G. C.), S10 RR023045 (to J. P. W.), and DK62248 (to M. T. B.). This work was also supported by the Canadian Institute of Health Research (to J. Y. M.).

[1] To whom correspondence should be addressed: Dept. of Chemistry and Biochemistry and the Molecular Biology Institute, UCLA, 607 Charles E. Young Dr. East, Los Angeles, CA. Tel.: 310-825-8754; Fax: 310-825-1968; E-mail: clarke@chem.ucla.edu.

[2] The abbreviations used are: PRMT, protein arginine methyltransferase; MMA, ω-N^G-monomethylarginine; ADMA, ω-N^G, N^G-asymmetric dimethylarginine; SDMA, ω-N^G,N'^G-symmetric dimethylarginine; AdoMet, *S*-adenosyl-L-methionine; [^{3}H]AdoMet, *S*-adenosyl-[*methyl*-^{3}H]L-methionine; HBR, H2B repression region; BisTris, 2-[bis(2-hydroxyethyl)amino]-2-(hydroxymethyl)propane-1,3-diol; ESI, electrospray ionization; ETD, electron transfer dissociation.

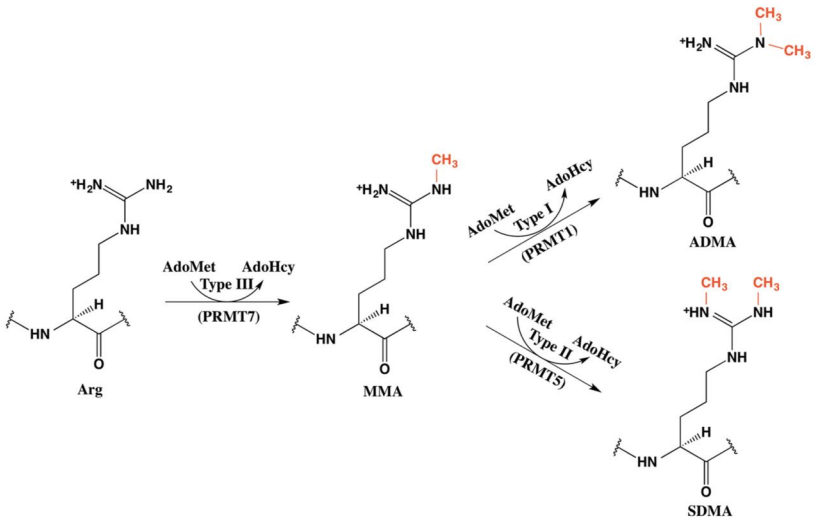

FIGURE 1. **Reactions catalyzed by type I, II, and III PRMTs.** AdoHcy, *S*-adenosylhomocysteine.

Its expression has been correlated with sensitivity to topoisomerase II inhibitors in Chinese hamster fibroblasts (12), resistance to the topoisomerase I inhibitor camptothecin in HeLa cells (13), and correlated by linkage-directed association analysis to etoposide cytotoxicity in human lymphoblastoid cell lines (14). Finally, a gene expression meta-analysis identified a possible role of PRMT7 in promoting breast cancer metastasis (15). These results suggest PRMT7 as a potential target for anticancer therapeutics.

Since its discovery as a methyltransferase (4), the type of methylation reaction catalyzed by PRMT7 has been under debate. A sole type III activity forming MMA has been reported (4, 5) as well as a type I/type II activity forming both ADMA and SDMA (16). A sole type III activity was also found for the worm and trypanosome homologs of PRMT7 (17, 18). In a number of studies, PRMT7 was expressed in mammalian cells as a FLAG-tagged species where the purification methods would be expected to also pull down the type II PRMT5 species (2, 3, 19). The potential contamination of PRMT7 with PRMT5 (and possibly other PRMTs, including the major PRMT1 species) in such studies would complicate the analysis of substrate specificity. These problems may have led to the misclassification of PRMT7 as a type II PRMT and confusion of its methylation sites with those of other PRMTs (9, 20). Given the roles of PRMTs in epigenetic regulation via histone methylation and the involvement of PRMT7 in both cell development and cancer (10–15), it is important to establish the catalytic pattern and substrate specificity of PRMT7.

Here, we report the expression and purification of mouse PRMT7 from insect cells with robust activity. We identify H2B as the best substrate among recombinant human core histones and detect the monomethylation of H2B Arg-29, Arg-31, Arg-33 and H4 Arg-17, Arg-19 by PRMT7 with high resolution amino acid analysis and top-down mass spectroscopy. We found that PRMT7 specifically targets arginine residues in R*X*R motifs surrounded by multiple lysines. Our work confirming the type III formation of MMA and our discovery of the unique substrate recognition motif of PRMT7 clarify two common ambiguities in the study of this methyltransferase, setting a foundation for exploring the kinetic mechanism, inhibitor discovery, and biological functions of PRMT7.

EXPERIMENTAL PROCEDURES

Mutagenesis—Mouse PRMT7-pEGFP-C1 plasmid was prepared as described (6). The wild-type plasmid was mutated to create a catalytically inactive enzyme that cannot bind AdoMet, with motif I residues LDIG changed to AAAA. Mutagenic primers were designed to be 45 bases in length with a T_m of 89 °C. Primers used were as follows: forward primer 5′-GGA CAG AAG GCC TTG GTT GCG GCC GCT GCG ACT GGC ACG GGA CTC-3′ and reverse primer 5′-GAG TCC CGT GCC AGT CGC AGC GGC CGC AAC CAA GGC CTT CTG TCC-3′. A PCR was set up according to the QuikChange site-directed mutagenesis kit (Agilent), using 50 ng of dsDNA template (GFP-PRMT7 wild type), 125 ng of both primers, and PfuUltra HF DNA polymerase. The PCR was run at 95 °C for 1 min, 18 cycles of 95 °C for 50 s, 60 °C for 50 s, and 68 °C for 10 min. There was an additional 7-min extension at 68 °C. Amplification products were then digested using 10 units of DpnI for 1 h at 37 °C to remove the parental dsDNA. Plasmids were then transformed into XL10-Gold ultracompetent *Escherichia coli* cells, plated on LB kanamycin plates, and grown overnight at 37 °C. Positive colonies were subjected to DNA sequencing on both strands to confirm the mutations (GeneWiz, Inc.).

Protein Expression and Purification—Wild-type and mutant mouse GFP-PRMT7 plasmid DNA prepared as described above were subcloned into a modified pFastBac baculovirus expression vector and expressed between GST (at the N terminus) and His tag (at the C terminus). The PRMT7 pFastBac vector was transformed into *E. coli* (DH10Bac), and the bacmid DNA was generated. *Spodoptera frugiperda* (Sf9) insect cells were then transfected with the bacmid DNA to produce virus particles. By

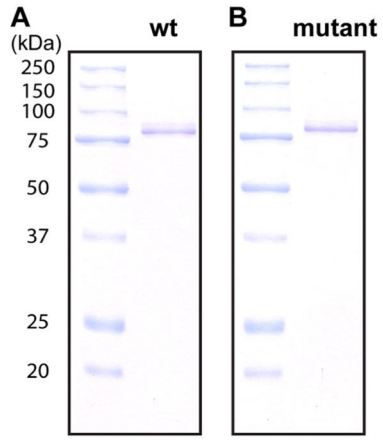

C

GPLGYMKVFCGRANPTTGSLEWLEEDEHYDYHQEIARSSYADMLHDKDRNIKYYQGIRAA
VSRVKDRGQKALV**LDIG**TGTGLLSMMAVTAGADFCYAIEVFKPMAEAAVKIVERNGFSDK
IKVINKHSTEVTVGPDGDLPCRANILITELFDTELIGEGALPSYEHAHKHLVQEDCEAVP
HRATVYAQLVESRRMWSWNKLFPVRVRTSLGEQVIVPPSELERCPGAPSVCDIQLNQVSP
ADFTVLSDVLPMFSVDFSKQVSSSAACHSRQFVPLASGQAQVVLSWWDIEMDPEGKIKCT
MAPFWAQTDPQELQWRDHWMQCVYFLPQEEPVVQGSPRCLVAHHDDYCVWYSLQRTSPDE
NDSAYQVRPVCDCQAHLLWNRPRFGEINDQDRTDHYAQALRTVLLPGSVCLCVSDGSLLS
MLAHHLGAEQVFTVESSVASYRLMKRIFKVNHLEDKISVINKRPELLTAADLEGKKVSLL
LGEPFFTTSLLPWHNLYFWYVRTSVDQHLAPGAVVMPQAASLHAVIVEFRDLWRIRSPCG
DCEGFDVHIMDDMIKHSLDFRESREAEPHPLWEYPCRSLSKPQEILTFDFQQPIPQQPMQ
SKGTMELTRPGKSHGAVLWMEYQLTPDSTISTGLINPAEDKGDCCWNPHCKQAVYFLSTT
LDLRVPLNGPRSVSYVVEFHPLTGDITMEFRLADTLS***ELALVPRGSSAHHHHHHHHHH***

FIGURE 2. **Recombinant mouse PRMT7 expressed in Sf9 insect cells.** *A,* SDS-PAGE followed by Coomassie Blue staining of the purified wild-type enzyme, revealing a single major polypeptide of ~80 kDa (expected mass is 81.2 kDa). This protein includes an N-terminal extension of GPLGY and a C-terminal extension of ELALVPRGSSAHHHHHHHHHH. The lane of marker proteins is shown on the *left* with the polypeptide sizes. *B,* SDS-PAGE analysis of the PRMT7 inactive mutant with motif I residues LDIG changed to AAAA. *C,* LC-MS/MS analysis of tryptic peptides of wild-type PRMT7. Sequences were searched against both the *S. frugiperda* and the mouse subsets of the UniRef100 database as well as the tagged expected sequence of PRMT7. Sequence coverage of the recombinant PRMT7 (85%) is shown by *underlining*; those residues not present in the endogenous protein are highlighted in *bold* and *italics*; the LDIG motif that was mutated in the PRMT7 mutant is shown in *bold*.

performing mini-infection assays, we selected the most efficient conditions for protein expression, which were 0.75–1.0 × 10^6 cells/ml with a ratio of 1:100 between virus suspension and media and 48 h of duration for infection. One liter of Sf9 cell culture pellet (infected with wild-type or mutant PRMT7-expressing baculovirus) was used for protein purification. The Sf9 cell pellet was lysed in 40 ml of PBS lysis buffer containing 1 mM EDTA, 0.05% Triton X-100, 1 mM DTT, 1 tablet of protease inhibitor mixture (Roche Applied Science), and a final concentration of 250 mM NaCl, using 20 strokes of a Dounce homogenizer followed by three 30-s periods of sonication. The total cell lysate was incubated for 30 min at 4 °C with 1 mM $MgCl_2$ and benzonase nuclease to remove DNA or RNA contamination followed by centrifugation at 38,724 × *g* for 30 min at 4 °C to get a clear soluble lysate. The soluble cell lysate was then incubated with Glutathione-Sepharose 4B beads (GE Healthcare) for 1 h in GST-binding buffer (lysis buffer without protease inhibitor) followed by washing the beads three times with washing buffer (GST binding buffer made up to a final concentration of 350 mM NaCl). The GST beads were then incubated with 5 mM ATP and 15 mM $MgCl_2$ for 1 h at 4 °C to prevent nonspecific binding of heat-shock proteins and washed again three times with washing buffer. GST beads were then washed with P5 buffer (50 mM sodium phosphate, 500 mM NaCl, 10% glycerol, 0.05% Triton X-100, 5 mM imidazole, pH 7.0) and incubated with PreScission protease (GE Healthcare; 4–8 units for 100 μl of GST beads) in P5 buffer for 6 h at 4 °C. GST-cleaved PRMT7 protein was collected as the supernatant after centrifugation and incubated with TALON cobalt metal affinity resin (Clontech; prewashed with P5 buffer) for 1 h in P5 buffer at 4 °C under rotation. The TALON resin was then washed three times (5 min each) with P30 buffer (P5 buffer with a final concentration of 30 mM imidazole). PRMT7 protein was then eluted from the resin with P500 buffer (P5 buffer with a final

concentration of 500 mM imidazole) with 5 min under rotation, and the elution step was repeated two times to elute maximum protein (21). Purified PRMT7 protein was analyzed for quality and quantity by SDS-PAGE with Coomassie Blue staining. The final sequence is GPLGY-(mouse PRMT7)-ELALVPRGSSAH-HHHHHHHHH, as shown in Fig. 2. PRMT7 protein was then dialyzed in storage buffer (Tris-Cl, pH 7.5, 150 mM NaCl, 10% glycerol, 1 mM DTT) at 4 °C for 1 h and stored in small aliquots at −80 °C.

PRMT1 was used as a His-tagged species purified from *E. coli* (22, 23) and was a kind gift from Drs. Heather Rust and Paul Thompson (Scripps Research Institute, Jupiter, FL). PRMT5 was used as a Myc-tagged species purified from HEK293 cells (24) and was a kind gift from Drs. Jill Butler and Sharon Dent (University of Texas MD Anderson Cancer Center, Houston, TX).

Peptide and Protein Substrates—Peptides H2B(23-37), H2B(23-37)R29K, H2B(23-37)R31K, H2B(23-37)R33K, H2B(23-37)R29K,R31K, H2B(23-37)R29K,R33K, H2B(23-37)R31K,R33K, H4(1-8), H4(14-22), H4(14-22)R17K, and H4(14-22)R19K were purchased from GenScript as HPLC-purified materials at >90% purity and verified by mass spectrometry by the vendor. Peptides H4(1-21), H4(1-21)R3K and H4(1-21)R3MMA were previously described (22, 23) and were a kind gift of Drs. Heather Rust and Paul Thompson (Scripps Research Institute). The sequences of all the peptides are listed in Table 1. GST-GAR was expressed in *E. coli* BL21 Star (DE3) cells (Invitrogen, C601003) and purified with glutathione-Sepharose 4B beads (Amersham Biosciences) by affinity chromatography as described previously (5). Recombinant human histone H2A (GenBank™ accession number AAN59960), H2B (GenBank™ accession number AAN59961), H3.3 (GenBank™ accession number P84243), and H4 (GenBank™ accession number AAM83108) were purchased from New England Biolabs as 1 mg/ml solutions in 20 mM sodium phosphate, 300 mM NaCl, and 1 mM EDTA. Histone H3.3 also included 1 mM DTT. In some cases, the histone preparations were dialyzed against 10,000 volumes of the reaction buffer (50 mM potassium HEPES, 10 mM NaCl and 1 mM DTT, pH 7.5) or H_2O, at 4 °C for 1 h. Alternatively, the original buffer was exchanged by diluting histones 40-fold in the reaction buffer and then reconcentrated using an Amicon centrifugation filter; this process was repeated twice.

In Vitro Methylation Assay and Acid Hydrolysis of Protein and Peptide Substrates—PRMT-catalyzed reactions were performed with 0.7 μM *S*-adenosyl-L-[*methyl*-^{3}H]methionine ([^{3}H]AdoMet; PerkinElmer Life Sciences, 75–85 Ci/mmol, from a stock of 0.55 mCi/ml in 10 mM H_2SO_4/EtOH (9:1, v/v)) and appropriate substrate in a final reaction volume of 60 μl unless otherwise specified. The reactions were buffered in 50 mM potassium HEPES, pH 7.5, 10 mM NaCl, and 1 mM DTT and incubated at room temperature (21–23 °C) for 20–24 h. When proteins were used as substrates, the methylation reactions were quenched with 12.5% (w/v) trichloroacetic acid, and 20 μg of bovine serum albumin was added as a carrier protein. After incubation at room temperature for 30 min, the precipitated protein was collected by centrifugation at 4000 × *g* for 30 min. The pellet was washed with cold acetone and air-dried. When peptides were used as substrates, the reaction mixture was quenched with trichloroacetic acid (final concentration is 1.6%), and peptides were isolated using an OMIX C18 ZipTip (Agilent Technologies) followed by vacuum centrifugation. Acid hydrolysis of all dried reaction mixtures was then carried out *in vacuo* at 110 °C for 20 h using 50 μl of 6 N HCl. Samples were then dried by vacuum centrifugation and dissolved in 50 μl of water.

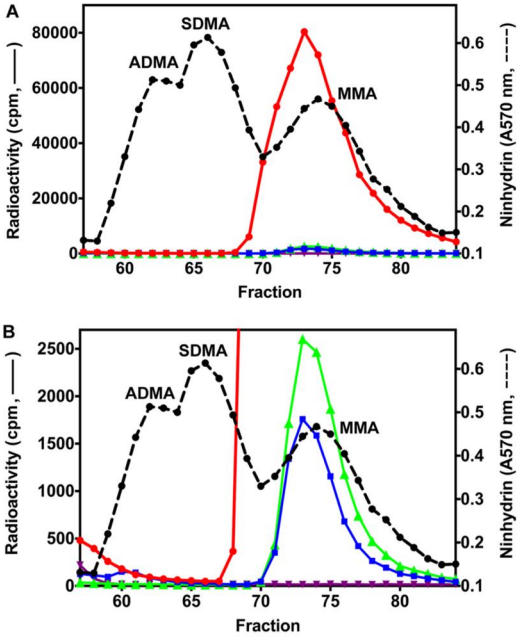

FIGURE 3. **Formation of [^{3}H]MMA from incubation of PRMT7 with [^{3}H]AdoMet and GST-GAR as a methyl-accepting substrate.** *A, in vitro* methylation reactions were performed as described under "Experimental Procedures" using 6 μg of GST-GAR and 1.2 μg of wild-type or mutant PRMT7 at a final concentration of 0.26 μM. Incubations in the absence of PRMT7 or GST-GAR were used as controls. The reactions were allowed to proceed at room temperature for 20 h. After acid hydrolysis, the methylated amino acid derivatives were analyzed by high resolution cation exchange chromatography together with standards of ADMA, SDMA, and MMA as described under "Experimental Procedures." ^{3}H radioactivity (*solid lines*) and the ninhydrin color of the methylated arginine standards (*dashed lines*; elution positions indicated) were determined with liquid scintillation counting and 570 nm absorbance, respectively. Because of a tritium isotope effect (5), the [^{3}H]methyl derivatives of ADMA, SDMA, and MMA elute on the high resolution cation exchange chromatography column 1–2 min earlier than the nonisotopically labeled standards. *Red,* wild-type PRMT7 with GST-GAR; *green,* wild-type PRMT7 alone; *blue,* mutant PRMT7 with GST-GAR; *purple,* GST-GAR alone. *B,* magnification of the radioactivity scale to show PRMT7 automethylation (*green*), the residual activity of mutant PRMT7 (*blue*), and the absence of ADMA and SDMA in the reaction products (*red*).

Amino Acid Analysis of Methylation Products by High Resolution Cation Exchange Chromatography—Amino acid analysis was performed to determine the products of enzymatic methylation reactions as described previously (5). Briefly, the hydrolyzed samples were mixed with 1 μmol each of ω-MMA (acetate salt, Sigma, M7033), SDMA (di(*p*-hydroxyazobenzene)-*p'*-sulfonate salt, Sigma, D0390), and ADMA (hydrochloride salt, Sigma, D4268) as internal standards. Samples were loaded onto a cation exchange column of PA-35 sulfo-

TABLE 1

Sequences of synthesized H2B and H4 peptides

Ac is acetyl.

Peptide	Sequence	Theoretical M_r	Observed M_r
H2B(23–37)	Ac-KKDGKKRKRSRKESY	1936.23	1935.60[a]
H2B(23–37)R29K	Ac-KKDGKKKKRSRKESY	1908.22	1908.00[a]
H2B(23–37)R31K	Ac-KKDGKKRKKSRKESY	1908.22	1907.80[a]
H2B(23–37)R33K	Ac-KKDGKKRKRSKKESY	1908.22	1908.00[a]
H2B(23–37)R29K,R31K	Ac-KKDGKKKKKSRKESY	1880.21	1879.60[a]
H2B(23–37)R29K,R33K	Ac-KKDGKKKKRSKKESY	1880.21	1879.60[a]
H2B(23–37)R31K,R33K	Ac-KKDGKKRKKSKKESY	1880.21	1879.60[a]
H4(1–21)	Ac-SGRGKGGKGLGKGGAKRHRKV	2132	2133[b]
H4(1–21)R3K	Ac-SGKGKGGKGLGKGGAKRHRKV	2104	2105[b]
H4(1–21)R3MMA	Ac-SGR(me)GKGGKGLGKGGAKRHRKV	2146	2147[b]
H4(1–8)	Ac-SGRGKGGK	787.87	787.60[a]
H4(14–22)	Ac-GAKRHRKVL	1106.33	1106.25[a]
H4(14–22)R17K	Ac-GAKKHRKVL	1078.32	1078.20[a]
H4(14–22)R19K	Ac-GAKRHKKVL	1078.32	1078.20[a]

[a] Data were provided by GenScript Inc.
[b] Data are from Refs. 22, 23.

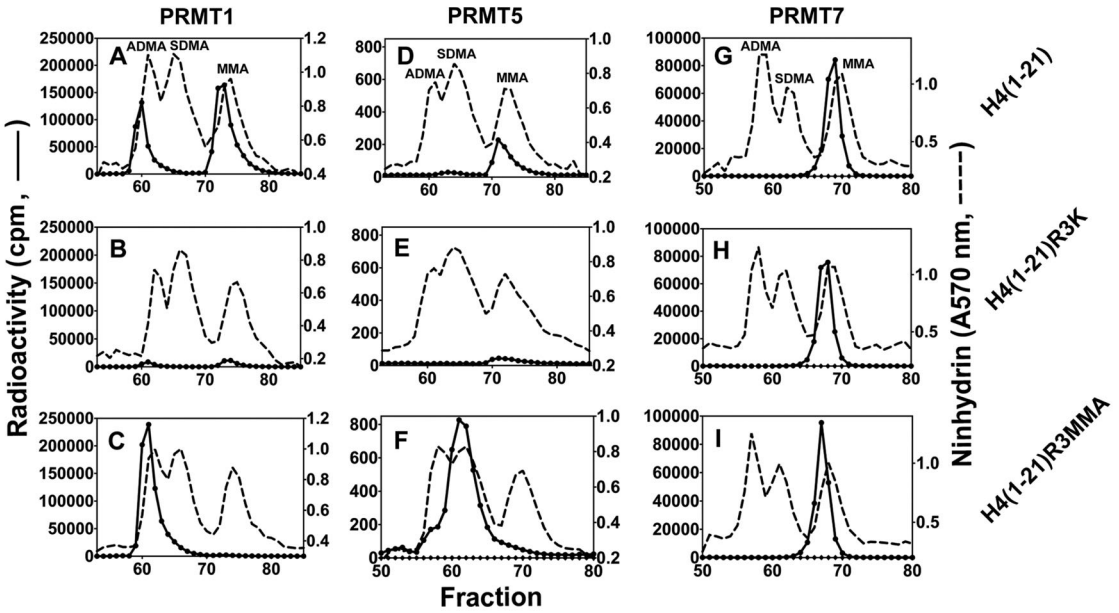

FIGURE 4. **Comparison of the methylation products of PRMT1, -5, and -7 using synthetic peptides derived from the N terminus of human histone H4.** Peptides (12.5 μM final concentration) were incubated with [^{3}H]AdoMet and PRMT1 (0.45 μM final concentration), PRMT5 (0.72 μM final concentration), or PRMT7 (0.26 μM final concentration) as described under "Experimental Procedures" and the reactions were allowed to proceed at room temperature for 20 h. The reaction mixtures were then acid-hydrolyzed and analyzed for methylated arginine species as described under "Experimental Procedures." *A–C* show PRMT1-catalyzed methylation products of peptides H4(1–21), H4(1–21)R3K, and H4(1–21)R3MMA (Table 1), respectively. *D–F* show PRMT5-catalyzed methylation products of these peptides. *G–I* show PRMT7-catalyzed methylation products of these peptides. The elution positions of the ADMA, SDMA, and MMA standards are specifically indicated in *A, D,* and *G* but are similar in all of the experiments.

nated polystyrene beads (6–12 μm; Benson Polymeric Inc., Sparks, NV) and eluted with sodium citrate buffer (0.35 M Na^+, pH 5.27) at 1 ml/min at 55 °C. Elution positions of the amino acid standards were determined by a ninhydrin assay. 50-μl aliquots of 1-ml column fractions were mixed with 100 μl of ninhydrin solution (20 mg/ml ninhydrin and 3 mg/ml hydrindantin in 75% (v/v) dimethyl sulfoxide and 25% (v/v) 4 M lithium acetate, pH 4.2) and incubated at 100 °C for 15–20 min, and the absorbance was measured at 570 nm using a SpectraMax M5 microplate reader with a path length of 0.5 cm. Radioactivity in column fractions was quantitated using a Beckman LS6500 counter and expressed as an average of three 5-min counting cycles after mixing 950 μl of each fraction with 10 ml of fluor (Safety Solve, Research Products International, 111177).

Fluorography of Histones Methylated by PRMT7—The enzymatic methylation reactions were set up with [^{3}H]AdoMet as described above. After 15–20 h of incubation at room temperature (21–23 °C), the reactions were quenched by SDS loading buffer and separated on 16% Tris-glycine gel (Novex, Invitrogen, EC6495BOX) or 4–12% BisTris gel (NuPAGE Novex, Invitrogen, NP0335BOX), stained with Coomassie Blue for 0.5 h, destained for 1 h, enhanced in autoradiography enhancing buffer (EN3HANCE^{TM}, PerkinElmer Life Sciences, 6NE9701) for 1 h, and vacuum-dried. The fluoroimage was

scanned after 3 h to 7 days of exposure to autoradiography film (Denville Scientific Inc., E3012). From the fluoroimage, the densitometry of each band was measured with ImageJ software, and the specific radioactivity was calculated by dividing the intensity of the fluorograph band with that of the Coomassie-stained band.

Top-down Mass Spectrometry of Proteins or Peptides Methylated by PRMT7—Methylation reactions were performed at the indicated concentration of AdoMet (Sigma, A2408, *p*-toluenesulfonate salt) in a buffer of 50 mM potassium HEPES, pH 7.5, 10 mM NaCl, and 1 mM DTT. Top-down mass spectrometry coupled with ETD (LTQ-Orbitrap) was used to determine the methylation sites targeted by PRMT7. Protein or peptide substrate was incubated with PRMT7 and 182–200 μM AdoMet in the reaction buffer at room temperature for 24 h. Then the methylation products were loaded onto OMIX C18 ZipTip (Agilent Technologies, A5700310), washed with 0.1% formic acid, and eluted with formic acid/acetonitrile/H_2O (0.1:50:50). The eluted sample was subjected directly to electrospray ionization (ESI), and ion isolation and ETD fragmentation were performed to identify and break down the positively charged methylated species. Unit resolution was achieved on all product ions by operating the instrument at 30,000 or 60,000 resolution (at 400 *m*/*z*). The mass spectra of multiply charged precursors were deconvoluted to monoisotopic zero-charge mass using Xtract 3.0 software. The ETD tandem mass spectra were analyzed with ProsightPC 2.0 software (Thermo Scientific) to match the identified c and z ions to the known amino acid sequences and to localize post-translational modifications, which remain a largely manual process.

RESULTS

Robust Mouse PRMT7 Expressed in Insect Cells Catalyzes the Formation of Monomethylated Arginine Residues Only—Previously, human PRMT7 was prepared as a GST fusion protein expressed in bacterial cells. This enzyme was shown to be a type III enzyme that formed MMA residues on a variety of proteins and peptides (4, 5). However, the enzymatic activity was relatively low. To study an enzyme with minimal exogenous residues that could be expressed in animal cells in potential complex with interacting proteins and with potential post-translational modifications, we prepared recombinant mouse PRMT7 with small N- and C-terminal tags in Sf9 insect cells. We observed a single major polypeptide of the expected size of PRMT7 with SDS-PAGE analysis (Fig. 2*A*). LC-MS/MS analysis demonstrated high sequence coverage (85%) of PRMT7 (Fig. 2*C*) and the absence of tryptic peptides corresponding to other PRMTs or other methyltransferases from mouse or *S. frugiperda*. Additionally, no tryptic peptides were detected consistent with the presence of additional stoichiometric subunits of PRMT7. As a control, a catalytic mutant was prepared where the AdoMet-binding motif I residues LDIG were changed to AAAA (Fig. 2*B*).

Methylation assays were then carried out with the previously characterized substrates GST-GAR, a protein containing the first 148 amino acids of human fibrillarin (5, 21), and synthetic peptides derived from the N terminus of human histone H4 (22, 23, 25–27). Using amino acid analysis employing high resolu-

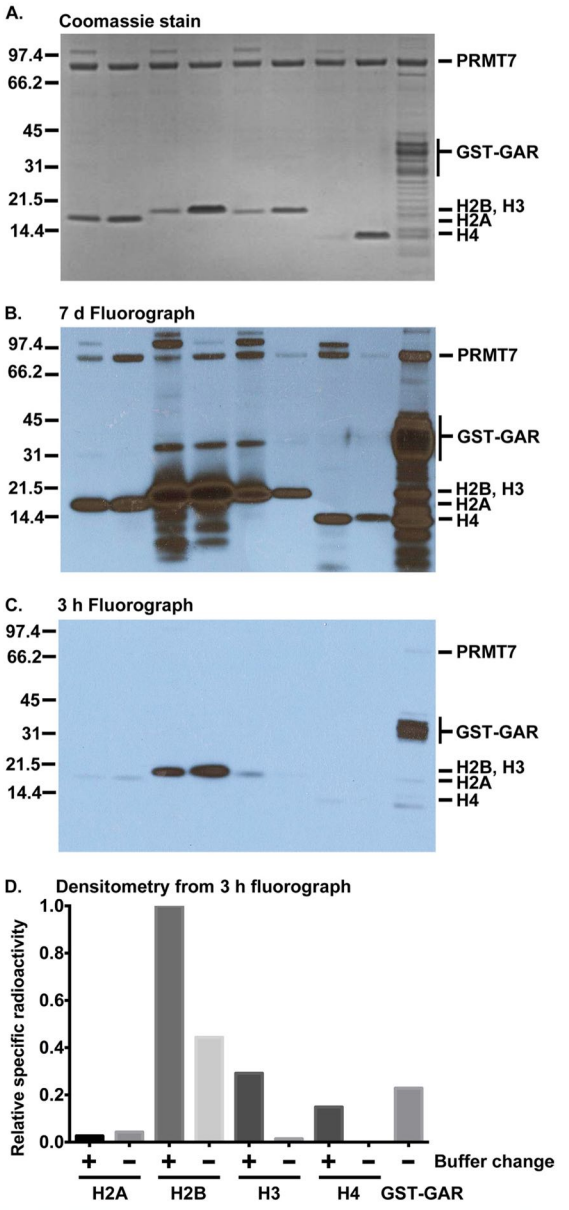

FIGURE 5. **PRMT7-catalyzed methylation of core histones with and without buffer change detected by fluorography.** 4 μg of human recombinant histones H2A, H2B, H3.3, and H4, either in the supplied buffer or exchanged into the reaction buffer (see "Experimental Procedures"), or 4 μg of GST-GAR were mixed with PRMT7 (0.26 μM final concentration) and [^{3}H]AdoMet and incubated at room temperature as described under "Experimental Procedures" for 20 h in a final volume of 40 μl. Samples were then mixed with SDS loading buffer, separated on 4–12% BisTris gel, and stained with Coomassie Blue (*A*). The protein substrate in each lane was labeled at the *bottom* of the graph. The expected position of molecular mass standards (Bio-Rad, broad range) is shown on the *left* in kDa. The fluoroimage was developed after 7 days (*d*) of film exposure (*B*) or 3 h of film exposure (*C*). As described under "Experimental Procedures," the density of radioactive bands from the film shown in *C* (where the density was mostly in the linear range) was divided by the density of the Coomassie-stained polypeptide to obtain the specific radioactivity (*D*). Data were normalized against the specific radioactivity of H2B (with buffer change).

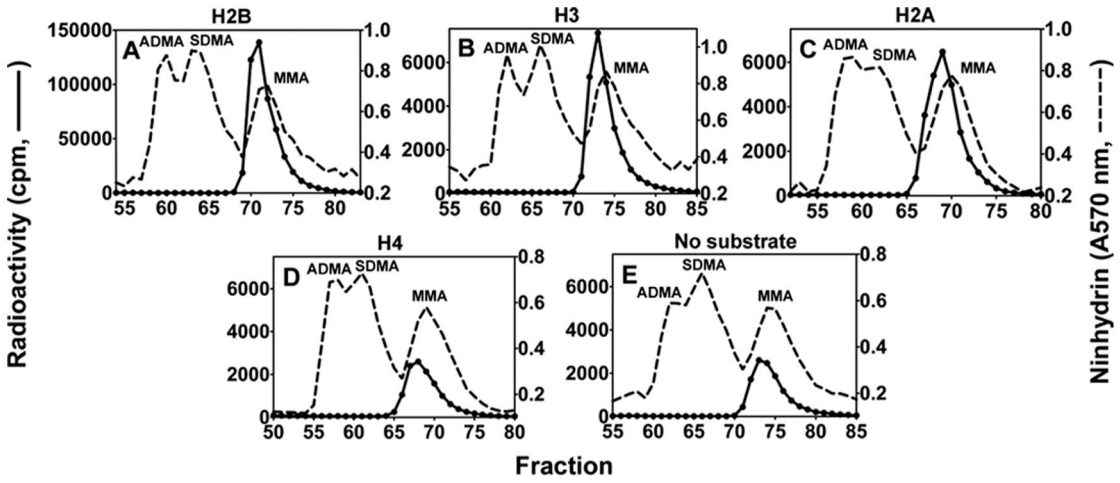

FIGURE 6. **Amino acid analysis of histones methylated by PRMT7.** 6 μg of recombinant human H2A, H2B, H3.3, or H4 was dialyzed against the reaction buffer and then incubated for 20 h with [^{3}H]AdoMet and PRMT7 (0.26 μM final concentration), hydrolyzed to amino acids, and analyzed by high resolution cation exchange chromatography as described in Fig. 2 legend. *A–D* show the PRMT7-catalyzed methylation products of H2B, H3.3, H2A, and H4. *E* shows the control of PRMT7 automethylation in the absence of histone substrates.

tion cation exchange chromatography, we were able to clearly separate MMA, SDMA, and ADMA and capture femtomole levels of methylation products from [^{3}H]AdoMet. In Fig. 3, we demonstrate the high catalytic activity of PRMT7 on GST-GAR, resulting in a peak radioactivity of $\sim 8 \times 10^4$ cpm in MMA with no SDMA or ADMA formation detected. The activity of this enzyme was about 18-fold greater than that of the GST fusion protein expressed in bacterial cells (5) when tested under similar conditions. The catalytic mutant PRMT7 retained only ~2% of this activity, confirming the absence of other PRMT enzymes in the preparation (Fig. 3*A*). Interestingly, PRMT7 alone showed relatively weak automethylation activity (a peak of $\sim 2.6 \times 10^3$ cpm), which has not been previously observed (Fig. 3*B*).

To confirm the catalytic activity forming only MMA, we compared the methylation products of a synthetic peptide based on residues 1–21 of human histone H4 along with its Arg-3 to Lys and Arg-3 to MMA derivatives (Table 1) catalyzed by PRMT7 with those catalyzed by the representative type I PRMT1 and type II PRMT5 enzymes. As shown in Fig. 4, PRMT1 formed ADMA and MMA on H4(1–21) as expected. When Arg-3 was replaced with Lys on the peptide, there was still residual activity left (~7%), indicating that Arg-17 and/or Arg-19 can also be weakly methylated by PRMT1. When the Arg-3-monomethylated peptide was used as a substrate, PRMT1 formed mainly ADMA, most likely on Arg-3, which confirms the major methylation site on the histone H4 N-terminal tail for PRMT1 (28). PRMT5 formed SDMA and MMA on H4(1–21) as expected (29). PRMT5 also showed weak activity (~20%) on the R3K mutant peptide, suggesting that Arg-17 and/or Arg-19 are its target sites as well. When Arg-3 is pre-monomethylated, PRMT5 formed mainly SDMA on H4(1–21)R3MMA, indicating Arg-3 as its major methylation site on H4 tail. Most interestingly, PRMT7 mediated formation of only MMA on all of the three H4 peptides, whether Arg-3 was mutated to Lys or MMA. These results indicate first, when there is already a methyl group on Arg-3, that PRMT7 does not add a second methyl group to it like PRMT1 and PRMT5; and second, on the H4 N-terminal tail, Arg-17 and/or Arg-19 are likely the major targets for PRMT7 rather than Arg-3.

PRMT7 Preferentially Methylates H2B among Core Histones—To study the substrate specificity of the PRMT7 enzyme expressed in insect cells, we compared the methylation level of all four core human recombinant histones catalyzed by PRMT7 in the presence of [^{3}H]AdoMet in an SDS-PAGE fluorography assay. As shown in Fig. 5, H2B was found to be a much better substrate than any of the other histones. After a 3-h exposure of the EN3HANCE^{TM} gel, only H2B appeared to be significantly methylated; after a 7-day exposure, the H2B band saturated the film response, and H2A, H3, and H4 bands became apparent. Of note, we found that replacing the histone storage buffer (300 mM NaCl, 1 mM EDTA, and 20 mM sodium phosphate, pH 7.0) with the reaction buffer (50 mM potassium HEPES, pH 7.5, 10 mM NaCl, and 1 mM DTT) significantly promoted the methylation of histone H2B, especially histones H3 and H4.

The specificity of PRMT7 for histone H2B was confirmed by amino acid analysis of the reaction products. Here, we observed a peak radioactivity of MMA of $\sim 1.4 \times 10^5$ cpm for H2B and 5% or less of this value for H2A, H3, and H4 (Fig. 6). No ADMA or SDMA products were observed in any of these reactions.

PRMT7 Targets Arg-29, Arg-31, and Arg-33 in Basic RXR Motifs on Histone H2B—Next, we aimed to identify the methylation sites of PRMT7 on H2B. First, high resolution top-down Fourier transform-MS analysis was conducted for intact H2B protein (Fig. 7*A*) and the product of H2B methylation with PRMT7 and AdoMet (Fig. 7*B*). Samples were subjected to LTQ-Orbitrap coupled with ETD, enabling us to confirm the monomethylation on H2B (Δm = 14 Da for monoisotopic mass) and selectively isolate and fragment the monomethylated species. Fig. 7*B* shows PRMT7-mediated production of a 20-charge monomethylated precursor ion ($\Delta m/z$ = 0.7 compared with the unmodified ion peak), which generated the

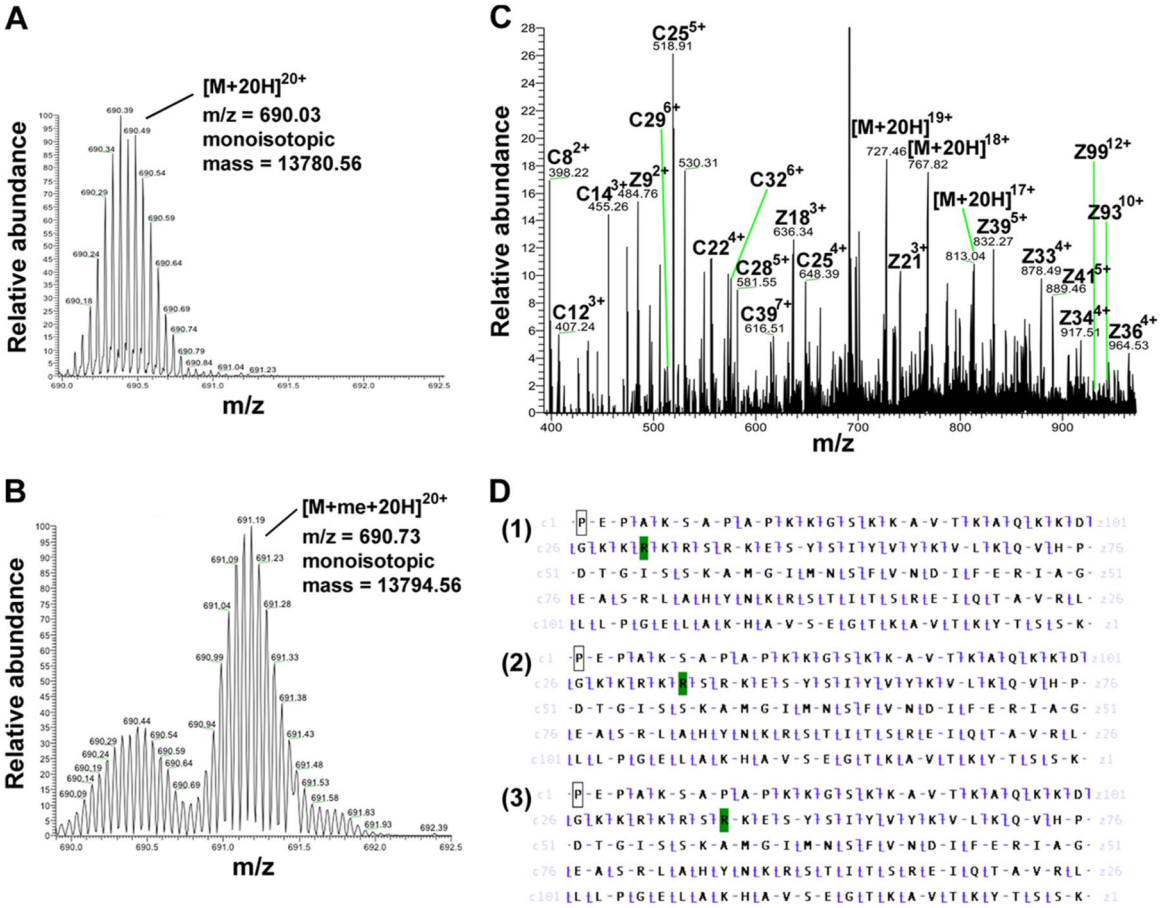

FIGURE 7. **Detection of PRMT7-formed monomethylarginine sites in histone H2B using top-down mass spectrometry.** 15 μg of H2B was incubated with 4.8 μg of PRMT7 (1 μM) and 200 μM AdoMet in the reaction buffer at room temperature for 24 h in a final volume of 60 μl. The methylation products were desalted using an OMIX C18 ZipTip and directly introduced into an LTQ-Orbitrap mass spectrometer by nano-ESI as described previously (30). *A,* control mass spectrum of unreacted H2B is shown with ion isolation of the 20-charge species (m/z = 690.03, monoisotopic mass = 13,780.56 Da; calculated monoisotopic mass 13,780.54 Da). *B,* mass spectrum of methylated H2B from the incubation mixture described above is shown with ion isolation of the 20-charge species (m/z = 690.73, monoisotopic mass = 13,794.56 Da; calculated monoisotopic mass 13,794.56 Da). *C,* ETD tandem mass spectrum of the 20-charge precursor of methylated H2B. Unit resolution was achieved on all product ions by operating the instrument at 30,000 resolution (at 400 m/z). To maximize signal intensity for better sequence coverage in the dissociation experiment, the ion isolation experimental window was kept wide enough that there was some contamination of the desired molecular ion with unmethylated H2B. The c and z ions were assigned assuming the methyl group is on H2B R29, as in panel D-1. *D,* c and z ion coverage for H2B when a methyl group is assigned on Arg-29 (D-1), Arg-R31 (D-2), or Arg-33 (D-3). The identified c and z ions are shown mapped onto the primary sequence (c ions of N-terminal origin are indicated by the *slash pointing up* and to the *left*; c ions, of C-terminal origin are indicated with a *slash pointing down* and to the *right*). In D-1, the presence of C29 and Z97 ions indicates the methylation of Arg-29. In D-2, the presence of C31 and Z97 ions indicates the methylation of either Arg-29 or Arg-31. In D-3, the presence of C34 and Z97 ions indicates the methylation of Arg-29, Arg-31, or Arg-33. Residues highlighted in *green* represent monomethylarginine sites.

product ions shown in Fig. 7*C* using ETD. The best matches for the fragment c and z ions were found for histone H2B monomethylated on either Arg-29, Arg-31, or Arg-33 (Fig. 7*D*). Analyses of other charge states of the methylated H2B also confirmed the same results. It is difficult at this point to distinguish between these three sites of methylation, although the presence of specific C29 and Z97 ions in Fig. 7*D* supports the presence of MMA at least at Arg-29. Nevertheless, it is clear that all of these sites are within the HBR region in the sequence KKRKRSRK.

To specifically map the PRMT7-catalyzed methylation sites in the N-terminal basic region of histone H2B, we prepared six peptides corresponding to residues 23–37 and containing 0, 1, or 2 Arg to Lys substitutions at Arg-29, Arg-31, and Arg-33 (Table 1). As shown in Fig. 8*A*, the wild-type peptide with three arginine residues was an excellent substrate for PRMT7 ($\sim 3 \times 10^5$ cpm in the MMA peak), confirming the results of the top-down mass spectrometry. When Arg-29 or Arg-33 was replaced, leaving R*X*R sequences, the peptides remained good substrates with 69 and 26% of the methyl-accepting activity of the wild-type peptide, respectively (Fig. 8, *C* and *D*). However, when the central Arg-31 residue was replaced, the methyl-accepting activity decreased to only ~3% of the wild-type peptide (Fig. 8*E*). More interestingly, when two of the three arginine residues were replaced by lysine residues, leaving only a single

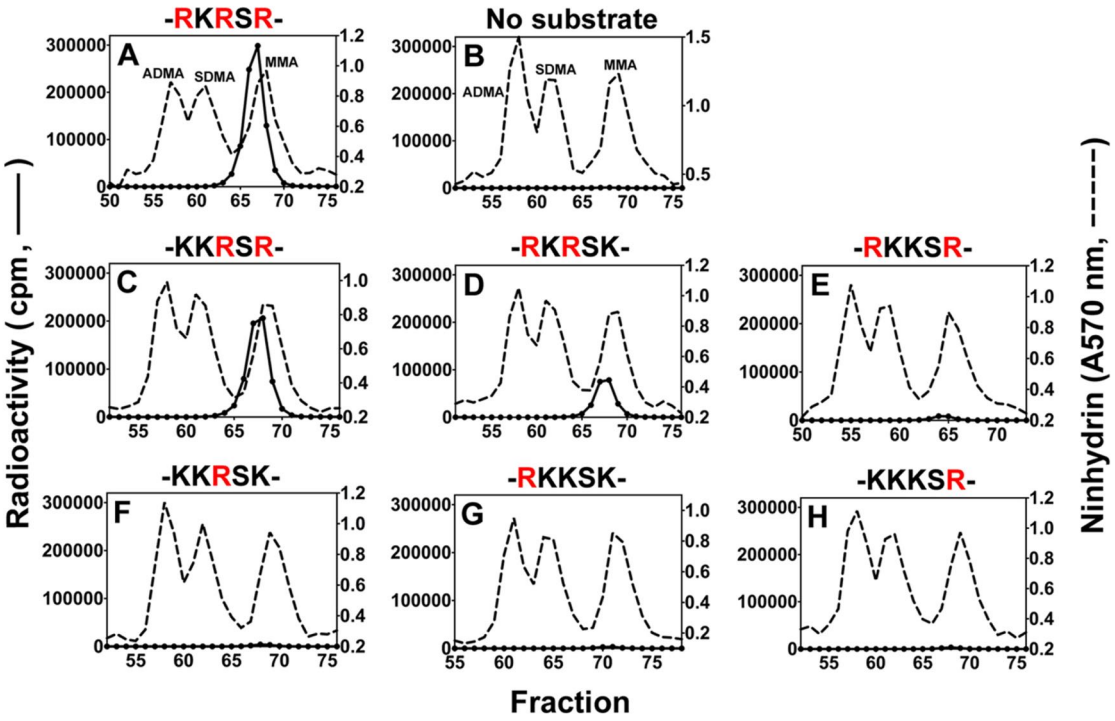

FIGURE 8. **Amino acid analysis of peptides derived from residues 23–37 of histone H2B methylated by PRMT7.** Peptides (12.5 μM final concentration; Table 1) were methylated by PRMT7 as described in Fig. 3 legend. *A–H* show PRMT7-catalyzed methylation products of H2B(23–37), no substrate, H2B(23–37)R29K, H2B(23–37)R33K, H2B(23–37)R31K, H2B(23–37)R29K,R33K, H2B(23–37)R31K,R33K, and H2B(23–37)R29K,R31K, respectively. Partial sequences containing the target arginine sites and their lysine mutations are indicated *above* the panels. The arginine methylation sites present in each peptide are highlighted in *red*.

arginine residue at positions 29, 31, or 33, the methyl-accepting activity dropped to only ~1% of the wild-type peptide (Fig. 8, *F–H*). These latter activities were only 3–4 times higher than the background MMA level formed by automethylation of PRMT7 under the same conditions (Fig. 8*B*). These data indicate that PRMT7 can monomethylate any of the three arginine residues in this region but that it shows a dramatically higher activity when at least two arginine residues are present and spaced with only one residue between them, suggesting a preferred R*X*R substrate recognition motif for PRMT7.

The k_{cat} and K_m values for selected H2B peptides containing the RKRKR sequence and its variants are shown in Table 2. Here, the value of the k_{cat}/K_m is about 4–29-fold lower when either terminal arginine residue is replaced by a lysine residue. When the central arginine residue is replaced by a lysine residue to eliminate the R*X*R motif, the k_{cat} value is over 50-fold lower, and the activity is too low to obtain a reliable K_m value. When these values are compared with those of other mammalian PRMTs reported in the literature, the k_{cat}/K_m value for PRMT7 is some 10–1000-fold lower than those for PRMT1, and -3–6, but similar to that of PRMT8 and some 50-fold greater than that of PRMT2. Although these values were determined using differing experimental conditions and substrates, it appears that there is a wide range of activity for mammalian PRMTs.

Finally, to pin down the localization of the methylation sites, we performed high resolution tandem MS analyses of the methylated wild-type H2B(23–37) peptide and its R29K mutant. Fig. 9*A* shows an example of the 5-charge state of H2B(23–37) with an m/z of 388.03, which was deconvoluted to the monoisotopic mass of the peptide (1935.12 Da). After the reaction was catalyzed by PRMT7, Fig. 9*B* shows the generation of singly, doubly, and triply methylated H2B(23–37) (m/z = 390.83, 393.63, and 396.43 and monoisotopic mass = 1949.13, 1963.14, and 1977.15 Da, respectively), with ~60% of singly methylated products, indicating the high conversion but low processivity of PRMT7 under our experimental conditions. As the amino acid analysis showed that all the methylated arginines were monomethylated (Fig. 8), the existence of triply methylated peptide confirms that all three arginines in H2B(23–37) can be methylated, although the chance of adding three methyl groups was very low. The singly methylated precursor ion generated the product ions in Fig. 9*C*, giving the best c and z ion coverage of the H2B(23–37) sequence when the methyl group was assigned to Arg-29, Arg-31, or Arg-33 (Fig. 9*D*). The c and z ions in D-1 and D-2 strongly suggested methylation of Arg-29 and Arg-31; those in D-3 did not support but could not exclude the methylation of Arg-33, probably because Arg-33 was methylated to a very low level. Thus, the singly methylated species was actually a mixture of peptides

TABLE 2

Comparison of kinetic parameters of PRMT7 with other mammalian PRMTs

Values of k_{cat} and K_m of PRMT7 were measured as described previously (26). Varied concentrations of the indicated H2B peptides (0–100 μM) were mixed with 0.1 μM PRMT7 and 10 μM *S*-adenosyl-[*methyl*-^{14}C]L-methionine (47 mCi/mmol, PerkinElmer Life Sciences) in 50 mM potassium HEPES, pH 7.5, 10 mM NaCl, 1 mM DTT, and 20 μM sodium EDTA, and incubated at room temperature for 4–5 h. Duplicate reactions mixtures were spotted onto Whatman P81 filters that were washed extensively in 50 mM $NaHCO_3$, pH 9, and counted by liquid scintillation as described previously (26). Data were analyzed by a nonlinear fit to the Michaelis-Menten equation using GraphPad Prism software; ± values reflect the standard error.

Enzyme (Ref.)	Substrate	k_{cat}	K_m (methyl-accepting substrate)	k_{cat}/K_m
		h^{-1}	μM	$\mu M^{-1}\ h^{-1}$
PRMT1 (26)	H4 (1–20)	38.4	0.34	106.8
PRMT1 (31)	H4 (1–21)	27.6	1.1	25.1
PRMT1 (32)	H4 protein	5.0	4.2	1.2
PRMT2 (32)	H4 protein	0.0065	3.3	0.0020
PRMT3 (33)	Ribosomal protein S2	6	1	6
PRMT4 (34)	H3 protein	25	≤0.2	≥50
PRMT5/MEP50 (26)	H4 (1–20)	2.6	0.63	4.1
PRMT6 (35)	H4 (1–21)	9.6	5.5	1.7
PRMT7 (this study)	H2B (23–37)	0.62 ± 0.02	6.9 ± 0.5	0.090 ± 0.007
PRMT7 (this study)	H2B (23–37)R29K	0.26 ± 0.01	11.0 ± 1.1	0.024 ± 0.003
PRMT7 (this study)	H2B (23–37)R31K	0.011 ± 0.002	[a]	
PRMT7 (this study)	H2B (23–37)R33K	0.094 ± 0.010	30.5 ± 7.7	0.0031 ± 0.0008
PRMT8 (36)	H4 protein	0.14	1.5	0.096

[a] Data values were too low for accurate determination.

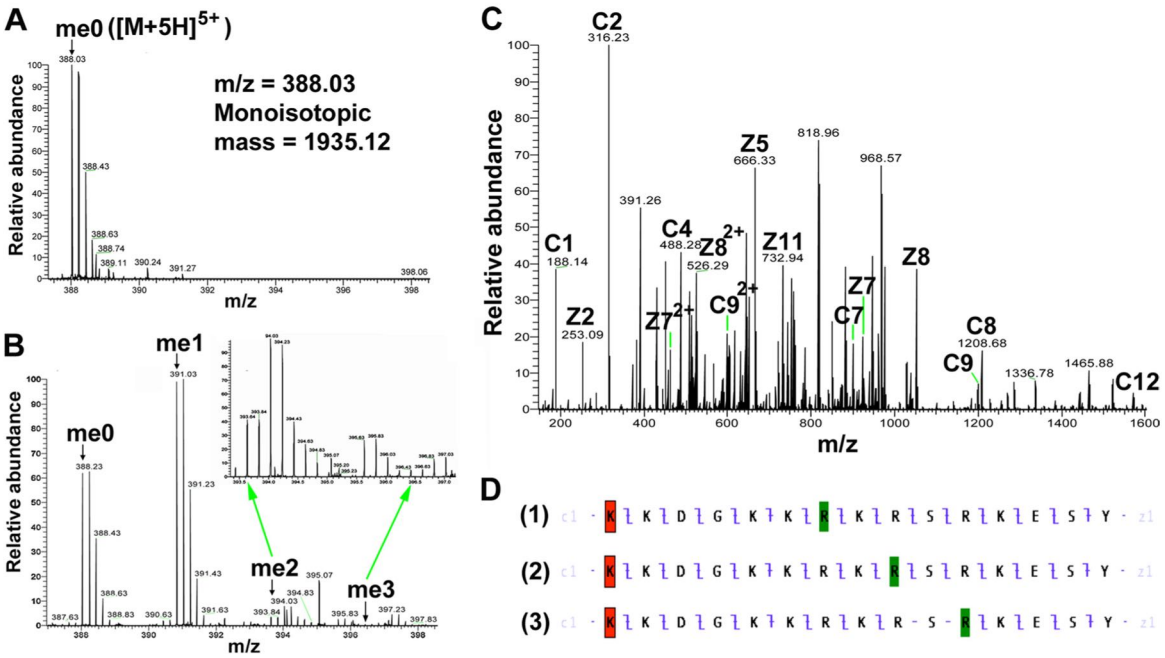

FIGURE 9. **Detection of PRMT7-formed monomethylarginine sites in a peptide corresponding to residues 23–37 of histone H2B by mass spectrometry.** 24 μM H2B(23–37) was incubated with 4.8 μg of PRMT7 (1.87 μM) and AdoMet (182 μM) in reaction buffer in a final volume of 33 μl at room temperature for 24 h. The methylation products were desalted with OMIX C18 ZipTip and directly introduced into an LTQ-Orbitrap mass spectrometer by nano-ESI, as in Fig. 6. *A,* control mass spectrum showing the +5 charged state of unmethylated H2B(23–37) (**me0**; *m/z* = 388.03, monoisotopic mass = 1935.11 Da; calculated monoisotopic mass = 1935.12 Da). *B,* LTQ-Orbitrap spectrum showing the +5 charged state of PRMT7-methylated H2B(23–37). The species detected included the unmethylated (**me0**), the monomethylated (**me1**; *m/z* = 390.83, monoisotopic mass = 1949.13 Da; calculated monoisotopic mass = 1949.14 Da), the doubly methylated (**me2**; *m/z* = 393.63, monoisotopic mass = 1963.14 Da; calculated monoisotopic mass = 1963.15 Da), and the triply methylated (**me3**; *m/z* = 396.43, monoisotopic mass = 1977.15 Da; calculated monoisotopic mass = 1977. 17 Da). The *inset* shows a magnification of the region for doubly and triply methylated H2B(23–37). *C,* ETD tandem mass spectrum of the 5-charge precursor of monomethylated H2B(23–37). The peaks corresponding to **me1** in *B* were isolated and fragmented with ETD. Unit resolution was achieved on all product ions by operating the instrument at 60,000 resolution (at 400 *m/z*). Note that **me1** is a mixture of Arg-29-methylated, Arg-31-methylated, and Arg-33-methylated species. The c and z ions were assigned assuming the methyl group is on Arg-31, as in panel D-2. *D,* c and z ion coverage for H2B(23–37) peptide when a methyl group is assigned on Arg-29 (D-1), Arg-31 (D-2), or Arg-33 (D-3). In D-1, the presence of C7 and Z9 ions indicates the monomethylation of Arg-29. In D-2, the presence of C9 and Z7 ions indicates the monomethylation of Arg-31. In D-3, the Z5 and Z6 ions supporting monomethylation of Arg-33 were not found, probably because Arg-33 is methylated to a very low extent, as suggested by *B* **me3**. Acetylation of the N-terminal lysine residue is indicated by *red shading*; monomethylation of arginine residues is indicated by *green shading*.

with monomethylation on different arginine residues, and Arg-29 and Arg-31 should be the major methylation sites on H2B. Additionally, the fragmentation pattern for the methylated H2B(23–37)R29K peptide is more consistent with the Arg-31 site of methylation (Fig. 10). Combined with the presence of a small amount of dimethylated peptide, these

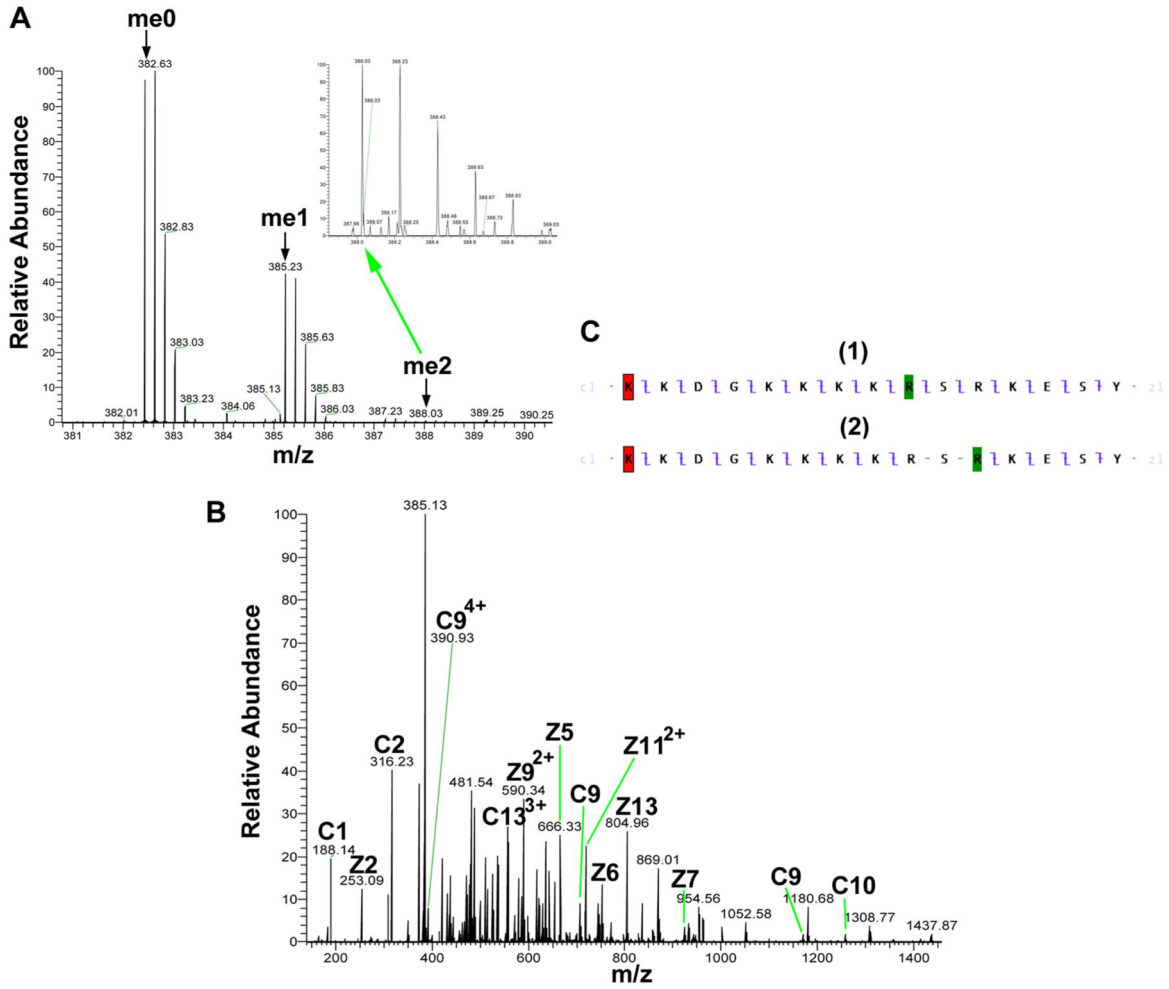

FIGURE 10. **Detection of PRMT7-formed monomethylarginine sites in a peptide corresponding to residues 23–37 of histone H2B with Arg-29 to Lys mutation by mass spectrometry.** 24 μM H2B(23–37)R29K was incubated with 4.8 μg of PRMT7 (1.87 μM) and AdoMet (182 μM) in the reaction buffer in a final volume of 33 μl at room temperature for 24 h. The methylation products were desalted with OMIX C18 ZipTip and directly introduced into an LTQ-Orbitrap mass spectrometer by nano-ESI as described above. *A,* mass spectrum showing the +5 charged state of PRMT7-methylated H2B(23–37)R29K. The species detected included the unmethylated (***me0***; m/z = 382.43, monoisotopic mass = 1907.11 Da; calculated monoisotopic mass = 1907.11 Da), the monomethylated (***me1***; m/z = 385.23, monoisotopic mass = 1921.12 Da; calculated monoisotopic mass = 1921.13 Da), doubly methylated (***me2***; m/z = 388.03, monoisotopic mass = 1935.11 Da; calculated monoisotopic mass = 1935.15 Da). The *inset* shows a magnification of the region for doubly methylated H2B(23–37)R29K. *B,* ETD tandem mass spectrum of the 5-charge precursor of monomethylated H2B(23–37)R29K. The peaks corresponding to ***me1*** in *A* were isolated and fragmented with ETD. The c and z ions were assigned assuming the methyl group is on Arg-31, as in *C-1*. *C,* c and z ion coverage for H2B(23–37)R29K when a methyl group is assigned on Arg-31 (B-1) or Arg-33 (B-2). In *C-1*, the presence of C9 and Z7 ions indicates the monomethylation of Arg-31. *C-2*, the Z5 and Z6 ions supporting monomethylation of R33 were not found, probably because Arg-33 is methylated to a very low extent, as suggested in *A,* ***me2***. Acetylation of the N-terminal lysine residue is indicated by *red shading*; monomethylation of arginine residues is indicated by *green shading*.

results also suggest that Arg-31 is a major site of methylation, and Arg-33 is a minor site.

Confirmation of the RXR Recognition Motif for PRMT7 Using Histone H4 N-terminal Peptides—Although the recombinant histone H4 protein did not appear to be a good substrate for PRMT7 (Fig. 6*D*), the H4(1–21) peptide was well methylated (Fig. 4*G*). To identify the methylation sites on H4 N-terminal tail, short H4 peptides were synthesized covering the 1–8 or 14–22 residues, and the Arg-17/Arg-19 to Lys derivatives were also made for the latter peptide. As shown in Fig. 11, H4(14–22) could still be methylated by PRMT7 ($\sim 4 \times 10^3$ cpm in the MMA peak), but the activity was much weaker compared with H4(1–21) (Fig. 4*G*, $\sim 8 \times 10^4$ cpm in the MMA peak), indicating that distant residues on the H4 N terminus also play a role in substrate recognition. Surprisingly, comparing Fig. 11, *B* and *C,* with *E*, the methyl-accepting activity of H4(14–22)R17K or R19K for PRMT7 was not much greater than PRMT7 automethylation (Fig. 11*E*). These results show again that a single arginine residue, even within a basic residue context, is not a good target for PRMT7. Consistent with this idea, the H4(1–8) peptide, containing a single arginine residue at position 3 that is a substrate for both PRMT1 and PRMT5 (28, 29), was not

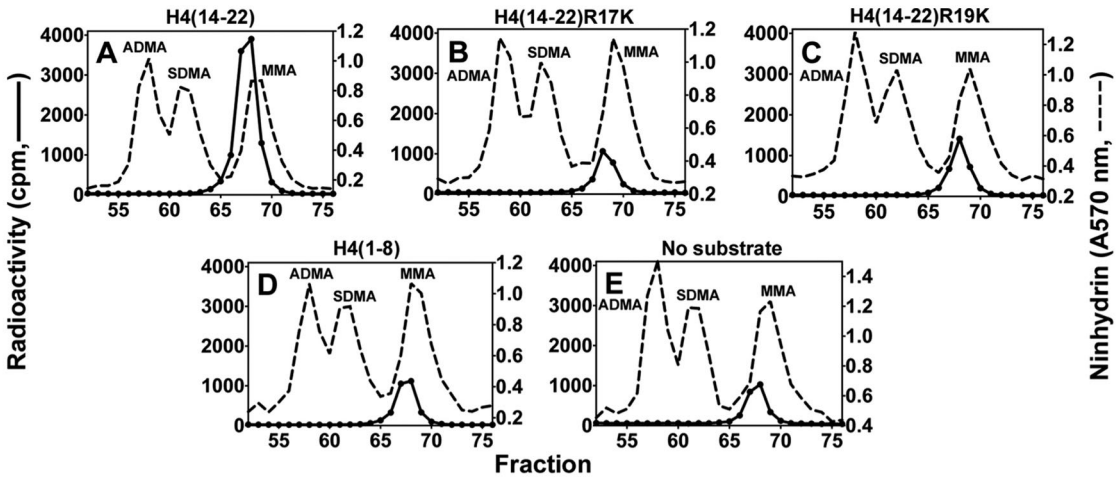

FIGURE 11. **Amino acid analysis of peptides derived from residues 14–22 of histone H4 methylated by PRMT7.** Peptides (12.5 μM; Table 1) were incubated with PRMT7 (0.26 μM) and [^{3}H]AdoMet (0.7 μM) as described under "Experimental Procedures," and the reactions were allowed to proceed at room temperature for 20 h. The reaction mixtures were then acid-hydrolyzed and analyzed for methylated arginine species as described. *A–D* show PRMT7-catalyzed methylation products of H4(14–22), H4(14–22)R17K, H4(14–22)R19K, and H4(1–8), respectively. *E* shows the control of PRMT7 automethylation.

detected as a substrate for PRMT7 (compare Fig. 11, *D* with *E*). Finally, tandem MS analysis of the PRMT7 methylated H4(1–21) peptide also suggested the absence of methylation at Arg-3 and the presence of methylation at Arg-17 and Arg-19 (Fig. 12). The 5-charge state of unmethylated H4(1–21) showed an m/z of 427.46, deconvoluting to a monoisotopic mass of 2132.26 Da. After the PRMT7-catalyzed reaction, the singly methylated peptide (m/z = 430.26, monoisotopic mass = 2146.27 Da) and doubly methylated peptide (m/z = 433.06, monoisotopic mass = 2160.28 Da) were also present, although the level for the latter was very low. ETD fragmentation gave informative c and z ions covering most of H4(1–21) sequence when a methyl group was assigned on Arg-17 (Fig. 12*D*) (2). But C17, C18 and Z3, Z4 ions were missed if a methyl group was assigned on Arg-19 (Fig. 12*D* (3)), indicating it was less strongly methylated. Putting a methyl group on Arg-3 significantly lowered the sequence coverage (Fig. 12*D*) (1), suggesting H4R3 was not likely the methylation site. Together, the MS data gave evidence for methylation of H4R17 and Arg-19 by PRMT7, with a preference for Arg-17.

DISCUSSION

We have shown that an insect cell-expressed mouse PRMT7 has a robust protein arginine methyltransferase activity, but one that is limited to the formation of MMA residues within specific R*X*R motifs. These results support the assignment of a type III activity to this enzyme that was previously observed for a GST-tagged PRMT7 expressed in bacteria (4, 5) and that is consistent with the type III assignment for the worm (17) and trypanosome (18) homologs. It is not clear at this point what contributes to the enhanced activity of the insect cell-expressed enzyme, although it is possible that insect cell post-translational modifications and differences in the N- and C-terminal tags can affect the activity. Initial mass spectrometric analysis of tryptic peptides of PRMT7 suggested possible sites of phosphorylation and methylation, but these results need to be verified. However, this analysis demonstrated no contamination of the insect cell-expressed enzyme with other methyltransferases.

Previous results suggesting that PRMT7 has the ability to form ADMA and/or SDMA (9, 16, 20) may have been compromised by contamination of enzyme preparations with other PRMTs, particularly when FLAG-tagged PRMT7 is purified in a protocol also known to purify nontagged PRMT5 (2, 3, 5, 19). Endogenous PRMT5 in mammalian cells has an affinity for the monoclonal M2 antibody used to purify FLAG-tagged proteins (19). As such, nontagged PRMT5 can be co-purified with FLAG-PRMT7, and the methyltransferase activity detected from such preparations would be from the mixture of both enzymes, leading to misidentification of SDMA generated by PRMT5 as a PRMT7 product. For example, the observation of methylation in peptide sites corresponding to Arg-3 of histone H2A and H4 (9) may be due to PRMT5 rather than PRMT7, especially because these sites are known substrates of PRMT5 (2, 26). Additionally, the reported methylation of Arg-3 on recombinant histone H4 and R2 on histone H3 (20) may also be due to PRMT5 contamination. The distinct preference of PRMT5 for Arg-3 and PRMT7 for Arg-17/Arg-19 in H4(1–21) is clearly shown in Fig. 4. Because the activity of PRMT5 is ~45 times greater than that of PRMT7 (Table 2), a small degree of contamination with PRMT5 can mask the activity of PRMT7. The very high relative activity of PRMT1 (Table 2) may also lead to misleading results if PRMT7 preparations are contaminated with this enzyme. Finally, we note that the H4(1–21) and H4(1–21)R3K peptides can be effectively used to distinguish PRMT7 activity from that of PRMT5 and PRMT1 as demonstrated in Fig. 4.

We have shown that PRMT7 automethylation occurs in the insect cell-expressed enzyme; such an automethylation activity can complicate substrate identification and necessitates enzyme-only controls. Automethylation has been previously observed in several other methyltransferases (37) and has

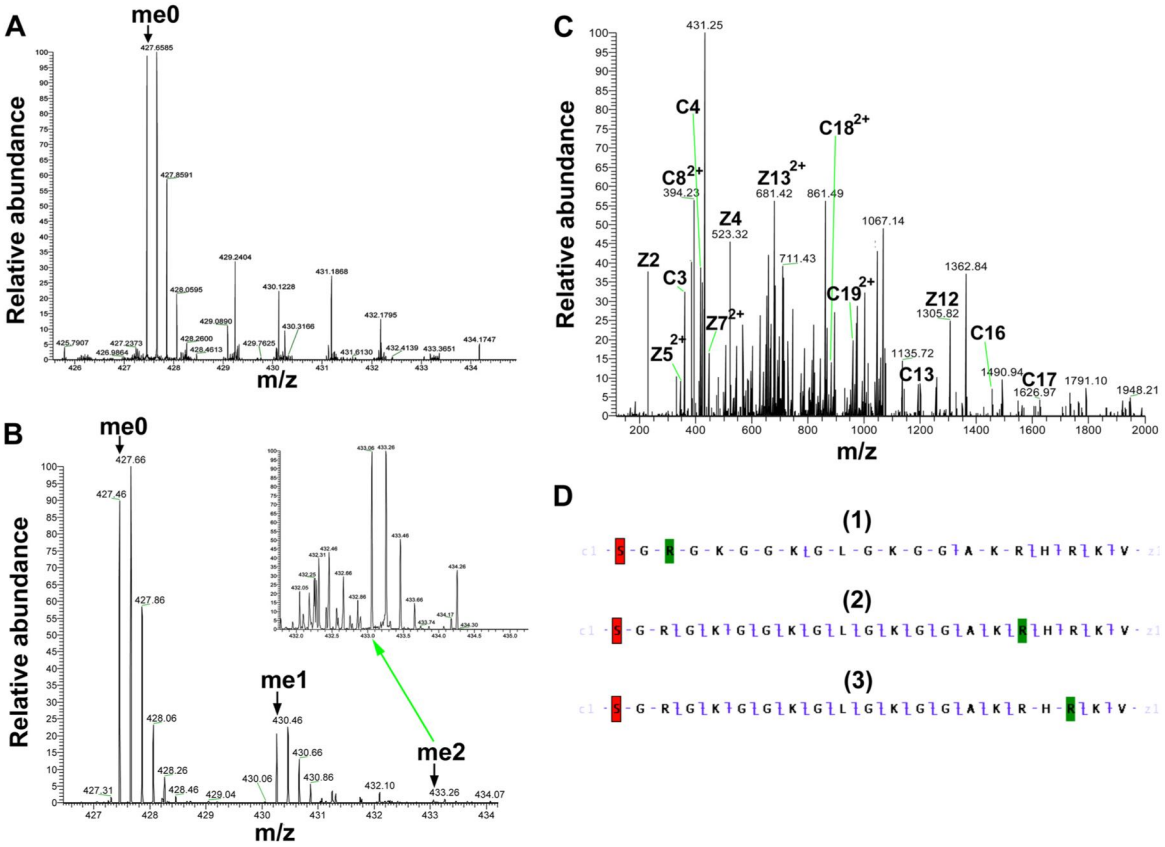

FIGURE 12. **Detection of PRMT7-formed monomethylarginine sites in a peptide corresponding to residues 1–21 of histone H4 by mass spectrometry.** 24 μM H4(1–21) was incubated with 4.8 μg of PRMT7 (1.87 μM) and AdoMet (182 μM) in the reaction buffer in a final volume of 33 μl at room temperature for 24 h. The methylation products were desalted with OMIX C18 ZipTip and directly introduced into an LTQ-Orbitrap mass spectrometer by nano-ESI as described above. *A*, control mass spectrum showing the +5 charged state of unmethylated H4(1–21) (***me0***; m/z = 427.46, monoisotopic mass = 2132.25 Da; calculated monoisotopic mass = 2132.26 Da). *B*, mass spectrum showing the +5 charged state of PRMT7-methylated H4(1–21). The species detected included the unmethylated (***me0***), the monomethylated (***me1***; m/z = 430.26, monoisotopic mass = 2146.27 Da; calculated monoisotopic mass = 2146.27 Da), the doubly methylated (***me2***; m/z = 433.06, monoisotopic mass = 2160.26 Da; calculated monoisotopic mass = 2160.29 Da). The *inset* shows a magnification of the region for doubly methylated H4(1–21). *C*, ETD tandem mass spectrum of the 5-charge precursor of monomethylated H4(1–21). The peaks corresponding to ***me1*** in *B* were isolated and fragmented with ETD. The c and z ions were assigned assuming the methyl group is on Arg-17, as in D-2. *D*, c and z ion coverage for H4(1–21) when a methyl group is assigned on Arg-3 (*D-1*), Arg-17 (*D-2*), or Arg-19 (*D-3*). D-1, the absence of majority of ions indicates that H4R3 is not a good methylation site for PRMT7. D-2, the presence of C17 and Z5 ions indicates monomethylation of Arg-17. D-3, the presence of C19 and Z5 ions indicates monomethylation of Arg-17 or Arg-19. Acetylation of the N-terminal lysine residue is indicated by *red shading*; monomethylation of arginine residues is indicated by *green shading*.

been associated with the regulation of activity in CARM1/PRMT4 (38).

The substrate specificity of PRMTs has been reviewed by Yang and Bedford (3). Most PRMTs, including PRMT1, -3, -6, and -8, target glycine- and arginine-rich motifs, which are involved in mediating nucleic acid and protein interactions (39, 40); CARM1/PRMT4 specifically methylates proline-, glycine-, and methionine-rich motifs (41), although PRMT5 works on both (41, 42). Adding to this substrate profile, we now demonstrate that PRMT7 shows a unique substrate specificity that is distinct from other known PRMT members. PRMT7 methylates two very basic regions on the H2B protein and peptides and H4 peptides where two or more closely positioned arginine residues are present in sequences rich in lysine residues. The mutation analyses on peptides H2B(23–37) and H4(14–22) also suggest that PRMT7 strongly prefers two arginines with one residue apart to a single arginine or two arginines with three residues apart, even if they are located in the same basic region. These results lead us to propose that PRMT7 specifically recognizes lysine- and arginine-rich (KAR) regions with an R*X*R motif. The binding selectivity for arginine over lysine is significant despite their similar chemical nature, as replacing one of the arginines with lysine decreases the methylation efficiency.

PRMT7 methylates the four core histones to different extents with a clear preference for the N-terminal basic motif of H2B. The very high methyl-accepting activity of H2B *in vitro* suggests that it might be a physiological substrate for PRMT7. Previous studies identified multiple post-translational modifications on human H2B, including acetylation on Lys-5, Lys-15,

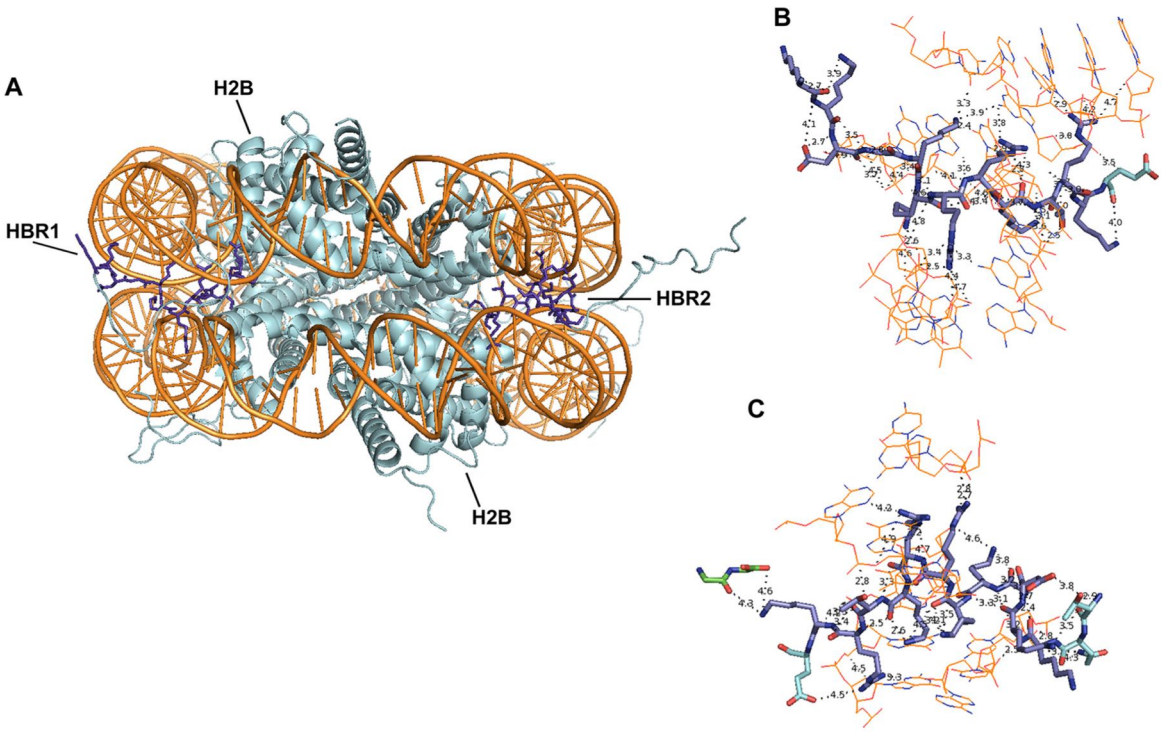

FIGURE 13. **Crystal structure of H2B N-terminal basic regions in a nucleosome core particle (Protein Data Bank code 1KX5, 1.9-Å resolution).** *A,* two molecules of histone H2B.2 (*Xenopus laevis*; *cyan*) from a histone octamer wrapped by two strands of nucleosomal DNA (*Homo sapiens*; *orange*). The H2B repression region (*HBR*; sequence, KKDGKKRRKTRK; residues highlighted as *blue sticks*) is at the root of the flexible N-terminal tail and exits the nucleosome through a minor groove channel formed by two DNA strands (1). *B* and *C* exhibit magnifications of HBR1 and HBR2 areas from *A*. They are both tightly associated with surrounding DNA. Noncovalent bonds with distance <5 Å are shown. *Green,* Gly-101 and Gly-102 are from histone H4.

Lys-16, and Lys-20 (43, 44), phosphorylation on Ser-14 (45), and methylation on Lys-46, Lys-57, and Lys-108 (43). However, arginine methylation on HBR has not been reported to our knowledge. These MMA modifications may have been missed because traditional tryptic digestion in bottom-up mass spectrometric analysis may cleave KAR regions like the methylated sequence -KKRKRSRK- in histone H2B into small fragments that are undetectable for LC-MS/MS analysis. A similar situation may occur with the -KRHRK- sequence in histone H4. It is also possible that the stoichiometry of methylation of these R*X*R sites in histones H2B and H4 is very low. We have shown that the histone-histone and histone-DNA interactions both inhibit H2B methylation *in vitro*. In the nucleosome structure, the target arginine residues of histones H2B and H4 are generally bound to DNA and may be largely inaccessible to PRMT7 until a conformational change occurs. Additional studies will be required to identify these potential new methylation sites *in vivo*, as well as sites on non-histone proteins.

With the revelation of its catalytic pattern and substrate specificity, it is intriguing to speculate on the biological consequences of potential PRMT7-mediated histone methylation. For histone H4, the KRHRK region has been shown to interact with the acidic islet of the H2A globular domain and possibly Arg-96 to Leu-99 of H2B from the neighboring nucleosome and to facilitate nucleosome array compaction (46–50). The same RHR region (residues 17–19) has also been demonstrated to interact with a C-terminal acidic patch of Dot1 methyltransferase, facilitating Dot1-mediated histone H3K79 methylation and telomeric silencing (51). For histone H2B, the N-terminal HBR region KKDGKKRKRSRK associates with DNA, stabilizes nucleosome structure, and silences gene expression (52, 53). Methylation of these basic regions may compromise their interaction with protein or DNA binding partners, affecting downstream processes, including transcription (54). It is thus possible that PRMT7 modulates chromatin stability and transcription initiation. Because the PRMT7-targeting basic region is located at the end of the flexible N-terminal tail of H2B and is in close contact with negatively charged DNA chains (Fig. 13), its modification by PRMT7 may not occur, although this region is tightly bound to surrounding DNA. It is also possible that H2B is methylated before it is incorporated into the nucleosome, perhaps as a marker for histone assembly as in the case of H3K56 acetylation during replication (55). A final possibility is that once H2B dissociates out of the nucleosome, PRMT7-mediated methylation targets it for ubiquitination and then degradation, as in the case for PRMT5-catalyzed methylation on Arg-111 and Arg-113 of E2F-1 (56).

In summary, our discovery of the sequence motif for PRMT7 recognition will facilitate the identification of physiological

substrates and the effects of protein arginine methylation on their functions in health and disease.

Acknowledgments—We thank Stéphane Richard (McGill University) for valuable suggestions in initiating the project. We thank Paul Thompson and Heather Rust (Scripps Research Institute) for the gifts of His-PRMT1 and the H4(1–21), H4(1–21)R3K, and H4(1–21)R3MMA peptides. We thank Jill Butler and Sharon Dent (MD Anderson Cancer Center) for the gift of Myc-PRMT5. We thank Yan Coulombe for assistance with protein purification. LC-MS/MS analyses of tryptic peptides of PRMT7 were performed at the University of Alabama at Birmingham CCC Proteomics Core. We also thank the previous and current members of the Clarke laboratory, in particular Alexander Patananan and Jonathan Lowenson for their help.

REFERENCES

1. Walsh, C. T. (2006) *Post-translational Modification of Proteins: Expanding Nature's Inventory,* pp. 1–490, Roberts and Co. Publishers, Englewood, CO
2. Bedford, M. T., and Clarke, S. G. (2009) Protein arginine methylation in mammals: who, what, and why. *Mol. Cell* **33,** 1–13
3. Yang, Y., and Bedford, M. T. (2013) Protein-arginine methyltransferases and cancer. *Nat. Rev. Cancer* **13,** 37–50
4. Miranda, T. B., Miranda, M., Frankel, A., and Clarke, S. (2004) PRMT7 is a member of the protein arginine methyltransferase family with a distinct substrate specificity. *J. Biol. Chem.* **279,** 22902–22907
5. Zurita-Lopez, C. I., Sandberg, T., Kelly, R., and Clarke, S. G. (2012) Human protein arginine methyltransferase 7 (PRMT7) is a type III enzyme forming ω-NG-monomethylated arginine residues. *J. Biol. Chem.* **287,** 7859–7870
6. Herrmann, F., Pably, P., Eckerich, C., Bedford, M. T., and Fackelmayer, F. O. (2009) Human protein-arginine methyltransferases *in vivo*–distinct properties of eight canonical members of the PRMT family. *J. Cell Sci.* **122,** 667–677
7. Auclair, Y., and Richard, S. (2013) The role of arginine methylation in the DNA damage response. *DNA Repair* **12,** 459–465
8. Gonsalvez, G. B., Tian, L., Ospina, J. K., Boisvert, F. M., Lamond, A. I., and Matera, A. G. (2007) Two distinct arginine methyltransferases are required for biogenesis of Sm-class ribonucleoproteins. *J. Cell Biol.* **178,** 733–740
9. Karkhanis, V., Wang, L., Tae, S., Hu, Y. J., Imbalzano, A. N., and Sif, S. (2012) Protein arginine methyltransferase 7 regulates cellular response to DNA damage by methylating promoter histones H2A and H4 of the polymerase δ catalytic subunit gene, POLD1. *J. Biol. Chem.* **287,** 29801–29814
10. Buhr, N., Carapito, C., Schaeffer, C., Kieffer, E., Van Dorsselaer, A., and Viville, S. (2008) Nuclear proteome analysis of undifferentiated mouse embryonic stem and germ cells. *Electrophoresis* **29,** 2381–2390
11. Dhar, S. S., Lee, S. H., Kan, P. Y., Voigt, P., Ma, L., Shi, X., Reinberg, D., and Lee, M. G. (2012) Trans-tail regulation of MLL4-catalyzed H3K4 methylation by H4R3 symmetric dimethylation is mediated by a tandem PHD of MLL4. *Genes Dev.* **26,** 2749–2762
12. Gros, L., Renodon-Cornière, A., de Saint Vincent, B. R., Feder, M., Bujnicki, J. M., and Jacquemin-Sablon, A. (2006) Characterization of prmt7α and -β isozymes from Chinese hamster cells sensitive and resistant to topoisomerase II inhibitors. *Biochim. Biophys. Acta* **1760,** 1646–1656
13. Verbiest, V., Montaudon, D., Tautu, M. T., Moukarzel, J., Portail, J. P., Markovits, J., Robert, J., Ichas, F., and Pourquier, P. (2008) Protein arginine *N*-methyl transferase 7 (PRMT7) as a potential target for the sensitization of tumor cells to camptothecins. *FEBS Lett.* **582,** 1483–1489
14. Bleibel, W. K., Duan, S., Huang, R. S., Kistner, E. O., Shukla, S. J., Wu, X., Badner, J. A., and Dolan, M. E. (2009) Identification of genomic regions contributing to etoposide-induced cytotoxicity. *Hum. Genet.* **125,** 173–180
15. Thomassen, M., Tan, Q., and Kruse, T. A. (2009) Gene expression meta-analysis identifies chromosomal regions and candidate genes involved in breast cancer metastasis. *Breast Cancer Res. Treat.* **113,** 239–249
16. Lee, J. H., Cook, J. R., Yang, Z. H., Mirochnitchenko, O., Gunderson, S. I., Felix, A. M., Herth, N., Hoffmann, R., and Pestka, S. (2005) PRMT7, a new protein arginine methyltransferase that synthesizes symmetric dimethylarginine. *J. Biol. Chem.* **280,** 3656–3664
17. Takahashi, Y., Daitoku, H., Yokoyama, A., Nakayama, K., Kim, J. D., and Fukamizu, A. (2011) The *C. elegans* PRMT-3 possesses a type III protein arginine methyltransferase activity. *J. Recept. Signal Transduct. Res.* **31,** 168–172
18. Fisk, J. C., Sayegh, J., Zurita-Lopez, C., Menon, S., Presnyak, V., Clarke, S. G., and Read, L. K. (2009) A type III protein arginine methyltransferase from the protozoan parasite *Trypanosoma brucei*. *J. Biol. Chem.* **284,** 11590–11600
19. Nishioka, K., and Reinberg, D. (2003) Methods and tips for the purification of human histone methyltransferases. *Methods* **31,** 49–58
20. Migliori, V., Müller, J., Phalke, S., Low, D., Bezzi, M., Mok, W. C., Sahu, S. K., Gunaratne, J., Capasso, P., Bassi, C., Cecatiello, V., De Marco, A., Blackstock, W., Kuznetsov, V., Amati, B., Mapelli, M., and Guccione, E. (2012) Symmetric dimethylation of H3R2 is a newly identified histone mark that supports euchromatin maintenance. *Nat. Struct. Mol. Biol.* **19,** 136–144
21. Buisson, R., Dion-Côté, A. M., Coulombe, Y., Launay, H., Cai, H., Stasiak, A. Z., Stasiak, A., Xia, B., and Masson, J. Y. (2010) Cooperation of breast cancer proteins PALB2 and piccolo BRCA2 in stimulating homologous recombination. *Nat. Struct. Mol. Biol.* **17,** 1247–1254
22. Osborne, T. C., Obianyo, O., Zhang, X., Cheng, X., and Thompson, P. R. (2007) Protein arginine methyltransferase 1: positively charged residues in substrate peptides distal to the site of methylation are important for substrate binding and catalysis. *Biochemistry* **46,** 13370–13381
23. Obianyo, O., Osborne, T. C., and Thompson, P. R. (2008) Kinetic mechanism of protein arginine methyltransferase 1. *Biochemistry* **47,** 10420–10427
24. Butler, J. S., Zurita-Lopez, C. I., Clarke, S. G., Bedford, M. T., and Dent, S. Y. (2011) Protein-arginine methyltransferase 1 (PRMT1) methylates Ash2L, a shared component of mammalian histone H3K4 methyltransferase complexes. *J. Biol. Chem.* **286,** 12234–12244
25. Feng, Y., Xie, N., Jin, M., Stahley, M. R., Stivers, J. T., and Zheng, Y. G. (2011) A transient kinetic analysis of PRMT1 catalysis. *Biochemistry* **50,** 7033–7044
26. Feng, Y., Wang, J., Asher, S., Hoang, L., Guardiani, C., Ivanov, I., and Zheng, Y. G. (2011) Histone H4 acetylation differentially modulates arginine methylation by an in *cis* mechanism. *J. Biol. Chem.* **286,** 20323–20334
27. Antonysamy, S., Bonday, Z., Campbell, R. M., Doyle, B., Druzina, Z., Gheyi, T., Han, B., Jungheim, L. N., Qian, Y., Rauch, C., Russell, M., Sauder, J. M., Wasserman, S. R., Weichert, K., Willard, F. S., Zhang, A., and Emtage, S. (2012) Crystal structure of the human PRMT5:MEP50 complex. *Proc. Natl. Acad. Sci. U.S.A.* **109,** 17960–17965
28. Strahl, B. D., Briggs, S. D., Brame, C. J., Caldwell, J. A., Koh, S. S., Ma, H., Cook, R. G., Shabanowitz, J., Hunt, D. F., Stallcup, M. R., and Allis, C. D. (2001) Methylation of histone H4 at arginine 3 occurs *in vivo* and is mediated by the nuclear receptor coactivator PRMT1. *Curr. Biol.* **11,** 996–1000
29. Pal, S., Baiocchi, R. A., Byrd, J. C., Grever, M. R., Jacob, S. T., and Sif, S. (2007) Low levels of miR-92b/96 induce PRMT5 translation and H3R8/H4R3 methylation in mantle cell lymphoma. *EMBO J.* **26,** 3558–3569
30. Thangaraj, B., Ryan, C. M., Souda, P., Krause, K., Faull, K. F., Weber, A. P., Fromme, P., and Whitelegge, J. P. (2010) Data-directed top-down Fourier-transform mass spectrometry of a large integral membrane protein complex: photosystem II from *Galdieria sulphuraria*. *Proteomics* **10,** 3644–3656
31. Rust, H. L., Zurita-Lopez, C. I., Clarke, S., and Thompson, P. R. (2011) Mechanistic studies on transcriptional coactivator protein arginine methyltransferase 1. *Biochemistry* **50,** 3332–3345
32. Lakowski, T. M., and Frankel, A. (2009) Kinetic analysis of human protein arginine *N*-methyltransferase 2: formation of monomethyl- and asymmetric dimethyl-arginine residues on histone H4. *Biochem. J.* **421,** 253–261

33. Siarheyeva, A., Senisterra, G., Allali-Hassani, A., Dong, A., Dobrovetsky, E., Wasney, G. A., Chau, I., Marcellus, R., Hajian, T., Liu, F., Korboukh, I., Smil, D., Bolshan, Y., Min, J., Wu, H., Zeng, H., Loppnau, P., Poda, G., Griffin, C., Aman, A., Brown, P. J., Jin, J., Al-Awar, R., Arrowsmith, C. H., Schapira, M., and Vedadi, M. (2012) An allosteric inhibitor of protein arginine methyltransferase 3. *Structure* **20,** 1425–1435
34. Schurter, B. T., Koh, S. S., Chen, D., Bunick, G. J., Harp, J. M., Hanson, B. L., Henschen-Edman, A., Mackay, D. R., Stallcup, M. R., and Aswad, D. W. (2001) Methylation of histone H3 by coactivator-associated arginine methyltransferase 1. *Biochemistry* **40,** 5747–5756
35. Obianyo, O., and Thompson, P. R. (2012) Kinetic mechanism of protein arginine methyltransferase 6 (PRMT6). *J. Biol. Chem.* **287,** 6062–6071
36. Dillon, M. B., Rust, H. L., Thompson, P. R., and Mowen, K. A. (2013) Automethylation of protein arginine methyltransferase 8 (PRMT8) regulates activity by impeding *S*-adenosylmethionine sensitivity. *J. Biol. Chem.* **288,** 27872–27880
37. Sayegh, J., Webb, K., Cheng, D., Bedford, M. T., and Clarke, S. G. (2007) Regulation of protein arginine methyltransferase 8 (PRMT8) activity by its N-terminal domain. *J. Biol. Chem.* **282,** 36444–36453
38. Wang, L., Charoensuksai, P., Watson, N. J., Wang, X., Zhao, Z., Coriano, C. G., Kerr, L. R., and Xu, W. (2013) CARM1 automethylation is controlled at the level of alternative splicing. *Nucleic Acids Res.* **41,** 6870–6880
39. Boffa, L. C., Karn, J., Vidali, G., and Allfrey, V. G. (1977) Distribution of N^G, N^G,N^G-dimethylarginine in nuclear protein fractions. *Biochem. Biophys. Res. Commun.* **74,** 969–976
40. Thandapani, P., O'Connor, T. R., Bailey, T. L., and Richard, S. (2013) Defining the RGG/RG motif. *Mol. Cell* **50,** 613–623
41. Cheng, D., Côté, J., Shaaban, S., and Bedford, M. T. (2007) The arginine methyltransferase CARM1 regulates the coupling of transcription and mRNA processing. *Mol. Cell* **25,** 71–83
42. Branscombe, T. L., Frankel, A., Lee, J. H., Cook, J. R., Yang, Z., Pestka, S., and Clarke, S. (2001) PRMT5 (Janus kinase-binding protein 1) catalyzes the formation of symmetric dimethylarginine residues in proteins. *J. Biol. Chem.* **276,** 32971–32976
43. Beck, H. C., Nielsen, E. C., Matthiesen, R., Jensen, L. H., Sehested, M., Finn, P., Grauslund, M., Hansen, A. M., and Jensen, O. N. (2006) Quantitative proteomic analysis of post-translational modifications of human histones. *Mol. Cell. Proteomics* **5,** 1314–1325
44. Golebiowski, F., and Kasprzak, K. S. (2005) Inhibition of core histones acetylation by carcinogenic nickel(II). *Mol. Cell. Biochem.* **279,** 133–139
45. Cheung, W. L., Ajiro, K., Samejima, K., Kloc, M., Cheung, P., Mizzen, C. A., Beeser, A., Etkin, L. D., Chernoff, J., Earnshaw, W. C., and Allis, C. D. (2003) Apoptotic phosphorylation of histone H2B is mediated by mammalian sterile twenty kinase. *Cell* **113,** 507–517
46. Zoroddu, M. A., Kowalik-Jankowska, T., Kozlowski, H., Molinari, H., Salnikow, K., Broday, L., and Costa, M. (2000) Interaction of Ni(II) and Cu(II) with a metal binding sequence of histone H4: AKRHRK, a model of the H4 tail. *Biochim. Biophys. Acta* **1475,** 163–168
47. Allahverdi, A., Yang, R., Korolev, N., Fan, Y., Davey, C. A., Liu, C. F., and Nordenskiöld, L. (2011) The effects of histone H4 tail acetylations on cation-induced chromatin folding and self-association. *Nucleic Acids Res.* **39,** 1680–1691
48. Luger, K., Mäder, A. W., Richmond, R. K., Sargent, D. F., and Richmond, T. J. (1997) Crystal structure of the nucleosome core particle at 2.8 Å resolution. *Nature* **389,** 251–260
49. Chodaparambil, J. V., Barbera, A. J., Lu, X., Kaye, K. M., Hansen, J. C., and Luger, K. (2007) A charged and contoured surface on the nucleosome regulates chromatin compaction. *Nat. Struct. Mol. Biol.* **14,** 1105–1107
50. Zhou, J., Fan, J. Y., Rangasamy, D., and Tremethick, D. J. (2007) The nucleosome surface regulates chromatin compaction and couples it with transcriptional repression. *Nat. Struct. Mol. Biol.* **14,** 1070–1076
51. Fingerman, I. M., Li, H. C., and Briggs, S. D. (2007) A charge-based interaction between histone H4 and Dot1 is required for H3K79 methylation and telomere silencing: identification of a new trans-histone pathway. *Genes Dev.* **21,** 2018–2029
52. Parra, M. A., Kerr, D., Fahy, D., Pouchnik, D. J., and Wyrick, J. J. (2006) Deciphering the roles of the histone H2B N-terminal domain in genome-wide transcription. *Mol. Cell. Biol.* **26,** 3842–3852
53. Wyrick, J. J., and Parra, M. A. (2009) The role of histone H2A and H2B post-translational modifications in transcription: a genomic perspective. *Biochim. Biophys. Acta* **1789,** 37–44
54. Casadio, F., Lu, X., Pollock, S. B., LeRoy, G., Garcia, B. A., Muir, T. W., Roeder, R. G., and Allis, C. D. (2013) H3R42me2a is a histone modification with positive transcriptional effects. *Proc. Natl. Acad. Sci. U.S.A.* **110,** 14894–14899
55. Li, Q., Zhou, H., Wurtele, H., Davies, B., Horazdovsky, B., Verreault, A., and Zhang, Z. (2008) Acetylation of histone H3 lysine 56 regulates replication-coupled nucleosome assembly. *Cell* **134,** 244–255
56. Cho, E. C., Zheng, S., Munro, S., Liu, G., Carr, S. M., Moehlenbrink, J., Lu, Y. C., Stimson, L., Khan, O., Konietzny, R., McGouran, J., Coutts, A. S., Kessler, B., Kerr, D. J., and Thangue, N. B. (2012) Arginine methylation controls growth regulation by E2F-1. *EMBO J.* **31,** 1785–1797

CHAPTER 4

Substrate Specificity of Human Protein Arginine Methyltransferase 7 (PRMT7):

The Importance of Acidic Residues in the Double E loop

Substrate Specificity of Human Protein Arginine Methyltransferase 7 (PRMT7)

*THE IMPORTANCE OF ACIDIC RESIDUES IN THE DOUBLE E LOOP**

Received for publication, September 6, 2014, and in revised form, October 6, 2014 Published, JBC Papers in Press, October 7, 2014, DOI 10.1074/jbc.M114.609271

You Feng, Andrea Hadjikyriacou, and Steven G. Clarke[1]

From the Department of Chemistry and Biochemistry and the Molecular Biology Institute, UCLA, Los Angeles, California 90095-1569

Background: Mammalian PRMT7 has been implicated in multiple biological processes, but its *in vivo* substrates have not been identified.
Results: Mutagenesis studies indicate key residues that affect the unique substrate preference of PRMT7.
Conclusion: Acidic residues within the double E loop confer specificity to PRMT7.
Significance: Understanding how PRMT7 recognizes its substrates will enhance our knowledge of its physiological role.

Protein arginine methyltransferase 7 (PRMT7) methylates arginine residues on various protein substrates and is involved in DNA transcription, RNA splicing, DNA repair, cell differentiation, and metastasis. The substrate sequences it recognizes *in vivo* and the enzymatic mechanism behind it, however, remain to be explored. Here we characterize methylation catalyzed by a bacterially expressed GST-tagged human PRMT7 fusion protein with a broad range of peptide and protein substrates. After confirming its type III activity generating only ω-N^G-monomethylarginine and its distinct substrate specificity for R*X*R motifs surrounded by basic residues, we performed site-directed mutagenesis studies on this enzyme, revealing that two acidic residues within the double E loop, Asp-147 and Glu-149, modulate the substrate preference. Furthermore, altering a single acidic residue, Glu-478, on the C-terminal domain to glutamine nearly abolished the activity of the enzyme. Additionally, we demonstrate that PRMT7 has unusual temperature dependence and salt tolerance. These results provide a biochemical foundation to understanding the broad biological functions of PRMT7 in health and disease.

Protein arginine methyltransferases (PRMTs)[2] are a family of enzymes that direct posttranslational methylation on targeted arginine residues in eukaryotes (1–4). Most mammalian PRMTs have been characterized as either type I enzymes that transfer up to two methyl groups from *S*-adenosyl-L-methionine (AdoMet) to the same terminal nitrogen atom forming ω-N^G-monomethylarginine (MMA) and ω-N^G,N^G-asymmetric dimethylarginine (ADMA) (PRMT1, -2, -3, -4, -6, and -8) or type II enzymes that transfer up to two methyl groups to different terminal nitrogen atoms, forming MMA and ω-N^G,N'^G-symmetric dimethylarginine (SDMA) (PRMT5) (1–4). However, PRMT7 has been found to produce MMA residues only, which defines it as the first type III PRMT (5–9). Recent work utilizing an insect cell-expressed mouse PRMT7 demonstrated a unique substrate specificity for R*X*R motifs among multiple basic residues (8). No other PRMT has been shown to have such narrow sequence specificity. These results led to the question of how the substrate selectivity of PRMT7 is restricted.

The human *PRMT7* gene encodes a protein containing ancestrally duplicated methyltransferase domains (1, 5). Although the advantage of duplicating the catalytic domain is unknown, it has been shown that deletion of either domain abolishes its activity (5). A number of studies have indicated that *PRMT7* expression in mammalian cells is regulated and can affect many biological processes, including pluripotency (10–12). Consistent with this role, *PRMT7* knockdown stimulates neuronal differentiation (13). Genetic variation of *PRMT7* may lead to increased sensitivity of cell lines to etoposide, a chemotherapeutic agent that targets topoisomerase II (14, 15). In addition, down-regulation of *PRMT7* sensitizes tumor cells to the topoisomerase I inhibitor camptothecin (16) and modulates cell response to DNA-damaging agents (17, 18). The role of PRMT7 has also been implicated in male germ line imprinting (19), Sm ribonucleoprotein methylation, and small nuclear ribonucleoprotein biogenesis (20) as well as breast cancer metastasis (21, 22). Thus, PRMT7 appears to participate in broad cellular processes under normal and disease conditions and is of therapeutic interest.

Given the extensive biological involvement of PRMT7, it is particularly important to get a clear understanding of its fundamental catalytic mechanism and cellular substrate specificity. Although the insect cell-expressed mouse PRMT7 showed higher catalytic activity than the bacterially expressed GST-

* This work was supported, in whole or in part, by National Institutes of Health Grant GM026020 (to S. G. C.) and GM007185, a Ruth L. Kirschstein National Research Service Award (to A. H.).

[1] To whom correspondence should be addressed: Dept. of Chemistry and Biochemistry and the Molecular Biology Institute, University of California, Los Angeles, 607 Charles E. Young Dr. E., Los Angeles, CA 90095-1569. Tel.: 310-825-8754; Fax: 310-825-1968; E-mail: clarke@mbi.ucla.edu.

[2] The abbreviations used are: PRMT, protein arginine methyltransferase; MMA, ω-N^G-monomethylarginine; [^{3}H]MMA, [*methyl*-^{3}H]ω-N^G-monomethylarginine; ADMA, ω-N^G,N^G-asymmetric dimethylarginine; SDMA, ω-N^G,N'^G-symmetric dimethylarginine; AdoMet, *S*-adenosyl-L-methionine; [^{3}H]AdoMet, *S*-adenosyl-[*methyl*-^{3}H]-L-methionine; [^{14}C]AdoMet, *S*-adenosyl-L-[*methyl*-^{14}C]methionine; GAR, glycine- and arginine-rich domain of human fibrillarin; TAT, trans-activator of transcription protein; RPL3, ribosomal protein L3; SmD3, small nuclear ribonucleoprotein D3; HBR, H2B repression domain; LDIG(69–72)AAAA, L69A/D70A/I71A/G72A mutant; LFD(145–147)WMG, L145W/F146M/D147G mutant; FD(146–147)LG, F146L/D147G mutant.

tagged human PRMT7 (7, 8), site-directed mutagenesis and protein expression and purification are facilitated in the bacterial system. In this work, we used the bacterial system to determine which residues of human PRMT7 are important for substrate recognition. We determined the substrate specificity with multiple peptide and protein substrates and then performed mutagenesis and kinetic analysis to probe the roles of specific residues of PRMT7 in the methylation reaction. We were able to demonstrate that two acidic residues within the catalytic double E loop are essential for its substrate specificity. Additionally, we revealed that mammalian PRMT7 is relatively tolerant to low temperature but is very sensitive to high temperature and salt. These findings will broaden our understanding of the reaction catalyzed by PRMT7 and set directions for future studies of its cellular functions.

EXPERIMENTAL PROCEDURES

Protein Expression and Purification—Human PRMT7 was subcloned into a pGEX-2T vector and expressed in *Escherichia coli* BL21 Star (DE3) cells (Invitrogen, C601003) as a GST fusion protein (7). The enzyme was purified using a glutathione-Sepharose affinity chromatography method modified from that described previously (7). Cells containing GST-PRMT7 plasmid were grown to an optical density at 600 nm of 0.6–0.8, and protein expression was induced with 0.4 mM isopropyl-D-thiogalactopyranoside at 16 °C overnight. The cells were lysed with sonication in a phosphate-buffered saline solution (137 mM NaCl, 2.7 mM KCl, 10 mM Na_2HPO_4, 2 mM KH_2PO_4, pH 7.4) containing 1 mM phenylmethylsulfonyl fluoride. The cell lysate was centrifuged for 50 min at 23,000 × *g* at 4 °C, and the supernatant containing GST-PRMT7 was loaded to glutathione-Sepharose 4B beads (Amersham Biosciences) according to the manufacturer's instructions. After washing with the phosphate-buffered saline solution, the bound protein was eluted with an elution buffer containing 30 mM glutathione, 50 mM HEPES, 120 mM NaCl, and 5% glycerol (pH 8.0). Glutathione in the eluted protein solution was reduced by 10–30-fold by adding fresh elution buffer without glutathione and reconcentrating using an Amicon centrifugation filter. Protein was quantified by a Lowry assay after trichloroacetic acid precipitation and stored at −80 °C as 50-μl aliquots. GST-GAR was expressed in *E. coli* BL21 Star (DE3) cells and purified with glutathione-Sepharose 4B affinity chromatography as described previously (7).

Mutagenesis—Primers for site-directed mutagenesis of GST-PRMT7 were synthesized by Integrated DNA Technologies (San Diego, CA). To create a catalytically inactive enzyme that cannot bind *S*-adenosylmethionine, quadruple mutations (L69A/D70A/I71A/G72A) were made using the forward primer 5′-GGACAGAAGGCCTTGGTTGCGGCCGCTGCGACTGGCACGGGACTC-3′ and the reverse primer 5′-GAGTCCCGTGCCAGTCGCAGCGGCCGCAACCAAGGCCTTCTGTCC-3′ (T_m = 89 °C). Other forward and reverse primers included 5′-GGTCACAGAGTTGTTTGGCACAGAGCTGATCGG-3′ and 5′-CCGATCAGCTCTGTGCCAAACAACTCTGTGACC-3′ (T_m = 80 °C) for D147G, 5′-CAGAGTTGTTTGACACAATGCTGATCGGGGAGGGGGC-3′ and 5′-GCCCCCTCCCCGATCAGCATTGTGTCAAACAACTCTG-3′ (T_m = 81 °C) for E149M, 5′-CCATCCACGTGCAGGAGAGCCTCGGAGAGCAGG-3′ and 5′-CCTGCTCTCCGAGGCTCTCCTGCACGTGGATGG-3′ (T_m = 79 °C) for T203E, 5′-CCACGTGCAGACCGAGCTCGGAGAGCAGGTCATCG-3′ and 5′-CGATGACCTGCTCTCCGAGCTCGGTCTGCACGTGG-3′ (T_m = 81 °C) for S204E, 5′-CTCTCCTCCTGGGCCAGCCGTTCTTCAC-3′ and 5′-GTGAAGAACGGCTGGCCCAGGAGGAGAG-3′ (T_m = 80 °C) for E478Q, 5′-AACATCCTGGTCACAGAGTGGATGGGCACAGAGCTGATCGGGGAG-3′ and 5′-CTCCCCGATCAGCTCTGTGCCCATCCACTCTGTGACCAGGATGTT-3′ (T_m = 78 °C) for triple mutation LFD(145–147)WMG, and 5′-CCTGGTCACAGAGTTGTTAGGCACAGAGCTGATCGG-3′ and 5′-CCGATCAGCTCTGTGCCTAACAACTCTGTGACCAGG-3′ (T_m = 89 °C) for the double mutation F146L/D147G. PCRs were set up according to the QuikChange Lightning site-directed mutagenesis kit (Agilent Technologies, Inc.), using 50 ng of the human PRMT7 pGEX-2T plasmid template, a 0.2 μM concentration of both primers, and 1 μl of QuikChange Lightning enzyme. The PCR was run at 95 °C for 2 min, followed by 18 cycles of reactions at 95 °C for 20 s, 60 °C for 10 s, and 68 °C for 4 min. There was an additional 5-min extension at 68 °C before the reaction was stopped at 4 °C. Amplification products were then digested using 2 μl of DpnI restriction enzyme for 5 min at 37 °C to remove the parental dsDNA. The mutant plasmid (3 μl) was then transformed into XL10-Gold ultracompetent *E. coli* cells, which were grown overnight at 37 °C on LB plates with ampicillin. Plasmid DNA from positive colonies was then sequenced on both strands to confirm the mutation (GeneWiz, Inc.). Mutant proteins, purified as described above, appeared to be folded correctly because their sensitivities to limited proteolysis were similar to the wild-type enzyme.

Peptide Substrates—Peptides H2B(23–37), H2B(23–37)R29K, H2B(23–37)R31K, H2B(23–37)R33K, H2B(23–37)R29K/R31K, H2B(23–37)R29K/R33K, H2B(23–37)R31K/R33K, H4(1–8), H4(14–22), H4(14–22)R17K, and H4(14–22)R19K were purchased from GenScript as HPLC-purified preparations with ≥90% purity. Peptides H4(1–21), H4(1–21)R3K, and H4(1–21)R3MMA were a kind gift from Drs. Heather Rust and Paul Thompson (Scripps Research Institute, Jupiter, FL) and were described previously (23, 24). P-SmD3 (a 28-residue fragment of pre-mRNA splicing protein SmD3) was a kind gift from Dr. Sidney Pestka (UMDNJ, Robert Wood Johnson Medical School, Piscataway, NJ) and was described previously (25). P-RPL3 (a 16-residue fragment of ribosomal protein L3) was purchased from Biosynthesis Inc. All peptides were verified by mass spectrometry with sequences listed in Table 1.

P81 Paper-based Methyl Transfer Assay—Enzymatic reactions contained 10–20 μM *S*-adenosyl-L-[*methyl*-^{14}C]methionine ([^{14}C]AdoMet; PerkinElmer Life Sciences; from a 425 μM stock (47 mCi/mmol) in 10 mM H_2SO_4/EtOH (9:1, v/v)) or 0.7 μM *S*-adenosyl-L-[*methyl*-^{3}H]methionine ([^{3}H]AdoMet; PerkinElmer Life Sciences; from a 7.0 μM stock (78.2 Ci/mmol) in 10 mM H_2SO_4/EtOH (9:1, v/v)), the indicated amounts of GST-PRMT7/mutant and peptide/protein substrate, and the indicated reaction buffer (typically 50 mM HEPES (pH 7.5), 10 mM NaCl, and 1 mM DTT) in a final reaction volume of 30 μl. After incubation, the reactions were quenched by loading 25 μl of the mixture onto a 2.5-cm diameter P81 phosphocellulose

ion exchange filter paper (Whatman), which was then washed three times at room temperature for 45 min in 300 ml of 0.05 M $NaHCO_3$ (pH 9). Positively charged peptides and proteins bind tightly to the phosphocellulose, whereas unreacted radioactive AdoMet washes off (26). After air drying at room temperature, the filters were submerged in 10 ml of Safety-Solve scintillation mixture (Research Products International, 111177) and subjected to liquid scintillation counting for three cycles of 3 min using a Beckman LS6500 instrument.

Amino Acid Analysis of Protein and Peptide Substrates by High Resolution Cation Exchange Chromatography—Substrates were methylated with the indicated amount of GST-PRMT7 wild-type or mutant protein and 0.7 μM [^{3}H]AdoMet in a final reaction volume of 60 μl. The reactions were incubated for 18–20 h at 23 °C in 50 mM potassium HEPES (pH 7.5), 10 mM NaCl, and 1 mM DTT. Control reactions were performed in the absence of substrate or enzyme or in the presence of the catalytically inactive enzyme mutant. When GST-GAR protein and P-SmD3 peptide were used as substrates, 60 μl of 25% (w/v) trichloroacetic acid with 20 μg of the carrier protein bovine serum albumin was added and incubated at 23 °C for 30 min prior to centrifugation at 4000 × *g* for an additional 30 min. The pellet was air-dried after washing with −20 °C acetone. When smaller peptides were used as substrates, 3–4 μl of 25% (w/v) trichloroacetic acid was used to lower the pH of the reaction mixture, and the peptides were isolated using OMIX C18 Zip-Tip® pipette tips (Agilent Technologies) followed by vacuum centrifugation to remove the elution buffer (trifluoroacetic acid/acetonitrile/H_2O (0.1:50:50)). Acid hydrolysis of all samples was performed *in vacuo* at 110 °C for 20 h with 50 μl of 6 N HCl. After removal of the HCl by vacuum centrifugation, samples were dissolved in 50 μl of water and mixed with 1 μmol each of ω-MMA (acetate salt; Sigma, M7033), SDMA (di-(*p*-hydroxyazobenzene)-*p′*-sulfonate salt; Sigma, D0390), and ADMA (hydrochloride salt; Sigma, D4268) as internal standards. High resolution cation exchange chromatography was then performed as described previously (8). The positions of the amino acid standards were determined using 570-nm absorbance after ninhydrin assay with 50 μl of column fractions (8). Radioactivity in 950 μl of each fraction was determined with liquid scintillation as described (8) but using the average of three 3-min counting cycles.

Fluorography of Methylated GST-GAR after SDS-PAGE—Methyl transfer reactions were set up with [^{3}H]AdoMet, GST-GAR, and GST-PRMT7 wild-type or mutant protein as described above for the amino acid analysis. For the time course, 10 μg of GST-GAR was preincubated at 23 °C for 5 h in the reaction buffer before the addition of the enzyme and [^{3}H]AdoMet. For the temperature dependence assays, reactions were set up using GST-GAR (10 μg, 4.8 μM final concentration), 0.8 μM GST-PRMT7, and 0.7 μM [^{3}H]AdoMet and were incubated for 16 h. In both cases, the reactions were quenched by the addition of SDS loading buffer and separated on 12.6% Tris-glycine gels, stained with Coomassie Blue for 1 h, destained overnight, treated in autoradiography-enhancing buffer (EN^{3}HANCE, PerkinElmer, 6NE9701) for 1 h and vacuum-dried. Dried gels were then exposed to autoradiography film (Denville Scientific Inc., E3012) for 3–4 days at −80 °C (Denville Scientific Inc., E3012). After exposure to film, ImageJ densitometric analysis was done on scanned images of the film and quantified as relative activity.

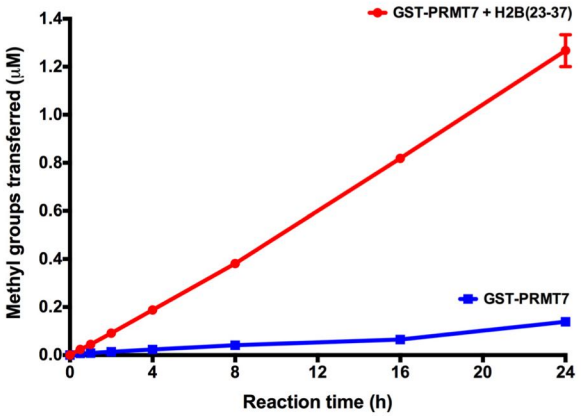

FIGURE 1. **Time course of the GST-PRMT7-catalyzed methylation reaction using the P81 paper assay.** Reactions were performed using 0.4 μM GST-PRMT7, 100 μM H2B(23–37) peptide, and 20 μM [^{14}C]AdoMet in a reaction buffer containing 50 mM potassium HEPES (pH 7.5), 10 mM NaCl, and 1 mM DTT in a total volume of 150 μl at 23 °C (*red points* and *line*). A control reaction was performed in the absence of the H2B(23–37) peptide substrate (*blue points* and *line*). At each time point, 20 μl of reaction mixture was spotted on a Whatman P81 filter, and the radioactive products were quantitated with liquid scintillation as described under "Experimental Procedures." Measurements were made in duplicate; when the range of values was larger than the plot symbol it is indicated with an *error bar*.

RESULTS

GST-PRMT7 Specifically Recognizes RXR Motifs Surrounded by Multiple Basic Residues in Peptide Sequences Based on Histone and Nonhistone Proteins—Full-length human PRMT7 was expressed and purified as a GST fusion protein from *E. coli* to avoid contamination from other PRMTs (27). Using a P81 filter paper assay as described under "Experimental Procedures," we optimized reaction conditions (temperature, pH, and salt) where product formation was linear over a 24-h period (Fig. 1). Importantly, at the 24 h point, only 6.3% of the initial AdoMet and only 1.3% of the initial peptide were converted to products, indicating that initial velocity conditions prevailed. To characterize the recognition sites for GST-PRMT7, methylation assays were first carried out with synthetic peptides containing the histone H2B repression domain (HBR, residues 27–34 (KKRKRSRK) (28)) that previously was observed to be methylated by insect cell-expressed PRMT7 (8). Peptides consisting of residues 23–37 were prepared with Arg-29, Arg-31, and Arg-33 as in the wild-type sequence or with one or two Arg → Lys substitutions at these sites (Table 1). The methylation products of these peptides were analyzed with high resolution amino acid analysis (Fig. 2). The wild-type peptide H2B(23–37) bearing the three arginines in the R*X*R*X*R sequence was well methylated by GST-PRMT7, producing only MMA (Fig. 2*A*). Peptides R29K and R33K, in which either the first or third arginine was mutated but where the R*X*R motif was retained remained good substrates with peak MMA radioactivity compared with the unmodified peptide of ~33 and ~6%, respectively (Fig. 2, *B* and *D*). However, peptide R31K with an R*XXX*R motif was rel-

TABLE 1

Peptide sequences

All arginine residues are highlighted in boldface type. Ac, acetyl.

Peptide	Sequence	Theoretical M_r	Observed M_r
H2B(23–37)	Ac-KKDGKK**R**K**R**S**R**KESY	1936.23	1935.60[a]
H2B(23–37)R29K	Ac-KKDGKKKK**R**S**R**KESY	1908.22	1908.00[a]
H2B(23–37)R31K	Ac-KKDGKK**R**KKS**R**KESY	1908.22	1907.80[a]
H2B(23–37)R33K	Ac-KKDGKK**R**K**R**SKKESY	1908.22	1908.00[a]
H2B(23–37)R29K/R31K	Ac-KKDGKKKKKS**R**KESY	1880.21	1879.60[a]
H2B(23–37)R29K/R33K	Ac-KKDGKKKK**R**SKKESY	1880.21	1879.60[a]
H2B(23–37)R31K/R33K	Ac-KKDGKK**R**KKSKKESY	1880.21	1879.60[a]
H4(1–21)	Ac-SG**R**GKGGKGLGKGGAK**R**H**R**KV	2133.47	2133[b]
H4(1–21)R3K	Ac-SGKGKGGKGLGKGGAK**R**H**R**KV	2105.46	2105[b]
H4(1–21)R3MMA	Ac-SG**R**(me)GKGGKGLGKGGAK**R**H**R**KV	2147.50	2147[b]
H4(1–8)	Ac-SG**R**GKGGK	787.87	787.60[a]
H4(14–22)	Ac-GAK**R**H**R**KVL	1106.33	1106.25[a]
H4(14–22)R17K	Ac-GAKKH**R**KVL	1078.32	1078.20[a]
H4(14–22)R19K	Ac-GAK**R**HKKVL	1078.32	1078.20[a]
H3(1–7)	Ac-A**R**TKQTA	816.91	816.50[a]
P-SmD3	AG**R**G**R**GKAAILKAQVAA**R**G**R**G**R**GMG**R**GN-amide	2792.25	2791[c]
P-RPL3	WGTKKLP**R**KTH**R**GL**R**K	1962.36	1961[c]
P-TAT	YG**R**KK**RR**Q**RRR**	1559.83	1559.60[a]
GAR (residues 1–148 of human fibrillarin)	MKPGFSP**R**GGGFGG**R**GGFGD**R**GG**R**GG**R**GGFGGG**R**G**R**GGGF**R**G**R**G**R**GGGGGGGGGGGGGG **R**GGGGFHSGGN**R**G**R**G**R**GGK**R**GNQSGKNVMVEPH**R**HEGVFIC**R**GKEDALVTKNLVPG ESVYGEK**R**VSISEGDDKIEY**R**AWNPF**R**SKLAAAI	14,815	

[a] Data provided by GenScript Inc.
[b] Data from Refs. 23 and 24.
[c] Data from MALDI-TOF analysis.

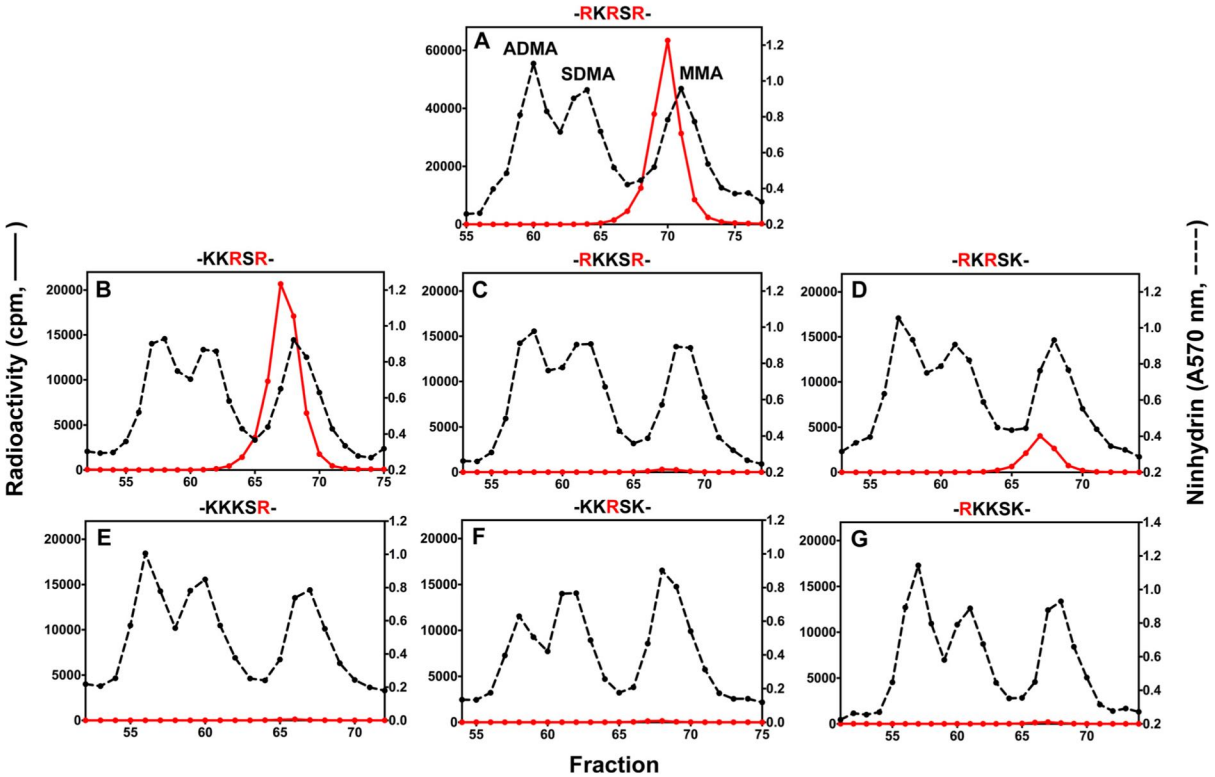

FIGURE 2. **Monomethylation of peptides derived from the DNA repression region of histone H2B by GST-PRMT7.** Peptides (12.5 μM; Table 1) were incubated with GST-PRMT7 (0.48 μM) and [^{3}H]AdoMet (0.7 μM) at 23 °C for 20 h as described under "Experimental Procedures." The reaction mixtures were then desalted with OMIX C18 ZipTip pipette tips, acid-hydrolyzed, and analyzed for methylated arginine species by amino acid analysis using high resolution cation exchange chromatography. The *red solid line* indicates the radioactivity of ^{3}H-methylated species; the *black dashed line* indicates the ninhydrin absorbance (570 nm) of ADMA, SDMA, and MMA standards. The ^{3}H-methyl derivatives of ADMA, SDMA, and MMA elute on this high resolution cation exchange column 1–2 min earlier than the non-labeled standards due to a tritium isotope effect (7, 8). *A–G*, PRMT7-catalyzed methylation products of H2B(23–37), H2B(23–37)R29K, H2B(23–37)R31K, H2B(23–37)R33K, H2B(23–37)R29K/R31K, H2B(23–37)R29K/R33K, and H2B(23–37)R31K/R33K, respectively. Partial sequences containing the target arginine sites (*highlighted* in *red*) are listed *above* the *panels*.

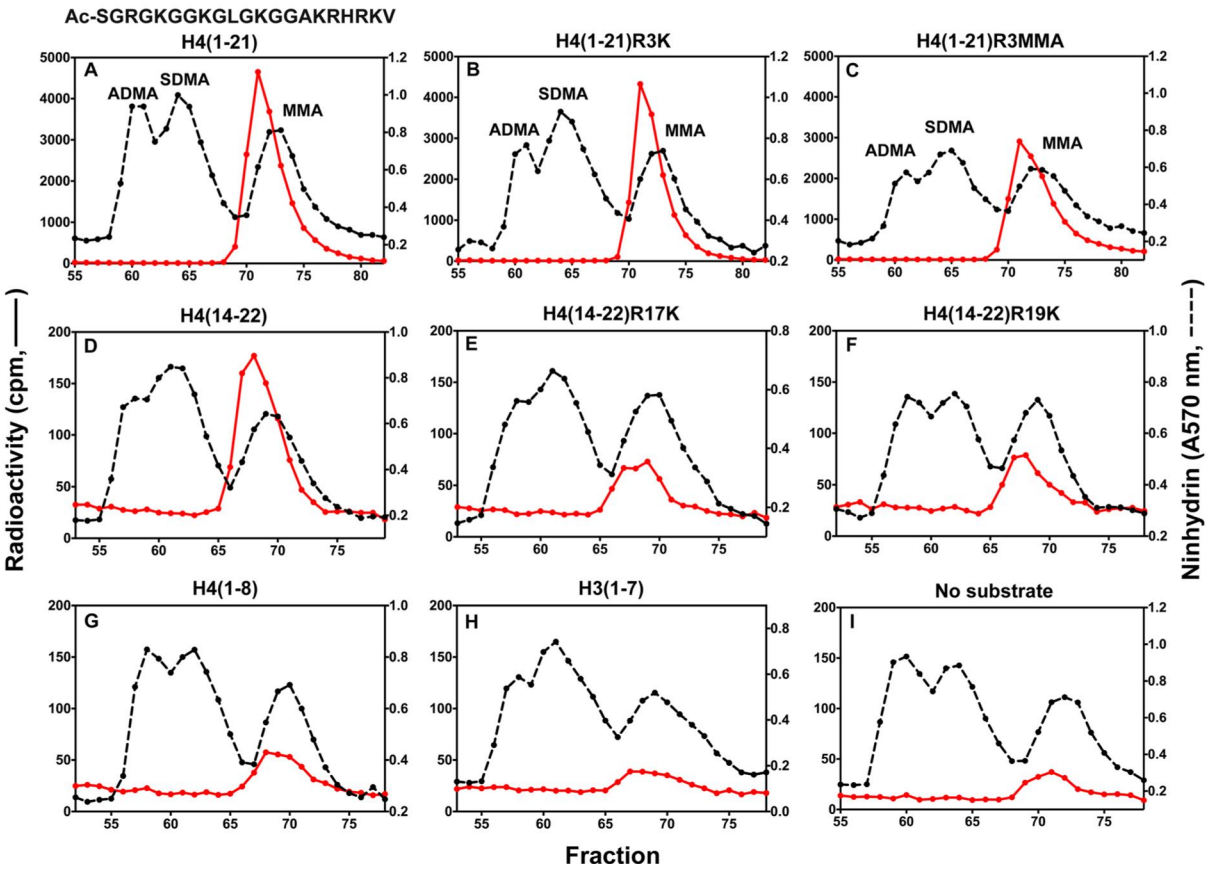

FIGURE 3. **Selective monomethylation in the R*X*R sequence of peptides derived from the N terminus of human histone H4.** Peptides (12.5 μM; Table 1) were incubated with [^{3}H]AdoMet (0.7 μM) and GST-PRMT7 (0.48 μM) at 23 °C for 20 h, as described under "Experimental Procedures." The reaction mixtures were desalted and tested by amino acid analysis, as described in the legend to Fig. 2. *A–C*, the GST-PRMT7-catalyzed methylation products of peptides H4(1–21), H4(1–21)R3K, and H4(1–21)R3MMA, respectively. The elution positions of the ADMA, SDMA, and MMA standards are indicated. *D–F*, GST-PRMT7-catalyzed methylation of peptides H4(14–22), H4(14–22)R17K, and H4(14–22)R19K. Control reactions with peptide H4(1–8), peptide H3(1–7), and no substrate (PRMT7 automethylation) are shown in *G–I*, respectively.

atively poorly methylated by GST-PRMT7, giving a peak radioactivity of only about 0.4% (Fig. 2*C*). Furthermore, when only a single arginine was present, as in peptides R29K/R31K, R29K/R33K, and R31K/R33K, less than 0.3% of the control radioactivity was seen (Fig. 2, *E–G*).

We also analyzed peptide substrates derived from the N-terminal 1–21, 1–8, or 14–22 residues of human histone H4 (Table 1). Peptide H4(1–21) was shown to be a good substrate for GST-PRMT7, with a single MMA peak (Fig. 3*A*). The replacement of Arg-3, the target site of PRMT1 and PRMT5 (23, 24, 26, 29–32), by either lysine or MMA in the peptide did not greatly decrease MMA formation or result in SDMA or ADMA formation (Fig. 3, *B* and *C*). Analysis of shorter peptides containing residues 14–22 of H4 and its R17K and/or R19K derivatives revealed that the loss of either the Arg-17 or Arg-19 residue markedly decreased MMA formation (Fig. 3, *D–F*). Finally, peptides containing residues 1–8 of H4 and residues 1–7 of H3 that lack the R*X*R motif were analyzed; little increase in MMA formation was seen over the small amount in the no-substrate control that reflects enzyme automethylation (Fig. 3, *G–I*). We did, however, find a role for the N-terminal residues in facilitating PRMT7-substrate interactions, because MMA formation in the H4(14–22) peptide was some 250-fold less than in the H4(1–21) peptide (Fig. 3, *A* and *D*).

We also searched for substrates for GST-PRMT7 with similar basic R*X*R motifs that were not derived from histones. Three peptides, P-TAT bearing a RKKRRQRRR sequence, P-SmD3 bearing RGRGK and RGRGR sequences, and P-RPL3 bearing a HRGLRK sequence, were analyzed (Table 1 and Fig. 4). Each of these peptides was recognized by GST-PRMT7 and only formed MMA. With P-TAT, the incorporation of ^{3}H-methyl groups approached the incorporation seen with the histone H2B(23–37) peptide (Fig. 2*A*), validating the preference of PRMT7 for the R*X*R motif in a high density of basic residues. P-SmD3 incorporated about 20% of the radioactivity seen with P-TAT, suggesting the importance of basic residues adjacent to the methylation sites. Finally, the P-RPL3 peptide only incorporated about 5% of the radioactivity of P-TAT. Here the insertion of a single residue between the pair of arginine residues appears to decrease PRMT7 recognition. Although we have not identified the precise sites of methylation in these peptides, all of them contain either R*X*R motifs or R*XX*R motifs in basic contexts.

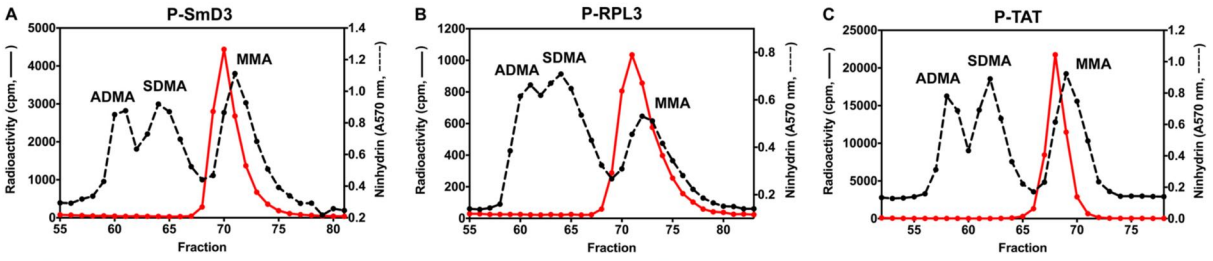

FIGURE 4. **Methylation of peptides derived from nonhistone substrates by GST-PRMT7.** Peptides (12.5 μM; Table 1) were methylated by GST-PRMT7 (0.48 μM) with [^{3}H]AdoMet (0.7 μM) at 23 °C for 18 h and detected by amino acid analysis as described in the legend to Fig. 2, except that trichloroacetic acid precipitation was used with the P-SmD3 substrate. *A–C*, PRMT7-catalyzed methylation products of peptides derived from SmD3, RPL3, and TAT proteins, respectively.

Taken together, the results shown in Figs. 2–4 suggest that bacterially expressed GST-human PRMT7 specifically recognizes pairs of arginine residues separated by one residue in a highly basic context to form only the monomethylated derivatives. This specificity is similar to that previously seen with the insect cell-expressed mouse PRMT7 enzyme (8).

Identification of Residues in PRMT7 Involved in Recognition of Basic RXR Substrates—Because the specific targeting of a basic R*X*R site by PRMT7 is unique among PRMT family members, we next tried to identify the residues in the enzyme important for substrate recognition. In all PRMT enzymes, the region following methyltransferase motif II has been associated with substrate binding (1, 2, 33) (Fig. 5). Here, PRMTs contain two highly conserved glutamate residues in a "double E" loop that directly bind the target arginine residue. We were intrigued to note that human PRMT7 has an aspartate residue (Asp-147) as the third residue following the initial glutamate in a position where all other PRMTs (except for PRMT9) contain a glycine residue. In addition, PRMT7 is the only human PRMT with an acidic residue (Glu-149) as the fifth residue following the initial glutamate of the double E loop. From the crystal structures of mouse and *Caenorhabditis elegans* PRMT7 (34, 35), Asp-147 and Glu-149 would be expected to face the substrate binding cavity. Interestingly, trypanosome PRMT7, which contains Gly and Met instead of Asp and Glu at these two positions (Fig. 5), methylates histone H4 at the non-R*X*R Arg-3 site, indicating that it may have a different substrate specificity from the human or mouse PRMT7 (9). However, it is clear that all of these species are type III PRMTs that only produce MMA as a product. We thus hypothesized that Asp-147 and Glu-149 might be important for targeting basic R*X*R sequences. Therefore, D147G and E149M mutations were made, changing the former into the conserved residue of the other PRMTs and the latter into the corresponding residue in TbPRMT7. We also constructed enzymes where residues 145–147 (LFD) in the double E loop of GST-PRMT7 were mutated to the conserved WMG sequence present in the type I PRMT1, -2, -3, -6, and -8 enzymes or mutated to the LLG sequence in the type II PRMT5 enzyme (Fig. 5). The C-terminal domain of human PRMT7 is not well conserved, with only one glutamate (Glu-478) present in the residues corresponding to the double E loop (Fig. 5, *red box*). To test the importance of this glutamate residue, a E478Q mutation was introduced. Finally, LC-MS/MS analysis on insect cell-

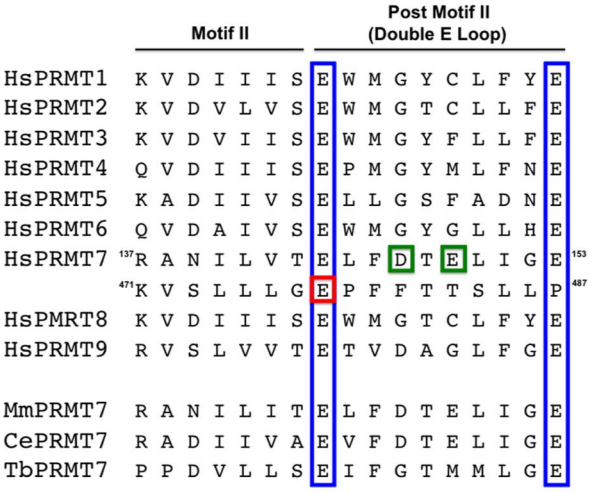

FIGURE 5. **Sequence alignment of the substrate binding motif II and post-motif II (double E loop) of PRMTs.** The two catalytic glutamate residues on the double E loop are *highlighted* with *blue boxes*. Two additional acidic residues (Asp-147 and Glu-149) in the N-terminal domain post-motif II in HsPRMT7 are *highlighted* with *green boxes*. The only acidic residue (Glu-478) on the C-terminal domain post-motif II in HsPRMT7 is *highlighted* with a *red box*. *Hs*, *Homo sapiens*; *Mm*, *Mus musculus*; *Ce*, *C. elegans*; *Tb*, *Trypanosoma brucei*; *HsPRMT9*, the gene product on human chromosome 4q31.

expressed mouse PRMT7 (8) indicated possible phosphorylation sites on residues Thr-203 and Ser-204, which are conserved in human PRMT7. To determine whether these modifications might regulate the activity of the enzyme, T203E and S203E mutations were made to mimic the phosphorylated Thr-203 and Ser-204 residues.

Amino acid analysis was carried out on all of the GST-PRMT7 mutants with the H2B(23–37) peptide as a substrate. As indicated in Fig. 6, all the mutations lowered the methyl group incorporation in H2B(23–37) to different levels compared with the wild-type enzyme (Fig. 6*H*), although none of them altered the type III methyltransferase activity because only MMA product was observed. The radioactivity in MMA generated by GST-D147G and GST-E149M with the peptide (Fig. 6, *A* and *B*) was ~6 and ~17% of that by the wild-type enzyme, respectively. However, the enzyme automethylation in these mutants in the absence of peptide was 4- and 3-fold higher when compared with that of the wild type (Fig. 6*H*, *blue line*). Thus, these two mutants were more active with auto-

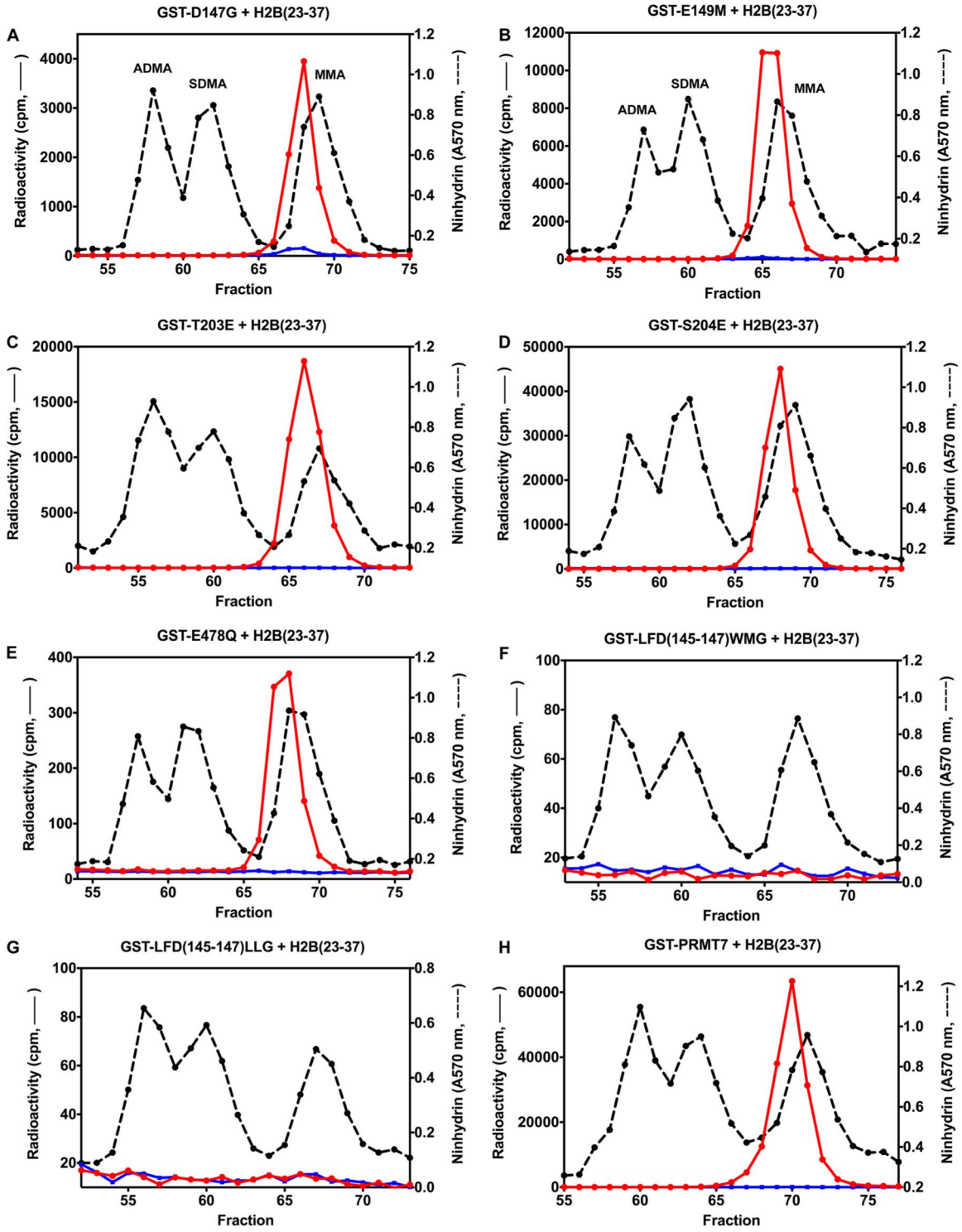
A
GST-D147G + H2B(23-37)
ADMA
SDMA
MMA
B
GST-E149M + H2B(23-37)
C
GST-T203E + H2B(23-37)
D
GST-S204E + H2B(23-37)
E
GST-E478Q + H2B(23-37)
F
GST-LFD(145-147)WMG + H2B(23-37)
G
GST-LFD(145-147)LLG + H2B(23-37)
H
GST-PRMT7 + H2B(23-37)
Radioactivity (cpm, ——)
Ninhydrin (A570 nm, - - - -)
Fraction

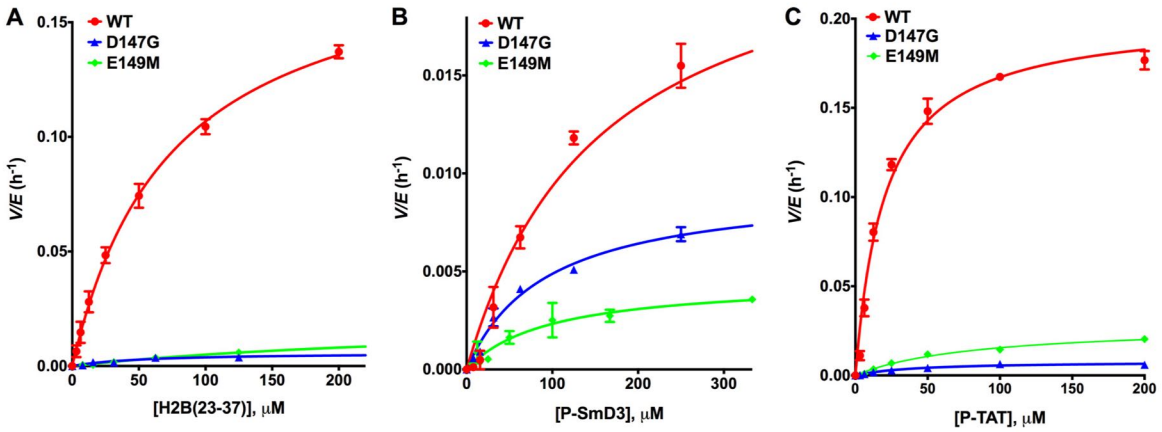

FIGURE 7. **Michaelis-Menten analyses for GST-PRMT7 mutants with H2B(23–37) (*A*), P-SmD3 (*B*), and P-TAT (*C*) as substrates.** Kinetic initial rate measurements were taken, and data were fit to the Michaelis-Menten equation as described in the legend to Table 2. Each assay was performed in duplicate, and the *error bars* indicate the range. The *solid lines* represent the curves from the fitted k_{cat} and K_m values shown in Table 2. Data are shown for the wild-type enzyme (*red*), the D147G mutant (*blue*), and the E149M mutant (*green*).

methylation but less active with the H2B(23–37) peptide containing the HBR domain, giving a clue that Asp-147 and Glu-149 might be essential in regulating the substrate specificity. Although the T203E and T204E mutants showed similar levels of product accumulation to the wild-type enzyme (Fig. 6, *C* and *D*), the E478Q mutant surprisingly displayed only <1% of radioactivity incorporation to H2B(23–37) (Fig. 6*E*), demonstrating the importance of the acidic residue Glu-478 in the region corresponding to the double E loop in the C-terminal domain. Little or no activity was observed for the LFD(145–147)WMG and the FD(146–147)LG mutants designed to mimic the double E loops of the type I and type II enzymes, respectively (Figs. 5 and 6 (*F* and *G*)).

Substrate Specificity Changes Determined by Kinetic Analysis of GST-PRMT7 Mutants with Peptide Substrates—We then performed detailed kinetic characterization on the wild-type GST-PRMT7 and mutants GST-D147G, GST-E149M, and GST-S204E using different peptide substrates. Under our conditions, product formation catalyzed by GST-PRMT7 is linear for 24 h at 23 °C (Fig. 1). In these experiments, we incubated the reactions for 5 h, a time at which substrate consumption would be expected to be less than 2%. The concentration of peptide substrate was varied, whereas the [^{14}C]AdoMet was fixed at 15 μM for the kinetic analyses. As shown in Fig. 7, the Michaelis-Menten curves showed similar patterns for H2B(23–37) and P-TAT, which both contain very basic R*X*R target sites. The D147G and E149M mutants showed very little activity toward these two peptides compared with the wild type. However, the catalytic pattern of the wild-type and mutant enzymes for the P-SmD3 substrate containing the less basic RGRG repeats was distinct. Although the P-SmD3 peptide was a markedly poorer substrate than H2B(23–37) and P-TAT, the relative activities of

TABLE 2

Kinetic data for selected GST-PRMT7 mutants with different substrates

P81 paper assays were performed with varying concentrations of each substrate (typically 0–200 μM) incubated with 15 μM [^{14}C]AdoMet and 0.5 or 0.75 μM GST-PRMT7 or its mutant in the reaction buffer (50 mM potassium HEPES (pH 7.5), 10 mM NaCl, and 1 mM DTT) in a total volume of 30 μl at 23 °C. After 5 h, 25 μl of the reaction mixture was spotted onto the P81 filter paper, which was washed and dried as described under "Experimental Procedures." The radioactivity on the P81 paper was detected by liquid scintillation as described. The initial velocity as a function of substrate concentration was fit to the Michaelis-Menten equation with the Prism 6 program, which gave the k_{cat} and K_m and their S.E. values as shown below.

Enzyme	Substrate	k_{cat}	K_m	k_{cat}/K_m
		$\times 10^{-3}\ h^{-1}$	μM	$\times 10^{-4}\ \mu M^{-1}\ h^{-1}$
GST-PRMT7	H2B (23–37)	186 ± 6	75 ± 5	25 ± 2
	P-SmD3	24 ± 2	155 ± 27	1.6 ± 0.3
	P-TAT	201 ± 7	21 ± 2	98 ± 11
GST-D147G	H2B (23–37)	5.9 ± 0.5	55 ± 15	1.1 ± 0.3
	P-SmD3	9.4 ± 0.4	92 ± 12	1.0 ± 0.1
	P-TAT	7.9 ± 0.7	42 ± 10	1.9 ± 0.5
GST-E149M	H2B (23–37)	21 ± 1	325 ± 36	0.65 ± 0.08
	P-SmD3	4.6 ± 0.6	96 ± 29	0.48 ± 0.16
	P-TAT	29 ± 2	84 ± 12	3.5 ± 0.5
GST-S204E	H2B (23–37)	85 ± 5	63 ± 8	13 ± 2
	P-SmD3	7.5 ± 0.6	26 ± 7	2.9 ± 0.8
	P-TAT	81 ± 1	7.7 ± 0.6	110 ± 8

the D147G and E149M mutations were much greater with the P-SmD3 substrate. These results suggest that Asp-147 and Glu-149 are particularly important in recognizing the basic residues surrounding the target site. Interestingly, the activity of the E149M enzyme was greater than that of the D147G enzyme with the more basic H2B(23–37) and P-TAT substrates but lower with the less basic P-SmD3 substrate. The k_{cat} and K_m values for all of the mutants tested are shown in Table 2, where the k_{cat}/K_m value best reflects the overall substrate specificity. Compared with wild-type GST-PRMT7, the k_{cat}/K_m values are 23- and 38-fold lower for GST-D147G and GST-E149M in

FIGURE 6. **Methylated product analyses of PRMT7 mutants with the H2B(23–37) peptide as a substrate.** Peptide (12.5 μM) was methylated by a 0.48 μM concentration of the indicated GST-PRMT7 mutant (*A–G*) with [^{3}H]AdoMet (0.7 μM) in a 60-μl reaction for 18 h. The products were acid-hydrolyzed and subjected to cation exchange coupled with amino acid analysis as described in the legend to Fig. 2. The *red line* shows radioactivity with the full reaction mixture; the *blue line* shows the radioactivity in enzyme automethylation (no H2B(23–37) was present). For ease of comparison, the data for wild-type GST-PRMT7 (*H*) are combined from the data shown in Fig. 2*A* and Fig. 3*I*. In *H*, the reaction was incubated for 20 h but under conditions otherwise identical to those shown in *A–G*, where the incubation was 18 h.

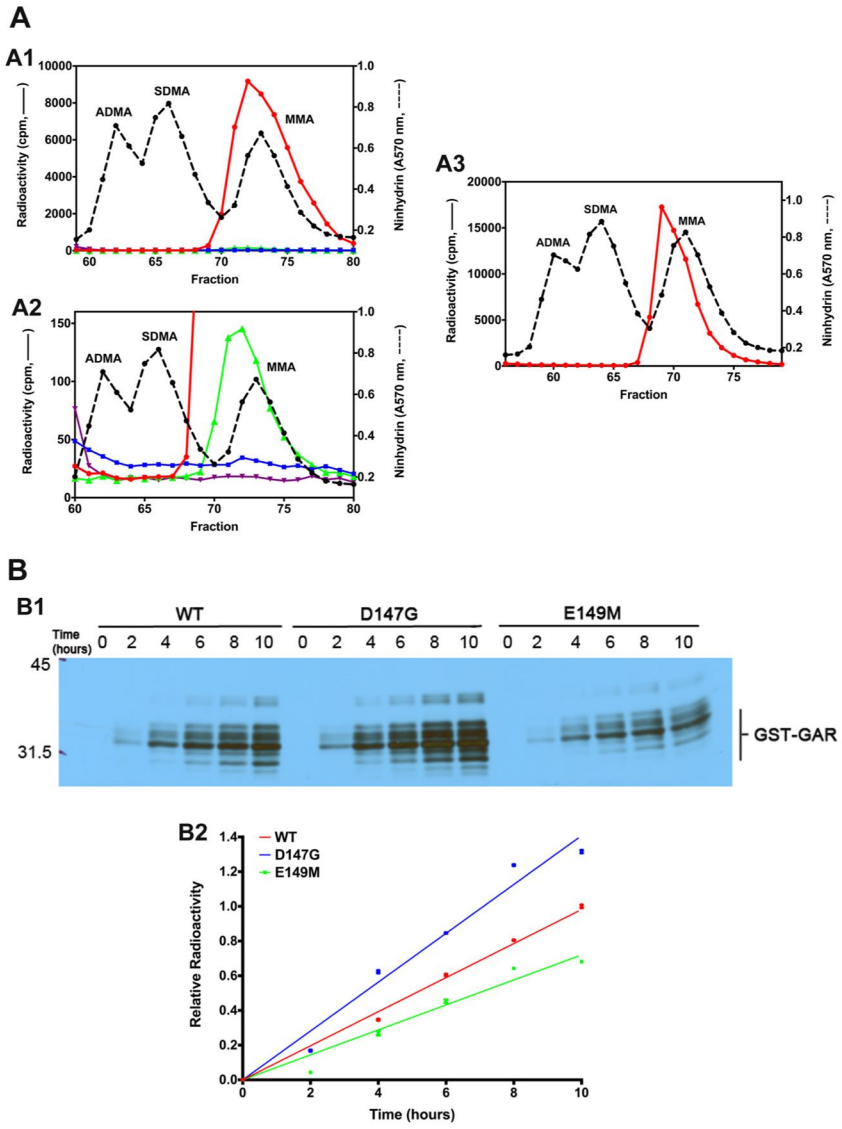

FIGURE 8. **Methylation of the GST-GAR protein by GST-PRMT7 and its mutants.** *A*, GST-PRMT7-catalyzed formation of MMA on GST-GAR. *A1*, *in vitro* methylation reactions were performed as described in the legend to Fig. 2 using 6 μg of GST-GAR (2.9 μM) and 3 μg of wild-type GST-PRMT7 or mutant LDIG(69–72)AAAA (0.48 μM). The reactions were allowed to proceed at 23 °C for 20 h before quenching by trichloroacetic acid precipitation. Incubations in the absence of GST-PRMT7 or GST-GAR were used as controls. After acid hydrolysis, the methylated amino acid derivatives were analyzed by high resolution cation exchange chromatography together with standards of ADMA, SDMA, and MMA as described under "Experimental Procedures." ^{3}H radioactivity (*solid lines*) and ninhydrin absorbance of the methylated arginine standards (*dashed lines*; elution positions indicated) were detected with liquid scintillation counting and 570-nm absorbance, respectively. *Red*, wild-type GST-PRMT7 with GST-GAR; *green*, wild-type GST-PRMT7 alone; *blue*, LDIG(69–72)AAAA mutant enzyme with GST-GAR; *purple*, GST-GAR alone. *A2*, magnification of the radioactivity scale to show PRMT7 automethylation (*green*), the residual activity of LDIG(69–72)AAAA (*blue*), and the absence of ADMA and SDMA in the reaction products (*red*). *A3*, premethylated GST-GAR generates only MMA in a PRMT7-catalyzed reaction. GST-GAR (6 μg) was preincubated with unlabeled AdoMet (125 μM final) and GST-PRMT7 (3 μg) in 40 μl of reaction buffer at 23 °C for 24 h to enrich for MMA. Next, the unlabeled AdoMet concentration was lowered to 0.05 μM by adding fresh reaction buffer, and the sample was concentrated using an Amicon Ultra centrifugal filter (Millipore). Then [^{3}H]AdoMet (0.7 μM) and extra GST-PRMT7 (2.4 μg) were added into the reaction mixture, which was incubated at 23 °C for another 20 h before acid hydrolysis and cation exchange chromatography. The radioactivity of ^{3}H-labeled protein residue was plotted in comparison with the standards. *B*, time course of GST-GAR methylation by double E loop GST-PRMT7 mutants. *B1*, fluorography of ^{3}H-methylated GST-GAR after reaction with wild type or mutant GST-PRMT7 as described under "Experimental Procedures." Dried gels were exposed to autoradiography film for 4 days at −80 °C. Reactions were run in duplicate on separate gels, one of which is shown here. *B2*, quantification of GST-GAR methylation catalyzed by wild type GST-PRMT7 (*red*), D147G (*blue*), and E149M (*green*). Data were acquired from the densitometric analysis of the autoradiography film and are shown as activity relative to that at the 10-h time point for the wild-type enzyme. *Error bars*, range of duplicate experiments.

methylating H2B(23–37) and 52- and 28-fold lower for these two mutants in methylating P-TAT, whereas they are only 2- and 3-fold lower for them in methylating P-SmD3. These data indicate that Asp-147 and Glu-149 are responsible for the selectivity of PRMT7 for R*X*R residues in basic sequence contexts. Looking at the H2B(23–37) substrate only, GST-D147G

showed a 32-fold smaller k_{cat} and a similar K_m compared with the wild type, indicating that Asp-147 in the double E loop is mainly involved in catalysis; GST-E149M showed a 9-fold smaller k_{cat} and a 4-fold larger K_m compared with the wild type, indicating that Glu-149 in the double E loop is involved in both catalysis and substrate binding. As for GST-S204E, the k_{cat}/K_m values for all three substrates are generally similar to the wild type because the k_{cat} and K_m for individual peptide are both decreased. It is possible that the potential phosphorylation on Ser-204 might increase the substrate binding affinity.

Specificity of GST-PRMT7 Mutants for the Protein Substrate GST-GAR—To confirm the alteration of substrate specificity for the GST-D147G and GST-E149M PRMT7 mutant enzymes, we also analyzed the substrate GST-GAR, consisting of residues 1–148 of human fibrillarin (7, 36) and containing similar RGRG repeats as in the P-SmD3 peptide (Table 1). We first performed amino acid analysis on the reaction products. Fig. 8*A* shows that wild-type GST-PRMT7 generated only [^{3}H]MMA on GST-GAR (Fig. 8*A1*). A small amount of [^{3}H]MMA automethylation was found for the enzyme-alone control (about 1.4% of that with GST-GAR) (Fig. 8*A2*, *green line*); less than 0.1% of [^{3}H]MMA was detected with the AdoMet binding-deficient mutant enzyme GST-LDIG(69–72)AAAA and GST-GAR (Fig. 8*A2*, *blue line*). In addition, to verify if PRMT7 adds a second methyl group to monomethylated arginine residues, GST-GAR was premethylated with unlabeled AdoMet to enrich for MMA, and then [^{3}H]AdoMet was added for detection of methylated product. Again, only the [^{3}H]MMA peak was observed with no detectable [^{3}H]SDMA or [^{3}H]ADMA formation (Fig. 8*A3*). These results confirm that GST-PRMT7 is unable to transfer a second methyl group to the arginine site where one methyl group is already present.

Next, SDS-PAGE and fluorography were performed to monitor the time courses of GST-GAR methylation catalyzed by wild-type GST-PRMT7 and mutants GST-D147G and GST-E149M (Fig. 8*B*). The density of methylated GST-GAR bands on the fluoroimage (Fig. 8*B1*) was quantified, and product formation indicated by the relative radioactivity was linear for up to 10 h with the wild-type and mutant enzymes (Fig. 8*B2*). Importantly, the activities of the mutant enzymes were similar to that of the wild-type enzyme; GST-D147G showed, in fact, a higher catalytic activity. These results stand in marked contrast to those obtained above with the H2B(23–37) and P-TAT peptides, where very little activity was seen in the mutants compared with the wild type (Fig. 7, *A* and *C*). Therefore, the substrate specificity change is confirmed here: mutation of Asp-147 and Glu-149 on the double E loop does not greatly affect the specificity of PRMT7 for RGRG-containing GST-GAR but dramatically decreases its selectivity for substrates rich in basic residues.

Unusual Dependence of PRMT7 Activity on Temperature and Salt Concentration—During the reaction condition optimization, we found that PRMT7 had an unusual temperature dependence. When we tested the temperature effect on bacterially expressed human GST-PRMT7 with H2B(23–37) as a substrate in the P81 paper assay (Fig. 9*A*), the peak activity was found between 15 and 25 °C. The enzyme remained ~50% active when the temperature was lowered to 5 °C, whereas its

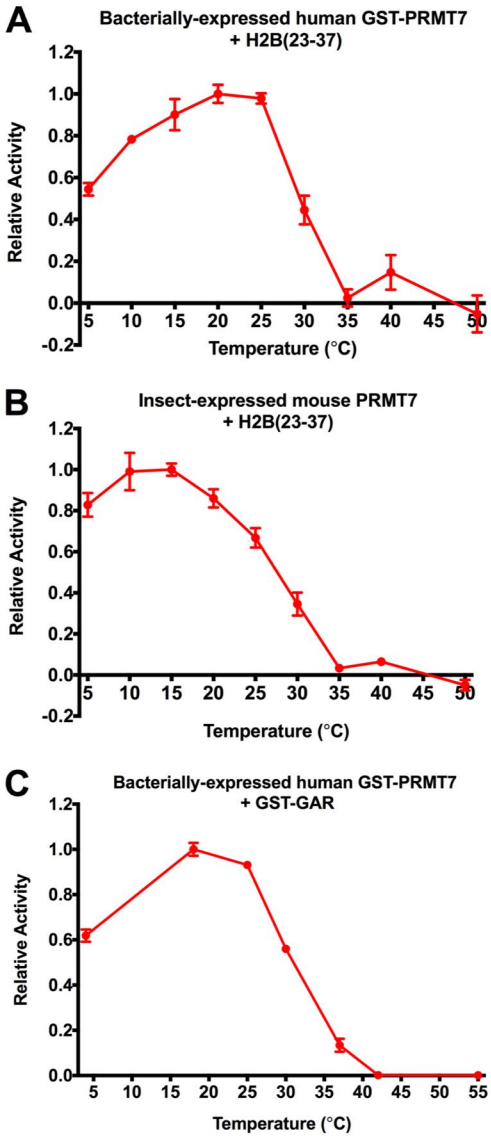

FIGURE 9. **Effect of temperature on PRMT7 activity.** *A*, temperature dependence of bacterially expressed human GST-PRMT7 with the H2B(23–37) peptide as a substrate. The reactions contained 0.4 μM GST-PRMT7, 40 μM H2B(23–37), and 10 μM [^{14}C]AdoMet in a 30-μl reaction buffer of 50 mM potassium HEPES (pH 7.5), 10 mM NaCl, and 1 mM DTT. The reactions were incubated at the indicated temperature for 16 h. After incubation, the reaction mixtures were spotted on Whatman P81 filter paper and washed, and the radioactivity in the protein products was determined by liquid scintillation counting, as described under "Experimental Procedures." The reaction background (radioactivity in the absence of enzyme) was subtracted, and the relative activity is shown in comparison with the activity at 20 °C. *B*, temperature dependence of insect cell-expressed mouse PRMT7 with the H2B(23–37) peptide as a substrate. The reactions contained 0.1 μM PRMT7, 10 μM H2B(23–37), and 10 μM [^{14}C]AdoMet in 50 mM potassium HEPES (pH 7.5), 10 mM NaCl, and 1 mM DTT and were analyzed as in *A*, except that the relative activity is shown in comparison with the value at 15 °C. *C*, temperature dependence of bacterially expressed human GST-PRMT7 with GST-GAR as a substrate. 4.8 μM GST-GAR, 0.8 μM GST-PRMT7, and 0.7 μM [^{3}H]AdoMet were incubated in the reaction buffer for 16 h. The methylated products were separated with 12.6% SDS-PAGE, treated with EN^{3}HANCE buffer, vacuum-dried, and exposed to autoradiography film for 3 days at −80 °C. Densitometric analysis was done on scanned images of the film, and quantification of the data is shown as activity relative to that at 18 °C. In each case, the assays were done in duplicate, and the *error bars* show the range of the data.

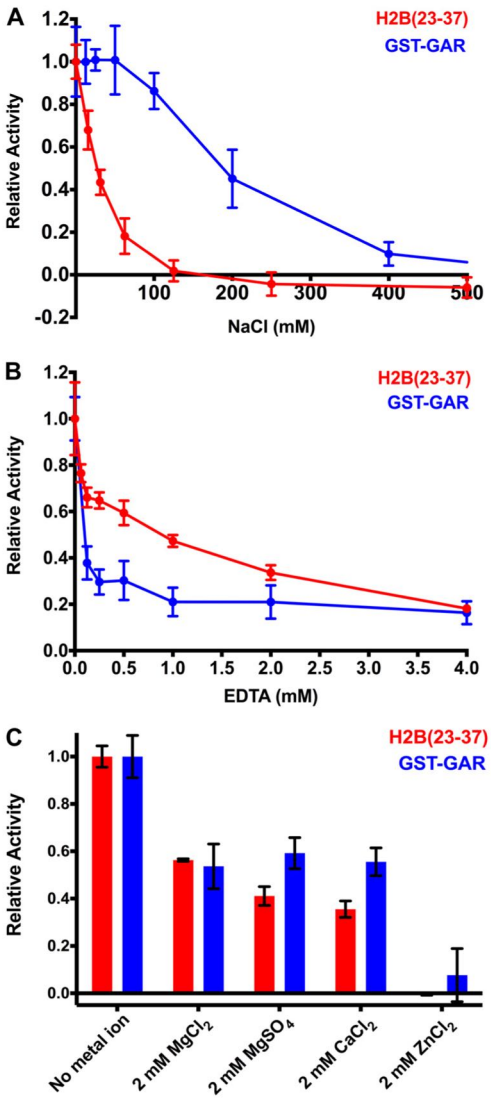

FIGURE 10. **Effect of NaCl, EDTA, and metal ions on PRMT7 activity.** A, salt effect. The reaction buffer contained 50 mM potassium HEPES (pH 7.5), 1 mM DTT, and different concentrations of NaCl. When H2B(23–37) peptide was used as a substrate (*red*), 20 μM peptide, 0.4 μM GST-PRMT7, and 10 μM [^{14}C]AdoMet were incubated for 16 h at 23 °C. When GST-GAR was used as a substrate (*blue*), 2 μg of GST-GAR, 0.8 μg of GST-PRMT7, and 0.7 μM [^{3}H]AdoMet were incubated for 18 h at 23 °C. The reaction mixtures were then spotted on Whatman P81 filter paper and washed, and the radioactivity in the methylated products was determined by liquid scintillation as described under "Experimental Procedures." Radioactivity in controls lacking enzyme (peptide assay) or enzyme and substrate (protein assay) were subtracted. *B*, EDTA effect. The reaction buffer contained 50 mM potassium HEPES (pH 7.5), 10 mM NaCl, 1 mM DTT, and different concentrations of EDTA. When H2B(23–37) was used as a substrate (*red*), 40 μM H2B(23–37), 0.4 μM GST-PRMT7, and 10 μM [^{14}C]AdoMet were incubated at 23 °C for 16.5 h. When GST-GAR was used as a substrate (*blue*), 4.5 μg of GST-GAR, 0.8 μg of GST-PRMT7, and 0.7 μM [^{3}H]AdoMet were incubated at 23 °C for 18 h. Product formation was analyzed as in *A* above; radioactivity in controls lacking enzyme (peptide assay) or enzyme and substrate (protein assay) were subtracted. *C*, metal ion effect. When H2B(23–37) was used as a substrate (*red bars*), the reactions containing 40 μM H2B(23–37), 0.4 μM GST-PRMT7, and 10 μM [^{14}C]AdoMet were incubated in the presence of 2 mM $MgCl_2$, $MgSO_4$, $CaCl_2$, or $ZnCl_2$ at 23 °C for 16 h. The positive control was performed in absence of metal ion; the negative control was performed in absence of enzyme and metal ion and was subtracted as background. When GST-GAR was used as a substrate (*blue bars*), the reactions containing 4.5 μg of GST-GAR, 0.8 μg of GST-PRMT7 and 0.7 μM [^{3}H]AdoMet were incubated in the presence of the indicated metal ions at 23 °C for 18 h. The negative control contained only [^{3}H]AdoMet and the buffer components and was subtracted as background. All measurements were performed in duplicate; *error bars* indicate the range.

activity dropped dramatically above 30 °C. These results were surprising for a mammalian enzyme presumably working at body temperatures of about 37 °C. To confirm this phenomenon, we also analyzed the temperature effect on the insect-expressed mouse PRMT7 (8) with H2B(23–37) as a substrate in the P81 paper assay (Fig. 9*B*) and the bacterially expressed human GST-PRMT7 with GST-GAR as a substrate in the fluorography assay (Fig. 9*C*). In both of these cases, a similar temperature dependence was found. These results indicate that PRMT7 is an unusual mammalian enzyme with significant activity at sub-physiological temperatures.

We also detected an unusual sensitivity of GST-PRMT7 to salt and the metal chelator EDTA. Using the peptide H2B(23–37), we found half-inhibition at about 30 mM NaCl (Fig. 10*A*). With the GST-GAR substrate, less salt sensitivity was seen, with a half-inhibition at about 180 mM NaCl. EDTA also showed an inhibitory effect on GST-PRMT7, with either the H2B(23–37) or GST-GAR substrate (Fig. 10*B*). At an EDTA concentration of 1 mM, enzyme activity was reduced by over 50% for both substrates. In experiments supplementing reaction mixtures with 2 mM $MgCl_2$, $MgSO_4$, $CaCl_2$, or $ZnCl_2$, we observed no increase in activity (Fig. 10*C*). The mechanism of inhibition of PRMT7 by EDTA remains to be established, although we note that zinc has been detected in the crystal structure of mouse PRMT7 (34).

DISCUSSION

We have confirmed the type III activity of bacterially expressed GST-tagged human PRMT7 on basic R*X*R sequence motifs under our optimized reaction conditions. Product formation was significantly improved as we adjusted several conditions from our previous study (7), particularly the reaction temperature. The type III activity of GST-PRMT7 forming only MMA product has been confirmed with both GST-GAR protein derived from fibrillarin and various peptides derived from histone H4, histone H2B, splicing protein SmD3, ribosomal protein RPL3, and HIV-1 TAT protein as well as for PRMT7 automethylation. These results are consistent with previous reports on human and mouse PRMT7 (7, 8) as well as studies on the trypanosome PRMT7 (6, 9). Although PRMT7 may work synergistically with type I or type II PRMTs or other modulators *in vivo*, PRMT7 by itself only generates MMA residues.

We find that effective substrates for GST-tagged human PRMT7 consist of sequences with at least two closely spaced arginine residues with adjacent basic residues. Out of all of the peptides tested (Table 1), H2B(23–27) bearing a KKRKRSRK sequence and P-TAT bearing an RKKRRQRRR sequence are the best PRMT7 substrates, probably because they contain a high density of positive charges and multiple arginine residues, which may be preferably recognized by the extra two acidic residues (Asp-147 and Glu-149) in the double E loop (Fig. 7). H4(1–21) bearing a KRHRK sequence, P-SmD3 bearing

RGRGK and RGRGR sequences, and P-RPL3 bearing an HRGLRK sequence are moderate substrates for PRMT7, suggesting the essential role of basic residue density. The H2B and H4 mutant peptides, where R*X*R sequences are modified to R*X*K or K*X*R sequences, are poor substrates. This demonstrates the importance of at least two arginine residues as the recognition site, which is also supported by the poor methylation of H4(1–8) and H3(1–7) sequences with a single arginine residue. These results are consistent with and extend those found earlier for the insect-expressed mouse enzyme (8).

Through site-directed mutagenesis, we show that the two additional acidic residues (Asp-147 and Glu-149) in the double E loop may be crucial elements in the substrate specificity of PRMT7 (Fig. 7). Enzymes where these residues are substituted with glycine and methionine, respectively, demonstrate dramatically decreased activity toward the H2B(23–37) and P-TAT substrates with high basic residue density but only moderately affected activity toward the P-SmD3 and GST-GAR substrates with relatively low basic residue density. It thus appears that the D147G and E149M mutations compromise the selectivity of PRMT7 for very basic R*X*R sites and that these two unique acidic residues in the PRMT7 double E loop are probably determinants for the preferable recognition of basic residues adjacent to or near the methylatable arginine residues.

We have also prepared PRMT7 with mutations in the double E loop designed to mimic conserved residues in type I and type II PRMTs (LFD to WMG and FD to LG, respectively). However, we found that neither of the mutated proteins displayed methyl transfer activity. Although the acidic residues do play an important role in conferring substrate specificity, mutating multiple residues in the double E loop destroys the ability of PRMT7 to methylate substrates. All of these mutations are within the catalytic N-terminal domain. PRMT7 also has an ancestrally duplicated C-terminal domain where many of the residues important for binding AdoMet or substrates have been altered. For example, only one of the glutamate residues in the corresponding region of the double E loop is present in the C-terminal domain (Glu-478). However, this domain is still required for enzyme activity (5), and in this study, we have shown that the E478Q mutation reduces the activity of PRMT7 to $<1\%$ of the wild-type activity. Although this second domain in PRMT7 is poorly conserved in sequence (5), it is certainly not redundant for substrate binding or catalysis.

In this study, we found special unique features of PRMT7 catalysis. First, the enzyme is more active at temperatures below the physiological mammalian value of 37 °C and in fact can perform catalysis even at 5 °C. Second, NaCl, EDTA, and some common metal ions were found to have a relatively strong inhibitory effect on PRMT7. These phenomena have not been observed for other members of the mammalian PRMT family. The unusual sensitivity to temperature may indicate that PRMT7 may be activated by cold stress to tissues.

Unfortunately, no *in vivo* substrates for PRMT7 have yet been unambiguously identified. Our results here, however, indicate that PRMT7-targeting sequences are often nucleotide binding sequences that compact and stabilize the structure of DNA/RNA, such as the HBR domain on histone H2B (28, 37), the RKKRRQRRR region (residues 49–57) on HIV-1 TAT protein (38), and the KRHRK region on histone H4 (39). The HBR domain at the end of the H2B N-terminal tail closely interacts with neighboring nucleosomal DNA and represses gene transcription (28, 37). In yeast, it was found that HBR is necessary and sufficient for repressing ~8.6% of genes, many of which are located near telomeres or involved in the metabolism of vitamins and carbohydrates (28). No *in vivo* evidence has been found for posttranslational modifications on the HBR domain, although *in vitro* data are very clear that insect-expressed mouse PRMT7 monomethylates Arg-29, Arg-31, and Arg-33 in this region (8). HIV-1 TAT residues 49–57 bear a nuclear localization signal and RNA-binding motif. This region has been reported to be asymmetrically dimethylated on Arg-52 and Arg-53 by PRMT6, leading to weaker interaction with the viral RNA and down-regulation of the transactivation capacity of TAT (40, 41). Our study suggests that arginine monomethylation may also occur in this region. Posttranslational modifications catalyzed by PRMT7 at these arginine and lysine-rich regions, although poorly characterized, may play an essential role in modulating their interactions with DNA/RNA. More efforts are needed to validate these possible methylation sites and the biological consequences of their modification *in vivo*.

Acknowledgments—We thank Paul Thompson and Heather Rust (Scripps Research Institute) for the kind gift of peptides H4(1–21), H4(1–21)R3K, and H4(1–21)R3MMA. We thank the previous and current members of the Clarke laboratory, in particular Alexander Patananan, Mingle Zhang, Kanishk Jain, Qais Al-Hadid, Cecilia Zurita-Lopez, and Jonathan Lowenson, for help.

REFERENCES

1. Bedford, M. T., and Clarke, S. G. (2009) Protein arginine methylation in mammals: who, what, and why. *Mol. Cell* **33,** 1–13
2. Herrmann, F., Pably, P., Eckerich, C., Bedford, M. T., and Fackelmayer, F. O. (2009) Human protein arginine methyltransferases *in vivo*: distinct properties of eight canonical members of the PRMT family. *J. Cell Sci.* **122,** 667–677
3. Yang, Y., and Bedford, M. T. (2013) Protein arginine methyltransferases and cancer. *Nat. Rev. Cancer* **13,** 37–50
4. Baldwin, R. M., Morettin, A., and Côté, J. (2014) Role of PRMTs in cancer: could minor isoforms be leaving a mark? *World J. Biol. Chem.* **5,** 115–129
5. Miranda, T. B., Miranda, M., Frankel, A., and Clarke, S. (2004) PRMT7 is a member of the protein arginine methyltransferase family with a distinct substrate specificity. *J. Biol. Chem.* **279,** 22902–22907
6. Fisk, J. C., Sayegh, J., Zurita-Lopez, C., Menon, S., Presnyak, V., Clarke, S. G., and Read, L. K. (2009) A type III protein arginine methyltransferase from the protozoan parasite *Trypanosoma brucei*. *J. Biol. Chem.* **284,** 11590–11600
7. Zurita-Lopez, C. I., Sandberg, T., Kelly, R., and Clarke, S. G. (2012) Human protein arginine methyltransferase 7 (PRMT7) is a type III enzyme forming ω-N^G-monomethylated arginine residues. *J. Biol. Chem.* **287,** 7859–7870
8. Feng, Y., Maity, R., Whitelegge, J. P., Hadjikyriacou, A., Li, Z., Zurita-Lopez, C., Al-Hadid, Q., Clark, A. T., Bedford, M. T., Masson, J. Y., and Clarke, S. G. (2013) Mammalian protein arginine methyltransferase 7 (PRMT7) specifically targets R*X*R sites in lysine- and arginine-rich regions. *J. Biol. Chem.* **288,** 37010–37025
9. Wang, C., Zhu, Y., Caceres, T. B., Liu, L., Peng, J., Wang, J., Chen, J., Chen, X., Zhang, Z., Zuo, X., Gong, Q., Teng, M., Hevel, J. M., Wu, J., and Shi, Y. (2014) Structural determinants for the strict monomethylation activity by *Trypanosoma brucei* protein arginine methyltransferase 7. *Structure* **22,** 756–768

10. Kim, C., Lim, Y., Yoo, B. C., Won, N. H., Kim, S., and Kim, G. (2010) Regulation of post-translational protein arginine methylation during HeLa cell cycle. *Biochim. Biophys. Acta* **1800,** 977–985
11. Lu, H., Cui, J. Y., Gunewardena, S., Yoo, B., Zhong, X. B., and Klaassen, C. D. (2012) Hepatic ontogeny and tissue distribution of mRNAs of epigenetic modifiers in mice using RNA-sequencing. *Epigenetics* **7,** 914–929
12. Buhr, N., Carapito, C., Schaeffer, C., Kieffer, E., Van Dorsselaer, A., and Viville, S. (2008) Nuclear proteome analysis of undifferentiated mouse embryonic stem and germ cells. *Electrophoresis* **29,** 2381–2390
13. Dhar, S. S., Lee, S. H., Kan, P. Y., Voigt, P., Ma, L., Shi, X., Reinberg, D., and Lee, M. G. (2012) Trans-tail regulation of MLL4-catalyzed H3K4 methylation by H4R3 symmetric dimethylation is mediated by a tandem PHD of MLL4. *Genes Dev.* **26,** 2749–2762
14. Baldwin, E. L., and Osheroff, N. (2005) Etoposide, topoisomerase II and cancer. *Curr. Med. Chem. Anticancer Agents* **5,** 363–372
15. Bleibel, W. K., Duan, S., Huang, R. S., Kistner, E. O., Shukla, S. J., Wu, X., Badner, J. A., and Dolan, M. E. (2009) Identification of genomic regions contributing to etoposide-induced cytotoxicity. *Hum. Genet.* **125,** 173–180
16. Verbiest, V., Montaudon, D., Tautu, M. T., Moukarzel, J., Portail, J. P., Markovits, J., Robert, J., Ichas, F., and Pourquier, P. (2008) Protein arginine (*N*)-methyl transferase 7 (PRMT7) as a potential target for the sensitization of tumor cells to camptothecins. *FEBS Lett.* **582,** 1483–1489
17. Gros, L., Delaporte, C., Frey, S., Decesse, J., de Saint-Vincent, B. R., Cavarec, L., Dubart, A., Gudkov, A. V., and Jacquemin-Sablon, A. (2003) Identification of new drug sensitivity genes using genetic suppressor elements: protein arginine n-methyltransferase mediates cell sensitivity to DNA-damaging agents. *Cancer Res.* **63,** 164–171
18. Gros, L., Renodon-Cornière, A., de Saint Vincent, B. R., Feder, M., Bujnicki, J. M., and Jacquemin-Sablon, A. (2006) Characterization of prmt7α and β isozymes from Chinese hamster cells sensitive and resistant to topoisomerase II inhibitors. *Biochim. Biophys. Acta* **1760,** 1646–1656
19. Jelinic, P., Stehle, J. C., and Shaw, P. (2006) The testis-specific factor CTCFL cooperates with the protein methyltransferase PRMT7 in H19 imprinting control region methylation. *PLoS Biol.* **4,** e355
20. Gonsalvez, G. B., Tian, L., Ospina, J. K., Boisvert, F. M., Lamond, A. I., and Matera, A. G. (2007) Two distinct arginine methyltransferases are required for biogenesis of Sm-class ribonucleoproteins. *J. Cell Biol.* **178,** 733–740
21. Thomassen, M., Tan, Q., Kruse, T. A. (2009) Gene expression meta-analysis identifies chromosomal regions and candidate genes involved in breast cancer metastasis. *Breast Cancer Res. Treat.* **113,** 239–249
22. Yao, R., Jiang, H., Ma, Y., Wang, L., Wang, L., Du, J., Hou, P., Gao, Y., Zhao, L., Wang, G., Zhang, Y., Liu, D. X., Huang, B., and Lu, J. (2014) PRMT7 induces epithelial-to-mesenchymal transition and promotes metastasis in breast cancer. *Cancer Res.* **74,** 5656–5667
23. Osborne, T. C., Obianyo, O., Zhang, X., Cheng, X., and Thompson, P. R. (2007) Protein arginine methyltransferase 1: positively charged residues in substrate peptides distal to the site of methylation are important for substrate binding and catalysis. *Biochemistry* **46,** 13370–13381
24. Obianyo, O., Osborne, T. C., and Thompson, P. R. (2008) Kinetic mechanism of protein arginine methyltransferase 1. *Biochemistry* **47,** 10420–10427
25. Lee, J. H., Cook, J. R., Yang, Z. H., Mirochnitchenko, O., Gunderson, S. I., Felix, A. M., Herth, N., Hoffmann, R., and Pestka, S. (2005) PRMT7, a new protein arginine methyltransferase that synthesizes symmetric dimethylarginine. *J. Biol. Chem.* **280,** 3656–3664
26. Feng, Y., Wang, J., Asher, S., Hoang, L., Guardiani, C., Ivanov, I., and Zheng, Y. G. (2011) Histone H4 acetylation differentially modulates arginine methylation by an in *cis* mechanism. *J. Biol. Chem.* **286,** 20323–20334
27. Gary, J. D., and Clarke, S. (1998) RNA and protein interactions modulated by protein arginine methylation. *Prog. Nucleic Acid Res. Mol. Biol.* **61,** 65–131
28. Parra, M. A., Kerr, D., Fahy, D., Pouchnik, D. J., and Wyrick, J. J. (2006) Deciphering the roles of the histone H2B N-terminal domain in genome-wide transcription. *Mol. Cell Biol.* **26,** 3842–3852
29. Feng, Y., Xie, N., Jin, M., Stahley, M. R., Stivers, J. T., and Zheng, Y. G. (2011) A transient kinetic analysis of PRMT1 catalysis. *Biochemistry* **50,** 7033–7044
30. Antonysamy, S., Bonday, Z., Campbell, R. M., Doyle, B., Druzina, Z., Gheyi, T., Han, B., Jungheim, L. N., Qian, Y., Rauch, C., Russell, M., Sauder, J. M., Wasserman, S. R., Weichert, K., Willard, F. S., Zhang, A., and Emtage, S. (2012) Crystal structure of the human PRMT5:MEP50 complex. *Proc. Natl. Acad. Sci. U.S.A.* **109,** 17960–17965
31. Strahl, B. D., Briggs, S. D., Brame, C. J., Caldwell, J. A., Koh, S. S., Ma, H., Cook, R. G., Shabanowitz, J., Hunt, D. F., Stallcup, M. R., and Allis, C. D. (2001) Methylation of histone H4 at arginine 3 occurs *in vivo* and is mediated by the nuclear receptor coactivator PRMT1. *Curr. Biol.* **11,** 996–1000
32. Pal, S., Baiocchi, R. A., Byrd, J. C., Grever, M. R., Jacob, S. T., and Sif, S. (2007) Low levels of miR-92b/96 induce PRMT5 translation and H3R8/H4R3 methylation in mantle cell lymphoma. *EMBO J.* **26,** 3558–3569
33. Zhang, X., and Cheng, X. (2003) Structure of the predominant protein arginine methyltransferase PRMT1 and analysis of its binding to substrate peptides. *Structure* **11,** 509–520
34. Cura, V., Troffer-Charlier, N., Wurtz, J. M., Bonnefond, L., and Cavarelli, J. (2014) Structural insight into arginine methylation by the mouse protein arginine methyltransferase 7: a zinc finger freezes the mimic of the dimeric state into a single active site. *Acta Crystallogr. D Biol. Crystallogr.* **70,** 2401–2412
35. Hasegawa, M., Toma-Fukai, S., Kim, J. D., Fukamizu, A., and Shimizu, T. (2014) Protein arginine methyltransferase 7 has a novel homodimer-like structure formed by tandem repeats. *FEBS Lett.* **588,** 1942–1948
36. Tang, J., Gary, J. D., Clarke, S., and Herschman, H. R. (1998) PRMT3, a type I protein arginine *N*-methyltransferase that differs from PRMT1 in its oligomerization, subcellular localization, substrate specificity, and regulation. *J. Biol. Chem.* **273,** 16935–16945
37. Wyrick, J. J., and Parra, M. A. (2009) The role of histone H2A and H2B post-translational modifications in transcription: a genomic perspective. *Biochim. Biophys. Acta* **1789,** 37–44
38. Truant, R., and Cullen, B. R. (1999) The arginine-rich domains present in human immunodeficiency virus type 1 Tat and Rev function as direct importin β-dependent nuclear localization signals. *Mol. Cell Biol.* **19,** 1210–1217
39. Ebralidse, K. K., Grachev, S. A., and Mirzabekov, A. D. (1988) A highly basic histone H4 domain bound to the sharply bent region of nucleosomal DNA. *Nature* **331,** 365–367
40. Boulanger, M. C., Liang, C., Russell, R. S., Lin, R., Bedford, M. T., Wainberg, M. A., and Richard, S. (2005) Methylation of Tat by PRMT6 regulates human immunodeficiency virus type 1 gene expression. *J. Virol.* **79,** 124–131
41. Xie, B., Invernizzi, C. F., Richard, S., and Wainberg, M. A. (2007) Arginine methylation of the human immunodeficiency virus type 1 Tat protein by PRMT6 negatively affects Tat interactions with both cyclin T1 and the Tat transactivation region. *J. Virol.* **81,** 4226–4234

CHAPTER 5

PRMT9 is a Type II methyltransferase that methylates

the splicing factor SAP145

PRMT9 is a Type II methyltransferase that methylates the splicing factor SAP145

Yanzhong Yang[1,2], Andrea Hadjikyriacou[3], Zheng Xia[4], Sitaram Gayatri[1], Daehoon Kim[1], Cecilia Zurita-Lopez[3], Ryan Kelly[3], Ailan Guo[5], Wei Li[4], Steven G. Clarke[3] & Mark T. Bedford[1]

The human genome encodes a family of nine protein arginine methyltransferases (PRMT1–9), whose members can catalyse three distinct types of methylation on arginine residues. Here we identify two spliceosome-associated proteins—SAP145 and SAP49—as PRMT9-binding partners, linking PRMT9 to U2 snRNP maturation. We show that SAP145 is methylated by PRMT9 at arginine 508, which takes the form of monomethylated arginine (MMA) and symmetrically dimethylated arginine (SDMA). PRMT9 thus joins PRMT5 as the only mammalian enzymes capable of depositing the SDMA mark. Methylation of SAP145 on Arg 508 generates a binding site for the Tudor domain of the Survival of Motor Neuron (SMN) protein, and RNA-seq analysis reveals gross splicing changes when PRMT9 levels are attenuated. These results identify PRMT9 as a nonhistone methyltransferase that primes the U2 snRNP for interaction with SMN.

[1] Department of Molecular Carcinogenesis, The University of Texas MD Anderson Cancer Center, Smithville, Texas 78957, USA. [2] Department of Radiation Biology, Beckman Research Institute, City of Hope Cancer Center, Duarte, California 91010, USA. [3] Department of Chemistry and Biochemistry, Molecular Biology Institute, University of California Los Angeles, Los Angeles, California 90095, USA. [4] Division of Biostatistics, Department of Molecular and Cellular Biology, Baylor College of Medicine, Houston, Texas 77030, USA. [5] Cell Signaling Technology Inc., Danvers, Massachusetts 01923, USA. Correspondence and requests for materials should be addressed to Y.Y. (email: yyang@coh.org) or to M.T.B. (email: mtbedford@mdanderson.org).

Protein arginine methylation is an abundant post-translational modification, with ~0.5% of all arginine residues present in the methylated state in mouse embryonic fibroblasts[1]. Arginine methylation is enriched on RNA-binding proteins[2,3]. Indeed, over 50% of the arginine methylation found in mammalian cells is concentrated on heterogeneous nuclear ribonucleoproteins[4]. In addition, a number of well-characterized methylation sites are found on histone tails[5] and splicing factors[6]. Three distinct types of methylated arginine residues occur in mammalian cells. The most prevalent is omega-N^G,N^G-dimethylarginine[7]. In this case, two methyl groups are placed on one of the terminal nitrogen atoms of the guanidino group; this derivative is commonly referred to as asymmetric dimethylarginine (ADMA). Two other methyl-arginine derivatives occur, namely the symmetrically dimethylated arginine (SDMA) derivative, where one methyl group is placed on each of the terminal guanidino nitrogens, and the omega-monomethylated derivative (ω-MMA). These three types of arginine methylation are catalysed by the nine members of the family of protein arginine methyltransferases (PRMTs)[8]. The PRMTs are classified according to their methylation products[9]. Types I, II and III are able to generate MMA. Type I enzymes include PRMT1, PRMT2, PRMT3, PRMT4/CARM1, PRMT6 and PRMT8, and they all perform a second methylation step to generate the ADMA mark. PRMT5 is the lone Type II enzyme described to date, generating the SDMA mark. PRMT7 is a Type III enzyme and only generates a MMA mark[10]. PRMT9 has not yet been characterized, and it is the subject of this study.

PRMT9 has two distinguishing features: (1) similar to PRMT7, it contains an ancestral amino-acid sequence duplication that harbours a second putative *S*-adenosylmethionine (AdoMet)-binding motif, and (2) unique among the PRMTs, it has three N-terminal tetratricopeptide repeats (TPRs). PRMT9 was identified as a potential human PRMT at the same time as we described PRMT8 (ref. 11). In that study, we noted the presence of a gene on chromosome 4q31 encoding a protein most similar to PRMT7 that was relatively well expressed in different tissues and designated it as PRMT9 (ref. 11). In the past, the PRMT9 designation has also been used for the product of the human *FBXO11* gene on chromosome 2p16 (ref. 12), although FBXO11 is unlikely to be a *bona fide* PRMT[13]. In some literature and protein databases, the gene on human chromosome 4q31 has previously also been referred to as PRMT10, although PRMT9 is the approved symbol and recommended gene name by the HUGO Gene Nomenclature Committee. The characterization of the PRMT9 protein (Q6P2P2 in the UniProt database) has been elusive, mainly because well-known PRMT substrates such as histones and glycine-arginine-rich (GAR) motif-containing proteins are not recognized (or poorly recognized) by the enzyme. Fortuitously, we found that PRMT9 can monomethylate and symmetrically dimethylate a protein that it interacts with, the spliceosome-associated protein, SAP145 (SF3B2). Thus, PRMT9 joins PRMT5 as the only mammalian Type II enzymes. SAP145 is a component of the U2 snRNP (small nuclear ribonucleoprotein) that is recruited to the branch region located near the 3′ splice site, and plays a critical role in the early stages of splicing. We were able to functionally link PRMT9 levels to the regulation of alternative splicing. Thus, we identified PRMT9 as a modulator of the SAP145/SAP49 protein complex that likely plays an important role in snRNP maturation in the cytoplasm.

Results

PRMT9 identification and primary sequence features. The gene encoding PRMT9 was identified a number of years ago[11]. A scan of the PRMT9 amino-acid sequence for protein domains identified three TPRs at its N terminus (Supplementary Fig. 1). TPRs are helical features that often mediate protein–protein interactions[14]. In addition, similar to PRMT7, PRMT9 harbours two putative AdoMet-binding domains with a clear duplication and partial conservation of most of the six signature PRMT motifs present (Fig. 1a). A phylogenetic tree analysis of the encoded amino-acid sequences of all nine members of the PRMT family reveals that it is most closely related to PRMT7 (Fig. 1b). The PRMT9 protein, with its defining TPR motifs and ancestrally duplicated sequence, is highly conserved among vertebrates, and is occasionally present in invertebrate animals, but has no orthologues in fungal species or prokaryotes (Supplementary Fig. 1).

PRMT9 associates with the SAP145 and SAP49 splicing factors. To help establish what biological processes PRMT9 may be associated with, we identified proteins that co-purified with PRMT9 expressed in HeLa cells. We performed tandem affinity purification of a TAP-tagged PRMT9 fusion, followed by tryptic digestion and mass spectrometry of the major interacting bands to identify the primary PRMT9 protein complex. The two major interacting proteins were identified as SAP145 and SAP49 (Fig. 2a). These splicing factors, also known, respectively, as SF3B2 and SF3B4, are tightly associated with each other[15]. We next developed a monoclonal antibody that specifically recognized the human PRMT9 protein (Supplementary Fig. 2a–f). Subcellular localization studies, using this antibody, revealed that PRMT9 is mainly a cytoplasmic protein (Supplementary Fig. 2d,e). Using this αPRMT9 antibody and antibodies against endogenous SAP145, we found that PRMT9 and SAP145 were reciprocally co-immunoprecipitated from HeLa cells (Fig. 2b). Similarly, green fluorescent protein (GFP)-tagged SAP49 co-immunoprecipitated with endogenous PRMT9 (immunoprecipitating antibodies to endogenous SAP49 are unavailable; Fig. 2c). To determine whether the interaction between PRMT9 and SAP145 is specific for this arginine methyltransferase, we transfected the complete set of GFP-tagged PRMTs into HeLa cells and immunoprecipitated them. Only GFP-PRMT9 was able to co-immunoprecipitate SAP145 (Fig. 2d). We have previously shown that PRMT3 interacts strongly with its substrate, RPS2 (refs 16,17), and this interaction serves as a control here.

Interaction of PRMT9 with SAP145. Next, we mapped the region of SAP145 that interacts with PRMT9. To do this, we broke the SAP145 protein into four roughly equal fragments (F1–4) and expressed them as glutathione *S*-transferase (GST) fusion proteins (Fig. 3a), which we then used to perform a GST pull-down assay with HeLa cell lysates. Western blot analysis revealed that cellular PRMT9 interacts with fragment F3 of SAP145, which encodes for amino acids 401–550 (Fig. 3b). This fragment has no distinctive structural features that could help explain the specificity of PRMT9 for this region. We also tested whether the recombinant GST-SAP49 can pull down endogenous PRMT9 using the similar experimental strategy. Interestingly, GST-SAP49 does not interact with PRMT9, suggesting that PRMT9 resides in the SAP145/SAP49 complex through an interaction with SAP145 (Supplementary Fig. 3a). We then attempted to perform reciprocal mapping of this interaction to establish which region of PRMT9 associates with SAP145. To do this, we generated a series of flag-tagged PRMT9 deletion constructs (Supplementary Fig. 3b). We were particularly interested in the possibility that the TPR motifs would interact with SAP145. However, these motifs proved not to be sufficient for SAP145 binding. Indeed, none of the PRMT9 deletion constructs could interact with SAP145 (or SAP49; Supplementary Fig. 3c),

even though the full-length tagged enzyme retained its binding abilities. This suggests that complete structural integrity of PRMT9 is required to maintain the PRMT9/SAP145/SAP49 protein complex. Supporting this idea, we found that the catalytically inactive form of PRMT9 lost its ability to interact with SAP145 (Fig. 3c,d). In addition, while SAP145 and SAP49 were associated with wild-type GFP-PRMT9 expressed in HEK293 cells, neither splicing factor was found to be associated with a catalytically inactive GFP-PRMT9 similarly expressed (data not shown). These results suggest that the integrity of the AdoMet-binding domain of PRMT9 is critical for its interaction with SAP145, and that PRMT9 may release SAP145 after substrate methylation, once it takes on its *S*-adenosylhomocysteine (AdoHcy)-bound form. Thus, to test whether PRMT9 bound to its product inhibitor AdoHcy would also not interact with SAP145, we treated HeLa cells with adenosine-2′,3′-dialdehyde, which results in elevated cellular AdoHcy levels[18]. We then performed a co-immunoprecipitation (co-IP) experiment to evaluate the impact of the AdoMet/AdoHcy switch on the PRMT9/SAP145 interaction. Interestingly, adenosine-2′,3′-dialdehyde treatment did not affect the PRMT9/SAP145 interaction, indicating that the AdoHcy-bound form of PRMT9 still likely interacts with its substrate (Supplementary Fig. 3d).

PRMT9 is a Type II PRMT that methylates SAP145. Using *in vitro* methylation assays with insect cell expressed HA (haemagglutinin)-PRMT9 and the four fragments of SAP145 as potential substrates, we found that only the F3 fragment that physically interacted with PRMT9 (Fig. 3b) was also a good methyl-acceptor for the enzyme (Fig. 4a). The F2 fragment could not be expressed well, and thus cannot be excluded as a possible substrate. No methylation of the F3 fragment was seen in a similarly expressed PRMT9 enzyme that was mutated in the AdoMet-binding site (Fig. 4a). We find that PRMT9 has little or no activity on the typical substrates of other PRMTs including core histones or GAR motif-containing proteins (data not shown). To determine the methylated arginine products of PRMT9, the *in vitro* ^{3}H-methylated F3 fragment of SAP145 was

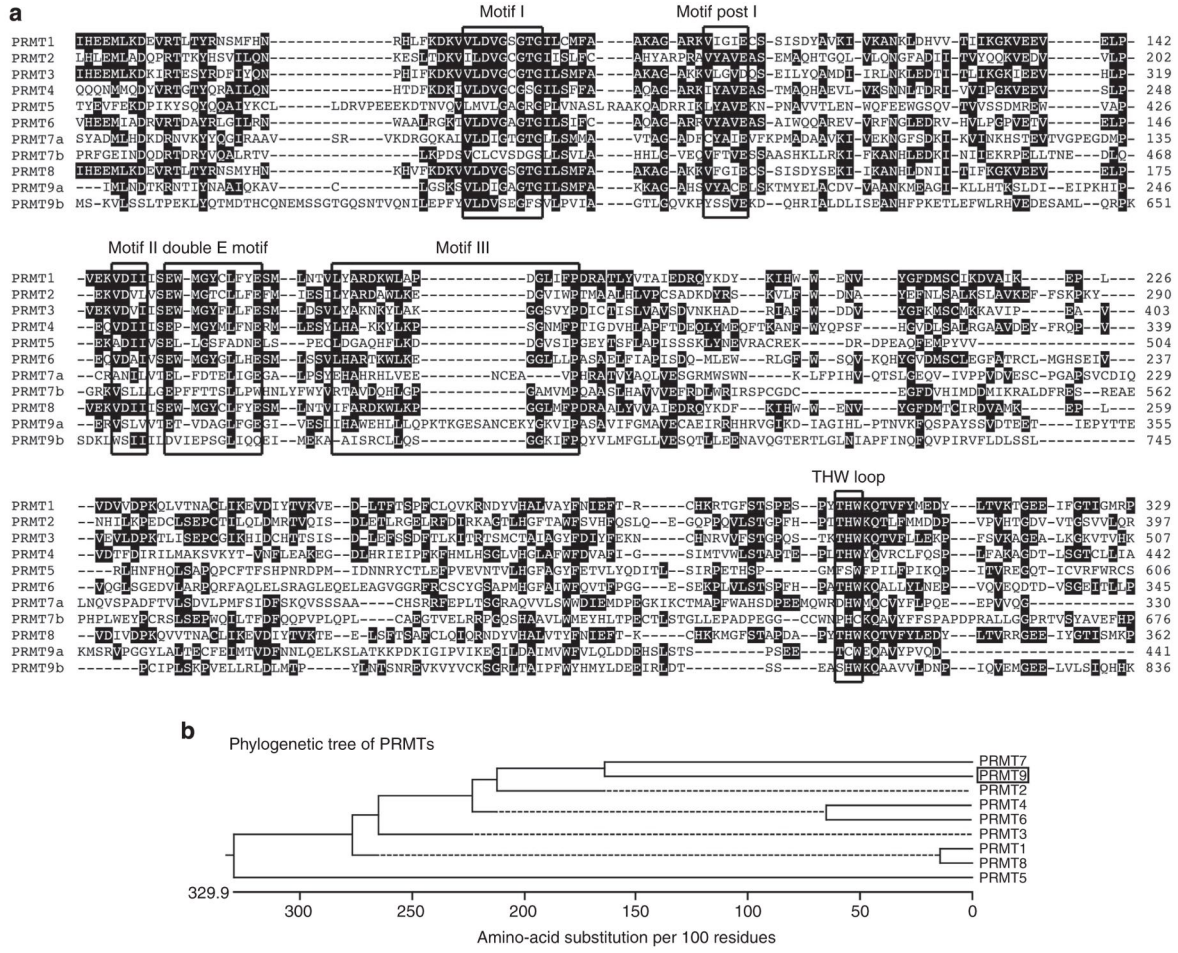

Figure 1 | Amino-acid sequence alignment of human PRMTs. (**a**) The amino-acid sequences from the catalytic domain of PRMTs are compared using ClustalW. The signature sequence motifs are boxed with black squares, including the motifs common to seven beta strand enzymes (Motif I, Motif Post I, Motif II and Motif III) as well as the Double E Motif and THW Loop motifs that are specific to PRMTs. The number on the right indicates the positions of amino acid of individual PRMT, starting at the initiator methionine. Human PRMT sequences used included PRMT1: NP_001527.3; PRMT2: NP_996845.1; PRMT3: NP_005779.1; PRMT4: NP_954592.1; PRMT5: NP_006100.2; PRMT6: NP_060607.2; PRMT7: NP_061896.1; PRMT8: NP_062828.3; and PRMT9: NP_612373.2. (**b**) A straight branched phylogenetic tree of all human PRMTs (shown in phenogram) was generated using ClustalW to demonstrate the evolutionary relationships among these enzymes. Protein sequence accession numbers used in the analysis are listed above.

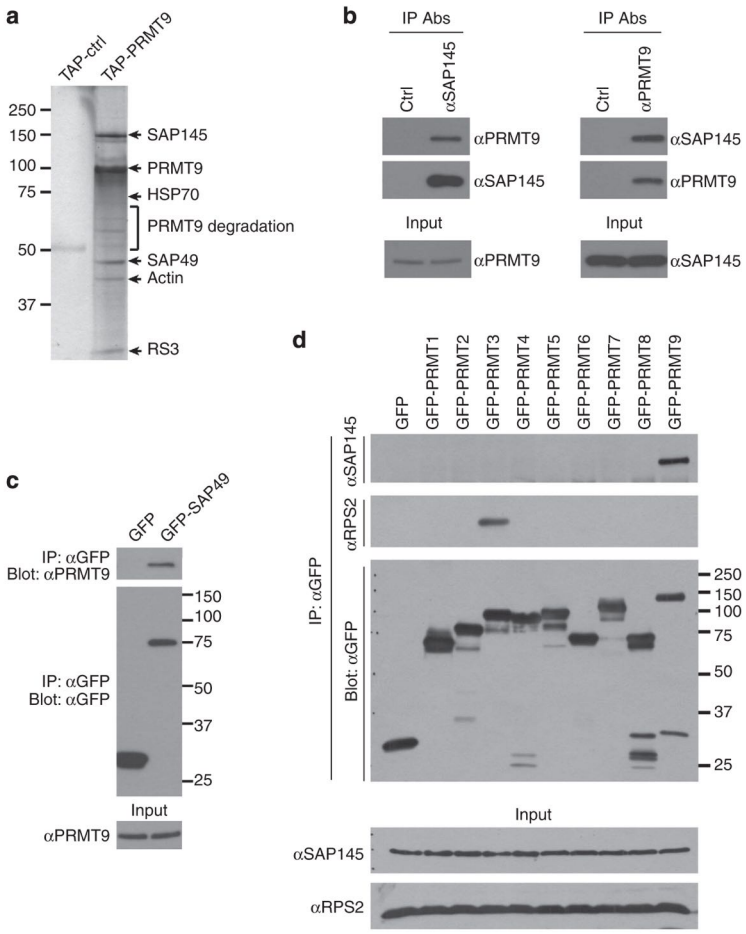

Figure 2 | PRMT9 interacts with SAP145 and SAP49. (**a**) TAP-tag purification of the PRMT9 protein complex from HeLa cells. HeLa cells were transiently transfected with either empty TAP-tag vector (TAP-Ctrl) or TAP-tag PRMT9 (TAP-PRMT9). A standard TAP procedure was applied. The eluted protein complex was separated by SDS–PAGE and silver-stained. The indicated gel slices were processed for protein identification using mass spectrometry. Actin, heat-shock protein 70 (HSP70) and 40S Ribosomal Protein S3 (RS3) are likely nonspecific interacting proteins. (**b**) PRMT9 and SAP145 co-immunoprecipitate. Reciprocal co-IP was performed in HeLa cells. Total cell lysates were immunoprecipitated with rabbit control IgG, αSAP145 antibody (left) and mouse control IgG, αPRMT9 antibody (right). The eluted protein samples were detected by western blotting with αPRMT9 and αSAP145 antibodies. The input samples were detected with αPRMT9 and αSAP145 antibodies, respectively. (**c**) PRMT9 and SAP49 co-immunoprecipitate. HeLa cells were transiently transfected with either GFP control vector or GFP-SAP49 plasmids. Total cell lysates were immunoprecipitated with αGFP antibody. The eluted protein samples were detected by western blotting with αPRMT9 and αGFP antibodies. The input samples were detected with αPRMT9. (**d**) Among all the PRMTs, only PRMT9 interacts with SAP145. HeLa cells were transiently transfected with control GFP vector and GFP-PRMTs (1 through 9). The total cell lysates were immunoprecipitated with αGFP antibody. The eluted protein samples were detected by western blotting with αSAP145, αRPS2 and αGFP antibodies. The input samples were detected with αSAP145 and αRPS2 antibodies.

subjected to amino-acid analysis. Mammalian expressed GFP-tagged PRMT9 was found to catalyse the formation of both MMA and SDMA only in the presence of the SAP145 fragment (Fig. 4b). No methylation was observed in control experiments with the PRMT9 fusion protein mutated in the AdoMet-binding site, demonstrating that the observed activity is intrinsic to tagged PRMT9 and not to another enzyme that might be co-purifying with it (Fig. 4a,b). To confirm the formation of SDMA, the radioactive peak from the cation-exchange amino-acid analysis column (corresponding to fractions 57–60) was subjected to thin-layer chromatography under conditions that separated MMA, SDMA and ADMA by their hydrophobic properties. We found that all of the radioactivity comigrated with SDMA (Fig. 4c), demonstrating that PRMT9 is a bona fide type II PRMT and joins PRMT5 as only the second enzyme of this type in mammals. A time course of *in vitro* methylation over a period of 20 h showed a steady accumulation of both MMA and the final product, SDMA (Supplementary Fig. 4a,b).

To localize the site or sites of methylation by PRMT9 on SAP145, each of the 10 arginine residues in the F3 fragment was replaced with a lysine residue. The F3 fragments containing lysine residues at nine of these sites were equally good methyl-acceptors. However, when R508 was mutated to lysine, methylation was greatly diminished, indicating the specificity of PRMT9 for this residue (Fig. 4d).

Importantly, PRMT9 is an active enzyme when purified from insect cell (Fig. 4a) and from mammalian cells (Supplementary Fig. 5a), but shows little or no activity when isolated as a GST

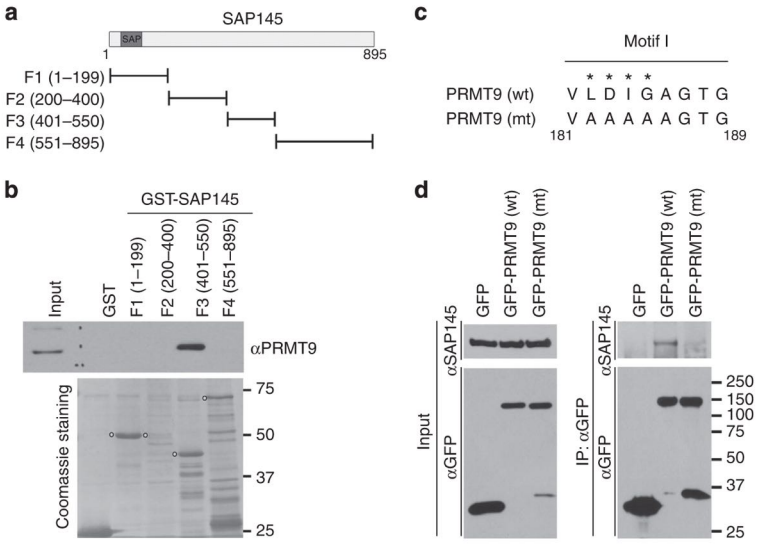

Figure 3 | Mapping the interaction regions of PRMT9 and SAP145. (**a**) A series of GST fusion truncations of SAP145 were generated. The location of the SAP (SAF-A/B, *A*cinus and *P*IAS) domain is indicated. (**b**) PRMT9 interacts with the amino acids 401–550 of SAP145. GST pull-down experiment was performed by incubating HeLa cell total lysates with purified GST or GST-tag SAP145 fragments described in **a**. The pull-down samples were eluted and detected by western blotting using the αPRMT9 antibody. The loading of the proteins was visualized by Coomassie staining of the membrane. The open circles indicate the individual GST-tag SAP145 fragments. (**c**) Generation of enzymatic mutant PRMT9. The asterisked amino acids (LDIG) located within the conserved Motif I of PRMT9 were mutated to AAAA, causing the loss of methyltransferase activity of enzyme. The numbers below indicate the location of the amino acids on the protein. (**d**) Wild-type, but not the enzymatic mutant, PRMT9 interacts with SAP145. Co-immunoprecipitation was performed in HeLa cells transiently transfected with GFP control vector, GFP-PRMT9 (wt) and GFP-PRMT9 (mt), as described in **c**. Total cell lysates were immunoprecipitated with the αGFP antibody. The eluted protein samples were detected by western blotting with αSAP145 and αGFP antibodies. The input samples were detected with αSAP145 and αGFP antibodies as well.

fusion protein from bacteria (Supplementary Fig. 5b). We next tested the ability of a set of eight GST-PRMTs to methylate SAP145-F3. We found that PRMT6 could also readily methylate the F3 fragment, but that no methylation was found with the other enzymes under these conditions (Supplementary Fig. 5b). Furthermore, we tested the ability of Myc-PRMT5 (GST-PRMT5 is inactive and was thus not tested in Supplementary Fig. 5b) to methylate SAP145-F3, and we found that it was unable to do so (Supplementary Fig. 5C). Importantly, further analysis using the mutated SAP145-F3 fragments as substrates revealed that PRMT6 mainly methylates the R515 site (Supplementary Fig. 5d); therefore, PRMT9 and PRMT6 modify distinct sites on SAP145. Thus, it appears that the SDMA mark at the R508 site of SAP145 is only deposited by PRMT9, and no other Type I or Type II PRMT modifies this site.

Reduced PRMT9 levels impact SAP145 methylation. To confirm the existence of the SAP145 R508me2s mark in cells, we generated a methyl-specific antibody against this site. Initially, we performed an *in vitro* characterization of this antibody and we showed that recombinant SAP145-F3 can only be recognized by the αSAP145 R508me2s antibody when it is subjected to prior methylation by PRMT9 (Fig. 5a). For immunoreactivity, the methyl-specific antibody also requires the presence of the R508 site. Thus, this antibody is indeed methyl-specific and site-specific (Fig. 5b). To establish whether this site is arginine-methylated in cells, we transfected HeLa cells with wild-type or mutant GFP-SAP145 (R508K), and performed western blot analysis with the αSAP145 R508me2s methyl-specific antibody (Fig. 5c). The antibody clearly detected the wild-type form of the ectopically expressed fusion protein, but not the mutant form. The endogenous untagged SAP145 protein is also detected as a band that migrates slightly faster than the tagged form. When we repeated this experiment, but co-transfected cells with both SAP145 and PRMT9, we observed a dramatic increase in the levels of the SAP145 methylation as detected with the methyl-specific antibody (Fig. 5d). Endogenous SAP145 methylation cannot be further enhanced by PRMT9 overexpression (data not shown), suggesting that endogenous SAP145 is fully methylated at the R508 site. This is not a unique phenomenon for a PRMT substrate, as we have previously shown that poly(A)-binding protein 1 (PABP1) is fully methylated by CARM1, and overexpression of CARM1 cannot further increase the PABP1 methylation level[19]. If this is the case, then the knockdown of PRMT9 should correlate well with the decrease in SAP145 methylation levels, and this is indeed what we observe; endoribonuclease-prepared siRNA (esiRNA)-mediated knockdown of PRMT9 concomitantly reduces the SAP145 methylation level as detected by αSAP145 R508me2s methyl-specific antibody (Fig. 5e).

The SMN interacts with methylated SAP145. PRMT9 seems to be a rather specific enzyme, and even though many methylated proteins can be detected in HeLa cell extract with pan-MMA and pan-SDMA antibodies, only SAP145 methylation is reduced when PRMT9 levels are lowered (Supplementary Fig. 6a). The SAP145 site (R508), which is the target of PRMT9 methylation, is highly conserved in vertebrates and invertebrates (Supplementary Fig. 6b), suggesting that it is a critical node of functional control, possibly through the regulation of protein–protein interactions. We first investigated whether methylation of this site regulated the interaction between SAP145 and SAP49. Overexpression of both PRMT9 and SAP145, which causes a dramatic increase in the R508me2s mark (Fig. 5d), does not alter the ability of SAP49 to interact with this protein complex (Supplementary Fig. 6c).

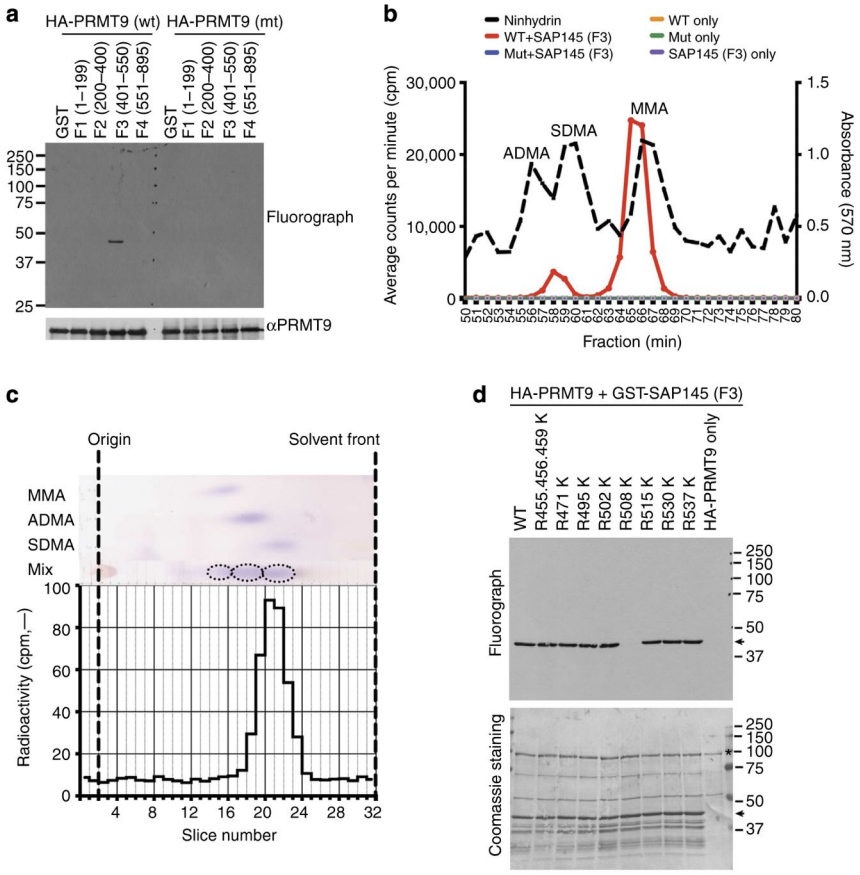

Figure 4 | PRMT9 catalyses symmetrical dimethylation of SAP145 at Arginine 508. (**a**) PRMT9 methylates SAP145 fragment F3 (a.a. 401–550). The *in vitro* methylation was performed by incubating either wild-type or enzymatic mutant recombinant HA-PRMT9 (purified from Sf21 cells) with GST or GST-tag SAP145 fragments (F1–F4, as described in Fig. 3a,b). The loading of PRMT9 was detected by western blotting using the αHA antibody. (**b**) PRMT9 symmetrically dimethylates SAP145 as detected by amino-acid analysis. Amino-acid analysis of *in vitro* methylation products from wild-type and enzymatic mutant GFP-PRMT9 as enzymes and GST-SAP145 (401–550) fragment as substrate. Black dashed line indicates elution of nonradiolabelled standards. The radioactive peaks elute 1–2 min before the nonradiolabelled standards due to a tritium isotope effect[39]. (**c**) PRMT9 symmetrically dimethylates SAP145 as detected by thin-layer chromatography (TLC). SDMA fractions from cation-exchange chromatography of the *in vitro* ^{3}H-methylation reaction were separated using TLC. Fractions were spotted on a cellulose plate along with the addition of 5 nmol MMA, 15 nmol ADMA and 5 nmol SDMA internal standards. Individual standards were also spotted in adjacent lanes to determine the migration distance of each methylated arginine derivative. The origin is indicated by fraction 2. The solvent front was run near the end of the plate to fraction 32. The plate was air-dried and each lane was subsequently sliced in 5-mm fractions and counted for three 30-min counting cycles. The radioactive peaks elute 1–2 min before the nonradiolabelled standards due to a tritium isotope effect[39]. This experiment was repeated three times, and similar migration patterns were observed. (**d**) PRMT9 methylates SAP145 at R508 *in vitro*. The *in vitro* methylation assay was performed by incubating recombinant HA-PRMT9 with a series of Arg to Lys (R to K) mutants of SAP145 fragment F3 (see Fig. 3a,b for description) for 1 h at 30 °C. After exposure at − 80 °C for 3 days, the membrane was stained with Coomassie blue to check the protein loading. Arrows indicate the positions of the substrates and stars indicate the positions of the recombinant HA-PRMT9.

Furthermore, disruption of the R508 methylation site does not affect the assembly of the SAP145/SAP49/PRMT9 complex (Supplementary Fig. 6d), suggesting that other protein–protein interactions may be regulated by this mark. Indeed, arginine methylation motifs create docking sites for the recognition by Tudor domain-containing proteins[20]. There are three Tudor domain-containing proteins that are well characterized as effector proteins for methyl-arginine marks, SPF30, Survival of Motor Neuron (SMN) and TDRD3 (ref. 5). SMN has been extensively studied and is involved in the assembly of ribonucleoprotein complexes, an important step for snRNP maturation, which regulates mRNA splicing[21]. When we performed a co-IP experiment, we observed the endogenous interaction of SMN with SAP145 (Fig. 6a). To address whether the Tudor domain of the SMN protein mediates this interaction, we performed a GST pull-down assay using the Tudor domains from three different proteins (SPF30, SMN and TDRD3). We incubated the GST-tagged recombinant proteins with HeLa cell lysates that were transiently transfected with either wild-type GFP-SAP145 or GFP-SAP145 (R508K) mutant. After pull-down and western blot analysis with αGFP antibody, we observed an interaction between the Tudor domain of SMN and ectopically expressed SAP145, but not with the methylation-deficient SAP145 (R508K; Fig. 6b). To further confirm this interaction in the cells, we performed co-IP of endogenous SMN with exogenously expressed GFP-SAP145 or GFP-SAP145 (R508K) mutant. Similar to what we observed in the pull-down experiment, endogenous SMN interacts with GFP-SAP145, but not with the methylation-deficient mutant (Fig. 6c).

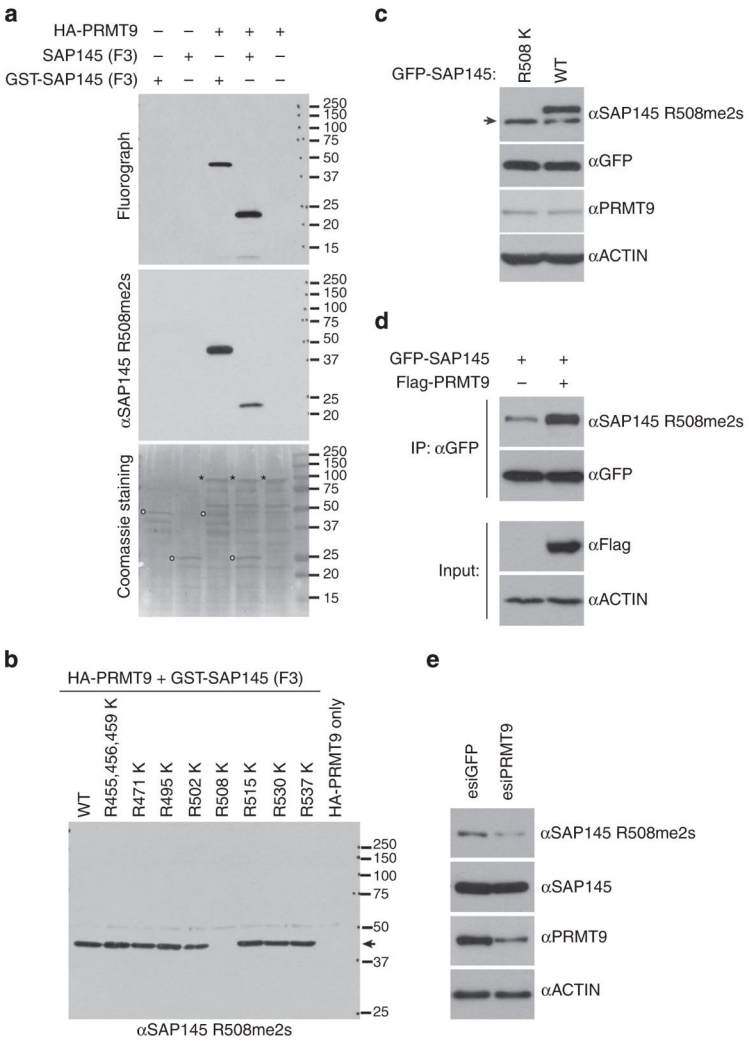

Figure 5 | PRMT9 symmetrically methylates SAP145 at Arg 508 *in vivo*. (**a**) SAP145 R508 methylation-specific antibody detects *in vitro* methylated SAP145. The *in vitro* methylation assay was performed using recombinant HA-PRMT9 as enzyme, either GST-tag SAP145 fragment F3 or SAP145 fragment F3 without GST-tag (cleaved by PreScission Protease) as substrates. The samples were run on a SDS-PAGE gel followed by exposure to X-ray film for 3 days. After exposure, the membrane was stripped and detected using SAP145 R508 methylation-specific antibody (αSAP145 R508me2s) by western blotting. The membrane was then stained with Coomassie blue to check the protein loading. Open circles indicate the positions of the substrates and stars indicate the position of the recombinant HA-PRMT9. (**b**) Arg to Lys mutation at the R508 site of SAP145 abolishes the recognition of αSAP145 R508me2s antibody. The same membrane, described in Fig. 4 (**d**), was stripped and detected using the αSAP145 R508me2s antibody by western blotting. The arrow indicates the position of specific signal detected by the antibody. (**c**) Arg 508 of SAP145 is symmetrically dimethylated in the cells. HeLa cells were transiently transfected with either GFP-SAP145 or GFP-SAP145 (R508K). 30 μg of total cell lysates were subjected to western blotting detection with αSAP145 R508me2s, αGFP, αPRMT9 and αActin antibodies. The arrow indicates the endogenous SAP145 methylation signals. (**d**) Overexpression of PRMT9 increases SAP145 R508 symmetrical dimethylation. HeLa cells were transfected with either GFP-SAP145 alone, or GFP-SAP145 and Flag-PRMT9. The total cell lysates were immunoprecipitated with αGFP antibody followed by western blotting with αSAP145 R508me2s and αGFP antibodies. The input samples were detected with αFlag and αActin antibodies. (**e**) Knockdown of PRMT9 decreases SAP145 R508-symmetric dimethylation. HeLa cells were transiently transfected with either control esiGFP (esiRNA targeting GFP) or esiPRMT9 (esiRNA targeting PRMT9). Total cell lysates (30 μg) were subjected to western blotting and detected with αSAP145 R508me2s, αSAP145, αPRMT9 and αActin antibodies.

To address whether SMN-SAP145 interaction is regulated by PRMT9, we transfected HeLa cells either with GFP-SAP145 alone or with GFP-SAP145 and Flag-PRMT9, followed by a co-IP assay to assess the influence of PRMT9 overexpression on the SMN–SAP145 interaction. Overexpression of PRMT9 dramatically increases the levels of the GFP-SAP145 methylation as detected with the methyl-specific antibody (Fig. 6d, right panel). Concomitantly, the interaction between SMN and GFP-SAP145 was greatly enhanced (Fig. 6d, left panel). These results demonstrate that SAP145 R508 methylation by PRMT9 creates a recognition motif for the Tudor domain of SMN, thus facilitating the assembly of the SMN–SAP145 complex. We next investigated whether the SMN–SAP145 interaction is important for U2 snRNP maturation. To do this, we transfected HeLa cells

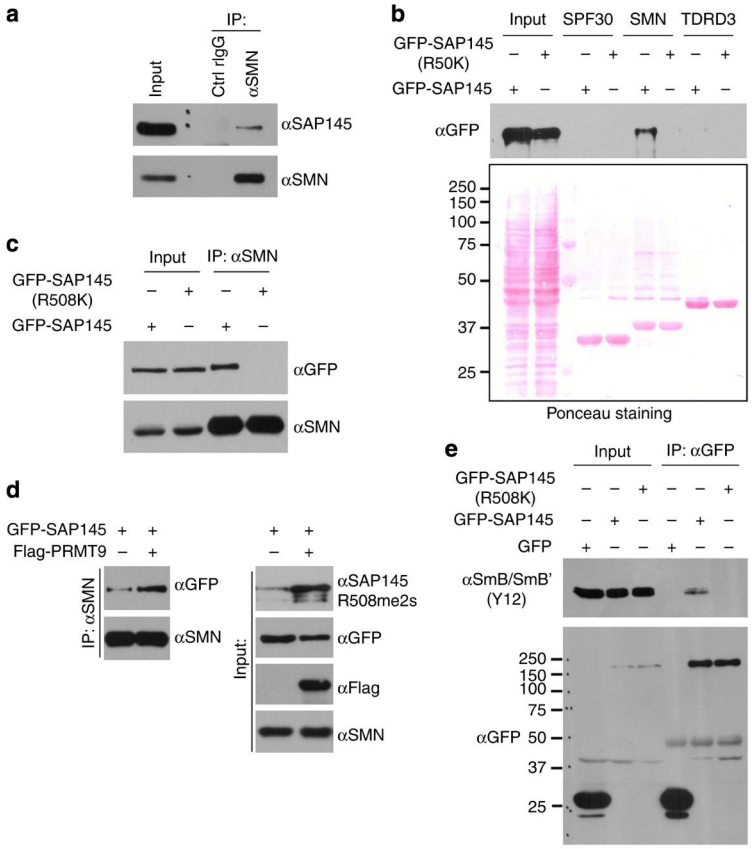

Figure 6 | Methylation of arginine 508 is required for SAP145–SMN interaction. (**a**) SMN interacts with SAP145 *in vivo*. Endogenous co-IP was performed by immunoprecipitating HeLa cell nuclear extracts using αSMN antibody, followed by western blotting detection using the αSAP145 antibody. (**b**) The Tudor domain of SMN interacts with wild-type but not R508K mutant form of SAP145. HeLa cells were transfected with either GFP-SAP145 or GFP-SAP145 (R508K). GST pull-down experiment was performed by incubating transfected cell lysates with recombinant GST-Tudor domains of SPF30, SMN and TDRD3. Eluted samples were detected by western blotting with αGFP antibody. Ponceau S staining displays the loading of total cell lysates and recombinant proteins. (**c**) SMN interacts with the wild-type but not the R508K mutant form of SAP145. HeLa cells were transfected with either GFP-SAP145 or GFP-SAP145 (R508K). The nuclear extracts were immunoprecipitated with αSMN antibody. The eluted samples and input samples were detected with the indicated antibodies. (**d**) Overexpression of PRMT9 enhances the interaction of SMN with GFP-SAP145. HeLa cells were transfected with the indicated plasmids. The nuclear extracts were immunoprecipitated with the αSMN antibody. The eluted samples and input samples were detected with the indicated antibodies. (**e**) An intact SAP145 R508 methylation site is required for U2 snRNP maturation. HeLa cells were transfected with either GFP-SAP145 or GFP-SAP145 (R508K). Cell lysates were immunoprecipitated with the αGFP antibody. The eluted samples and input samples were detected with αSmB (Y12) and with αGFP antibodies.

with either GFP-SAP145 or GFP-SAP145 (R508K), and then performed an αGFP immunoprecipitation. An intact methylation site was required for SmB/B′ association with GFP-SAP145, strongly suggesting that the PRMT9 methylation site is critical for SMN-mediated Sm core assembly of the U2 snRNP (Fig. 6e).

PRMT9 is required for efficient alternative splicing. The robust and specific interaction between PRMT9 and SAP145/SAP49 (Fig. 2), the ability of PRMT9 to methylate SAP145 (Fig. 4) and the regulation of methylation-dependent SMN–SAP145 interaction by PRMT9 (Fig. 6) strongly suggest that PRMT9 is involved in the regulation of mRNA splicing. To investigate this possibility, we extracted total RNA from control knockdown and esiRNA-mediated PRMT9 knockdown HeLa cells and subjected them to RNA-sequencing (RNA-seq) analysis, particularly focusing on changes in alternatively spliced events. To reduce the experimental variation, two sets of biological replicates were prepared. Western blot analysis demonstrated the efficient knockdown of endogenous PRMT9 in both replicate samples (Fig. 7a). For RNA-seq, we performed 75-nt paired-end sequencing and achieved ~220 million and 120 million unique mapped reads for control knockdown and PRMT9 knockdown, respectively. We used a mixture-of-isoform (MISO) model 2 to compute and quantify alternative splicing events. We were able to identify five types of alternative splicing events, which were significantly altered. These events included 34 skipped exons, 13 retained introns, 9 alternative 3′ splice sites, 9 alternative 5′ splice sites and 3 mutually exclusive exons (Supplementary Table 1). One example of the MISO output landscape is displayed in Fig. 7b, showing RNA-seq read coverage across EDEM1 exon 8 to exon 10 from esiGFP control and esiPRMT9 knockdown HeLa cells. To validate the alternative splicing called by MISO, reverse transcription–polymerase chain reaction (RT–PCR) was performed using the primers located within the flanking exons of the *EDEM1* gene. Knockdown of PRMT9 using esiRNA reduces the

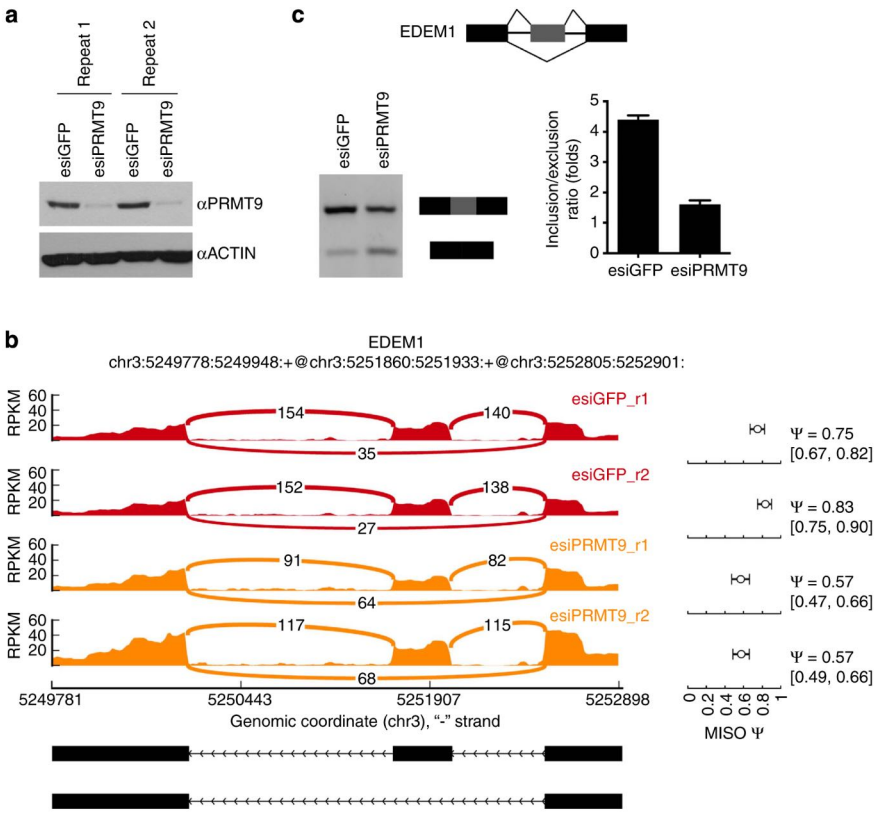

Figure 7 | PRMT9 regulates alternative splicing. (**a**) Two sets of biological replicated samples for RNA-seq. HeLa cells were transiently transfected with esiGFP control or esiPRMT9. The total RNA was extracted 72 h after transfection. Western blotting confirms the knockdown of the PRMT9 protein using αPRMT9 and αActin antibodies. (**b**) RNA-seq read coverage across EDEM1 exon 8 to exon 10 from esiGFP control and esiPRMT9 knockdown HeLa cells. MISO (Ψ) values and 95% confidence intervals were shown at right. (**c**) Validation of exon exclusion of EDEM1 exon 9 in response to PRMT9 knockdown. RT-PCR experiments were performed using RNA extracted from esiGFP control and esiPRMT9-transfected HeLa cells with primers located on exon 8 and exon 10 (left panel). The PCR products were quantified using the densitometric analysis. Inclusion versus exclusion ratio was calculated. Error bars represent s.d. calculated from three independent experiments (right panel).

inclusion/exclusion ratio to ~2.5-fold (Fig. 7c). At another gene loci (*NGLY1*), knockdown of PRMT9 expression increases the inclusion/exclusion ratio to ~2.5-fold (Supplementary Fig. 7a,b). It should be noted that esiRNA-mediated knockdown of PRMT9 only causes an ~50% decrease in the SAP145 R508 methylation level (Fig. 5e). A small amount of enzyme is still capable of carrying out substantial methylation. This may explain why we can only capture a small group of altered splicing events. Total removal of PRMT9 may have more profound effects on alternative splicing. Thus, PRMT9 is having an impact on alternative splicing in a number of different ways, possibly through its ability to methylate SAP145 and promote the interaction between SAP145 and SMN.

Discussion

We have demonstrated that PRMT9 is a Type II enzyme using both amino-acid analysis approaches and methyl-specific antibodies that recognize the SDMA mark on SAP145. It is unclear how many additional substrates PRMT9 might have; however, it is likely not as promiscuous as PRMT5, which methylates a broad swath of GAR motif-containing proteins. PRMT5 is the founding member of the Type II class of PRMTs, and clearly the dominant enzyme in this class. When cell lysates are subjected to western blot analysis using pan-SDMA antibodies, the majority of the bands detected in wild-type cells are lost in PRMT5 knockdown cell lines[1]. Quantification of the different types of arginine methylation across a large number of tissue and cell types have estimated the ratios to be roughly 1,500:3:2:1 for Arg:ADMA:MMA:SDMA[1,7,22]. Measurements of cellular SDMA levels using PRMT5 knockout (KO) cells are yet to be performed; however, this would establish what proportion of the SDMA is deposited by PRMT5 and PRMT9, respectively. Although PRMT5 and PRMT9 are both Type II enzymes, they do not display redundancy. In *in vitro* methylation assays these two PRMTs do not recognize each other's substrates (Supplementary Fig. 5c and data not shown). In addition, subsets of SDMA-specific antibodies selectively recognize PRMT5 or PRMT9 substrates as validated using the respective knockdown cell extracts (data not shown). The extended seven-amino-acid (CFKRKYL) PRMT9 methylation motif in SAP145 (Supplementary Fig. 6b) is not found in any other protein. However, when we reduce the search to a five-amino-acid motif (FKRKY) we did identify eight human proteins that could possibly be substrates for this newly characterized enzyme, and they will be tested in the near future.

After we designated the gene on human chromosome 4q31 as PRMT9 (ref. 11), this designation was also used for the *FBXO11*

gene on human chromosome 2p16 (ref. 12). FBXO11 does not contain the signature amino-acid sequence motifs of the PRMT family and the description of its activity as a PRMT likely was the result of contamination of the FLAG-tagged protein with PRMT5 (ref. 12). No methyltransferase activity has been observed with the nematode homologue of FBXO11 (ref. 13). It has been clearly shown that the monoclonal M2 antibody used to pull down FLAG-tagged proteins will also bring down endogenous PRMT5, thus contaminating any preparation of a FLAG-tagged protein[9,23]. Owing to the usage of PRMT9 for both of these gene products, PRMT10 has also been used to designate the 4q31 product. However, PRMT9 is now the approved symbol and recommended gene name by the HUGO Gene Nomenclature Committee for the PRMT characterized in this work.

Classic studies in the arginine methylation field first implicated this post-translational modification in the regulation of RNA metabolism[3,4]. More recently, large-scale proteomic analysis of arginine-methylated proteins revealed the identity of many of these RNA-binding proteins[24,25]. Both Type I and Type II PRMTs are involved in the regulation of splicing. The Type I enzyme, CARM1, enhances exon skipping in an enzyme-dependent manner[6,26]. It regulates splicing by methylating a number of splicing factors (CA150, SAP49, SmB and U1C), likely at transcriptionally active sites to which it is recruited as a transcriptional coactivator[6]. PRMT6 is another transcriptional co-regulator that does not exclusively modulate gene expression, but also has an impact on alternative splicing patterns[27]. Indeed, transcriptome analysis of PRMT6 knockdown cells revealed a number of gene-specific exon pattern changes, including altered exon retention and exon skipping[28]. The Type II enzyme, PRMT5, functions as a transcriptional repressor in the nucleus by symmetrically methylating histone H4R3 and H3R8 (ref. 29). In the cytoplasm, PRMT5 is primarily found in the 20S methylosome complex, along with MEP50, pICIn and various Sm proteins (SmB/B′, D1–3, E, F and G)[30–32]. In this complex, the Sm proteins are symmetrically dimethylated by PRMT5. In turn, the methylated Sm proteins interact with the Tudor domain of SMN[33], which helps to load the Sm proteins on spliceosomal snRNAs (U1, U2, U4, U5, U11 and U12)[21,34]. Thus, PRMT5 plays a critical role in spliceosomal U snRNP maturation. PRMT5 has a rather central role in pre-mRNA splicing, and it is assumed that pleiotropic splicing defects will be observed on PRMT5 loss; this is indeed the case. The conditional removal of PRMT5 in mouse neural progenitor cells results in defects in both constitutive splicing and alternative splicing[35]. Furthermore, in *Arabidopsis*, PRMT5 is essential for proper pre-mRNA splicing[36,37].

The splicing factors SAP145 and SAP49 are tightly associated with each other[15]. SAP145 and SAP49 are dedicated components of the nuclear U2 snRNP. The region of SAP145 that interacts with SAP49 has been mapped, and it lies adjacent to the R508me2s site[38]. Methylation of R508 does not have an impact on the SAP145/SAP49 interaction (Supplementary Fig. 6). The PRMT9/SAP145/SAP49 complex likely forms in the cytoplasm, where PRMT9 deposits the SAP145^{R508me2s} mark for subsequent recognition by SMN. In mammals, newly synthesized snRNAs are first exported to the cytoplasm, where they undergo maturation (partial snRNP complex assembly) before being imported back into the nucleus to form catalytically active snRNPs[21]. As described above, PRMT5 plays a critical role in the biogenesis of the Sm-class of spliceosomal snRNPs. PRMT9 seems to add another level of maturation, which is specific for U2 snRNA. A fairly unique feature of PRMT9 is its ability to strongly interact with its substrate, SAP145 (Fig. 2d); most PRMTs, with the exception of PRMT3, do not do this. The PRMT9/SAP145 interaction occurs in the cytoplasm. However, copious quantities of SAP145 are observed in the nucleus[38]. Thus, it is likely that some signals, perhaps a post-translational modification, regulate the dissociation of PRMT9 and SAP145 to facilitate nuclear translocation of the maturing U2 snRNP. Indeed, we observe reduced SmB/B′ association with mutant SAP145 (GFP-SAP145^{R508K}), which is indicative of an U2 snRNP maturation defect. This flaw in U2 snRNP maturation could modify the fidelity of branch point recognition and alter a subset of alternative splicing events.

Methods

Plasmids and antibodies. Human PRMT9 cDNA (NM_138364.2) was subcloned into a pGEX-6p-1 vector (GE Healthcare Life Sciences), a pEGFP-C1 vector (Clontech) and a 3XFlag vector (Invitrogen). NTAP-PRMT9 used for tandem affinity purification was generated by cloning human PRMT9 cDNA into pCeMM NTAP(GS) vector (EUROSCARF). Human SAP49 cDNA, SAP145 cDNA and its truncated cDNAs were cloned into pEGFP-C1 vector. Both wild-type and mutant HA-PRMT9 were cloned into pBacPAK vector (Clontech) for insect cell expression. Rabbit anti-GFP polyclonal antibody was purchased from Invitrogen (Cat no. A6455, used for IP, 2 µl per IP). Mouse anti-HA monoclonal antibody was purchased from Covance (Cat no. MMS-101P-200, used for western blot, 1:2,000 dilution). Mouse anti-Flag M2 monoclonal antibody was purchased from Sigma (Cat no. A2220, used for IP, 20 µl per IP). Rabbit anti-SAP145 polyclonal antibody was purchased from Novus Biologicals (Cat no. NB100-79848 used for western blot analysis, 1:3,000 dilution and IP, 5 µl per IP). Rabbit anti-SAP49 polyclonal antibody was purchased from Abcam (Cat no. ab66659, used for western blot analysis, 1:1,000 dilution). Mouse anti-PRMT9 monoclonal antibody was raised, using the recombinant GST-PRMT9 as antigen, by the Antibody Facility Core at M.D. Anderson Cancer Center (used for western blot analysis, 1:1,000 dilution and IP, 10 µl per IP). The SAP145^{R508me2s} antibody was identified in a screen for SDMA-specific antibodies (used for western blot, 1:1,000 dilution). Cell Signaling Technology generated this panel of antibodies using the XXXXR^{me2s}XXR^{me2s}XXXXR^{me2s}XXXR^{me2s}XXXX peptide as an antigen. The resulting antibodies were screened on PRMT5 KO cells, and the majority displayed a loss of immunoreactivity. However, two of these antibodies, BL8244 and BL8245, strongly recognized a band of roughly 150 kDa, which is not lost in PRMT5 KO cells. When we tested these two antibodies on PRMT9 knockdown cells, the immunoreactivity of this 150-kDa band was reduced. We thus went on to characterize these antibodies *in vitro* (Fig. 5). Uncropped immunoblots for each figure are shown in Supplementary Fig. 8.

Tandem affinity purification. HEK293 cells (from ATCC) were transfected with NTAP-PRMT9. A total of 1×10^8 cells were used for tandem affinity purification. In brief, cells were first lysed in lysis buffer containing 50 mM Tris-HCl (pH 7.5), 125 mM NaCl, 5% glycerol, 0.2% NP-40, 1.5 mM $MgCl_2$, 25 mM NaF, 1 mM Na_3VO_4 and protease inhibitors. After centrifugation at maximum speed for 10 min, the supernatant was incubated with rabbit-IgG Sepharose (GE Healthcare Life Sciences) at 4 °C for 4 h. The bound beads were first washed with lysis buffer and then with TEV-protease cleavage buffer (10 mM Tris-HCl (pH 7.5), 100 mM NaCl and 0.2% NP-40). The bound protein complexes were eluted by addition of 50 µg TEV protease (4 °C, overnight). TEV-protease cleavage products were then incubated with Streptavidin agarose (Millipore) at 4 °C for 2 h. The bound proteins were heated at 100 °C for 5 min in SDS sample buffer and analysed using SDS–PAGE followed by either silver staining or SYPRO Ruby staining. After comparison with the control samples, differentially expressed bands were cut from the gel and proteins were identified with liquid chromatography-tandem mass spectrometry (LC-MS/MS) using the Protein and Metabolite Analysis Core Facility at UT Austin.

Baculovirus expression and protein purification. HA-PRMT9 (both wild-type and the enzymatic mutant as described below) in pBacPAK8 vector were co-transfected with linearized Baculovirus DNA (BD Biosciences) using the FuGENE 6 transfection reagent (Roche). The expression and purification of recombinant proteins were followed according to the instruction manual of Baculovirus Expression Vector System (6th Edition, May 1999), except that HA-conjugated beads and HA peptide (Sigma) were used to bind and elute the recombinant proteins, respectively. Purified proteins were then dialysed in 1 × TBS buffer (50 mM Tris-Cl, pH 7.5, 150 mM NaCl) and used for the *in vitro* methylation assay.

Immunoprecipitation. HeLa cells were washed with ice-cold PBS and lysed with 1 ml of co-IP buffer (50 mM Tris-HCl (pH 7.5), 150 mM NaCl, 0.1% NP-40, 5 mM EDTA, 5 mM EGTA, 15 mM $MgCl_2$) with protease inhibitor cocktail. After sonication, insoluble materials were removed by centrifugation at maximum speed for 10 min. Whole-cell lysates were incubated with 2 µg of immunoprecipitation antibody overnight. After incubation with Protein A/G agarose beads, the bound proteins were eluted and analysed using western blot analyses.

Immunofluorescence. HeLa cells (from ATCC) were grown on glass coverslips to desired confluence before fixation. Cells were rinsed with PBS and fixed with 4% paraformaldehyde for 15 min at room temperature. After blocking with 20% newborn calf serum, cells were incubated with monoclonal PRMT9 antibody (1:1,000) at 4 °C overnight. Cells were then stained with secondary antibody and DAPI sequentially. The coverslips were then sealed and examined under a NIKON Eclipse E800 fluorescent microscope.

GST pull down. GST and different recombinant proteins were expressed and purified from *Escherichia coli*. The individual protein was incubated with HeLa cell lysates at 4 °C overnight. The protein complex was then incubated with Glutathione Sepharose 4B resin (GE Healthcare Life Sciences) for 1 h at 4 °C. The eluted samples were loaded on SDS–PAGE gel and detected with western blot analyses using the indicated antibodies. Equal loading of the recombinant proteins was visualized by either Coomassie blue staining or ponceau staining.

Nuclear and cytoplasmic extraction. Cytoplasmic and nuclear fractions of HeLa cells were extracted following the protocol as described in the instructions from the NE-PER Nuclear and Cytoplasmic Extraction Kit (Pierce Biotech).

esiRNA knockdown. esiRNA used for transient knockdown of PRMT9 was designed using the website http://cluster-12.mpi-cbg.de/cgi-bin/riddle/search. The preparation of dsRNA was followed according to the instructions of the MEGAscript RNAi Kit (Invitrogen). dsRNA was then digested with RNase III to produce a blender of 18- to 30-bp siRNA mixture. After purification, the esiRNA was dissolved in H_2O and tested for knockdown efficiency.

Site-directed mutagenesis. Human PRMT9 was mutated to create a catalytically inactive mutant by introducing quadruple mutations (L182A, D183A, I184A and G185A) in the conserved motif I in both the HA-PRMT9 and GFP-PRMT9 plasmid vectors. Mutant primers (IDT, San Diego, CA) were as follows: forward 5′-TGTTTGGGGTCCAAAAGTGTTGCGGCCGCTGCGGCAGGAACTGGAATACTAAGC-3′ and reverse primer 5′-GCTTAGTATTCCAGTTCCTGCCGCAGCGGCCGCAACACTTTTGGACCCCAAACA-3′ ($Tm = 86.7$ °C). PCR reactions were set up according to the QuikChange XL Site-Directed Mutagenesis kit (Agilent Technologies Inc.). GST-SAP145 Arginine to Lysine series mutants were generated using the same strategy. All mutations were confirmed on positive colonies by DNA sequencing.

***In vitro* methylation assay.** *In vitro* methylation reactions were carried out in 30 µl of PBS (pH = 7.4.) containing 0.5–1.0 µg of substrate, 3 µg of recombinant enzymes and 0.42 µM S-adenosyl-l-[methyl-^{3}H]methionine (79 Ci mmol^{-1} from a 7.5 µM stock solution; PerkinElmer Life Sciences). The reaction was incubated at 30 °C for 1 h and then separated on SDS–PAGE, transferred to a polyvinylidene difluoride membrane, treated with En3Hance (PerkinElmer Life Sciences) and exposed to a film for 1–3 days at –80 °C.

High-resolution cation-exchange chromatography. *In vitro* methylation reactions were set up with ~2 µg of enzyme protein, ~5 µg of substrate and 0.7 µM *S*-adenosyl-L-[*methyl*-^{3}H]methionine (PerkinElmer Life Sciences, 75-85 Ci mmol^{-1}, 0.55 mCi ml^{-1} in 10 mM H_2SO_4/EtOH (9:1, v/v)) in a final reaction volume of 60 µl. The reactions were incubated and rotated for 1, 5 or 20 h at 37 °C, in a reaction buffer of 50 mM potassium HEPES, 10 mM NaCl and 1 mM dithiothreitol, pH 8.0. To quench the reaction, a final concentration of 12.5% trichloroacetic acid was added with 20 µg of the carrier protein bovine serum albumin. After a 30-min incubation at room temperature, the precipitated proteins were centrifuged at 4,000 × *g* for 30 min and washed with cold acetone to remove excess [^{3}H]AdoMet, and the pellet was air-dried before acid hydrolysis. Fifty microlitres of 6 N HCl were added to each dried pellet, and 200 µl of 6 N HCl was added to a Waters PicoTag Chamber. Each sample was acid-hydrolysed *in vacuo* at 110 °C for 20 h. After acid hydrolysis, the pellets were dried using vacuum centrifugation. To prepare samples for high-resolution cation-exchange chromatography, the hydrolysed samples were resuspended in 50 µl of water and mixed with sodium citrate buffer (0.2 M in Na+, pH 2.2) and standards including 1 µmol each of ω-MMA (acetate salt, Sigma, M7033), SDMA (di(p-hydroxyazobenzene)-p′-sulfonate salt, Sigma, D0390) and ADMA (hydrochloride salt, Sigma, D4268). Samples were loaded on sulfonated polystyrene resin and eluted using 0.35 M sodium citrate running buffer, pH 5.25, at 55 °C. One-milliliter fractions were collected and the positions of the internal standards were determined using a ninhydrin assay using only 50 µl of each fraction. Fractions (950 µl) were assayed for radioactivity by the addition of 10 ml of Safety Solve Scintillation cocktail (Research Products International, 111177) and data were reported as the average of three 5-min counting cycles on a Beckman LS6500 Liquid Scintillation instrument.

Thin-layer chromatography. Fraction samples were spotted on a cellulose plate along with the addition of 5 nmol MMA, 15 nmol ADMA and 5 nmol SDMA of internal standards as described above. Individual standards were also spotted in adjacent lanes to determine the migration distance of each methylated arginine derivative. The origin is indicated by fraction 2. The solvent front was run near the end of the plate to fraction 32. The plate was air-dried and each lane was subsequently sliced in 5-mm fractions and counted using liquid scintillation counting for three 30-min counting cycles. This experiment was repeated three times and similar migration patterns were observed.

Protein sequence alignment using ClustalW. The parameters for the alignment using ClustalW were set as follows: Gap Penalty: 10, Gap Length Penalty: 0.2, Delay Divergent Seqs (%) 30, Protein Weight Matrix: Gonnet Series for multiple alignment parameters, and for pairwise alignment, Gap Penalty: 10, Gap Length 0.1, Protein Weight Matrix: Gonnet 250.

Deep-sequencing and alternative splicing analysis by MISO. Paired-end strand-specific RNA-seq reads were aligned to the human genome (hg19) using TopHat 2.0.91. We performed 75-nt paired-end sequencing and achieved ~220 million and 120 million unique mapped reads for control knockdown and PRMT9 knockdown, respectively. On the basis of the alignment result from TopHat, MISO model2 was used to compute 'percentage spliced in' (PSI or Ψ) values to quantify alternative splicing, indicating the fraction of a gene's mRNAs that include the alternative region. Five types of alternative splicing were analysed, including skipped exons, alternative 3′/5′ splice sites, mutually exclusive exons and retained intron. Then, change of Ψ and Bayes factor (>10) was used to identify significantly altered splicing in PRMT9 knockdown.

References

1. Dhar, S. *et al.* Loss of the major Type I arginine methyltransferase PRMT1 causes substrate scavenging by other PRMTs. *Sci. Rep.* **3,** 1311 (2013).
2. Gary, J. D. & Clarke, S. RNA and protein interactions modulated by protein arginine methylation. *Prog. Nucleic Acid Res. Mol. Biol.* **61,** 65–131 (1998).
3. Liu, Q. & Dreyfuss, G. *In vivo* and *in vitro* arginine methylation of RNA-binding proteins. *Mol. Cell Biol.* **15,** 2800–2808 (1995).
4. Boffa, L. C., Karn, J., Vidali, G. & Allfrey, V. G. Distribution of NG, NG,-dimethylarginine in nuclear protein fractions. *Biochem. Biophys. Res. Commun.* **74,** 969–976 (1977).
5. Gayatri, S. & Bedford, M. T. Readers of histone methylarginine marks. *Biochim. Biophys. Acta* **1839,** 702–710 (2014).
6. Cheng, D., Cote, J., Shaaban, S. & Bedford, M. T. The arginine methyltransferase CARM1 regulates the coupling of transcription and mRNA processing. *Mol. Cell* **25,** 71–83 (2007).
7. Paik, W. K. & Kim, S. *Natural Occurrence of Various Methylated Amino Acid Derivatives* (John Wiley & sons, 1980).
8. Yang, Y. & Bedford, M. T. Protein arginine methyltransferases and cancer. *Nat. Rev. Cancer* **13,** 37–50 (2013).
9. Bedford, M. T. & Clarke, S. G. Protein arginine methylation in mammals: who, what, and why. *Mol. Cell* **33,** 1–13 (2009).
10. Feng, Y. *et al.* Mammalian protein arginine methyltransferase 7 (PRMT7) specifically targets RXR sites in lysine- and arginine-rich regions. *J. Biol. Chem.* **288,** 37010–37025 (2013).
11. Lee, J., Sayegh, J., Daniel, J., Clarke, S. & Bedford, M. T. PRMT8, a new membrane-bound tissue-specific member of the protein arginine methyltransferase family. *J. Biol. Chem.* **280,** 32890–32896 (2005).
12. Cook, J. R. *et al.* FBXO11/PRMT9, a new protein arginine methyltransferase, symmetrically dimethylates arginine residues. *Biochem. Biophys. Res. Commun.* **342,** 472–481 (2006).
13. Fielenbach, N. *et al.* DRE-1: an evolutionarily conserved F box protein that regulates C. elegans developmental age. *Dev. Cell* **12,** 443–455 (2007).
14. Zeytuni, N. & Zarivach, R. Structural and functional discussion of the tetra-trico-peptide repeat, a protein interaction module. *Structure* **20,** 397–405 (2012).
15. Champion-Arnaud, P. & Reed, R. The prespliceosome components SAP 49 and SAP 145 interact in a complex implicated in tethering U2 snRNP to the branch site. *Genes Dev.* **8,** 1974–1983 (1994).
16. Swiercz, R., Person, M. D. & Bedford, M. T. Ribosomal protein S2 is a substrate for mammalian PRMT3 (protein arginine methyltransferase 3). *Biochem. J.* **386,** 85–91 (2005).
17. Swiercz, R., Cheng, D., Kim, D. & Bedford, M. T. Ribosomal protein rpS2 is hypomethylated in PRMT3-deficient mice. *J. Biol. Chem.* **282,** 16917–16923 (2007).
18. Chen, D. H., Wu, K. T., Hung, C. J., Hsieh, M. & Li, C. Effects of adenosine dialdehyde treatment on *in vitro* and *in vivo* stable protein methylation in HeLa cells. *J. Biochem.* **136,** 371–376 (2004).
19. Zeng, H. *et al.* A TR-FRET-based functional assay for screening activators of CARM1. *Chembiochem* **14,** 827–835 (2013).
20. Chen, C., Nott, T. J., Jin, J. & Pawson, T. Deciphering arginine methylation: Tudor tells the tale. *Nat. Rev. Mol. Cell Biol.* **12,** 629–642 (2011).

21. Matera, A. G. & Wang, Z. A day in the life of the spliceosome. *Nat. Rev. Mol. Cell Biol.* **15 (2014).**
22. Matsuoka, M. [Epsilon-N-methylated lysine and guanidine-N-methylated arginine of proteins. 3. Presence and distribution in nature and mammals]. *Seikagaku* **44,** 364–370 (1972).
23. Nishioka, K. & Reinberg, D. Methods and tips for the purification of human histone methyltransferases. *Methods* **31,** 49–58 (2003).
24. Guo, A. *et al.* Immunoaffinity enrichment and mass spectrometry analysis of protein methylation. *Mol. Cell Proteomics* **13,** 372–387 (2013).
25. Uhlmann, T. *et al.* A method for large-scale identification of protein arginine methylation. *Mol. Cell Proteomics* **11,** 1489–1499 (2012).
26. Ohkura, N., Takahashi, M., Yaguchi, H., Nagamura, Y. & Tsukada, T. Coactivator-associated arginine methyltransferase 1, CARM1, affects pre-mRNA splicing in an isoform-specific manner. *J. Biol. Chem.* **280,** 28927–28935 (2005).
27. Harrison, M. J., Tang, Y. H. & Dowhan, D. H. Protein arginine methyltransferase 6 regulates multiple aspects of gene expression. *Nucleic Acids Res.* **38,** 2201–2216 (2010).
28. Dowhan, D. H. *et al.* Protein arginine methyltransferase 6-dependent gene expression and splicing: association with breast cancer outcomes. *Endocr. Relat. Cancer* **19,** 509–526 (2012).
29. Di Lorenzo, A. & Bedford, M. T. Histone arginine methylation. *FEBS Lett.* **585,** 2024–2031 (2011).
30. Friesen, W. J. *et al.* The methylosome, a 20S complex containing JBP1 and pICln, produces dimethylarginine-modified Sm proteins. *Mol. Cell Biol.* **21,** 8289–8300 (2001).
31. Friesen, W. J. *et al.* A novel WD repeat protein component of the methylosome binds Sm proteins. *J. Biol. Chem.* **277,** 8243–8247 (2002).
32. Meister, G. *et al.* Methylation of Sm proteins by a complex containing PRMT5 and the putative U snRNP assembly factor pICln. *Curr. Biol.* **11,** 1990–1994 (2001).
33. Friesen, W. J., Massenet, S., Paushkin, S., Wyce, A. & Dreyfuss, G. SMN, the product of the spinal muscular atrophy gene, binds preferentially to dimethylarginine-containing protein targets. *Mol. Cell* **7,** 1111–1117 (2001).
34. Meister, G. & Fischer, U. Assisted RNP assembly: SMN and PRMT5 complexes cooperate in the formation of spliceosomal UsnRNPs. *EMBO J.* **21,** 5853–5863 (2002).
35. Bezzi, M. *et al.* Regulation of constitutive and alternative splicing by PRMT5 reveals a role for Mdm4 pre-mRNA in sensing defects in the spliceosomal machinery. *Genes Dev.* **27,** 1903–1916 (2013).
36. Deng, X. *et al.* Arginine methylation mediated by the *Arabidopsis* homolog of PRMT5 is essential for proper pre-mRNA splicing. *Proc. Natl Acad. Sci. USA* **107,** 19114–19119 (2010).
37. Sanchez, S. E. *et al.* A methyl transferase links the circadian clock to the regulation of alternative splicing. *Nature* **468,** 112–116 (2010).
38. Terada, Y. & Yasuda, Y. Human immunodeficiency virus type 1 Vpr induces G2 checkpoint activation by interacting with the splicing factor SAP145. *Mol. Cell Biol.* **26,** 8149–8158 (2006).
39. Zurita-Lopez, C. I., Sandberg, T., Kelly, R. & Clarke, S. G. Human protein arginine methyltransferase 7 (PRMT7) is a type III enzyme forming omega-NG-monomethylated arginine residues. *J. Biol. Chem.* **287,** 7859–7870 (2012).

Acknowledgements

We thank Maria Person for mass spectrometry analysis at the 'Protein and Metabolite Analysis Facility' (UT Austin) supported by RP110782 (CPRIT). M.T.B. is supported by an NIH grant (DK062248); S.G.C. is supported by an NIH grant (GM026020). A.H. and C.Z.-L. were supported by an NIH training grant (GM007185). M.T.B. is a cofounder of EpiCypher.

Author contributions

Y.Y., A.H., S.G.C. and M.T.B. conceived the project. Y.Y., A.H., S.G., D.K., C.Z.-L. and R.K. carried out the experiments. Z.X. and W.L. analysed the RNA-Seq data. A.G. developed the methyl-specific antibodies. M.T.B. wrote the manuscript and supervised the work. Y.Y., A.H. and S.G.C. provided valuable support with the writing.

Additional information

Accession codes: Deep-sequencing data can be accessed with GEO accession number GSE63953.

Supplementary Information accompanies this paper at http://www.nature.com/naturecommunications

Competing financial interests: The authors declare no competing financial interests.

Reprints and permission information is available online at http://npg.nature.com/reprintsandpermissions/

How to cite this article: Yang, Y. *et al.* PRMT9 is a Type II methyltransferase that methylates the splicing factor SAP145. *Nat. Commun.* 6:6428 doi: 10.1038/ncomms7428 (2015).

CHAPTER 6

Unique Features of Human Protein Arginine Methyltransferase 9 (PRMT9)

and Its Substrate RNA Splicing Factor SF3B2

Unique Features of Human Protein Arginine Methyltransferase 9 (PRMT9) and Its Substrate RNA Splicing Factor SF3B2*

Received for publication, April 17, 2015, and in revised form, May 14, 2015 Published, JBC Papers in Press, May 15, 2015, DOI 10.1074/jbc.M115.659433

Andrea Hadjikyriacou[‡], Yanzhong Yang[§1], Alexsandra Espejo[§], Mark T. Bedford[§], and Steven G. Clarke[‡2]

From the [‡]Department of Chemistry and Biochemistry and the Molecular Biology Institute, UCLA, Los, Angeles, California 90095 and the [§]Department of Epigenetics and Molecular Carcinogenesis, University of Texas MD Anderson Cancer Center, Smithville, Texas 78957

Background: Newly discovered protein arginine methyltransferase 9 (PRMT9) modulates alternative splicing by methylation of SF3B2.
Results: Biochemical probes of PRMT9 and its substrate protein revealed domains and residues required for methylation.
Conclusion: PRMT9 is unique among PRMTs in its narrow range of methyl-accepting substrates.
Significance: Understanding PRMT9 catalysis will help elucidate how it may control the activity of SF3B2 and other potential endogenous substrates.

Human protein arginine methyltransferase (PRMT) 9 symmetrically dimethylates arginine residues on splicing factor SF3B2 (SAP145) and has been functionally linked to the regulation of alternative splicing of pre-mRNA. Site-directed mutagenesis studies on this enzyme and its substrate had revealed essential unique residues in the double E loop and the importance of the C-terminal duplicated methyltransferase domain. In contrast to what had been observed with other PRMTs and their physiological substrates, a peptide containing the methylatable Arg-508 of SF3B2 was not recognized by PRMT9 *in vitro*. Although amino acid substitutions of residues surrounding Arg-508 had no great effect on PRMT9 recognition of SF3B2, moving the arginine residue within this sequence abolished methylation. PRMT9 and PRMT5 are the only known mammalian enzymes capable of forming symmetric dimethylarginine (SDMA) residues as type II PRMTs. We demonstrate here that the specificity of these enzymes for their substrates is distinct and not redundant. The loss of PRMT5 activity in mouse embryo fibroblasts results in almost complete loss of SDMA, suggesting that PRMT5 is the primary SDMA-forming enzyme in these cells. PRMT9, with its duplicated methyltransferase domain and conserved sequence in the double E loop, appears to have a unique structure and specificity among PRMTs for methylating SF3B2 and potentially other polypeptides.

Protein arginine methylation is an important post-translational modification in eukaryotic cells catalyzed by the family of PRMTs[3] (1–4). Each member of this family contains a conserved core methyltransferase domain, consisting of *S*-adenosyl-L-methionine (AdoMet)-binding sequences in motif I and post-motif I, and substrate-binding sequences in motif II, post-motif II (including the double E loop), and the THW loop (1–5). The mammalian family of PRMTs has been divided into three groups based on their activities. Type I PRMTs (PRMT1–4, PRMT6, and PRMT8) transfer up to two methyl groups on the same terminal guanidino nitrogen of arginine to form ω-N^G-monomethylarginine (MMA) and ω-N^G,N^G-asymmetric dimethylarginine (ADMA) residues. Type II PRMTs (PRMT5 and PRMT9) transfer methyl groups on different terminal guanidino nitrogen atoms to form MMA and ω-N^G,N'^G-symmetric dimethylarginine (SDMA) residues. Finally, type III enzymes transfer only a single methyl group to form MMA residues (PRMT7) (1–8). Both histone and non-histone proteins have been identified as PRMT substrates (2, 4–6, 9), indicating very diverse and important roles for these arginine-modifying enzymes. For example, dysregulation of PRMT1, the major asymmetric dimethylating enzyme, results in a variety of cancers, including breast, colon, bladder, lung, and various leukemias (5, 10, 11). Overexpression of other PRMTs (2–8) has also been linked to cancer development (particularly breast cancer) through increased cellular proliferation, conferred resistance to DNA-damaging agents, and increased cell invasion (3, 5). The mammalian PRMTs have important roles in transcriptional regulation, signal transduction, nuclear/cytoplasmic shuttling, DNA repair, mRNA splicing, and male germ line gene imprinting (2, 3).

Although most of the mammalian arginine methyltransferases have been extensively studied, the catalytic activity of PRMT9 was unknown until our recent work identified it as the second SDMA-forming enzyme in mammals (7). This enzyme

* This work was supported, in whole or in part, by National Institutes of Health Grants GM026020 (to S. G. C.), DK062248 (to M. T. B.), and GM007185, a Ruth L. Kirschstein National Research Service Award (to A. H.). The authors declare that they have no conflicts of interest with the contents of this article.

[1] Present address: Dept. of Radiation Biology, Beckman Research Institute, City of Hope Cancer Center, Duarte, CA 91010.

[2] To whom correspondence should be addressed: Dept. of Chemistry and Biochemistry and the Molecular Biology Institute, UCLA, 607 Charles E. Young Dr. E., Los Angeles, CA 90095-1569. Tel.: 310-825-8754; Fax: 310-825-1968; E-mail: clarke@mbi.ucla.edu.

[3] The abbreviations used are: PRMT, protein arginine methyltransferase; MMA, ω-N^G-monomethylarginine; ADMA, ω-N^G,N^G-asymmetric dimethylarginine; SDMA, ω-N^G,N'^G-symmetric dimethylarginine; AdoMet, *S*-adenosyl-L-methionine; [*methyl*-^{3}H]AdoMet, *S*-adenosyl-L-[*methyl*-^{3}H]methionine; GAR, glycine- and arginine-rich domain of human fibrillarin; MBP, myelin basic protein; OHT, 4-hydroxytamoxifen; OPA, *o*-phthalaldehyde; MEF, mouse embryo fibroblast; ΔTPR, GST-PRMT9 mutant missing residues 21–139; ΔN, GST-PRMT9 mutant missing residues 21–350; ΔC 529, GST-PRMT9 mutant missing residues 530–895; ΔC 350, mutant missing residues 351–895; Bistris, 2-[bis(2-hydroxyethyl)amino]-2-(hydroxymethyl)propane-1,3-diol.

should be distinguished from the FBXO11 gene product, previously erroneously termed PRMT9, that is a component of an E3 ubiquitin ligase complex (7, 12). Biological assays showed that PRMT9 levels are functionally linked to the regulation of alternative splicing, and PRMT9 was thus identified as a modulator of small nuclear ribonucleoprotein maturation (7). PRMT9 is found in a cellular complex with the splicing factors SF3B2 and SF3B4, also known as SAP145 and SAP49, respectively (7). PRMT9 catalyzes the formation of MMA and SDMA in SF3B2 but had little or no activity on the common *in vitro* substrates of other PRMTs, such as polypeptides with glycine-arginine rich repeats (GAR) (7).

Splicing factor SF3B2 is highly conserved in nature, binds SF3B4 in a tight complex (13, 14), and has implied functional roles in cell cycle progression (14). Previous studies have shown that the HIV accessory protein Vpr interferes with the SF3B2-SF3B4 complex as a mechanism to induce G_2 checkpoint arrest and ensure colocalization in nuclear speckles (14). Because PRMT9 methylates SF3B2 within the highly conserved region that mediates its interaction with Vpr, understanding how SF3B2 is recognized and methylated by PRMT9 might provide a potential anti-HIV role for this enzyme.

PRMT9, like PRMT7, contains an ancestrally duplicated methyltransferase domain (7, 8). Other PRMTs contain only one methyltransferase domain, which makes this an unusual feature of these two "outlier" PRMTs. Crystallographic studies elucidating the structure of *Mus musculus* and *Caenorhabditis elegans* PRMT7 show that AdoMet only binds to the N-terminal domain, and the other methyltransferase domain at the C terminus may have a pseudodimer function (15, 16), mimicking the homodimer structure required for activity of other PRMTs upon binding their substrate (PRMT1, PRMT3, and PRMT5, and *Trypanosoma brucei* PRMT7) (15, 17–19). Deletion of either domain in PRMT7 abolishes its activity (20), as do amino acid substitutions in the C-terminal domain (8), consistent with a role in forming pseudodimers that are necessary for correct substrate binding. In addition, our recent work shows that a full-length PRMT9 is necessary for interaction with SF3B2 (7). In this study, we aimed to determine whether N- and C-terminal truncations in PRMT9 retain methylation activity on SF3B2 *in vitro*. In addition, PRMT9 harbors three tetratricopeptide repeats (TPRs), which often mediate protein-protein interactions (21). We thus wanted to elucidate the functional role of this TPR motif and the two methyltransferase domains.

We are also interested in determining how the specificity of PRMT9 is established, in particular what sets it apart from the other much more promiscuous PRMTs. In the substrate-binding double E loop, there are several residues that are present in the type II (PRMT5 and PRMT9) and type III (PRMT7) enzymes that are not found in the type I enzymes. In particular, the presence of acidic residues in the double E loop of PRMT7 has been shown to play a role in the specificity of this enzyme for methylating arginine residues in R*X*R sequences in an overall basic sequence context (8). It is intriguing that PRMT9 has a double E loop sequence similar to PRMT7. We therefore wanted to biochemically characterize this enzyme, probing for the structural features responsible for its type II activity and substrate specificity. We also hoped to use these studies to identify the residues around the methylated arginine in SF3B2 that are critical for its recognition by the methyltransferase.

PRMT5, the only other well characterized symmetrically dimethylating enzyme (4, 22, 23), has been previously reported to play an important role in spliceosomal U small nuclear ribonucleoprotein maturation (24). It is therefore interesting that PRMT9, the only other SDMA-generating enzyme as yet discovered, also modifies a protein involved in RNA splicing. In studies reported here, we have now used immunoblotting and amino acid analyses to examine whether the roles of PRMT5 and PRMT9 are redundant in the cell. Importantly, understanding the contribution of PRMT9 to the global cellular levels of SDMA will determine its contribution to SDMA-mediated biological activities.

Experimental Procedures

Phylogenetic Tree Construction and Sequence Alignments of PRMT9 and SF3B2 Orthologs—A protein BLAST search was performed using *Homo sapiens* PRMT9 (Q6P2P2) and SF3B2 (Q13435) as the query to determine top-ranked orthologs. Protein sequences were aligned using MUSCLE (multiple-sequence comparison by log expectation) in MEGA6 (Molecular Evolutionary Genetics Analysis) software (25). Phylogenetic trees were generated using the neighbor joining method, and evolutionary distances were determined using *p*-distance. Sequence alignments for comparison of important regions within each ortholog were done using Clustal Omega Multiple Sequence Alignment software (26).

Bacterial Protein Expression and Purification—Human *PRMT9* cDNA was subcloned into a pGEX-6p-1 vector (GE Healthcare, catalog no. 28-9546-48), as described previously (7), and expressed as a GST fusion protein in *Escherichia coli* BL21 Star DE3 cells (Invitrogen, catalog no. C601003), resulting in a fusion protein of the *Schistosoma japonicum* GST (Uniprot P08515) with a linker sequence SDLEVLFQGPLGS and residues 1–845 of PRMT9 (UniProt Q6P2P2-1). The DNA of the construct was sequenced on both strands to confirm insertion and protein identity. Cells containing the GST-PRMT9 plasmid were grown in 4 liters of LB broth (Difco, catalog no. 244610) with 100 μg/ml ampicillin (Fisher, catalog no. BP1760) at 37 °C to an OD_{600} of 0.6. Induction was performed at 18 °C with 0.4 mM isopropyl D-thiogalactopyranoside (Gold Bio, catalog no. I2481C25). After a 19-h induction, the cells were harvested at 5000 × *g* at 4 °C and washed two times with phosphate-buffered saline (PBS, 137 mM NaCl, 2.7 mM KCl, 10 mM Na_2HPO_4, 2 mM KH_2PO_4, pH 7.4). Cells were then either frozen at −80 °C until lysis or immediately resuspended in 16 ml of PBS containing 1 mM phenylmethylsulfonyl fluoride (Sigma, catalog no. P7626) and lysed using an Avestin EmulsiFlex-C3 homogenizer for two cycles at 18,000 p.s.i. (Ottawa, Ontario, Canada). After the lysate was centrifuged at 23,000 × *g* for 50 min, the supernatant containing GST-PRMT9 was added to 1 ml of a 50% slurry of glutathione-Sepharose 4B resin (GE Healthcare, catalog no. 17-0756-01) and rotated at 4 °C for 2 h. The resin was then washed with PBS, and the protein was eluted with 2 ml of 30 mM reduced L-glutathione (Sigma, catalog no. G4251) in 50 mM Tris-HCl, 120 mM NaCl, and 5% glycerol, pH 7.5. The GST-SF3B2(401–550) fragment was generated by subcloning human

TABLE 1
Primers for mutagenesis
Fwd is forward and Rev is reverse.

Primer name	Sequence	T_m
		°C
PRMT9		
L182A/D183A/I184A/G185A	Fwd: 5′-TGT TTG GGG TCC AAA AGT GTT GCG GCC GCT GCG GCA GGA ACT GGA ATA CTA AGC-3′	86.7
	Rev: 5′-GCT TAG TAT TCC AGT TCC TGC CGC AGC GGC CGC AAC ACT TTT GGA CCC CAA ACA-3′	
D258G	Fwd: 5′-A GTT GTA ACA GAA ACT GTC GGT GCA GGT TTA TTT GGA GAA G-3′	78.6
	Rev: 5′-C TTC TCC AAA TAA ACC TGC ACC GAC AGT TTC TGT TAC AAC T-3′	
G260E	Fwd: 5′-GTA ACA GAA ACT GTC GAT GCA GAG TTA TTT GGA GAA GGA ATT GTG G-3′	78.5
	Rev: 5′-C CAC AAT TCC TTC TCC AAA TAA CTC TGC ATC GAC AGT TTC TGT TAC-3′	
Δ TPR	Fwd: 5′-CGC TGG GGC AGC CGG CAA TTT TTA TCG TGT TGC-3′	81.6
	Rev: 5′-GCA ACA CGA TAA AAA TTG CCG GCT GCC CCA GCG-3′	
Δ N	Fwd: 5′-GCT GGG GCA GCC GGC CCT TAT ACA ACT GAA A-3′	80.3
	Rev: 5′-TTT CAG TTG TAT AAG GGC CGG CTG CCC CAG C-3′	
Δ C 350	Fwd: 5′-GCT TAT TCT TCT GTA GAT ACT GAA GAA ACA ATT GAA TAG TAG ACA ACT GAA AAG ATG AGT-3′	82.6
	Rev: 5′-ACT CAT CTT TTC AGT TGT CTA CTA TTC AAT TGT TTC TTC AGT ATC TAC AGA AGA ATA AGC-3′	
Δ C 529	Fwd: 5′-TG GAA TCT ACA GAA ATT GCT TTG CTT TAG TAG ATC CCA TAT CAT GAA GGC TTT AAA ATG G-3′	79.6
	Rev: 5′-C CAT TTT AAA GCC TTC ATG ATA TGG GAT CTA CTA AAG CAA AGC AAT TTC TGT AGA TTC CA-3′	
SF3B2		
K507A/K509A	Fwd: 5′-G CCA CGC CAC TGG TGT TTT GCG CGC GCA TAC CTG CAG GGC AAA C-3′	79.4
	Rev: 5′-G TTT GCC CTG CAG GTA TGC GCG CGC AAA ACA CCA GTG GCG TGG C-3′	
K507R/K509R	Fwd: 5′-CCA CGC CAC TGG TGT TTT AGG CGC AGA TAC CTG CAG G-3′	80.0
	Rev: 5′-C CTG CAG GTA TCT GCG CCT AAA ACA CCA GTG GCG TGG-3′	
K507R/R508K/K509R	Fwd: 5′-TGC CTG TGC CAC GCC ACT GGT GTT TTA GGA AGA GAT ACC TGC AGG GCA A-3′	78.4
	Rev: 5′-T TGC CCT GCA GGT ATC TCT TCC TAA AAC ACC AGT GGC GTG GCA CAG GCA-3′	
K507R/R508K	Fwd: 5′-TGT GCC ACG CCA CTG GTG TTT TAG GAA GAA ATA CCT GCA GGG CAA AC-3′	78.7
	Rev: 5′-GT TTG CCC TGC AGG TAT TTC TTC CTA AAA CAC CAG TGG CGT GGC ACA-3′	
F506A/Y510A	Fwd: 5′-GTG CCA CGC CAC TGG TGT GCT AAG CGC AAA GCC CTG CAG GGC AAA-3′	79.5
	Rev: 5′-TTT GCC CTG CAG GGC TTT GCG CTT AGC ACA CCA GTG GCG TGG CAC-3′	

SF3B2 cDNA into the pGEX-6p-1 vector (7). GST-SF3B2 401–550-residue wild type and mutant fragments were purified in a similar manner, but protein was expressed using 0.5 mM isopropyl D-thiogalactopyranoside and induced for 18–20 h, 250 rpm at 18 °C. GST-GAR was purified as described previously (27). Bovine myelin basic protein was purchased from Sigma (M1891, lyophilized powder). Recombinant human histones were purchased from New England Biolabs (histone H2A, catalog no. M2502S; histone H2B, catalog no. M2505S; histone H3.1, catalog no. M2503S; histone H4, catalog no. M2504; Ipswich, MA). Calf thymus histones type IIA-S were purchased from Sigma (catalog no. H7755). Human recombinant FLAG-tagged PRMT5/MEP50 was purchased from BPS Bioscience (catalog no. 51045, lot 140131). A His-tagged human myelin basic protein construct on a pET15b-TEV plasmid was a generous gift from Dr. Douglas Juers from Whitman College; protein expression was performed under similar conditions, and the protein was purified using HisPur Cobalt Resin (Thermo Scientific, catalog no. 89964), with washing in 50 mM phosphate buffer containing 10 mM imidazole, pH 7.0, and elution using a 50 mM phosphate buffer containing 150 mM imidazole, pH 7.0. The protein was dialyzed overnight into PBS to remove residual imidazole. Proteins were quantified using a Lowry assay after precipitation using 10% trichloroacetic acid, using bovine serum albumin as a standard.

Mutagenesis—PRMT9 was mutated to create a catalytically inactive enzyme by introducing quadruple mutations (L182A/D183A/I184A/G185A) in the conserved AdoMet-binding motif I in both the GST-PRMT9 plasmid described above and in the GFP-PRMT9 plasmid described previously (7). Truncation mutants and double E loop mutants were created on the GST-PRMT9 wild type plasmid using the mutagenized primers listed in Table 1. Double E loop mutants consisted of mutating residues Asp-258 to Gly (D258G) and Gly-260 to Glu (G260E). Truncation mutants for GST-PRMT9 were created using mutagenized primers to remove the indicated amino acids from the plasmid as follows: ΔTPR (residues 21–139), ΔN (residues 21–350), ΔC 529 (stop codons were placed upstream of the C-terminal domain, at positions 529 and 530), and ΔC 350 (stop codons were placed upstream of the C-terminal domain at positions 350 and 351). SF3B2 mutants were created on the GST-SF3B2 401–550 fragment wild type plasmid, using mutagenized primers listed in Table 1. Mutants included K507A/K509A (-FARAY-), K507R/K509R (-FRRRY-), K507R/R508K/K509R (-FRKRY-), K507R/R508K (-FRKKY-), and F506A/Y510A (-AKRKA-). The GST mutant constructs were transformed into BL21 DE3 *E. coli* cells for expression as described above. GFP mutant constructs were transfected into HEK293 cells as described below. Mutagenesis was performed with PCRs set up according to the QuikChange XL site-directed mutagenesis kit (Agilent Technologies Inc., catalog no. 200521), using 50 ng of the appropriate wild type plasmid template, 125 ng of each forward and reverse primer as shown in Table 1, and 1 μl of PfuUltra HF DNA polymerase (2.5 units/μl). The PCR was run at 95 °C for 1 min, 18 cycles of 95 °C for 50 s, 60 °C for 50 s, and 65 °C for 3 min, followed by a final extension at 68 °C for 7 min. Following PCR, 1 μl of DpnI enzyme was added to the reaction and incubated at 37 °C for 1 h to digest the parental supercoiled dsDNA. Mutated plasmids were transformed into XL10-Gold Ultracompetent cells (200315, Agilent Technologies, Inc.) and plated onto LB plates with ampicillin (100 μg/ml) for GST-PRMT9 mutants and GST-SF3B2 mutants or kanamycin (30 μg/ml) (Fisher, catalog no. BP906) for GFP-PRMT9. DNA sequencing on both strands confirmed the mutations in positive colonies (GeneWiz, San Diego).

Generation of a Stable Cell Line Expressing Wild Type and Mutant GFP-PRMT9—Wild type and mutant GFP-PRMT9 on plasmid pEGFP-N1 (7) were transfected into HEK293 Flp-In TREx cells (Invitrogen, catalog no. R780-07). Approximately 1 μg of wild type or mutant plasmid DNA was incubated with 50

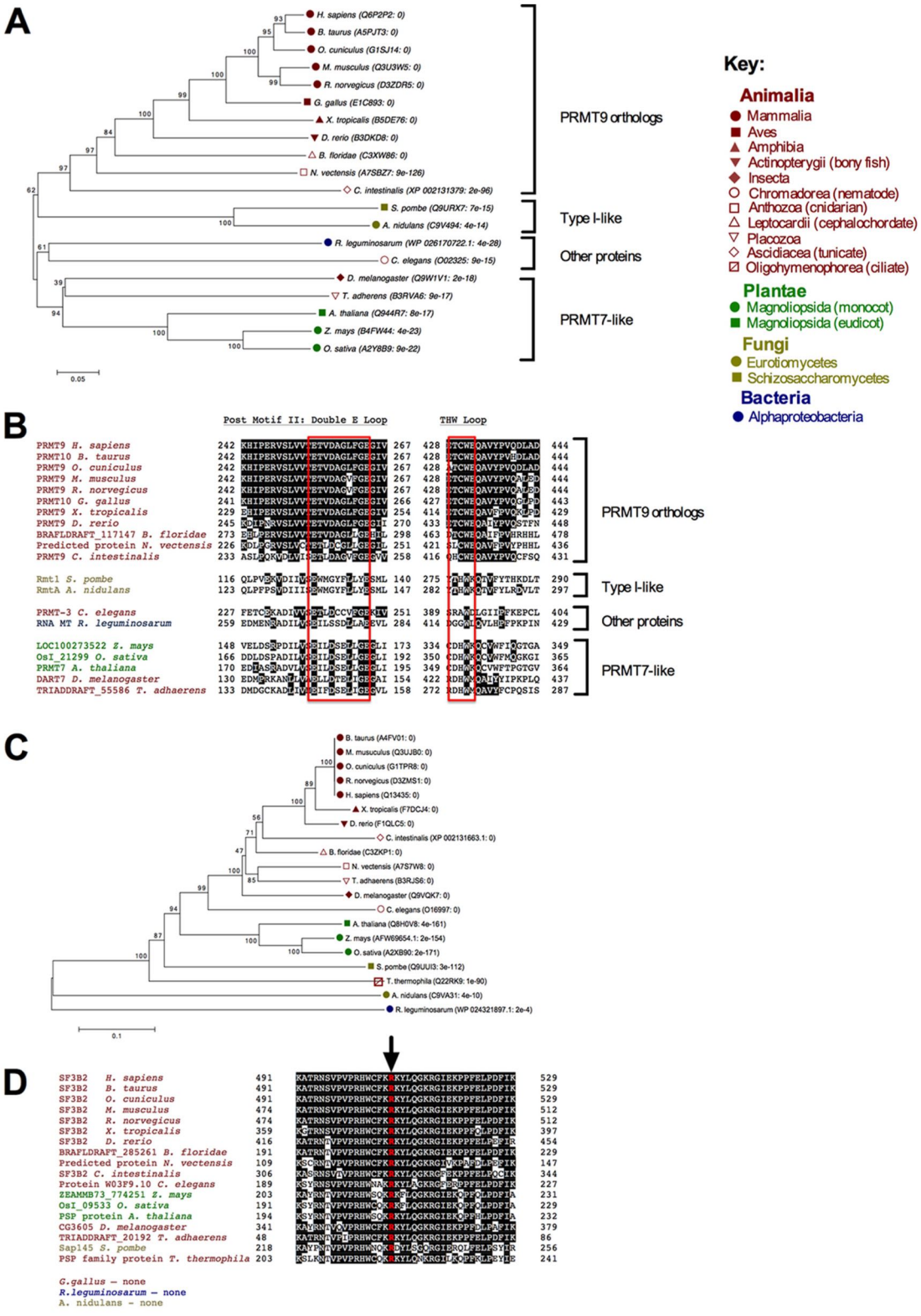
A
H. sapiens (Q6P2P2: 0)
B. taurus (A5PJT3: 0)
O. cuniculus (G1SJ14: 0)
M. musculus (Q3U3W5: 0)
R. norvegicus (D3ZDR5: 0)
G. gallus (E1C893: 0)
X. tropicalis (B5DE76: 0)
D. rerio (B3DKD8: 0)
B. floridae (C3XW86: 0)
N. vectensis (A7SBZ7: 9e-126)
C. intestinalis (XP 002131379: 2e-96)
S. pombe (Q9URX7: 7e-15)
A. nidulans (C9V494: 4e-14)
R. leguminosarum (WP 026170722.1: 4e-28)
C. elegans (O02325: 9e-15)
D. melanogaster (Q9W1V1: 2e-18)
T. adherens (B3RVA6: 9e-17)
A. thaliana (Q944R7: 8e-17)
Z. mays (B4FW44: 4e-23)
O. sativa (A2Y8B9: 9e-22)
0.05
PRMT9 orthologs
Type I-like
Other proteins
PRMT7-like
Key:
Animalia
Mammalia
Aves
Amphibia
Actinopterygii (bony fish)
Insecta
Chromadorea (nematode)
Anthozoa (cnidarian)
Leptocardii (cephalochordate)
Placozoa
Ascidiacea (tunicate)
Oligohymenophorea (ciliate)
Plantae
Magnoliopsida (monocot)
Magnoliopsida (eudicot)
Fungi
Eurotiomycetes
Schizosaccharomycetes
Bacteria
Alphaproteobacteria
B
Post Motif II: Double E Loop
THW Loop
PRMT9 H. sapiens 242 267 428 444
PRMT10 B. taurus 242 267 428 444
PRMT9 O. cuniculus 242 267 428 444
PRMT9 M. musculus 242 267 428 444
PRMT9 R. norvegicus 242 267 428 444
PRMT10 G. gallus 241 266 427 443
PRMT9 X. tropicalis 229 254 414 429
PRMT9 D. rerio 245 270 433 448
BRAFLDRAFT_117147 B. floridae 273 298 463 478
Predicted protein N. vectensis 226 251 421 436
PRMT9 C. intestinalis 233 258 416 431
PRMT9 orthologs
Rmt1 S. pombe 116 140 275 290
RmtA A. nidulans 123 147 282 297
Type I-like
PRMT-3 C. elegans 227 251 389 404
RNA MT R. leguminosarum 259 284 414 429
Other proteins
LOC100273522 Z. mays 148 173 334 349
OsI_21299 O. sativa 166 192 350 365
PRMT7 A. thaliana 170 195 349 364
DART7 D. melanogaster 130 154 422 437
TRIADDRAFT_55586 T. adhaerens 133 158 272 287
PRMT7-like
C
B. taurus (A4FV01: 0)
M. musculus (Q3UJB0: 0)
O. cuniculus (G1TPR8: 0)
R. norvegicus (D3ZMS1: 0)
H. sapiens (Q13435: 0)
X. tropicalis (F7DCJ4: 0)
D. rerio (F1QLC5: 0)
C. intestinalis (XP 002131663.1: 0)
B. floridae (C3ZKP1: 0)
N. vectensis (A7S7W8: 0)
T. adherens (B3RJS6: 0)
D. melanogaster (Q9VQK7: 0)
C. elegans (O16997: 0)
A. thaliana (Q8H0V8: 4e-161)
Z. mays (AFW69654.1: 2e-154)
O. sativa (A2XB90: 2e-171)
S. pombe (Q9UUI3: 3e-112)
T. thermophila (Q22RK9: 1e-90)
A. nidulans (C9VA31: 4e-10)
R. leguminosarum (WP 024321897.1: 2e-4)
0.1
D
SF3B2 H. sapiens 491 529
SF3B2 B. taurus 491 529
SF3B2 O. cuniculus 491 529
SF3B2 M. musculus 474 512
SF3B2 R. norvegicus 474 512
SF3B2 X. tropicalis 359 397
SF3B2 D. rerio 416 454
BRAFLDRAFT_285261 B. floridae 191 229
Predicted protein N. vectensis 109 147
SF3B2 C. intestinalis 306 344
Protein W03F9.10 C. elegans 189 227
ZEAMMB73_774251 Z. mays 203 231
OsI_09533 O. sativa 191 229
PSP protein A. thaliana 194 232
CG3605 D. melanogaster 341 379
TRIADDRAFT_20192 T. adhaerens 48 86
Sap145 S. pombe 218 256
PSP family protein T. thermophila 203 241
G.gallus – none
R.leguminosarum – none
A. nidulans – none

μl of Opti-MEM (Gibco, Invitrogen, catalog no. 31985062) for 5 min and then added to a solution containing 50 μl of Opti-MEM and 20 μl of FuGENE 6 transfection reagent (Promega, catalog no. E2691). The transfection solution was incubated for 20 min and added to the center of a 6-cm plate containing HEK293 cells in F-12/DMEM (1:1) (HyClone, Thermo Scientific, catalog no. SH30023.02), 10% fetal bovine serum (Tet-tested FBS, Gibco, catalog no. 16000), and 1% penicillin/streptomycin (Invitrogen, catalog no. 15140-122). Plates were incubated at 37 °C, 5% CO_2 for 4 days until the cells were about 80% confluent. At that time, 400 μg/ml geneticin (G418, Invitrogen, catalog no. 11811023) was added, and selection was monitored for 2 weeks. Cells positive for GFP-PRMT9 were confirmed by their ability to form colonies, their fluorescence, and by immunoblotting using an antibody to GFP (anti-rabbit GFP, Abcam).

Immunoprecipitation from HEK293 Cells Expressing GFP-PRMT9—Stable cell lines containing wild type and mutant GFP-PRMT9 DNA were grown to confluence in 1-liter roller bottles with DMEM, 10% Tet-tested FBS, and 1% penicillin/streptomycin. Cells were harvested and washed once with PBS. 220 μg of anti-rabbit GFP antibody (Abcam) was cross-linked to protein A beads (catalog no.156-0006, Bio-Rad) with 0.22 M dimethyl pimelimidate-HCl (Thermo Scientific, catalog no.21667) in 0.2 M sodium borate, pH 9.0. Beads were washed with 0.2 M ethanolamine and 0.2 M NaCl, pH 8.5, to inactivate residual cross-linker. Cells were lysed with LAP300 buffer (50 mM potassium HEPES, pH 7.4, 300 mM KCl, 1 mM EGTA, 1 mM $MgCl_2$, 10% glycerol, 0.3% Nonidet P-40) and protease inhibitor mixture (cOmplete, Roche Applied Science, catalog no.11697498001). The lysate was centrifuged at 28,400 × *g* for 10 min at 4 °C. The supernatant was then spun at 100,000 × *g* for 1 h at 4 °C, and this supernatant was collected and added to 0.4 ml of a 50% slurry of the GFP-protein A beads prepared as described above and equilibrated in LAP200 buffer (same as the LAP300 buffer described above but with 200 mM KCl). After incubation for 1 h at 4 °C, the beads were washed three times with LAP200 and stored in LAP100 buffer (100 mM KCl) at 4 °C.

Immunofluorescence and Localization of GFP-PRMT9 Wild Type and Mutant—Stable cell lines containing wild type and mutant GFP-PRMT9 in HEK293 cells were grown to confluency at 37 °C, 5% CO_2 on a poly-L-lysine-coated coverslip (BD Biosciences, catalog no. 354085) in a 24-well plate. After reaching confluency, cells were fixed using BRB80 buffer (0.4 M PIPES, 5 mM $MgCl_2$, and 5 mM EGTA, pH 6.8) with 4% paraformaldehyde (Electron Microscopy Science, catalog no. 15710). Cells were washed with PBS and permeabilized using 0.2% Triton X-100 for 1 min. Coverslips were then transferred to a moisture chamber and incubated for 30 min at room temperature with immunofluorescence (IF) buffer (PBS containing 5% fish gelatin (Sigma, G7765) and 0.1% Triton X-100). Antibodies were diluted in IF buffer and incubated for 1 h at room temperature. Antibodies used include anti-GFP (rabbit, 1:500) (Abcam) and Hoechst dye 33342 (1:1000) (Invitrogen, catalog no. H1399). Secondary donkey anti-rabbit fluorescein isothiocyanate (FITC) antibody (AffiniPure, Jackson ImmunoResearch, catalog no. 711-095-152) was also diluted (1:500) in IF buffer and incubated at room temperature for 30 min. Coverslips were then washed once with PBS, and 200 μl of anti-fade mounting solution (ProLong gold antifade mounting solution, Invitrogen, catalog no. P36934) was placed on the coverslips and sealed with clear nail polish. Cells were imaged at ×1000 magnification using a Leica TCS SPE I DMI4000 B inverted scanning confocal microscope with a Leica DFC360FX digital camera. Fixed cells on coverslips were kept at 25 °C during imaging. Images were acquired using Leica AF6000 software and analyzed using Fiji ImageJ software (National Institutes of Health).

LC-MS/MS to Identify Substrates and Interaction Partners—Immunoprecipitated GFP-PRMT9 wild type and catalytic mutant samples were sent to the Birmingham Proteomics and Mass Spectrometry Consortium, University of Alabama at Birmingham, for protein identification. Data were received as summary of protein peptide hits, among which were sorted for the top protein peptide hits identified and used in this study.

Amino Acid Analysis of Substrates Using High Resolution Cation Exchange Chromatography—In vitro methylation reactions included the indicated amount of enzyme and substrate proteins and 0.7 μM *S*-adenosyl-L-[*methyl*-^{3}H]methionine ([*methyl*-^{3}H]AdoMet; PerkinElmer Life Sciences, 75–85 Ci/mmol, 0.55 mCi/ml in 10 mM H_2SO_4/EtOH (9:1, v/v)) in a total volume of 60 μl. The reactions were performed at 37 °C in 50 mM potassium HEPES, 10 mM NaCl, and 1 mM DTT, pH 8.0. Reactions were stopped by adding trichloroacetic acid to 12.5% with 20 μg of the carrier protein bovine serum albumin. Acid hydrolysis and high resolution cation exchange chromatography were then performed as described previously (7). For ninhydrin assay, 50 μl of each fraction from the cation exchange column was used to determine the elution of nonradiolabeled standards, and the rest of the fraction (950 μl) was used for liquid scintillation counting. The efficiency of counting was determined to be about 51%. Under these conditions, about 90 cpm correspond to 1 fmol of radiolabeled methyl groups.

Detection of Methylated Substrates after SDS-PAGE—Methylation reactions were set up as described above for the amino acid analysis, but the reactions were quenched by the addition of SDS loading buffer. Reactions were then boiled for 5 min at 100 °C and separated on 12.6% Tris-glycine gels or 4–12% Bis-tris gel (NuPAGE Novex, Invitrogen, NP0335BOX), stained

FIGURE 1. **Evolutionary conservation of PRMT9 and SF3B2.** *A* and *C,* representative phylogenetic trees based on human PRMT9 (Q6P2P2) (*A*) and human SF3B2 (Q13435) (*C*) are shown for the selected organisms. UniProt IDs of top ranked orthologs with their respective *E* value are shown. The percentage of replicate trees in which the specific associated taxa clustered together in 500 replicates of the boot strap test is shown next to the branches. Evolutionary distances are displayed in units of the number of amino acid differences per site. All proteins were mutual best hits, and all organisms have complete genomes sequenced. Based on groupings in the phylogenetic tree, proteins were identified as "*PRMT9 orthologs*," "*type I-like*," "*other proteins*," and "*PRMT7-like*." *B,* sequence alignment of post-motif II; double E loop and THW loop residues, the two major distinguishing motifs found in PRMTs. *Shaded letters* indicate sequence identity. Double E loop residues and THW loop residues are *boxed* in *red*. *D,* sequence alignment of amino acids surrounding the Arg-508 site that is methylated by PRMT9. *Shaded letters* indicates sequence identity, using the same species, order and UniProt IDs as indicated in *C*. The Arg-508 methylation site indicated in *red* and an *arrow*.

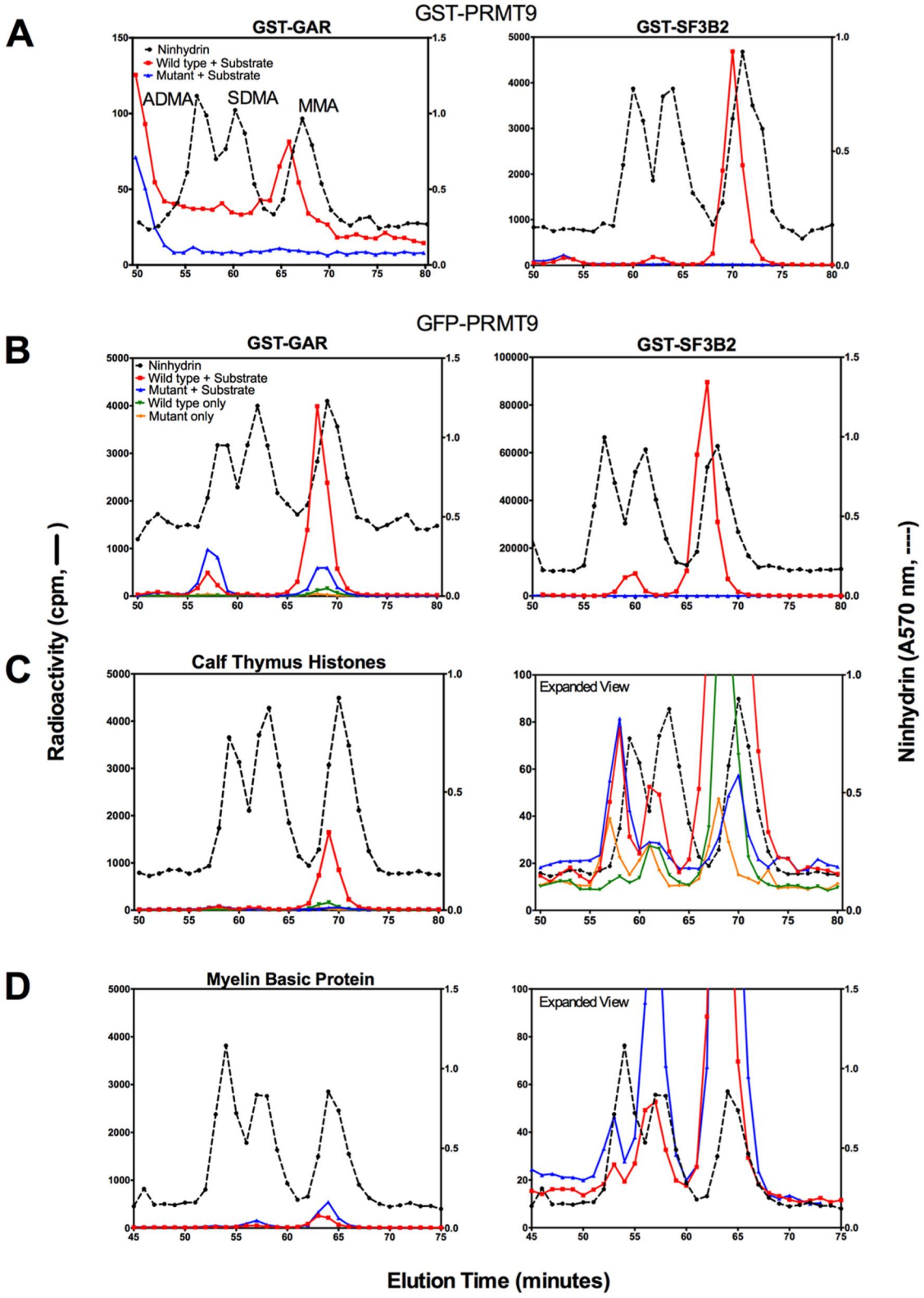
A
GST-PRMT9
GST-GAR
GST-SF3B2
Ninhydrin
Wild type + Substrate
Mutant + Substrate
ADMA
SDMA
MMA
B
GFP-PRMT9
GST-GAR
GST-SF3B2
Ninhydrin
Wild type + Substrate
Mutant + Substrate
Wild type only
Mutant only
C
Calf Thymus Histones
Expanded View
D
Myelin Basic Protein
Expanded View
Radioactivity (cpm, —)
Ninhydrin (A570 nm, ----)
Elution Time (minutes)

with Coomassie Blue for 1 h, and destained overnight. After destaining, the gel was treated with autoradiography enhancing buffer (EN^{3}HANCE, PerkinElmer Life Sciences, catalog no. 6NE9701) and vacuum dried. The dried gel was then exposed to autoradiography film (Denville Scientific, catalog no. E3012) at −80 °C for the indicated amount of time. For radioactive gel slice assay, gels were prepared, enhanced, and dried as described above, but the dried gel band was cut and submerged in 30% H_2O_2 for 24 h at 37 °C in a scintillation vial to solubilize. After incubation, 10 ml of Safety-Solve scintillation mixture (Research Products International, catalog no. 111177) was added to the vial, which was then counted for three 5-min cycles on a Beckman LS6500 liquid scintillation instrument. As described above, the specific activity of the label was about 90 cpm/fmol.

Generation of a PRMT5 Inducible Knock-out Cell Line—PRMT5 floxed mice were crossed with ER-Cre mice to generate *Prmt5*$^{F/F}$ER embryos and subsequently mouse embryonic fibroblasts (MEFs), as described previously (28). The MEFs, kindly provided by Drs. Marco Bezzi and Ernesto Guccione, were immortalized by maintaining cells on a 3T3 culture protocol in which 10^6 cells were passed onto gelatinized 10-cm dishes every 3 days.

PRMT5 Knock-out MEFs and Immunoblotting—To knock out PRMT5, Prmt5$^{F/F}$ER MEFs were treated with 2 μM 4-hydroxytamoxifen (OHT) for 14 or 30 days. Whole cell lysates of OHT-treated and untreated MEFs were separated by SDS-PAGE and transferred onto PVDF membranes. Blots were probed with a panel of antibodies, including anti-PRMT5 (1:1000) (Millipore), anti-SDMA (BL8243, 1:500) (Cell Signaling Technology, CST), anti-SDMA (BL8244, 1:200) (CST), anti-ADMA (D10F7, 1:2000)(CST), anti-MMA (1:2000, CST, catalog no. 8711), and anti-actin (1:10000) (Sigma, catalog no. A1978).

Amino Acid Analysis of Protein Hydrolysates and Quantification of SDMA—Approximately 40 mg of wet weight MEFs and 100 μl of 6 N HCl were added to a 6 × 50-mm glass tube and acid-hydrolyzed *in vacuo* as described above. After hydrolysis, the lysates were vacuum dried and resuspended in 100 μl of water and centrifuged at maximum speed (20,000 × *g*) for 10 min to remove debris. 75 μl was added to 250 μl of citrate loading buffer (0.2 M Na^+, pH 2.2), and amino acids were separated using the high resolution cation exchange chromatography method described above. Individual fractions collected with the known elution positions of ADMA, SDMA, MMA, and arginine were further derivatized using OPA for fluorescence detection and quantification using separation on a reverse phase HPLC (HP 1090 II liquid chromatograph coupled to a Gilson model 121 fluorometer with excitation filter of 305–395 nm and emission filter of 430–470 nm, with a setting of 0.001 relative fluorescence units), as described previously (29). An Agilent ZORBAX Eclipse AAA (analytical, 5 μm, 4.6-mm inner diameter, 150 mm in length) reverse phase column was used with 25-μl sample injection volumes at 32 °C and a flow rate of 1.7 ml/min. Solvent A consisted of 50 mM sodium acetate, pH 7.0, and solvent B of 100% methanol. The HPLC gradient used to separate the methylated OPA derivatives included a shallow gradient from 23 to 31.5% B for 20 min, a 5-min hold at 95% B, and a 14-min hold at 23% B. Because fractions containing arginine OPA derivatives commonly overloaded the detector, dilutions were made in the eluting buffer of the cation exchange column (sodium citrate, pH 5.25). The elution positions of methylated arginine derivatives were confirmed by comparison with standards. To quantify the data, the area under the curve for each amino acid peak of interest was determined using Excel by integration and area of summation by trapezoids. The total amount of each modification was calculated by summing the area of each cation exchange fraction that had the methylated amino acid present. Each replicate was normalized to cellular levels of arginine.

Results

Human PRMT9 and SF3B2 (SAP145) Are Evolutionarily Conserved among Vertebrates and Invertebrates—A BLAST search was used to identify homologs of human PRMT9 and SF3B2 in vertebrates, invertebrates, plants, and fungi. The sequences were aligned using MUSCLE, and a phylogenetic tree was assembled to show the conservation across various species (Fig. 1, *A* and *C*). Alignment of the post-motif II substrate-binding double E loop shows a clear conservation of the acidic residue Asp-258 and Gly-260 across all PRMT9 orthologs (Fig. 1*B*). Divergent sequences included PRMT7-like sequences in plants and invertebrates (Fig. 1*B*). Alignment of the THW loop also shows conservation of a cysteine residue in

FIGURE 2. **PRMT9 does not or very weakly methylates common PRMT substrates.** *A,* amino acid analysis of ^{3}H methylation reaction of bacterially expressed GST-PRMT9 wild type and catalytic mutant with GST-GAR (*left*) and GST-SF3B2 401–550-residue fragment (*right*) after 20 h of reaction at 37 °C, with 0.7 μM [*methyl*-^{3}H]AdoMet, and reaction buffer of 50 mM HEPES, 10 mM NaCl, 1 mM DTT, pH 8.0, in a final reaction volume of 60 μl. Approximately 5 μg of each substrate was reacted with 2 μg of wild type and catalytic mutant GST-PRMT9 enzyme. After TCA precipitation and acid hydrolysis, 1 μmol of ADMA, SDMA, and MMA standards were added, and amino acid analysis was carried out as described under "Experimental Procedures." The *dotted black line* indicates the ninhydrin absorbance at 570 nm for the elution of the nonradiolabeled standards. The *red line* indicates the elution of radioactive methylated amino acids from the reaction of the wild type enzyme with substrate, and the *blue line* indicates the elution of radioactive methylated amino acids from the methylation reaction of the catalytic mutant enzyme with the substrate. Radioactivity is given as the average of three counting cycles on a liquid scintillation counter. Because of the tritium isotope effect, radioactive methylated amino acids elute about 1 min prior to the nonisotopically labeled standards (45). *B,* amino acid analysis of methylation reactions of a more active mammalian-expressed GFP-PRMT9, with GST-GAR (*left*) and GST-SF3B2 401–550-residue fragment (*right*) after a 20-h reaction, using the same reaction conditions described in *A*. Approximately 5 μg of GST-GAR and GST-SF3B2 401–550-residue fragment were used in methylation reactions with 1 μg of GFP-PRMT9 wild type or catalytic mutant. The *red line* indicates the elution of radioactive methylated amino acids from the reaction of the wild type GFP-PRMT9 enzyme with the substrate. The *blue line* indicates the elution of the radioactive methylated amino acids from the reaction of the catalytic mutant GFP-PRMT9 enzyme with the substrate. The *green* and *orange lines* indicate the wild type and mutant enzyme only controls, respectively, showing any radioactivity due to background contamination in the GFP-PRMT9 enzymatic preparations. *C,* amino acid analysis of methylation reactions of 1 μg of GFP-PRMT9 wild type or catalytic mutant with 5 μg of calf thymus histones (*left*) after 20 h, using the same reaction conditions described above. *Right panel* is an expanded view of the radioactivity scale to show residual activity with the control reactions. *D,* amino acid analysis of methylation reactions of 1 μg of GFP-PRMT9 wild type or catalytic mutant preparations with 10 μg of bovine-purified MBP after 1 h (*left panel*), using the same reaction conditions described above. *Right panel* shows an expanded view of the radioactivity scale to show residual activity of the control reaction with the catalytic mutant.

A

Top Hits: (>5 peptide matches)	Species	UniProt ID	UniProt #	Size	Peptide Matches
60 kDa heat shock protein, mitochondrial	Homo sapiens	CH60_HUMAN	P10809	61 kDa	8
ATP synthase subunit alpha, mitochondrial	Hominidae	ATPA_HUMAN	P25705	60 kDa	11
DNA-dependent protein kinase catalytic sut	Homo sapiens	PRKDC_HUMAN	P78527	469 kDa	13
GFP-PRMT9			**GB0003**	**94 kDa**	**18**
Heat shock 70 kDa protein 1A/1B	Catarrhini	HSP71_HUMAN	P08107	70 kDa	8
Heat shock cognate 71 kDa protein	Eutheria	HSP7C_HUMAN	P11142	71 kDa	9
Heat shock protein HSP 90-beta	Homo sapiens	HS90B_HUMAN	P08238	83 kDa	5
Insulin receptor substrate 4	Homo sapiens	IRS4_HUMAN	O14654	134 kDa	5
Serum albumin	Bos taurus	ALBU_BOVIN	P02769	69 kDa	5
Sodium/potassium-transporting ATPase sut	Homo sapiens	AT1A1_HUMAN	P05023	113 kDa	8
Splicing factor 3B subunit 2	Hominidae	SF3B2_HUMAN	Q13435	100 kDa	21
Splicing factor 3B subunit 4	Catarrhini	SF3B4_HUMAN	Q15427	44 kDa	2
Translational activator GCN1	Homo sapiens	GCN1L_HUMAN	Q92616	293 kDa	5
Tubulin alpha-1B chain	Tetrapoda	TBA1B_HUMAN	P68363 (+1)	50 kDa	7
Tubulin beta chain	Amniota	TBB5_HUMAN	P07437	50 kDa	8

B

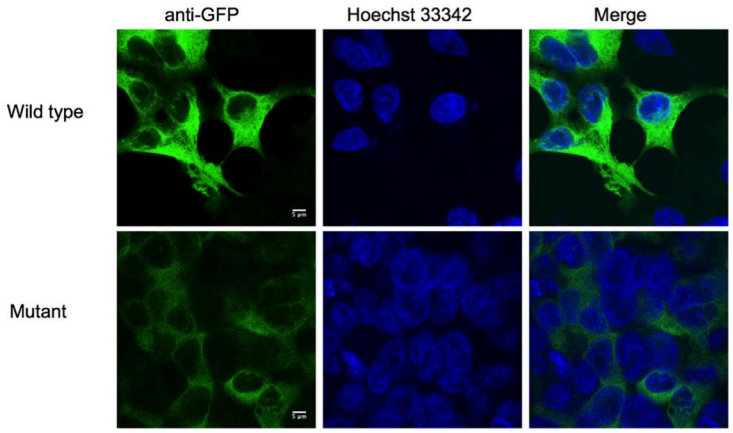

C

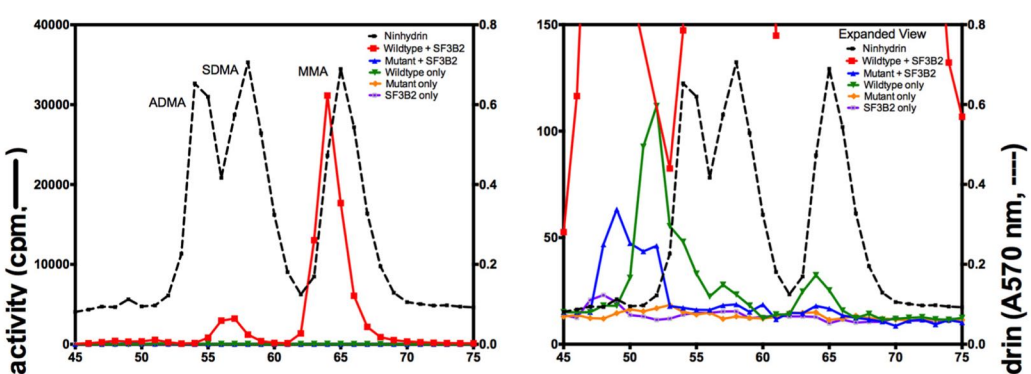

D

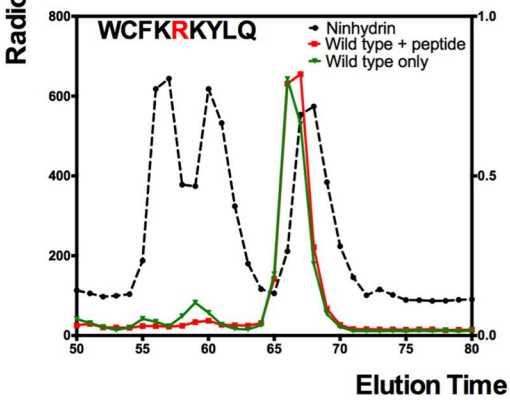

place of a histidine residue that is found in other types of PRMTs (Fig. 1*B*). Interestingly, the only other mammalian PRMT with a non-histidine residue at this position is PRMT5 (serine); the presence of smaller residues at this site has been suggested to correlate with the ability of PRMT5 and PRMT9 to form SDMA (4).

In our previous work, we identified Arg-508 on SF3B2 to be the target methylation site for PRMT9 (7). Analysis of the sequence surrounding Arg-508 of SF3B2 shows a strict conservation of this residue and the surrounding residues in vertebrates, invertebrates, plants, and fungi (Fig. 1*D*). The Lys-507 and Lys-509 residues are conserved in almost all species (Fig. 1*D*), with the exception of *Schizosaccharomyces pombe*, where the second lysine is replaced with an aspartate. Aromatic residues of Phe-506 and Tyr-510 are also well conserved, with differences found in the plants. Interestingly, the chicken *Gallus gallus* contains a PRMT9 ortholog, but an ortholog of SF3B2 does not appear to exist. In addition, *Nematostella vectensis* (a sea anemone) contains a PRMT9 ortholog, but this gene seems to have been lost in other species of the same phyla. In addition, organisms such as the fungi *Aspergillus nidulans* and the bacterium *Rhizobium leguminarosum* contain an SF3B2 ortholog but do not appear to have an ortholog of PRMT9, suggesting the enzyme plays a role unique to higher eukaryotes. The nematode *C. elegans* PRMT-3 protein (UniProt O02325 in Fig. 1*A*) is noteworthy because it is most closely related to PRMT9 (30), yet published studies show that it generates only MMA (31).

PRMT9 Is Poorly Active on Bona Fide PRMT Substrates—Most PRMTs are able to efficiently methylate a variety of substrate proteins; PRMT1 and PRMT5 have very broad substrate specificity, whereas PRMT4, PRMT6, and PRMT8 have a more limited specificity but still methylate a variety of substrates (2). We thus tested whether recombinant PRMT9 can methylate the common substrates of these other PRMTs, including a recombinant GST fusion of the N-terminal glycine and argi nine-rich region of fibrillarin (GST-GAR) that is recognized by PRMT1, PRMT3, and PRMT5–7 (2, 3, 8, 27, 32). In contrast to other PRMTs, we found that PRMT9 poorly methylates GST-GAR, as shown by amino acid analysis, with only a small radioactive MMA peak formed (Fig. 2*A*, *left panel*). Not surprisingly, PRMT9 is highly active on its biological substrate as the GST-SF3B2 401–550-residue fragment (Fig. 2*A*, *right panel*), producing both MMA (100-fold higher than GST-GAR) as well as SDMA products. A more active preparation of mammalian-expressed PRMT9 (GFP-PRMT9) proved to have enhanced methyltransferase activity on GST-GAR (Fig. 2*B*, *left panel*) and GST-SF3B2 (Fig. 2*B*, *right panel*), where both MMA (20-fold higher with GST-SF3B2 than that seen with GST-GAR) and SDMA were formed. Calf thymus histones were weakly methylated by the GFP-PRMT9 enzyme (MMA and some SDMA, Fig. 2*C*) but not to the level seen with SF3B2. MBP could not be methylated by PRMT9, as no activity was seen above that observed in the catalytic mutant (Fig. 2*D*). Here, the catalytically inactive GFP-PRMT9 was used as a control to rule out the possibility of another PRMT contaminant coimmunoprecipitating with the mammalian-expressed enzyme. We conclude that PRMT9 has little to no activity on the broadly methylated known substrates of the other mammalian PRMTs, and it appears to be relatively specific for the splicing factor SF3B2.

Mammalian-expressed PRMT9 Copurifies with Its Methylation Substrate SF3B2 and Is Localized to the Cell Cytoplasm—Mass spectrometry analysis of tryptic peptides was done on the immunoprecipitated wild type and catalytically inactive GFP-PRMT9 expressed in neuronally derived HEK293 cells (33) for protein identification of other possible binding partners and/or substrates. We previously showed that tandem affinity purification-tagged PRMT9 expressed in cervically derived HeLa cells was associated with SF3B2 and SF3B4 (7), and we sought to confirm this interaction with a different cell type. In HEK293 cells, wild type PRMT9 was associated with several proteins commonly brought down during the purification process but most interestingly brought down SF3B2 (SAP145) and SF3B4 (SAP49) as the top hits (Fig. 3*A*). Mass spectrometry analysis on the catalytic mutant GFP-PRMT9 did not identify any SF3B2 or SF3B4 peptides (data not shown), possibly suggesting that the binding of AdoMet is a prerequisite for complex formation or substrate binding. Immunofluorescence of wild type and mutant PRMT9 confirms the protein is primarily found in the cytoplasm, with some possible nuclear localization (Fig. 3*B*, *top panels*). Tissue-based mapping of the human proteome (34) confirms this localization, perhaps suggesting that variation of localization and expression is based on the cell type. The GFP-PRMT9 mutant protein was expressed in much lower

FIGURE 3. **Interaction partner identification, localization, and activity characterization of mammalian expressed PRMT9.** Mammalian expressed wild type and catalytic mutant GFP-PRMT9 constructs were immunoprecipitated from HEK293 cells as described under "Experimental Procedures." *A,* LC-MS/MS analysis was done on immunoprecipitated wild type and catalytic mutant GFP-PRMT9 samples to identify possible substrates and interaction partners. Identified peptide hits with greater than five peptide matches are listed (with the exception of SF3B4 with two peptide hits but was important for our analysis) for the wild type enzyme preparation, along with their UniProt ID and number, molecular weight, and the exact number of peptide hits. Catalytic mutant GFP-PRMT9 had similar peptide matches (data not shown), with the exception of the two splicing factors SF3B2 and SF3B4 identified in the wild type preparation were not identified with the mutant sample. *B,* immunofluorescence experiments to determine the intracellular localization of the wild type and catalytic mutant GFP-PRMT9 samples. Immunofluorescence was performed in HEK293 cells using anti-GFP antibody at 1:500 dilution. The *scale bar* indicates 5 μm. *C,* amino acid analysis (described under "Experimental Procedures" (7)) of methylation reactions with GFP-PRMT9 wild type or catalytic mutant enzymes and GST-SF3B2 401–550-residue fragment after 1 h at 37 °C. Approximately 1 μg of enzyme was reacted with 5 μg of substrate, in a final reaction volume of 60 μl consisting of 0.7 μM [*methyl*-^{3}H]AdoMet and reaction buffer of 50 mM HEPES, 10 mM NaCl, 1 mM DTT, pH 8.0. *Right panel* displays the expanded view of the radioactivity scale to show residual activity of the control reactions with the catalytic mutant and enzyme and substrate only controls. The *black dotted line* indicates the ninhydrin absorbance at 570 nm for the elution of the nonradiolabeled standards. The *solid line* indicates the elution of the radioactive methylated amino acids after the reaction of the enzyme with the substrate (*red*, wild type GFP-PRMT9, and *blue*, catalytic mutant GFP-PRMT9). The *green* and *orange lines* indicate the wild type and catalytic mutant GFP-PRMT9 enzyme only controls, respectively, and the *purple line* indicates the substrate only control. *D,* amino acid analysis of a highly active HA-tagged PRMT9 with a synthetic peptide consisting of the Arg-508 methylation site (highlighted in *red*), WCFKRKYLQ, indicated in the figure. The methylation reaction consisted of ~1 μg of HA-tagged PRMT9 and 12.5 μM peptide, 0.7 μM [*methyl*-^{3}H]AdoMet, and methylation reaction buffer of 50 mM HEPES, 10 mM NaCl, 1 mM DTT, pH 8.0, at 37 °C for 18 h. *Green line* indicates the enzyme only control reaction for background contamination.

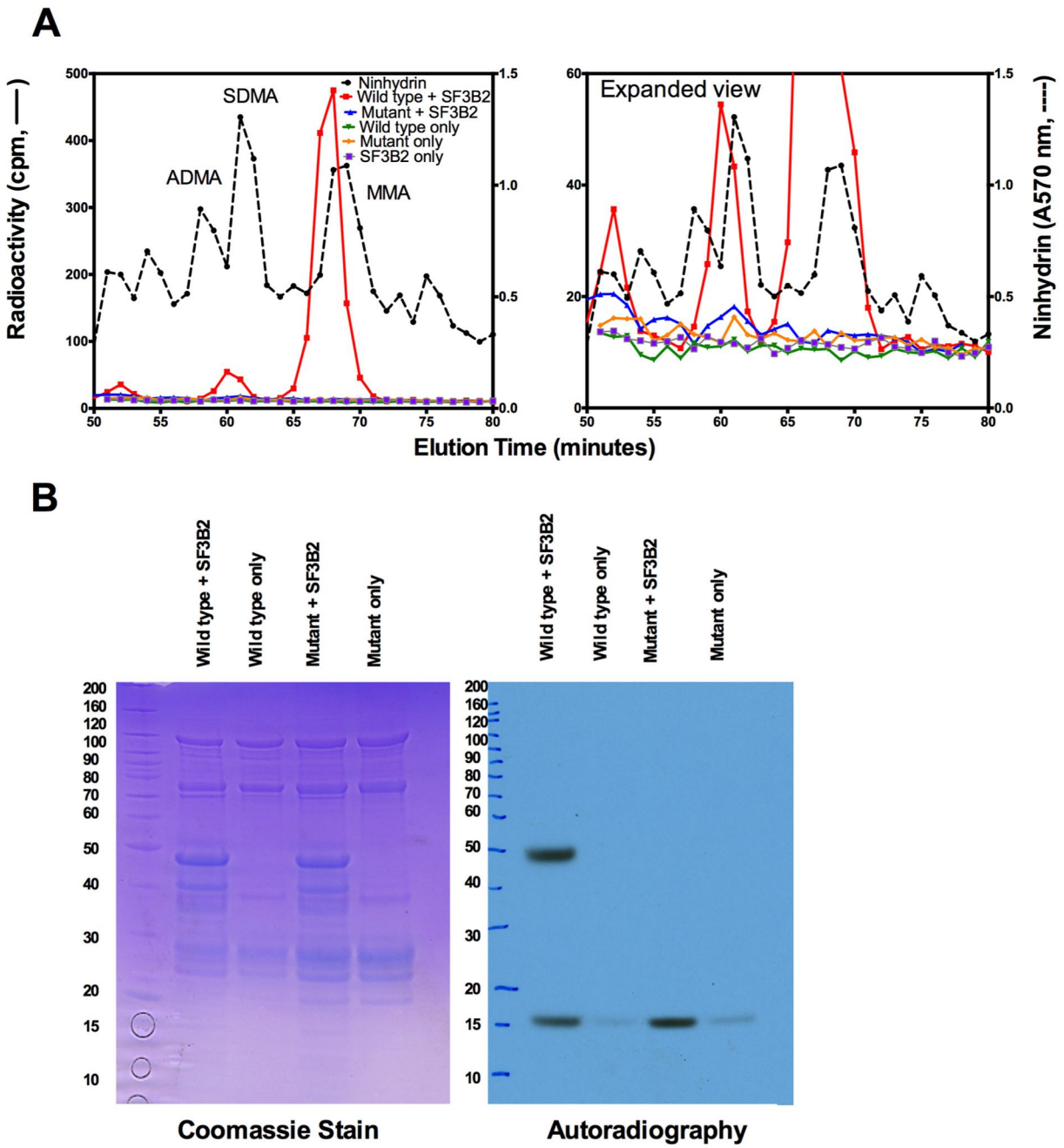

FIGURE 4. **Bacterially expressed GST-PRMT9 is very active on SF3B2 substrate.** *A,* amino acid analysis (described under "Experimental Procedures" (7)) using bacterially expressed GST-PRMT9 with GST-SF3B2 401–550-residue wild type fragment. Methylation reaction consisted of 2 μg of enzyme (wild type or catalytic mutant), 5 μg of GST-SF3B2 401–550-residue fragment, 0.7 μM [*methyl*-^{3}H]AdoMet, and methylation reaction buffer of 50 mM HEPES, 10 mM NaCl, 1 mM DTT, pH 8.0, at 37 °C for 1 h. The *dashed black line* indicates the ninhydrin absorbance at 570 nm for the elution of the nonradiolabeled standards. *Solid lines* indicate the elution of the radioactive methylated amino acids after the reaction of the enzyme with the substrate (*red*, wild type GST-PRMT9, and *blue*, catalytic mutant GST-PRMT9). *Green* and *orange lines* indicate the wild type and catalytic mutant enzyme only controls, respectively. The *purple line* indicates substrate only control. *B,* autoradiography of ^{3}H-methylated GST-SF3B2 401–550-residue fragment with wild type or catalytic mutant GST-PRMT9. Reactions were prepared as described in *A* for 1 h, and autoradiography was prepared as described above under "Experimental Procedures." The dried gel was then exposed to autoradiography film (Denville Scientific, E3012) for 7 days at −80 °C. BenchMark Protein Ladder (Invitrogen, catalog no. 10747-012) was used, with ~0.5 μg of each standard is shown. The identity of a nonspecific radiolabeled band shown at 16 kDa is unknown, but its formation is not dependent upon an active PRMT9 enzyme.

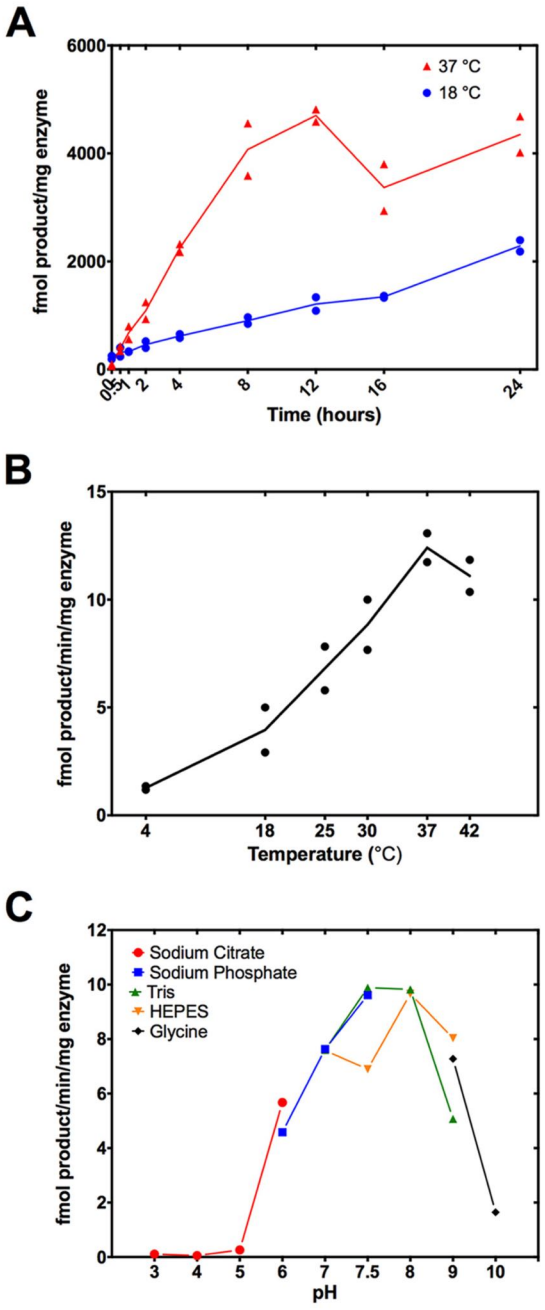

FIGURE 5. **Optimization of reaction conditions for PRMT9.** *A–C,* optimization of reaction conditions with GST-tagged PRMT9 for time (*A*), temperature (*B*), and buffer and pH (*C*). For all optimization conditions, reactions were quenched after the appropriate time by the addition of SDS loading buffer and run on a 12.6% Tris-glycine gel as described under "Experimental Procedures" for radioactive gel slice assay. *A,* time course reaction of GST-PRMT9 wild type enzyme with its substrate GST-SF3B2 401–550-residue wild type fragment. The reactions contained ~4 μg of GST-PRMT9, 6 μg of GST-SF3B2, 0.7 μM [*methyl*-^{3}H]AdoMet in a 60-μl reaction buffer of 50 mM potassium HEPES, pH 8.0, 10 mM NaCl, and 1 mM DTT. The reactions were run in duplicate at the indicated temperature (*red line,* 37 °C; *blue line*, 18 °C) for the indicated time (0, 0.5, 1, 2, 4, 8, 12, 16, and 24 h), run on SDS-PAGE, and counted as described under "Experimental Procedures." The specific activity determined for the [*methyl*-^{3}H]AdoMet (about 90 cpm/fmol) was used to calculate the amount of product formed. *B,* temperature dependence of GST-PRMT9 wild type with GST-SF3B2 401–550-residue wild type fragment. The reactions contained 4 μg of GST-PRMT9, 6 μg of GST-SF3B2, 0.7 μM [*methyl*-^{3}H]AdoMet in a 60-μl reaction buffer of 50 mM potassium HEPES, pH 8.0, 10 mM NaCl, and 1 mM DTT. Duplicate reactions were incubated at the indicated temperature for 18.5 h, run on SDS-PAGE, and counted as described above. The activity was calculated as in *A*. *C,* buffer type and pH influences activity of the enzyme with its substrate. Reactions contained 4 μg of GST-PRMT9 wild type, 6 μg of GST-SF3B2 401–550-residue wild type fragment, 0.7 μM [*methyl*-^{3}H]AdoMet, and the addition of 50 mM buffer (sodium citrate (pH 3.0, 4.0, 5.0, and 6.0, *red line*), sodium phosphate (pH 6.0, 7.0, and 7.5, *blue line*), Tris (pH 7.0, 7.5, 8.0, and 9.0, *green line*), HEPES (pH 7.0, 7.5, 8.0, and 9.0, *orange line*), and glycine (pH 9.0 and 10.0, *black line*)) at a final reaction volume of 60 μl. Reactions were run for 8.5 h at 37 °C. The reactions were quenched and run on a gel as described above and under "Experimental Procedures." Solubilized gel slices were counted and activity calculated as in *A*.

amounts (Fig. 3*B*, *bottom panels*), suggesting it may not be as stable as the wild type fusion protein. These localization studies suggest that PRMT9 methylates its substrate primarily in the cytoplasm, before SF3B2 is shuttled to the nucleus to participate in splicing. Amino acid analysis of GFP-PRMT9 with the bacterially expressed GST-SF3B2 fragment containing the methylation site (7) shows great methylation activity after only 1 h (Fig. 3*C*), with the controls of mutant enzyme, enzymes alone, or substrate alone showing negligible activity.

Our previous work has shown the site of PRMT9 methylation on SF3B2 is at Arg-508 (7). To study the effect of residues adjacent to Arg-508 on the methyltransferase activity of PRMT9, a synthetic peptide containing the SF3B2 sequence of residues 504–512 WCFKRKYLQ was generated (GenScript) and tested as a methyl-acceptor for PRMT9. Surprisingly, both GFP-PRMT9 (data not shown) and an even more active insect-expressed HA-tagged PRMT9 showed no activity above the enzyme only control (Fig. 3*D*). Other peptides derived from histone H2B and H4 residues and their mutants (H2B(23–37), H4(1–21), and H4(14–22) (6, 8)) containing a similar KRK sequence found in SF3B2 were also tested, and again no methylation activity was detected (data not shown). These results suggest that a specific conformation of the protein around the methylated arginine residue is required for PRMT9 methylation.

Bacterially Expressed GST-PRMT9 SDMA Forming Activity on Splicing Factor SF3B2—Because mammalian-expressed enzymes may be contaminated with endogenous PRMT family members, and because it is generally accepted that no PRMT activity has been observed in *E. coli* and other eubacteria (35–37), we bacterially expressed the GST-PRMT9 enzyme to further test for methylation activity. Using the GST-SF3B2 401–550-residue fragment fusion protein as a substrate in *in vitro* reaction mixtures with [*methyl*-^{3}H]AdoMet, we showed the formation of MMA and SDMA products by amino acid analysis (Fig. 4*A*) and the strong methylation of the polypeptide with the wild type enzyme but not with the catalytic mutant (Fig. 4, *A* and *B*). These results further validate SF3B2 as the biological substrate, because such activity with other substrates is not seen with the GST recombinant enzyme (Fig. 2*A*, *left panel*, and data not shown).

To study the effects of active site mutations on the GST-PRMT9 enzyme, we optimized reaction conditions to deter-

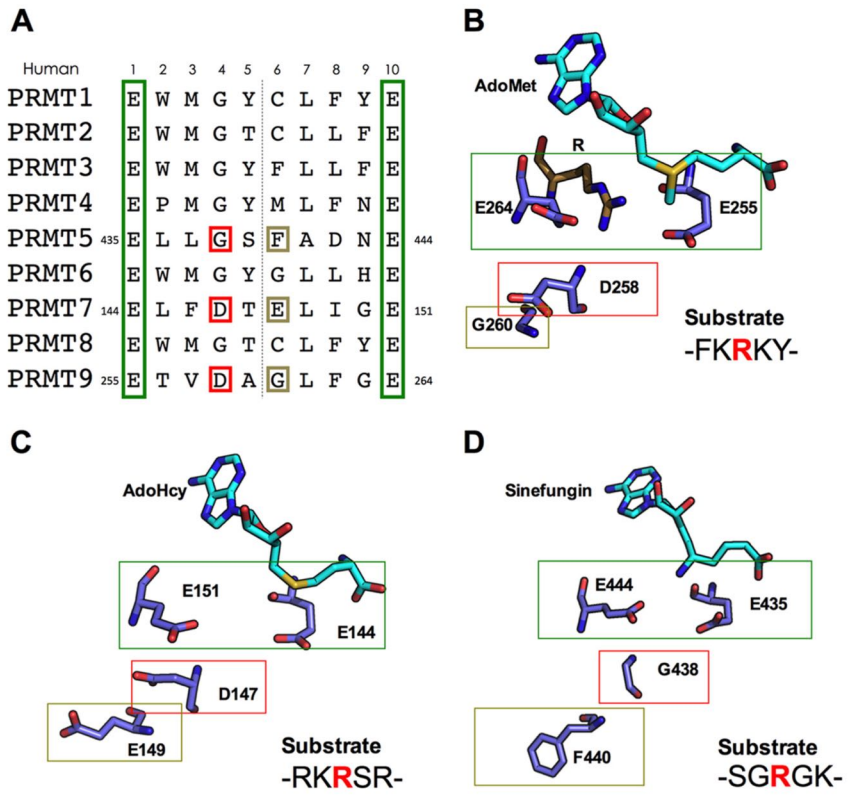

FIGURE 6. **Comparison of the double E loop residues of PRMT9 with known PRMT structures.** *A,* sequence alignment of the double E loop post motif II residues of the nine human PRMTs. The Glu residues making up the double E loop are *boxed* in *green*. Important residues unique to PRMT5, PRMT7, and PRMT9 are *boxed* in *red* and *yellow*. Sequences correspond to PRMT1 (UniProt ID, Q99873), PRMT2 (P55345), PRMT3 (O60678), PRMT4/CARM1 (Q86X55), PRMT5 (O14744), PRMT6 (Q96LA8), PRMT7 (Q9NVM4), PRMT8 (Q9NR22), and PRMT9 (Q6P2P2). *B,* predicted structure of *Homo sapiens* PRMT9 using modeling to other PRMTs with known structures generated by Phyre2.0 software, with AdoMet included as a ligand. A close look at important double E loop substrate-binding motif resides in relation to the AdoMet and substrate Arg. Acidic residues Glu-255 and Glu-264, which make up the ends of the double E loop, are boxed in *green*. Asp-258, in the middle of the double E loop, is boxed in *red*, and Gly-260, a position where other PRMTs have a distinguishing residue and PRMT7 contains a Glu, is *boxed* in *yellow*. The PRMT9 structure was modeled using Phyre2.0 (38) with input sequence from UniProt ID: Q6P2P2 and analyzed using PyMOL software. SF3B2 substrate sequence is listed, with substrate arginine highlighted in *red*. *C,* important residues of the double E loop in the crystal structure of *M. musculus* PRMT7 (Protein Data Bank code 4C4A (16)) with *S*-adenosylhomocysteine as a ligand. Mouse PRMT7 double E loop residues are identical to those of human PRMT7. Glu-144 and Glu-151 residues making up the ends of the double E loop are *boxed* in *green*. Acidic residues Asp-147 and Glu-149 are *boxed* in *red* and *yellow*, respectively. Structure was analyzed using PyMOL software. General substrate sequence is listed, with substrate arginine highlighted in *red*. *D,* a look at important residues of the double E loop in the crystal structure of *H. sapiens* PRMT5 (Protein Data Bank code 4GQB (39)) with sinefungin as a ligand. Gly-438 and Phe-440 in identical positions to those highlighted in *B* and *C* are *boxed* in *red* and *yellow*, respectively. Structure was analyzed using PyMOL software. General substrate sequence is listed, with substrate arginine highlighted in *red*.

mine the best conditions for methylation and also determine the amount of time needed to attain linear product formation. At 37 °C, enzyme activity was linear for 8 h, although at 18 °C it was linear for 12 h. In contrast to the PRMT7 enzyme (8), the activity was found to be ~4-fold higher at 37 °C than at 18 °C. Analysis of enzyme activity over the range of 4–42 °C demonstrated maximal activity at 37 °C (Fig. 5*B*). Using a variety of buffers, we found optimal activity at pH values between 7.5 and 8.0, although significant activity was detected from pH 6.0 to 9.0 (Fig. 5*C*).

Substrate-binding Double E Loop Residues Play an Important Role in Coordinating the Substrate Arginine—PRMTs contain a signature "double E loop" post-motif II, in which two glutamate residues that bind the methylatable arginine residue of the substrate protein are separated by eight residues (EX_8E (2)). Sequence alignment of these residues in the nine human PRMTs shows several conserved residues (Fig. 6*A*). Type I PRMTs (PRMT1–4, PRMT6, and PRMT8) all contain signature WMG or PMG sequences in positions 2–4, where the type II (PRMT5 and PRMT9) and type III (PRMT7) enzymes contain distinct sequences. PRMT7 and PRMT9 each contain an acidic Asp residue at position 4; PRMT7 has an additional acidic residue at position 6, although PRMT9 has a Gly residue there. The acidic residues at positions 4 and 6 have been shown to have an important role in substrate recognition for human PRMT7 (8). The predicted structure of the PRMT9 double E loop using Phyre2.0 modeling (38) shows the relative positions of the glutamate residues (residues 255 and 264) responsible for binding the substrate arginine. In this model, the carboxylate group of the position 4 Asp-258 points away from the substrate arginine, possibly to coordinate the binding of one or both of the two lysine residues adjacent to the methylated arginine in the FKRKY sequence of SF3B2 (Fig. 6*B*). The crystal structure of mouse PRMT7 (Fig. 6*C*) (16) shows a similar positioning of

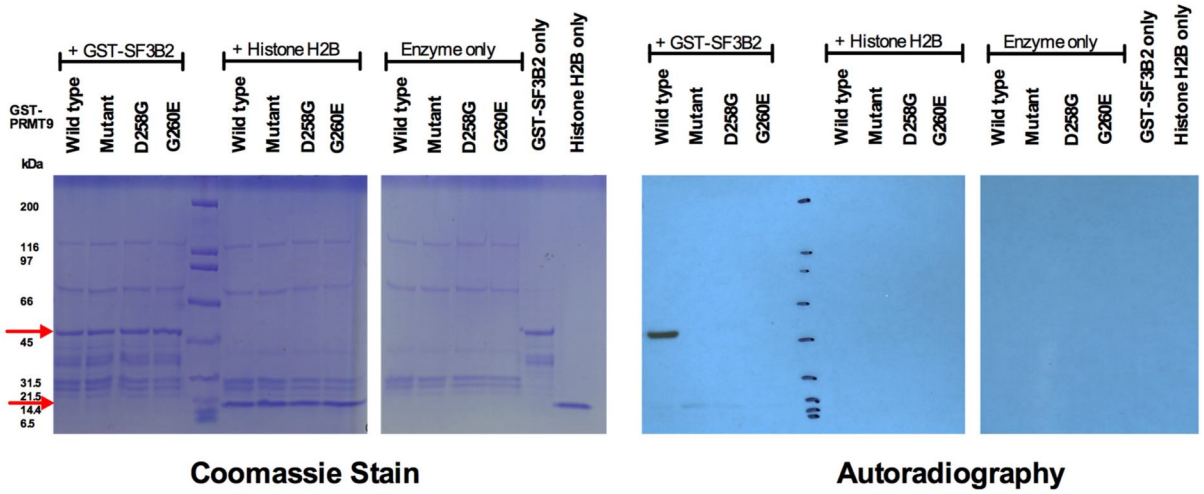

FIGURE 7. **Importance of a single acidic residue in the double E loop of PRMT9.** Site-directed mutagenesis was utilized to mutate the important residues mentioned in Fig. 6. Asp-258 was mutated to Gly to mimic type I enzymes, and Gly-260 was mutated to Glu to mimic PRMT7. The mutants were sequenced on both strands to confirm the mutation and bacterially expressed and purified as described under "Experimental Procedures." Methylation reactions were prepared using two PRMT substrates, PRMT9 substrate GST-SF3B2 401–550-residue wild type fragment (5 μg) purified as described under "Experimental Procedures" and PRMT7 protein substrate recombinant histone H2B (5 μg) purchased from New England Biolabs. Approximately 2 μg of enzyme (GST-PRMT9 wild type, catalytic mutant, D258G, or G260E) were added to the reaction with the indicated amount of substrate, along with 0.7 μM [*methyl*-^{3}H]AdoMet and methylation reaction buffer of 50 mM HEPES, 10 mM NaCl, 1 mM DTT, pH 8.0 at 37 °C for 1.5 h. Reactions were quenched by the addition of SDS loading buffer, run on 4–12% Bistris gel for SDS-PAGE, and dried as described under "Experimental Procedures." The dried gel was exposed to autoradiography film for 21 days at −80 °C. Molecular mass positions are indicated from 2 μg of unstained SDS-PAGE broad range markers (Bio-Rad, catalog no. 161-0317) electrophoresed in parallel lanes.

the corresponding residues, with both the position 4 Asp-147 and position 6 Glu-149 carboxyl groups also pointing away from the methylated arginine; this could account for the substrate specificity requirement of PRMT7 for an R*X*R motif (6). In addition, the crystal structure of human PRMT5 shows the position of the side chain of Phe-440, corresponding to Glu-149 in PRMT7 and Gly-260 in PRMT9, pointing away from the position of the methylated arginine (Fig. 6*D*) (39). These crystallographic and predicted structures led us to further probe these residues as being responsible for PRMT9's substrate specificity for the -FKRKY- sequence within the protein structure of SF3B2.

Site-directed Mutagenesis of Acidic Residue in PRMT9 Double E Loop Abolishes Recognition and Methylation of SF3B2—In probing for the residues responsible for PRMT9 substrate specificity, site-directed mutagenesis was done on residues in the double E loop described above and in Fig. 6. Asp-258 was mutated to Gly (D258G) to mimic type I enzymes, and Gly-260 was mutated to Glu (G260E) to mimic PRMT7. *In vitro* methylation reactions consisting of wild type, catalytic mutant, and mutants D258G and G260E were set up with GST-SF3B2 401–550-residue wild type fragment and recombinant histone H2B and analyzed by SDS-PAGE and autoradiography (Fig. 7). We found that PRMT9 lost all activity for SF3B2 when Asp-258 and Gly-260 were mutated, suggesting the importance of these residues in coordinating and binding of the substrate for methylation. *In vitro* methylation reactions with recombinant histone H2B, a good PRMT7 protein substrate due to its basic R*X*R sequences (6, 8), was also not recognized or methylated by either wild type enzyme or the D258G or G260E mutants. These results suggest that the local environment in the double E loop is crucial for catalysis.

Importance of PRMT9 Domains for Enzymatic Activity—Human PRMT9 contains three TPR motifs (residues 25–134) and two ancestrally duplicated methyltransferase domains (residues 135–530 and 531–895). This domain structure is unusual among the PRMT family, as no other PRMT contains a TPR motif, and only PRMT7 has a second methyltransferase domain. Several deletion constructs were made, in which the TPR motif was missing (ΔTPR), the N terminus was missing (ΔN; missing residues 21–350), and two C-terminal mutants ("ΔC 350," missing residues 351–895, and "ΔC 529," missing residues 530–895). These mutant enzymes were tested for enzymatic activity in *in vitro* methylation reactions by amino acid analysis (Fig. 8*A*). No activity was observed with any of the mutants after 16.5 h of incubation, a condition designed to detect any small amounts of product formation. Incubating the N- and C-terminal deletion constructs together did not result in enzyme activity (Fig. 8*A*). To rule out the possibility of degradation of the enzymes during the longer methylation reaction time, the reactions were set up in duplicate and incubated for 1 h, separated by SDS-PAGE, and subjected to autoradiography (Fig. 8*B*). Again, no activity was seen with the truncation mutants, suggesting that the intact, full-length PRMT9 protein is necessary for methylation activity.

Residues Surrounding the Arg-508 Methylation Site and the Position of the Methylated Arginine Are Important for Methyltransferase Activity—Because a synthetic peptide corresponding to the methylated region on SF3B2 could not be methylated by PRMT9 (Fig. 3*D*), the GST-SF3B2 401–550-residue wild type fragment was mutated to probe for the importance of the residues surrounding the Arg-508 site (-FKRKY-) using the more active GFP-PRMT9 enzyme (Fig. 9). The two flanking Lys residues were mutated to either Ala or Arg (Fig. 9, *B* and *C*). The

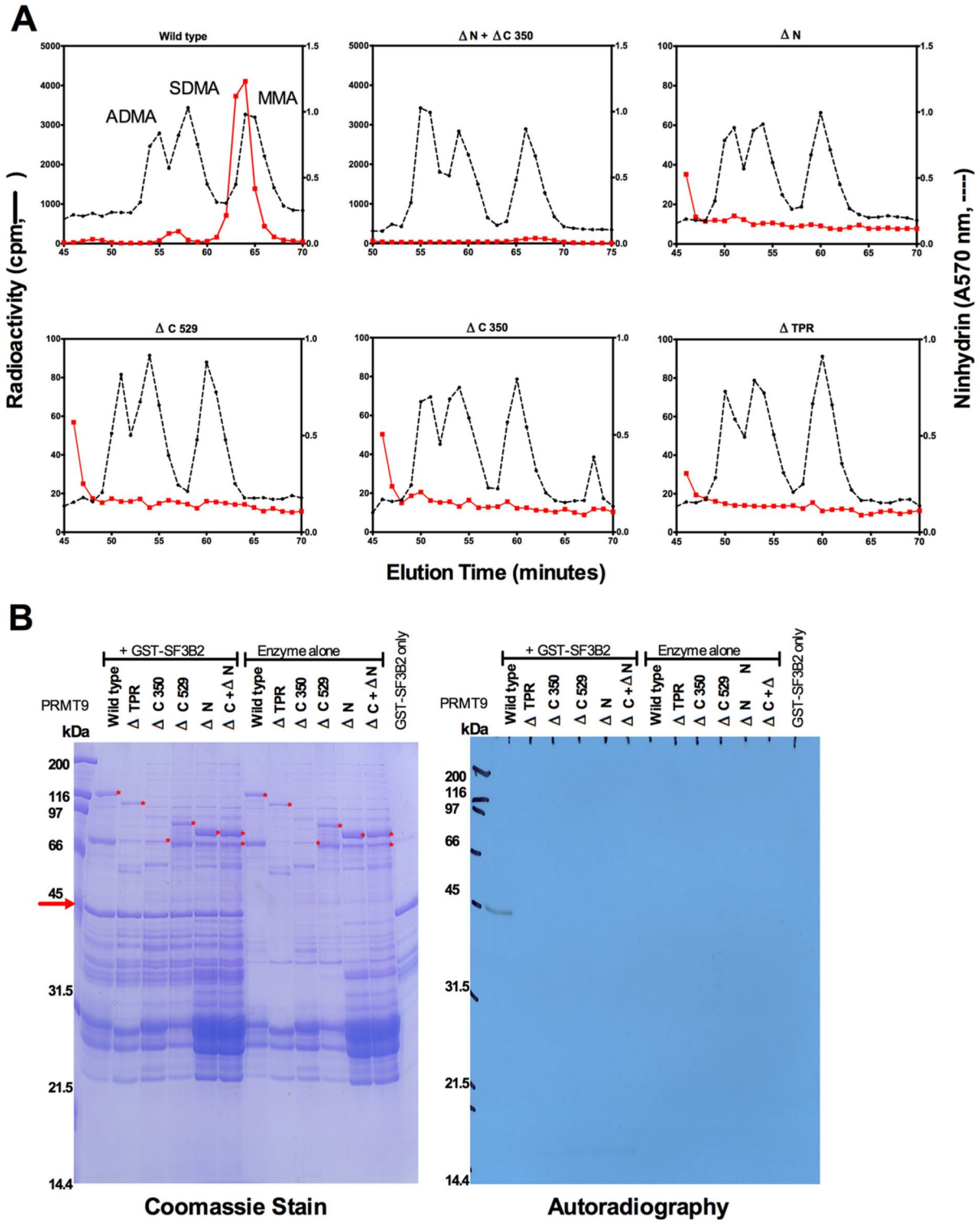
A
Wild type
ΔN + ΔC 350
ΔN
ΔC 529
ΔC 350
ΔTPR
ADMA
SDMA
MMA
Radioactivity (cpm, ——)
Ninhydrin (A570 nm, ----)
Elution Time (minutes)
B
+ GST-SF3B2
Enzyme alone
PRMT9
kDa
Wild type
ΔTPR
ΔC 350
ΔC 529
ΔN
ΔC+ΔN
GST-SF3B2 only
200
116
97
66
45
31.5
21.5
14.4
Coomassie Stain
Autoradiography

-FARAY- and the -FRRRY- mutant proteins were both substrates for PRMT9 with moderately diminished formation of MMA but a greatly reduced formation of SDMA (Fig. 9, *B* and *C*). We next probed for the importance of the position of the methylatable arginine residue in the -FKRKY- sequence by moving its position upstream or downstream by one residue. An -FRKRY- protein was generated with the lysine and arginine residues switched, which resulted in an ~200-fold loss of MMA production and the complete loss of SDMA production (Fig. 9*D*). When only one arginine residue was present at the −1 position (-FRKKY-), we detected less than 0.3% of the activity with the wild type -FKRKY- sequence (Fig. 9*E*). These results suggest the importance of the position of the methylated arginine residue in the protein. In additional experiments, we mutated the two aromatic residues Phe-506 and Tyr-510 to Ala to look at the importance of π stacking or aromaticity in the binding of the substrate. Interestingly, the mutant construct -AKRKA- had a similar methyl-accepting activity as the wild type -FKRKY- protein (Fig. 9*A*). To confirm these results, we analyzed the polypeptides methylated after SDS-PAGE and autoradiography using the bacterially expressed GST-tagged PRMT9 enzyme (Fig. 9*G*). No methylation was observed with the GST-SF3B2 fragment protein in the mutants where the arginine residue was moved, although full activity was seen in the -AKRKA- mutant and partial activity in the -FARAY- and -FRRRY- proteins, consistent with the results obtained in Fig. 9, *A–F,* by amino acid analysis with the GFP-tagged enzyme.

Relative Contribution of the Type II PRMTs (5 and 9) in Mouse Embryo Fibroblasts—PRMT5 and PRMT9 are the only type II SDMA-forming enzymes known in mammals. We were thus interested in the relative roles of these two enzymes in total SDMA production. Using mouse embryo fibroblasts constructed so that PRMT5 expression could be turned off by induction with OHT, we analyzed proteins by immunoblotting with anti-PRMT5, anti-SDMA, anti-MMA, anti-ADMA, and anti-actin antibodies (Fig. 10*A*). We were able to reduce the PRMT5 protein to undetectable levels. There was little or no change in immunoreactivity to antibodies against ADMA and some loss of reactivity to antibodies against MMA. However, we found almost all of the immunoreactivity to the anti-SDMA BL8243 antibody, and most of that to the anti-SDMA BL8244 antibody, was lost in cells lacking PRMT5 (Fig. 10*A*). Significantly, an immunoreactive band with the anti-SDMA BL8244 antibody was seen at 145 kDa, which corresponds to the full-length form of the SF3B2 protein. This band is still present when PRMT5 is lost, suggesting it represents a product of PRMT9. Interestingly, there are also other bands that are immunoreactive with the anti-SDMA BL8244 antibody when PRMT5 is lost, particularly a major band found at 30 kDa in addition to other minor bands, which may indicate there are other cellular PRMT9 substrates that have yet to be discovered.

We also analyzed the total content of SDMA, ADMA, and MMA in these cells by quantitating fluorescent OPA amino acid derivatives after acid hydrolysis (Fig. 10, *B* and *C*). Wild type and PRMT5 knock-out lysates were acid-hydrolyzed and separated using cation exchange chromatography and then further derivatized using OPA. Analysis of the wild type sample shows the presence of ADMA and SDMA peaks after derivatization (Fig 10*B*, *top left panel*). Quantification of MMA and arginine levels were also done; arginine levels were used to normalize the content of MMA, SDMA, and ADMA (Fig 10, *B*, *top right panel,* and *C*) (29). When this analysis was repeated for the PRMT5-deficient cells, SDMA was not detected, although the levels of MMA and ADMA were similar to those of wild type cells (Fig. 10, *B*, *lower panels,* and *C*). These results indicate that the bulk of SDMA formation in mouse embryo fibroblasts is catalyzed by PRMT5 and that PRMT9 is responsible for only a small percentage of SDMA production.

Methylation of Splicing Factor SF3B2 and Myelin Basic Protein by PRMT9 and PRMT5—Finally, we wanted to determine how much cross-reactivity there may be between PRMT9 and PRMT5 with their major substrates SF3B2 and myelin basic protein, respectively. We incubated these enzymes with each of the substrates and [*methyl*-^{3}H]AdoMet under conditions to ensure that methylation was in the linear range and detected SDMA and MMA formation by amino acid analysis (Fig. 11). We found PRMT5 formed over 10 times more SDMA product with myelin basic protein than with SF3B2 (Fig 11, *A* and *B*). Under the same conditions, however, PRMT9 formed 40 times more SDMA with the SF3B2 401–550-residue wild type fragment as a substrate compared with myelin basic protein (Fig. 11, *C* and *D*). These results, combined with those shown in Fig. 10, indicate that PRMT5 and PRMT9 are unlikely to play redundant roles in the cell. The lethality of PRMT5 mouse knock-outs and a definite role of PRMT5 in embryonic development further support the nonredundant functions of these enzymes (3, 40, 41).

Discussion

We have shown that mammalian-expressed and bacterially expressed human PRMT9 have a protein arginine methyltransferase activity, joining PRMT5 as the second type II SDMA-forming enzyme in the mammalian PRMT family. Our previous work had identified the enzyme and its substrate, splicing factor SF3B2, and also provided evidence for a biological role as a modulator of splicing (7). In this work,

FIGURE 8. **Full-length intact enzyme is required for methyltransferase activity.** *A,* amino acid analysis of methylation reactions using GST-tagged PRMT9 truncation mutants with GST-SF3B2 401–550-residue wild type fragment. Approximately 2 μg of each wild type and truncated enzyme was used in a 60-μl methylation reaction with 5 μg of GST-SF3B2 401–550-residue wild type fragment, 0.7 μM [*methyl*-^{3}H]AdoMet, and methylation reaction buffer of 50 mM HEPES, 10 mM NaCl, 1 mM DTT, pH 8.0, at 37 °C for 16.5 h. Acid hydrolysis and amino acid analysis was carried out as described under "Experimental Procedures." *B,* autoradiography of ^{3}H-methylated GST-SF3B2 wild type fragment after reaction with wild type or truncation mutant GST-PRMT9 enzymes. Reactions were set up as described in *A* but were run for only 1 h to prevent possible degradation of the enzymes. Reactions were quenched and run on SDS-PAGE as described under "Experimental Procedures." Dried gels were exposed to film for 3 days at −80 °C and run in experimental triplicates on separate gels, one of which is shown here. Molecular mass positions are indicated from 2 μg of unstained SDS-PAGE broad range markers (Bio-Rad, catalog no. 161-0317) electrophoresed in parallel lanes.

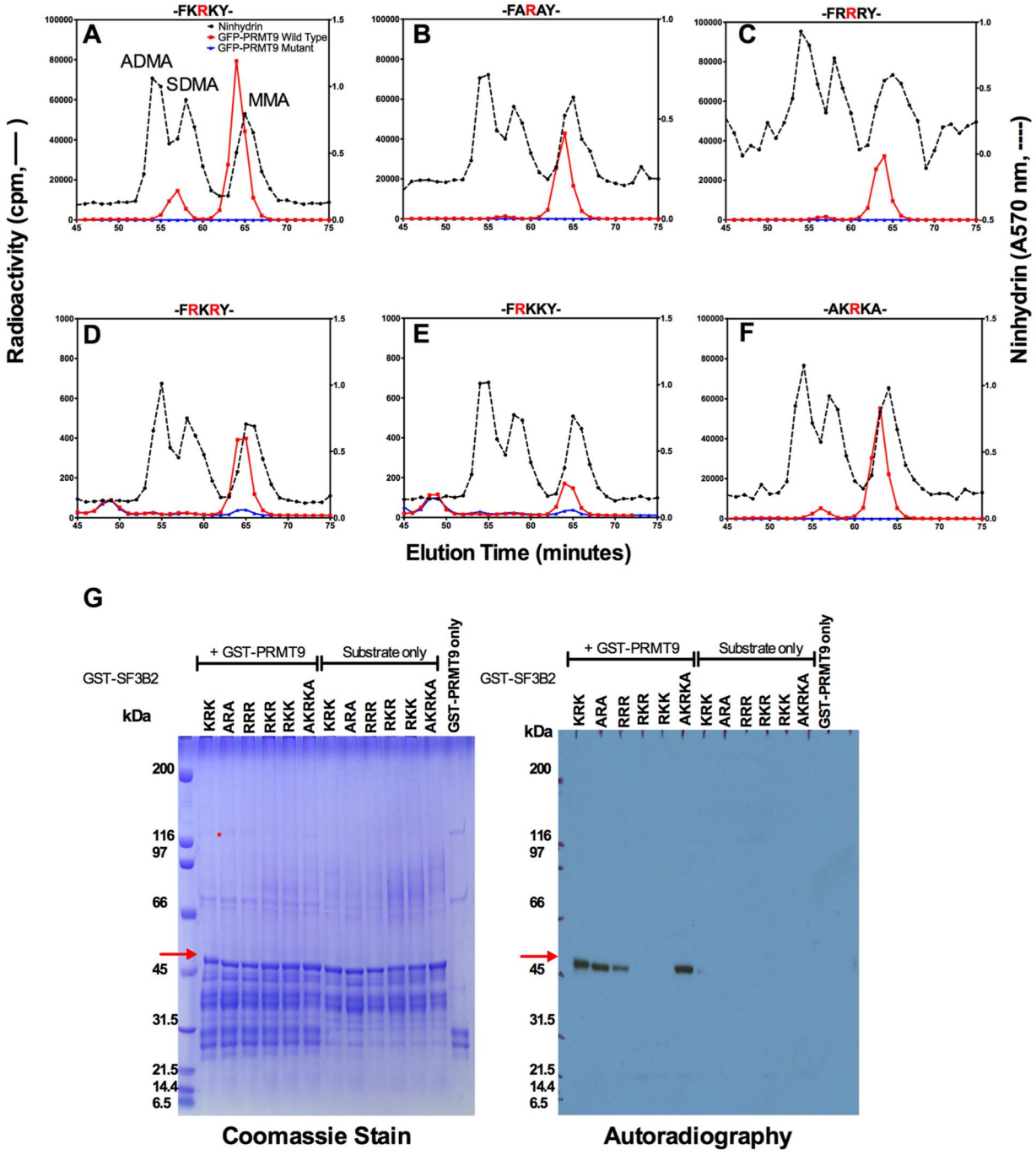

FIGURE 9. **Amino acids surrounding the Arg-508 site are important for substrate recognition and methylation.** *A–F,* point mutants were generated on the GST-SF3B2 401–550-residue wild type fragment where amino acids surrounding the Arg-508 methylation site were changed; mutants include K507A/K509A (-FARAY-), K507R/K509R (-FRRRY-), K507R/R508K/K509R (-FRKRY-), K507R/R508K (-FRKKY-), and F506A/Y510A (-AKRKA-). Methylation reactions were set up using mammalian-expressed wild type and catalytic mutant GFP-PRMT9 enzymes (1 μg) and GST-SF3B2 wild type or mutant fragments (5 μg), along with 0.7 μM [*methyl*-^{3}H]AdoMet, and methylation reaction buffer of 50 mM HEPES, 10 mM NaCl, 1 mM DTT, pH 8.0 at 37 °C for 16.5 h. Acid hydrolysis and amino acid analysis was carried out as described above under "Experimental Procedures." *G,* autoradiography of ^{3}H-methylated GST-SF3B2 401–550-residue wild type and mutant fragments (5 μg) with GST-PRMT9 wild type enzyme (2 μg) after a 16.5-h reaction. Reactions were set up with the same conditions as described in *A*. Reactions were quenched by addition of SDS-loading buffer, run on gels, and prepared for autoradiography as described under "Experimental Procedures." Dried gels were exposed to film for 3 days at −80 °C and run as experimental duplicates on separate gels, one of which is shown here. Molecular mass positions are indicated from 2 μg of unstained SDS-PAGE broad range markers (Bio-Rad, catalog no. 161-l0317) electrophoresed in parallel lanes.

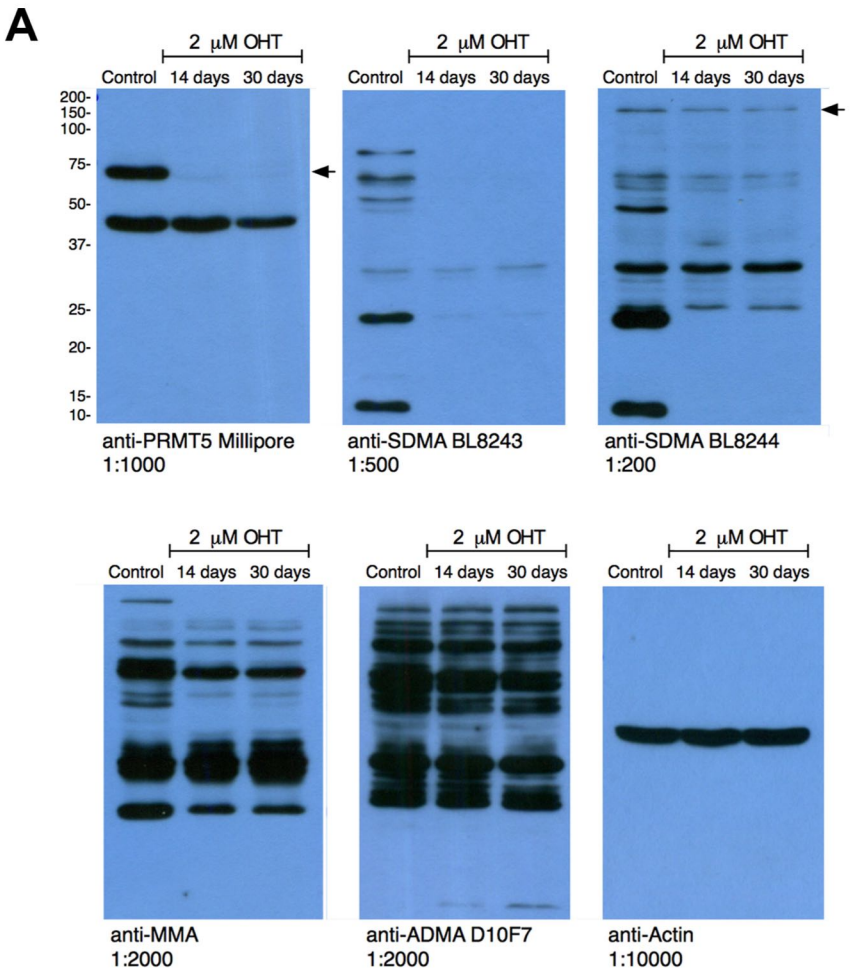

FIGURE 10. **Quantification of SDMA levels in protein hydrolysates of wild type and PRMT5 knock-out MEFs.** *A,* immunoblot showing wild type and PRMT5 knock-out MEFs treated for 14 and 30 days with 2 μM OHT. Whole cell lysates were prepared, run on SDS-PAGE, and immunoblotted using a panel of antibodies. Anti-PRMT5 (Millipore) antibody was used at a 1:1000 dilution to ensure efficient knockdown of PRMT5 in the OHT-treated cells. Anti-SDMA BL8243 and BL8244 were used at 1:500 and 1:200 dilution, respectively, to probe for cellular SDMA levels after PRMT5 knock-out. Anti-MMA (1:2000 dilution) and anti-ADMA D10F7 (1:2000 dilution) antibodies were also used to monitor cellular MMA and ADMA levels in wild type *versus* PRMT5 knock-out samples. Anti-actin (1:10,000 dilution) antibody was used to ensure equal loading. *B,* wild type and PRMT5 knock-out MEFs were harvested (40 mg), and the cell pellet was acid-hydrolyzed and run on amino acid analysis as described above under "Experimental Procedures," except no exogenous methylarginine standards were added to the samples. The resulting fractions from the amino acid analysis were derivatized using OPA for fluorescence quantification using reverse phase HPLC as described under "Experimental Procedures." Raw chromatographs show fluorescence at 455 nm, with peaks corresponding to individual fractions from the amino acid analysis that matched the elution of each methylated derivative (wild type, *top left*, PRMT5 knock-out, *bottom left*). Area comparison (wild type, *top right*; PRMT5 knock-out, *bottom right*) is shown as a quantification of the area under the peak for individual fractions from the amino acid analysis, using the raw data for ADMA (*red line*) and SDMA (*blue line*) peaks shown in the *left panels* and also quantifying MMA (*black dotted line*) amounts (raw chromatograms for MMA not shown). *C,* ratios of methylated arginine species/arginine. Quantification of arginine was used as an internal control for loading and easier comparison across sample replicates. To determine total area, the area under the raw chromatograph peaks (shown in *B*, *left* and *right panels*) was summed for each modification (ADMA, SDMA, and MMA) and corrected for dilution factors in preparation of the sample for OPA analysis. Total areas for each methylarginine species were then compared with the sum of the total area under the raw chromatographs for arginine, to give a ratio of modification/arginine. Data were gathered in experimental duplicate shown as the mean, and *bars* indicate the range of the data.

we have biochemically characterized the residues important for the PRMT9/SF3B2 enzyme-substrate interaction.

PRMT9 is an unusual protein arginine methyltransferase, as it has rather strict substrate specificity, an intact protein requirement for methylation, and contains a second methyltransferase domain and an additional acidic residue in its substrate-binding motif similar to human PRMT7. Its known substrate and binding partner in the cell, SF3B2, contains a methylatable sequence WCFKRKYLQ, which is not found in other proteins. Other proteins have similar sequences when -FKRKY- is searched, but no other proteins contain this extended sequence. PRMT9 has little or no activity on common PRMT substrates such as GST-GAR, myelin basic protein, or histones, suggesting an explicit role in splicing. We have shown that PRMT9 does not methylate a peptide with the WCFKRKYLQ sequence from SF3B2, suggesting that the substrate protein must be intact to make the correct contacts with the enzyme. In addition, we have demonstrated that N- and

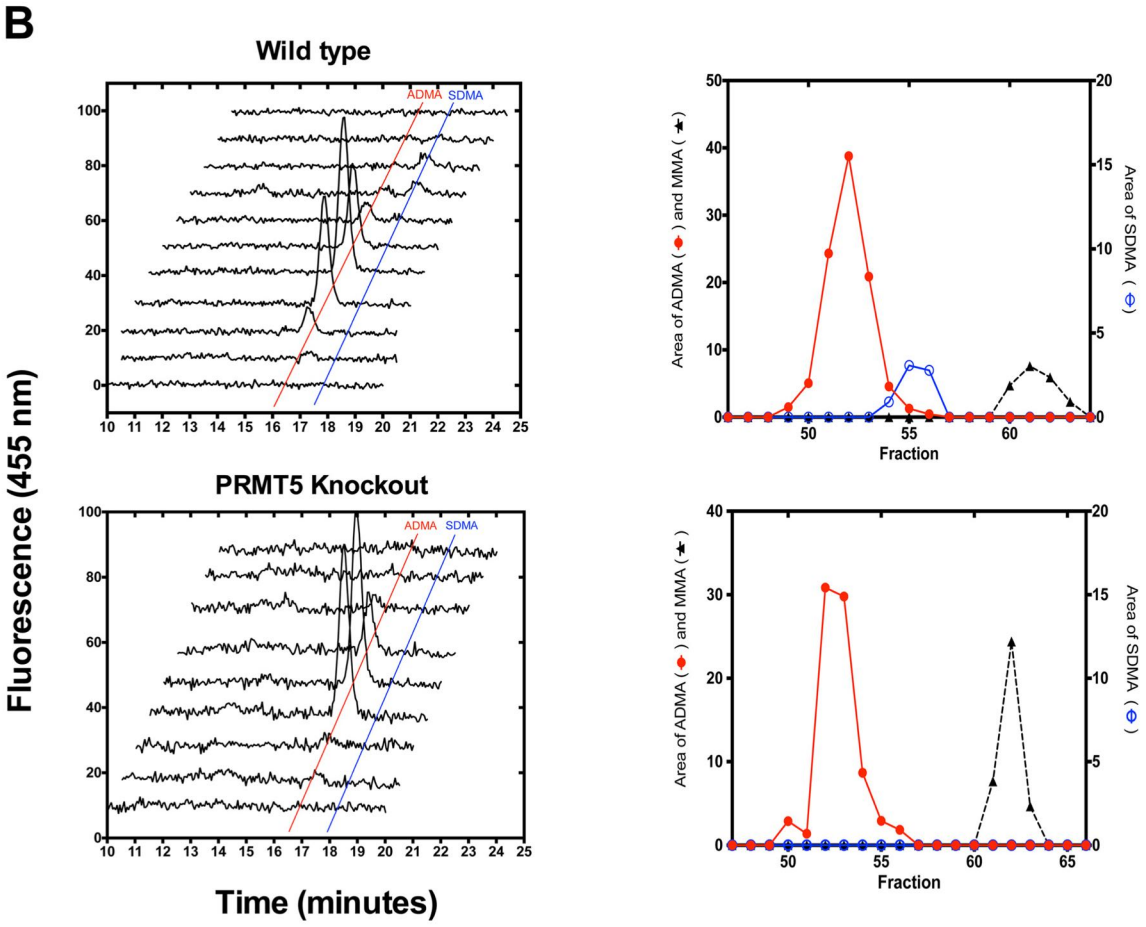

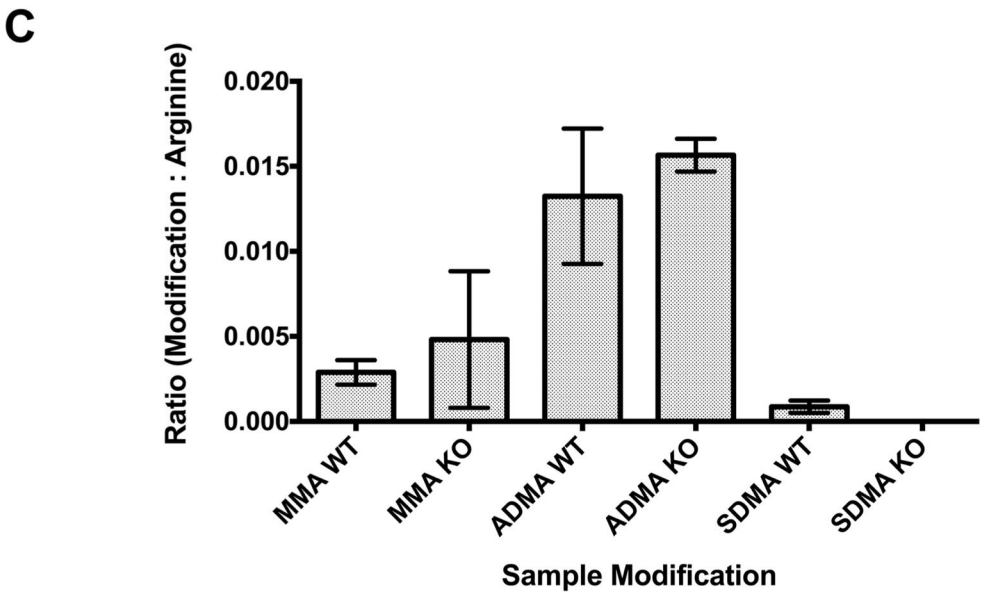

FIGURE 10—***Continued***

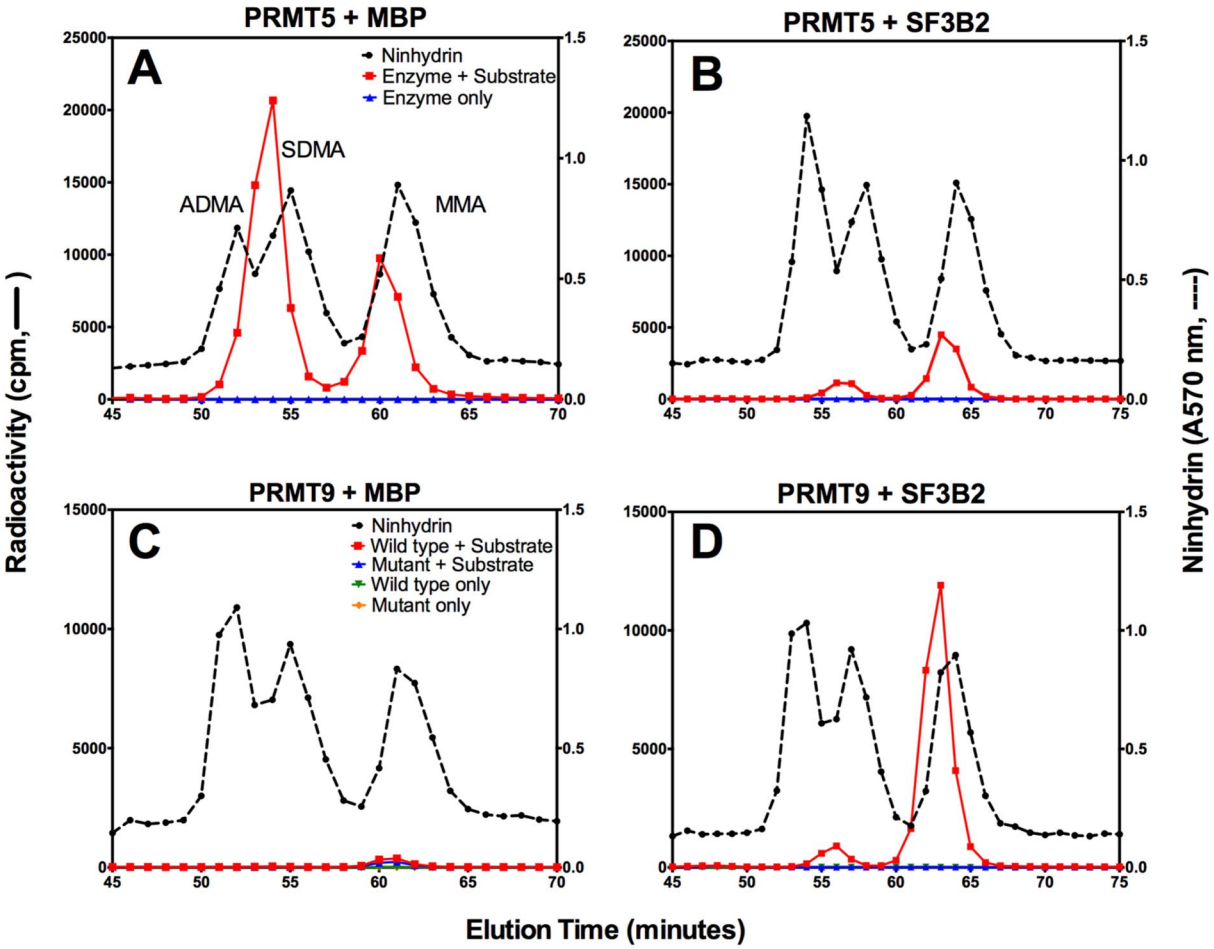

FIGURE 11. **PRMT5 and PRMT9 substrates are nonredundant.** *A,* amino acid analysis of PRMT5 (2.3 μg) and human His-tagged MBP (5 μg) after a 1-h *in vitro* methylation reaction, with 0.7 μM [*methyl*-^{3}H]AdoMet, and methylation reaction buffer of 25 mM Tris, 1 mM DTT, 8% glycerol, pH 8.0, at 37 °C in a 60-μl reaction volume. Acid hydrolysis and amino acid analysis was carried out as described under "Experimental Procedures." The *dotted black line* indicates ninhydrin absorbance at 570 nm for the nonradiolabeled methylated amino acid standards. The *red line* indicates the elution of the radioactive methylated amino acids of the wild type PRMT5 enzyme in reaction with the substrate. The *blue line* indicates the enzyme only control, to account for any background radioactivity. *B,* amino acid analysis of PRMT5 (2.3 μg) and GST-SF3B2 401–550-residue wild type fragment (5 μg) after a 1-h reaction, using same the conditions as described in *A*. *C,* amino acid analysis of *in vitro* methylation reaction of GFP-PRMT9 (wild type and catalytic mutant, 1 μg) with human His-tagged MBP (5 μg), with 0.7 μM [*methyl*-^{3}H]AdoMet, and methylation reaction buffer of 50 mM HEPES, 10 mM NaCl, 1 mM DTT, pH 8.0, at 37 °C in a 60-μl reaction volume. The *dotted black line* indicates the elution and ninhydrin absorbance at 570 nm for the nonradiolabeled methylated amino acids. The *red* and *blue lines* indicate the elution of the radioactive methylated amino acids of the substrate reacted with the wild type or catalytic mutant GFP-PRMT9, respectively. The *green* and *orange lines* indicate the wild type or catalytic mutant enzyme only controls. *D,* amino acid analysis of GFP-PRMT9 (wild type and catalytic mutant, 1 μg) with GST-SF3B2 401–550-residue wild type fragment (5 μg) after a 1-h reaction, using same conditions as described in *C*.

C-terminal deletions and TPR motif deletions of PRMT9 are inactive, further promoting the idea that the substrate must make correct contacts with both domains of the enzyme to be properly methylated. Structural studies have shown that PRMT1, PRMT3, and PRMT5 and *T. brucei* PRMT7 form homodimers in solution to methylate their substrates (15, 17–19), which may indicate that the second methyltransferase domain of PRMT9 functions to form a pseudodimer upon binding its substrate. Other studies have shown that substrates make important contacts on other parts of the enzyme, as is the case for PRMT1 with certain substrates (17), which would support our results. It should be noted, however, that PRMT1 and several other PRMTs like PRMT7, are also able to bind and methylate synthetic peptides (6, 8, 17, 39, 42).

Probing for the substrate residues important for methylation, we find that the position of the methylated arginine to be indispensable, possibly indicating a precise placement in the double E loop when AdoMet is bound (Fig. 6*B*). When the residues surrounding Arg-508 site are changed, SDMA is drastically reduced, and the amount of MMA formed is slightly affected. When the two lysines surrounding the target arginine are mutated to arginine, the presence of the extra positive charge in the active site seems to have detrimental effects, compared with when they are mutated to alanine. Furthermore, if the arginine residue is moved, we see almost completely abolished activity. Mutation of aromatic residues Phe-506 and Tyr-510 also seem to only slightly affect activity. This methylated sequence specificity is relatively uncommon, as the majority of PRMTs meth-

ylate RG-rich sequence motif (2, 3), with PRMT7 being the only other PRMT requiring a basic residue-rich environment for methylation (6, 8).

It is possible that the unique properties of PRMT9 within the PRMT family have been evolved to specifically recognize splicing factor SF3B2. In general, the phylogenetic distribution of PRMT9 and SF3B2 match each other (Fig. 1), although some organisms (higher plants) have the splicing factor but not PRMT9, and some organisms, such as chickens, have PRMT9 but not the splicing factor. It is also very interesting that although PRMT9 is found throughout the chordates, it is not widespread in invertebrates. For example, PRMT9 is clearly present in the sea anemone *N. vectensis* but is absent in the fruit fly *Drosophila melanogaster*. It is still unclear whether the *C. elegans prmt-3* gene encodes a PRMT9 ortholog. This protein, shown to methylate recombinant human histone H2A to form MMA only (31), has the conserved aspartate in position 4 of the double E loop but is more divergent than the chordate members of the PRMT9 family. No good orthologs of PRMT9 are found in plants, fungi, and other single cellular organisms. Novel BLAST-based methods have been developed to examine the evolutionary relationship between PRMTs in mammals and across various species, which provides insight into the evolutionary history of PRMTs (30, 43). Here, the closest relative of PRMT9 is PRMT7, with a close branch off of the PRMT5 outlier (30, 43). Interestingly, there is a wide evolutionary conservation of SF3B2 and the Arg-508 site across vertebrates, invertebrates, plants, fungi, and some unicellular organisms (Fig. 1, *C* and *D*). This may suggest that higher organisms found a need for regulation of splicing in the cell, and thus PRMT9 evolved or branched off from the rest of the PRMT family and PRMT7 to take on this function. Studies of orthologs of PRMT9 in other organisms would be of great interest, to determine whether the enzyme still has the same activity type, substrate specificity, and role in the cell. In addition, studying the relative distribution of the amounts of SDMA produced by PRMT9 compared with PRMT5 in other organisms would indicate an evolutionary relationship and need for regulation.

Tissue distribution studies show wide expression of PRMT9 in the body, with high protein expression in the testis, kidneys, skin, and hematopoietic and central nervous system (34, 44). PRMT9 has also been shown to have high expression in certain types of cancer, including lymphoma, melanoma, testicular, and pancreatic cancers (34). In addition, because of the involvement of SF3B2 in cell cycle progression and potential involvement in HIV hijacking/retroviral activity (14), it would be important to probe for the role of SF3B2 methylation in relation to viral and disease impact.

Although it does produce symmetrically dimethylated arginine, this enzyme is a minor contributor to the pool of SDMA in mouse embryo fibroblasts, compared with PRMT5 (Fig. 10). PRMT5 knock-out MEFs show no detectable SDMA by OPA analysis and greatly reduced SDMA by immunoblot analysis, indicating that PRMT9 SDMA methylation is likely restricted to a few substrates. Our OPA analysis results are consistent with similar studies quantifying relative amounts of these methylated arginine derivatives after the depletion of PRMT1 in cells (29). Furthermore, our results suggest that PRMT5 and PRMT9 do not appear to have redundant roles in cells, as they do not strongly methylate each other's substrates (Fig. 11). Immunoblots of PRMT5 knock-out MEF whole cell lysates with anti-SDMA antibodies show the presence of minor bands, which may indicate the presence of other possible substrates for PRMT9 in the cell. It will be interesting to characterize these possible substrates and identify other potential roles for PRMT9.

Acknowledgments—We thank Marco Bezzi and Ernesto Guccione (National University of Singapore) for providing primary Prmt5$^{F/F}$-ER-Cre MEFs. We also thank Jorge Torres, Xiaoyu Xia, and Ankur Gholkar (UCLA) for their advice and assistance with mammalian cell culture and immunofluorescence. We also thank the Margot Quinlan lab (UCLA) for their help with immunofluorescence studies and Douglas Juers (Whitman College, Washington) for the gift of the His-MBP plasmid. Alexander Patananan provided valuable advice and help with the OPA analysis as well as helpful comments on the manuscript. You Feng, Jonathan Lowenson, Kanishk Jain, Qais Al-Hadid, and Cecilia-Zurita Lopez provided helpful advice on the research and the manuscript.

References

1. Herrmann, F., Pably, P., Eckerich, C., Bedford, M. T., and Fackelmayer, F. O. (2009) Human protein arginine methyltransferases *in vivo*–distinct properties of eight canonical members of the PRMT family. *J. Cell Sci.* **122,** 667–677
2. Bedford, M. T., and Clarke, S. G. (2009) Protein arginine methylation in mammals: Who, what, and why. *Mol. Cell* **33,** 1–13
3. Yang, Y., and Bedford, M. T. (2013) Protein arginine methyltransferases and cancer. *Nat. Rev. Cancer* **13,** 37–50
4. Fuhrmann, J., Clancy, K. W., and Thompson, P. R. (2015) Chemical biology of protein arginine modifications in epigenetic regulation. *Chem. Rev.* 10.1021/acs.chemrev.5b00003
5. Lee, Y.-H., and Stallcup, M. R. (2009) Minireview: protein arginine methylation of nonhistone proteins in transcriptional regulation. *Mol. Endocrinol.* **23,** 425–433
6. Feng, Y., Maity, R., Whitelegge, J. P., Hadjikyriacou, A., Li, Z., Zurita-Lopez, C., Al-Hadid, Q., Clark, A. T., Bedford, M. T., Masson, J. Y., and Clarke, S. G. (2013) Mammalian protein arginine methyltransferase 7 (PRMT7) specifically targets RXR sites in lysine- and arginine-rich regions. *J. Biol. Chem.* **288,** 37010–37025
7. Yang, Y., Hadjikyriacou, A., Xia, Z., Gayatri, S., Kim, D., Zurita-Lopez, C., Kelly, R., Guo, A., Li, W., Clarke, S. G., and Bedford, M. T. (2015) PRMT9 is a Type II methyltransferase that methylates the splicing factor SAP145. *Nat. Commun.* 10.1038/ncomms7428
8. Feng, Y., Hadjikyriacou, A., and Clarke, S. G. (2014) Substrate specificity of human protein arginine methyltransferase 7 (PRMT7): the importance of acidic residues in the double E loop. *J. Biol. Chem.* **289,** 32604–32616
9. Molina-Serrano, D., Schiza, V., and Kirmizis, A. (2013) Cross-talk among epigenetic modifications: lessons from histone arginine methylation. *Biochem. Soc. Trans.* **41,** 751–759
10. Yoshimatsu, M., Toyokawa, G., Hayami, S., Unoki, M., Tsunoda, T., Field, H. I., Kelly, J. D., Neal, D. E., Maehara, Y., Ponder, B. A., Nakamura, Y., and Hamamoto, R. (2011) Dysregulation of PRMT1 and PRMT6, type I arginine methyltransferases, is involved in various types of human cancers. *Int. J. Cancer* **128,** 562–573
11. Baldwin, R. M., Morettin, A., and Côté, J. (2014) Role of PRMTs in cancer: Could minor isoforms be leaving a mark? *World J. Biol. Chem.* **5,** 115–129
12. Duan, S., Cermak, L., Pagan, J. K., Rossi, M., Martinengo, C., di Celle, P. F., Chapuy, B., Shipp, M., Chiarle, R., and Pagano, M. (2012) FBXO11 targets BCL6 for degradation and is inactivated in diffuse large B-cell lymphomas. *Nature* **481,** 90–93
13. Champion-Arnaud, P., and Reed, R. (1994) The prespliceosome compo-

nents SAP 49 and SAP 145 interact in a complex implicated in tethering U2 snRNP to the branch site. *Genes Dev.* **8,** 1974–1983
14. Terada, Y., and Yasuda, Y. (2006) Human immunodeficiency virus type 1 Vpr induces G2 checkpoint activation by interacting with the splicing factor SAP145. *Mol. Cell. Biol.* **26,** 8149–8158
15. Hasegawa, M., Toma-Fukai, S., Kim, J. D., Fukamizu, A., and Shimizu, T. (2014) Protein arginine methyltransferase 7 has a novel homodimer-like structure formed by tandem repeats. *FEBS Lett.* **588,** 1942–1948
16. Cura, V., Troffer-Charlier, N., Wurtz, J.-M., Bonnefond, L., and Cavarelli, J. (2014) Structural insight into arginine methylation by the mouse protein arginine methyltransferase 7: a zinc finger freezes the mimic of the dimeric state into a single active site. *Acta Crystallogr. D Biol. Crystallogr.* **70,** 2401–2412
17. Lee, D. Y., Ianculescu, I., Purcell, D., Zhang, X., Cheng, X., and Stallcup, M. R. (2007) Surface-scanning mutational analysis of protein arginine methyltransferase 1: roles of specific amino acids in methyltransferase substrate specificity, oligomerization, and coactivator function. *Mol. Endocrinol.* **21,** 1381–1393
18. Tang, J., Gary, J. D., Clarke, S., and Herschman, H. R. (1998) PRMT3, a type I protein arginine *N*-methyltransferase that differs from PRMT1 in its oligomerization, subcellular localization, substrate specificity, and regulation. *J. Biol. Chem.* **273,** 16935–16945
19. Lott, K., Zhu, L., Fisk, J. C., Tomasello, D. L., and Read, L. K. (2014) Functional interplay between protein arginine methyltransferases in *Trypanosoma brucei*. *Microbiol. Open* **3,** 595–609
20. Miranda, T. B., Miranda, M., Frankel, A., and Clarke, S. (2004) PRMT7 is a member of the protein arginine methyltransferase family with a distinct substrate specificity. *J. Biol. Chem.* **279,** 22902–22907
21. Blatch, G. L., and Lässle, M. (1999) The tetratricopeptide repeat: a structural motif mediating protein-protein interactions. *BioEssays* **21,** 932–939
22. Wang, M., Xu, R.-M., and Thompson, P. R. (2013) Substrate specificity, processivity, and kinetic mechanism of protein arginine methyltransferase 5. *Biochemistry* **52,** 5430–5440
23. Wang, M., Fuhrmann, J., and Thompson, P. R. (2014) Protein arginine methyltransferase 5 catalyzes substrate dimethylation in a distributive fashion. *Biochemistry* **53,** 7884–7892
24. Meister, G., Eggert, C., Bühler, D., Brahms, H., Kambach, C., and Fischer, U. (2001) Methylation of Sm proteins by a complex containing PRMT5 and the putative U snRNP assembly factor pICln. *Curr. Biol.* **11,** 1990–1994
25. Tamura, K., Stecher, G., Peterson, D., Filipski, A., and Kumar, S. (2013) MEGA6: Molecular evolutionary genetics analysis version 6.0. *Mol. Biol. Evol.* **30,** 2725–2729
26. McWilliam, H., Li, W., Uludag, M., Squizzato, S., Park, Y. M., Buso, N., Cowley, A. P., and Lopez, R. (2013) Analysis tool web services from the EMBL-EBI. *Nucleic Acids Res.* **41,** 597–600
27. Zurita-Lopez, C. I., Sandberg, T., Kelly, R., and Clarke, S. G. (2012) Human protein arginine methyltransferase 7 (PRMT7) is a Type III enzyme forming ω-N^G-monomethylated arginine residues. *J. Biol. Chem.* **287,** 7859–7870
28. Bezzi, M., Teo, S. X., Muller, J., Mok, W. C., Sahu, S. K., Vardy, L. A., Bonday, Z. Q., and Guccione, E. (2013) Regulation of constitutive and alternative splicing by PRMT5 reveals a role for Mdm4 pre-mRNA in sensing defects in the spliceosomal machinery. *Genes Dev.* **27,** 1903–1916
29. Dhar, S., Vemulapalli, V., Patananan, A. N., Huang, G., Di Lorenzo, A., Richard, S., Comb, M. J., Guo, A., Clarke, S. G., and Bedford, M. T. (2013) Loss of the major Type I arginine methyltransferase causes substrate scavenging by Type II and III enzymes. *Sci. Rep.* **3,** 1311. doi: 10.1038/srep01311
30. Wang, Y. C., Wang, J. D., Chen, C. H., Chen, Y. W., and Li, C. (2015) A novel BLAST-based relative distance (BBRD) method can effectively group members of protein arginine methyltransferases and suggest their evolutionary relationship. *Mol. Phylogenet. Evol.* **84,** 101–111
31. Takahashi, Y., Daitoku, H., Yokoyama, A., Nakayama, K., Kim, J.-D., and Fukamizu, A. (2011) The *C. elegans* PRMT-3 possesses a type III protein arginine methyltransferase activity. *J. Recept. Signal Transduct. Res.* **31,** 168–172
32. Branscombe, T. L., Frankel, A., Lee, J. H., Cook, J. R., Yang, Z., Pestka, S., and Clarke, S. (2001) PRMT5 (Janus kinase-binding protein 1) catalyzes the formation of symmetric dimethylarginine residues in proteins. *J. Biol. Chem.* **276,** 32971–32976
33. Shaw, G., Morse, S., Ararat, M., and Graham, F. L. (2002) Preferential transformation of human neuronal cells by human adenoviruses and the origin of HEK 293 cells. *FASEB J.* **16,** 869–871
34. Uhlén, M., Fagerberg, L., Hallström, B. M., Lindskog, C., Oksvold, P., Mardinoglu, A., Sivertsson, Å., Kampf, C., Sjöstedt, E., Asplund, A., Olsson, I., Edlund, K., Lundberg, E., Navani, S., Szigyarto, C. A., *et al.* (2015) Proteomics. Tissue-based map of the human proteome. *Science* **347,** 10.1126/science.1260419
35. Katz, J. E., Dlakić, M., and Clarke, S. (2003) Automated identification of putative methyltransferases from genomic open reading frames. *Mol. Cell. Proteomics* **2,** 525–540
36. Gary, J. D., and Clarke, S. G. (1998) RNA and protein interactions modulated by protein arginine methylation. *Prog. Nucleic Acids Res. Mol. Biol.* **61,** 65–131
37. Bachand, F. (2007) Protein arginine methyltransferases: from unicellular eukaryotes to humans. *Eukaryot. Cell* **6,** 889–898
38. Kelley, L. A., and Sternberg, M. J. (2009) Protein structure prediction on the web: a case study using the Phyre server. *Nat. Protoc.* **4,** 363–371
39. Antonysamy, S., Bonday, Z., Campbell, R. M., Doyle, B., Druzina, Z., Gheyi, T., Han, B., Jungheim, L. N., Qian, Y., Rauch, C., Russell, M., Sauder, J. M., Wasserman, S. R., Weichert, K., Willard, F. S., *et al.* S. (2012) Crystal structure of the human PRMT5: MEP50 complex. *Proc. Natl. Acad. Sci. U.S.A.* **109,** 17960–17965
40. Tee, W. W., Pardo, M., Theunissen, T. W., Yu, L., Choudhary, J. S., Hajkova, P., and Surani, M. A. (2010) Prmt5 is essential for early mouse development and acts in the cytoplasm to maintain ES cell pluripotency service Prmt5 is essential for early mouse development and acts in the cytoplasm to maintain ES cell pluripotency. *Genes Dev.* **24,** 2772–2777
41. Dacwag, C. S., Bedford, M. T., Sif, S., and Imbalzano, A. N. (2009) Distinct protein arginine methyltransferases promote ATP-dependent chromatin remodeling function at different stages of skeletal muscle differentiation. *Mol. Cell. Biol.* **29,** 1909–1921
42. Gui, S., Wooderchak-Donahue, W. L., Zang, T., Chen, D., Daly, M. P., Zhou, Z. S., and Hevel, J. M. (2013) Substrate-induced control of product formation by protein arginine methyltransferase 1. *Biochemistry* **52,** 199–209
43. Wang, Y. C., and Li, C. (2012) Evolutionarily conserved protein arginine methyltransferases in non-mammalian animal systems. *FEBS J.* **279,** 932–945
44. Petryszak, R., Burdett, T., Fiorelli, B., Fonseca, N. A., Gonzalez-Porta, M., Hastings, E., Huber, W., Jupp, S., Keays, M., Kryvych, N., McMurry, J., Marioni, J. C., Malone, J., Megy, K., Rustici, G., et al. (2014) Expression Atlas update–a database of gene and transcript expression from microarray- and sequencing-based functional genomics experiments. *Nucleic Acids Res.* **42,** D926–D932
45. Gottschling, H., and Freese, E. (1962) A tritium isotope effect on ion exchange chromatography. *Nature* **196,** 829–831

CHAPTER 7

Protein Arginine Methyltransferase Product Specificity is Mediated by Distinct Active-site Architectures

Protein Arginine Methyltransferase Product Specificity Is Mediated by Distinct Active-site Architectures*

Received for publication, June 1, 2016, and in revised form, July 5, 2016 Published, JBC Papers in Press, July 7, 2016, DOI 10.1074/jbc.M116.740399

Kanishk Jain[‡], **Rebeccah A. Warmack**[‡], **Erik W. Debler**[§1], **Andrea Hadjikyriacou**[‡], **Peter Stavropoulos**[§¶], and **Steven G. Clarke**[‡2]

From the [‡]*Department of Chemistry and Biochemistry and the Molecular Biology Institute, UCLA, Los Angeles, California 90095 and the* [§]*Laboratory of Cell Biology and* [¶]*Laboratory of Lymphocyte Biology, The Rockefeller University, New York, New York 10065*

In the family of protein arginine methyltransferases (PRMTs) that predominantly generate either asymmetric or symmetric dimethylarginine (SDMA), PRMT7 is unique in producing solely monomethylarginine (MMA) products. The type of methylation on histones and other proteins dictates changes in gene expression, and numerous studies have linked altered profiles of methyl marks with disease phenotypes. Given the importance of specific inhibitor development, it is crucial to understand the mechanisms by which PRMT product specificity is conferred. We have focused our attention on active-site residues of PRMT7 from the protozoan *Trypanosoma brucei*. We have designed 26 single and double mutations in the active site, including residues in the Glu-Xaa$_8$-Glu (double E) loop and the Met-Gln-Trp sequence of the canonical Thr-His-Trp (THW) loop known to interact with the methyl-accepting substrate arginine. Analysis of the reaction products by high resolution cation exchange chromatography combined with the knowledge of PRMT crystal structures suggests a model where the size of two distinct subregions in the active site determines PRMT7 product specificity. A dual mutation of Glu-181 to Asp in the double E loop and Gln-329 to Ala in the canonical THW loop enables the enzyme to produce SDMA. Consistent with our model, the mutation of Cys-431 to His in the THW loop of human PRMT9 shifts its product specificity from SDMA toward MMA. Together with previous results, these findings provide a structural basis and a general model for product specificity in PRMTs, which will be useful for the rational design of specific PRMT inhibitors.

Methylation of proteins is a major type of post-translational modification involved in the regulation of a variety of cellular processes mediated by protein-protein interactions, including splicing, transcription, translation, and signaling (1–3). Recent studies have implicated arginine methylation in altering the metabolic landscape of the cell, linking it to cancer metastasis (4–6), DNA damage (7), pluripotency (8), and parasite infection (9, 10). Catalysis of arginine methylation on the terminal nitrogen atoms of the guanidine group is mediated by a family of enzymes designated as protein arginine methyltransferases (PRMTs).[3] Most of these enzymes harbor a conserved ~310-residue core that comprises the methyltransferase domain conserved in *S*-adenosylmethionine (AdoMet)-dependent methyltransferases and a β-barrel domain unique to the PRMT family. These enzymes can be further categorized based on which methylarginine product they catalyze as follows: type I PRMTs catalyze the production of ω-N^G-monomethylarginine (MMA) and asymmetric ω-N^G,N^G-dimethylarginine (ADMA); type II PRMTs catalyze the production of MMA and symmetric ω-N^G,N'^G-dimethylarginine (SDMA); type III PRMTs catalyze the production of only MMA; and type IV PRMTs catalyze δ-N^G-monomethylarginine production (11). Notably, most PRMTs fall under the first three types of PRMTs. Type IV enzymes have only been reported in yeast and plants, although the presence of free δ-N^G-monomethylarginine has been reported in human plasma in a recent proteomic study (12).

ADMA and SDMA methyl marks on histones are recognized by different "reader" proteins and can lead to distinct downstream outcomes. For example, whether a particular arginine residue on histone tails is asymmetrically or symmetrically dimethylated can lead to gene repression or activation (13–17). However, few studies have been conducted to determine the role of MMA marks (18). It has been proposed that MMA marks are used mainly as precursors for dimethylation by the various type I and II PRMTs (17, 19).

Given the biological significance of the type of methylated arginine derivative formed, it is important to understand how product specificity is determined in PRMTs. It has been suggested that small variations in the structure of the active site of these enzymes govern the methylation activity type (2, 3, 20–23). Although previous studies utilizing site-directed mutagenesis have given some support for this hypothesis, efforts to efficiently change the activity type of PRMTs have not yet been fruitful. Two such studies using moderately sensitive analytical techniques have been reported for PRMT1 (14) and

* This work was supported by National Institutes of Health Grant GM026020 (to S. G. C.) and Ruth L. Kirschstein National Service Award GM007185 (to K. J., R .A. W., and A. H.). The authors declare that they have no conflicts of interest with the contents of this article. The content is solely the responsibility of the authors and does not necessarily represent the official views of the National Institutes of Health.

[1] Frey Fellow of the Damon Runyon Cancer Research Foundation supported by Grant DRG-1977-08.

[2] To whom correspondence should be addressed: Dept. of Chemistry and Biochemistry and Molecular Biology Institute, UCLA, 607 Charles E. Young Dr. East, Los Angeles, CA 90095. Tel.: 310-825-8754; E-mail: clarke@mbi.ucla.edu.

[3] The abbreviations used are: PRMT, protein arginine methyltransferase; MMA, ω-N^G-monomethylarginine; ADMA, ω-N^G,N^G-asymmetric dimethylarginine; SDMA, ω-N^G,N'^G-symmetric dimethylarginine; AdoHcy, *S*-adenosyl-L-homocysteine; AdoMet, *S*-adenosyl-L-methionine; [*methyl*-^{3}H]-AdoMet, *S*-adenosyl-[*methyl*-^{3}H]-L-methionine; ITC, isothermal titration calorimetry.

TABLE 1

Product analyses of wild-type and mutant *Tb*PRMT7 enzymes with the H4(1–21) R3MMA peptide

The number of experiments is indicated in parenthesis. As shown under the "Experimental Procedures," 86 cpm correspond to 1 fmol of methyl groups.

	[^{3}H]Methyl group radioactivity in MMA (average cpm)	[^{3}H]Methyl group radioactivity in ADMA (average cpm)	[^{3}H]Methyl group radioactivity in SDMA (average cpm)
***Tb*PRMT7 enzyme**			
Wild type (n = 4)	11,093	0	0
Automethylation (n = 4)	122	0	0
Double E loop mutants			
G180N (n = 1)	6,648	0	0
G180Y (n = 1)	5,365	0	0
E172Q (n = 1)	0	0	0
E181D (n = 3)	294	161	0
E181Q (n = 1)	62	0	0
I173G (n = 1)	0	0	0
I173A (n = 1)	121	0	0
I173V (n = 1)	7,231	0	0
I173P F174 M (n = 1)	0	0	0
I173L F174L (n = 1)	29,487	0	0
G175D M177E (n = 1)	0	0	0
E172D E181D (n = 1)	0	0	0
E181D I173G (n = 2)	64	0	0
THW loop mutants			
Q329A (n = 1)	420	0	0
Q329F (n = 1)	95	0	0
Q329H (n = 1)	23,218	0	0
W330A (n = 1)	437	0	0
Q329N (n = 1)	3,322	0	0
Helix αY mutants			
F71A (n = 1)	123	0	0
M75A (n = 1)	205	0	0
M75F (n = 1)	644	0	0
Double E loop and THW loop double mutants			
E181D W330A (n = 1)	52	0	0
E181D Q329A (n = 2)	89	0	500
E181D Q329N (n = 1)	0	0	0
Double E loop and helix αY double mutants			
E181D M75A (n = 1)	65	0	0
E181D F71A (n = 1)	143	0	0

PRMT5 (24), but they have not put forth a general model for the factors that guide product specificity for the three main types of PRMTs.

Using an approach where MMA, ADMA, and SDMA can be detected with sub-femtomole sensitivity, we have been able to demonstrate the transformation of PRMT7 from *Trypanosoma brucei* (*Tb*PRMT7) from an enzyme that strictly produces MMA to one also forming ADMA by replacing a glutamate residue in the double E loop (Glu-181) with an aspartate residue (Fig. 1) (25). The double E loop is a conserved feature of PRMTs that has been shown to directly interact with the methyl-accepting arginine residue (2, 11). *Tb*PRMT7 had been initially characterized for a possible role in the transcriptional control of gene expression in this organism (26). Here, we have focused on *Tb*PRMT7 because it displays robust type III activity and has been amenable to structural analysis (25–27). Within this work, we further examine the effects of key active-site residues on the enzymatic activity of *Tb*PRMT7 through mutagenesis and highly sensitive amino acid analysis techniques to demonstrate the importance of the THW loop (MQW for *Tb*PRMT7) (Fig. 1) (2). Complementary studies with PRMT9 from *Homo sapiens*, previously characterized as a type II enzyme (28, 29), corroborate our PRMT7 results. Based on this evidence, we propose a structural model for how PRMTs can limit their activities to type I, type II, or type III methylation.

Results

TbPRMT7 Active-site Double Mutation, E181D/Q329A, Converts the Enzyme to an SDMA-producing PRMT—Given the ability of the double E loop E181D mutation of *Tb*PRMT7 to alter the methylation type (25), seven *Tb*PRMT7 double mutants were generated with the E181D background to probe the effects of further increasing the size of the active site. Notably, the double mutant E172D/E181D was previously tested and found inactive (Table 1) (25). The additional substitutions in the six new double mutants included M75A, Q329A, Q329N, W330A, F71A, and I173G, each with the E181D mutation, based on their immediate vicinity to the sulfur atom of AdoHcy from which the methyl group of AdoMet is transferred to the arginine residue in protein and peptide substrates (Fig. 1). Using [*methyl*-^{3}H]AdoMet as a cofactor, we analyzed the hydrolyzed products of arginine methylation with high resolution cation exchange chromatography. Two of these double mutants showed little or no activity toward either the H4(1–21) peptide, comprised of the acetylated 21 N-terminal residues of the human histone H4 protein (data not shown), or the acetylated H4(1–21) R3MMA peptide, ω-monomethylated at the third arginine (Table 1). The H4(1–21) R3MMA peptide was used to enhance the detection of dimethylarginine derivatives by providing a substrate where a single methyla-

tion reaction at the primary site of modification could result in dimethylation of the peptide. Strikingly, one of the double mutants, E181D/Q329A, produced SDMA when incubated with the H4(1–21) R3MMA peptide (Fig. 2, *A* and *B*). The small amount of MMA produced in the reaction of the E181D/Q329A mutant with the H4(1–21) R3MMA peptide is most likely due to methylation of the secondary Arg-17 and Arg-19 sites on the histone peptide because the level of radioactivity here is higher than the level recorded for the enzyme alone (Fig. 2*B*). Importantly, although this enzyme contains the ADMA-producing mutation E181D (25), as well as a Q329A mutation in the THW loop, no ADMA formation was detected. SDMA production catalyzed by the E181D/Q329A mutant was confirmed by TLC analysis where the radioactive product co-migrated with the non-radioactive SDMA standard (Fig. 2*C*). The wild-type *Tb*PRMT7 does not produce any dimethylarginine products with either H4(1–21) or H4(1–21) R3MMA peptide (Fig. 3). The single Q329A mutant shows no evidence of dimethylarginine formation (Table 1).

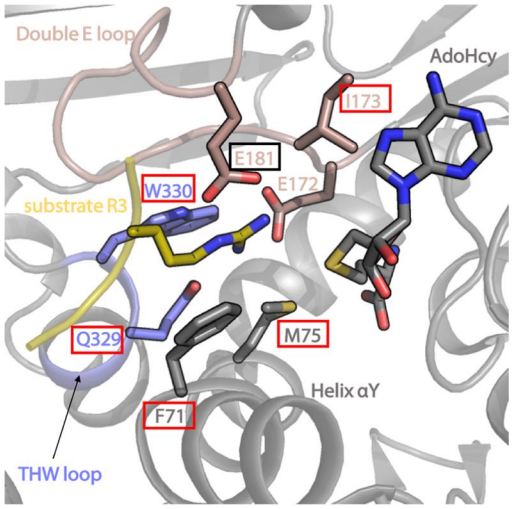

FIGURE 1. **Active site of *T. brucei* PRMT7.** Residue Glu-181, highlighted in the *black box*, is the site of mutation (E181D) shared by the six double mutants in this study with their second mutated residue highlighted in a *red box* (W330A, Q329A, Q329N, F71A, M75A, and I173G). The double mutant E172D/E181D was previously analyzed and Glu-172 is therefore not highlighted here (25). The double E loop is shown in *dark salmon*, the THW loop in *slate*, the substrate arginine residue in *yellow*, and the AdoHcy cofactor, helix αY, and adjacent residues of *Tb*PRMT7 (Protein Data Bank code 4M38) in *gray*.

TbPRMT7 E181D/Q329A Shows Higher Binding Affinity for the Monomethylated Histone H4(1–21) Peptide Than for the Unmethylated Peptide—Using isothermal titration calorimetry (ITC) with H4(1–21) and H4(1–21) R3MMA peptides, we previously demonstrated that the wild-type *Tb*PRMT7 enzyme binds its substrate H4(1–21) with higher affinity than its monomethylated product, H4(1–21) R3MMA, whereas the ADMA-producing *Tb*PRMT7 E181D mutant has markedly increased affinity for H4(1–21) R3MMA that even surpasses that for H4(1–21) (25). Similarly, we measured the affinity of the SDMA-producing *Tb*PRMT7 E181D/Q329A enzyme and

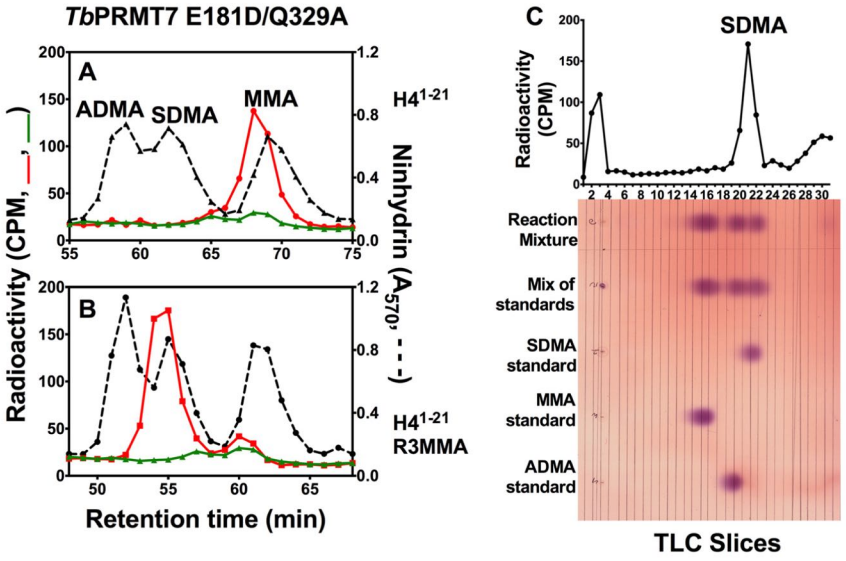

FIGURE 2. ***Tb*PRMT7 E181D/Q329A double mutant produces SDMA with the H4(1–21) R3MMA peptide.** The specificity of this mutant was determined using cation exchange chromatography and TLC as described under "Experimental Procedures." *Tb*PRMT7 E181D/Q329A (4.8 μg of protein) was incubated with the H4(1–21) or H4(1–21) R3MMA peptide (10 μM) and [*methyl*-^{3}H]AdoMet in a final volume of 60 μl. *A, Tb*PRMT7 E181D/Q329A double mutant with the H4(1–21) peptide. *B, Tb*PRMT7 E181D/Q329A with the H4(1–21) R3MMA peptide. The *red lines* in *A* and *B* represent radioactivity of the E181D/Q329A mutant with the different substrates, and the *green lines* indicate radioactivity of the methylation reaction with no substrate. As noted previously (25), radioactive methylarginine derivatives elute 1 min earlier than their non-radioactive counterparts due to the isotope effect (39, 40). As given under "Experimental Procedures," 86 cpm correspond to 1 fmol of methyl groups. For the number of biological replicates, see Table 1. *C,* representative TLC for hydrolysates of the reaction mixture and individual and mixed standards of ADMA, MMA, and SDMA. The *lower portion* shows the ninhydrin staining of the TLC plate; the *upper portion* shows the radioactivity corresponding to the TLC slices of the reaction mixture lane. Note: the ninhydrin standards on the TLC plate are the same as those shown in Fig. 4*D* of Ref. 25 where a different reaction mixture was chromatographed adjacent to the ADMA standard lane. The experiment is one of two biological replicates.

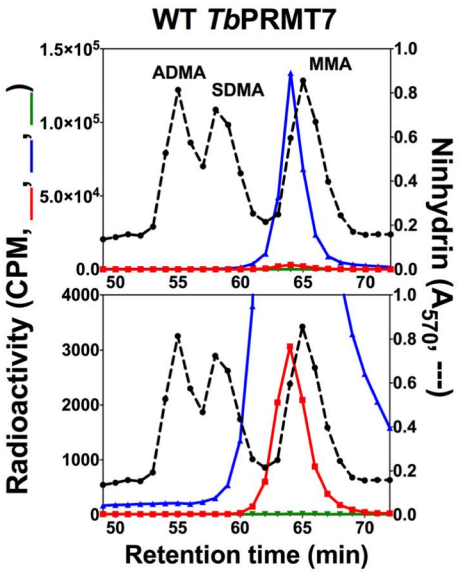

FIGURE 3. **Wild-type *Tb*PRMT7 displays no dimethylarginine production with H4(1–21) and H4(1–21) R3MMA peptides.** *In vitro* methylation and cation exchange chromatography were used as described under "Experimental Procedures" to assess wild-type *Tb*PRMT7 activity and product specificity with H4(1–21) (*blue*), H4(1–21) R3MMA peptides (*red*), or with the enzyme alone (*green*). *Dashed black lines* indicate elution profile of non-radioactive methylarginine species as measured by a ninhydrin assay (see "Experimental Procedures"). The *lower panel* represents enlargement of the radioactivity in the *upper panel* to show low levels of methylation. As given under the "Experimental Procedures," 86 cpm correspond to 1 fmol of methyl groups. For the number of biological replicates, see Table 1.

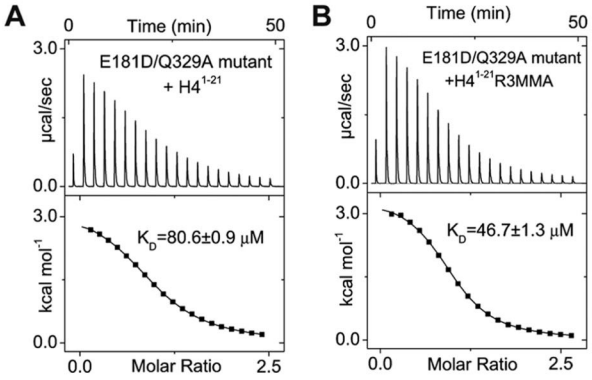

FIGURE 4. **Isothermal titration calorimetry of the *Tb*PRMT7 E181D/Q329A mutant with H4(1–21) (*A*) and H4(1–21) R3MMA (*B*), respectively.** Each titration was performed twice.

found that this mutant displays higher affinity for H4(1–21) R3MMA (K_D = 46.7 μM) *versus* its unmethylated counterpart H4(1–21) (K_D = 80.6 μM) (Fig. 4). Thus, the two mutant enzymes capable of dimethylation consistently favor binding of the bulkier H4(1–21) R3MMA peptide, which can be rationalized by providing a more spacious binding pocket, stabilizing the MMA substrate-enzyme interactions and enabling dimethylation.

Active-site Mutations Lead to Decreases in Type III PRMT7 Activity and Shifts in Recognition Site Specificity—Overall, we have reacted 26 single and double mutants of *Tb*PRMT7 with the H4(1–21) R3MMA peptide to test whether active-site mutations could display changes in the methylation type when presented with a primed monomethylarginine (Table 1). These mutations were generated based on their location in the active site of *Tb*PRMT7, including residues in the double E loop, the AdoMet-binding motif, the THW loop, and an N-terminal extension (helix αY). The majority of the active-site mutations result in decreases in enzyme activity. However, monomethylation is still observed, indicating that the modification of Arg-17 and Arg-19 on the substrate peptide is occurring, as Arg-3 is already methylated in this peptide. This finding suggests that there may be a change in recognition site specificity from glycine-arginine-rich regions to arginine residues in basic regions (26, 30). Notably, the THW (MQW) loop mutant Q329H showed significant increases in MMA production. Most remarkably, the double mutant E181D/Q329A produced both MMA and SDMA, as described above.

Mutation in the THW Loop of Human PRMT9, a Type II PRMT, Shifts Product Specificity from SDMA toward MMA—The human PRMT9 has recently been characterized as a type II PRMT, joining PRMT5 as an enzyme that catalyzes SDMA production (28, 29). This methyltransferase contains a Thr-Cys-Trp (TCW) sequence in place of the canonical Thr-His-Trp (THW) residues (28). To further investigate the role of spatial restrictions conferred by key active-site residues, the cysteine residue was mutated to a bulkier histidine residue to mimic type I and type III PRMTs. These mutant and wild-type enzymes were reacted with a GST fusion of the splicing factor SF3B2, a known substrate of PRMT9 (28). Comparison of wild-type and mutant activities reveals an impressive 8-fold increase in MMA production and almost complete elimination of SDMA production (<0.037%) (Fig. 5).

Rattus norvegicus PRMT1 M48F Mutant Enzyme Does Not Produce SDMA with Histone H4 Peptides—A previous study (24) reported a mutation in rat PRMT1 at Met-48, a residue conserved in the αY helix of many PRMTs, to Phe. This change led to the apparent production of SDMA along with ADMA and MMA, the wild-type products of a type I PRMT, as determined by *o*-phthalaldehyde-derivatized reverse-phase liquid chromatography and LC-MS analysis. However, it appeared that the degree of dimethylarginine formation was quite different when analyzed by these two methods. In our studies with *Tb*PRMT7, the homologous mutation, M75F, showed no change in PRMT7's type III activity with substrates, including RBP16 (25) and the H4(1–21) R3MMA peptide (Table 1). To validate the PRMT1 mutant activity (24), we compared the product specificity of the wild-type human PRMT1 (Fig. 6*A*) with the H4(1–21) and H4(1–21) R3MMA peptides to that of the rat PRMT1 M48F enzyme (Fig. 6*B*). We chose these peptides because H4(1–21) has been shown to be a robust PRMT1 substrate (31, 32). However, in contrast to the earlier work (24), we were unable to distinguish any difference in the product specificity of the wild-type human PRMT1 and the rat PRMT1 M48F mutant with the H4 peptide substrates using high resolution cation exchange chromatography (Fig. 6). With both enzymes, only MMA and ADMA were formed under conditions where we could detect SDMA at a level of less than 0.4% of

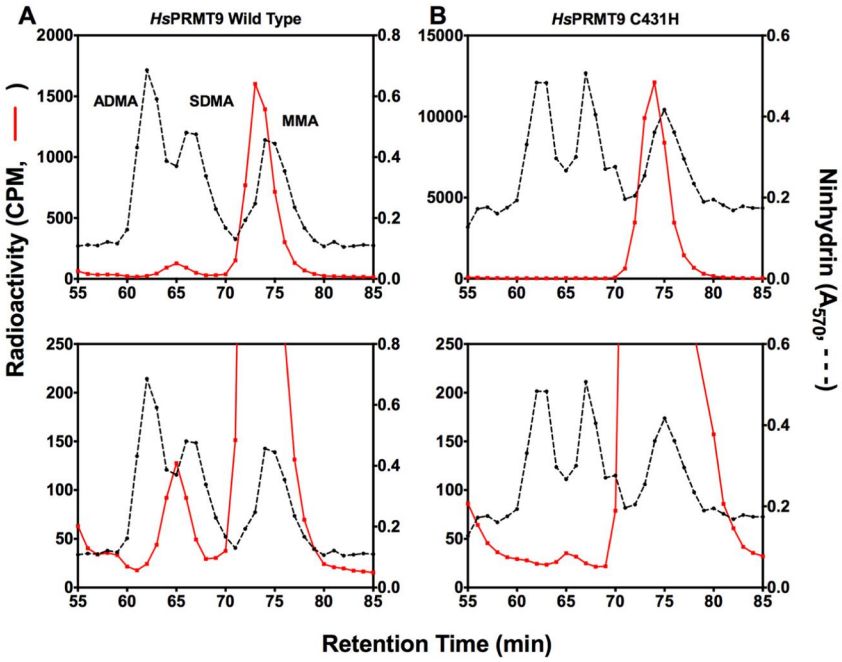

FIGURE 5. ***Hs*PRMT9 C431H mutant displays diminished SDMA and greatly increased MMA production with GST-SF3B2.** *A,* amino acid analysis of methylated arginine derivatives produced by the wild-type human GST-PRMT9 (*Hs*PRMT9) with substrate GST-SF3B2 as described under "Experimental Procedures." *B,* amino acid analysis of methylated arginine derivatives produced by the C431H mutant human GST-PRMT9 with substrate GST-SF3B2. In each case, the *lower panels* represent enlargement of the radioactivity in the *upper panels* to show low levels of methylation. As given under the "Experimental Procedures," 86 cpm correspond to 1 fmol of methyl groups. This experiment is one of two biological replicates.

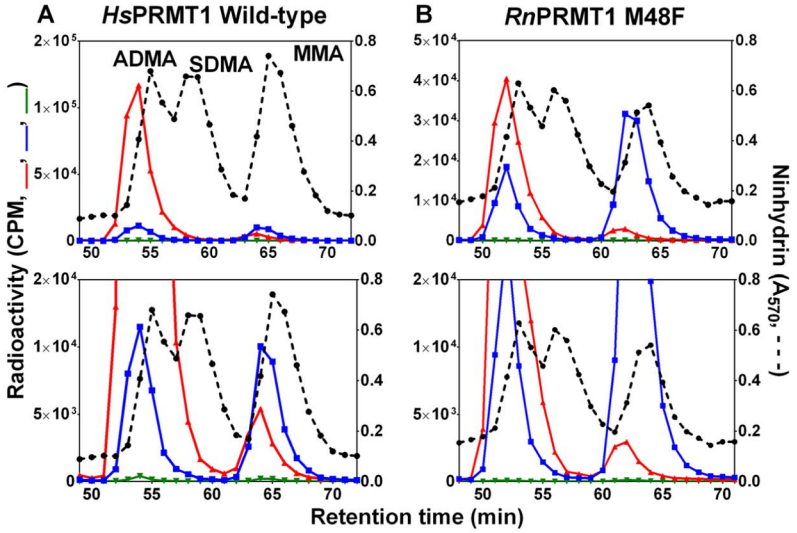

FIGURE 6. ***Rn*PRMT1 M48F mutant enzyme does not produce SDMA with histone H4 peptides.** *In vitro* methylation and cation exchange chromatography were used as described under the "Experimental Procedures" to assess PRMT1 activity and product specificity with H4(1–21) (*blue*), H4(1–21) R3MMA (*red*), and the enzyme alone (*green*). *Dashed black lines* indicate elution profile of non-radioactive methylarginine species as measured by a ninhydrin assay (see "Experimental Procedures"). *A,* amino acid analysis of methylated arginine derivatives produced by human PRMT1 (*Hs*PRMT1). *B,* amino acid analysis of methylated arginine derivatives produced by rat PRMT1 (*Rn*PRMT1) M48F mutant. In each case, the *lower panels* represent enlargement of the radioactivity in the *upper panels* to show low levels of methylation. As given under the "Experimental Procedures," 86 cpm correspond to 1 fmol of methyl groups. This experiment represents one of two biological replicates.

the radioactivity in ADMA. Significantly, in the presence of an already methylated substrate such as H4(1–21) R3MMA, the rat PRMT1 M48F was still unable to produce any SDMA (Fig. 6*B*). Additionally, there is MMA production above automethylation levels for wild-type human PRMT1 and rat PRMT1 M48F when given H4(1–21) R3MMA as a substrate. The MMA

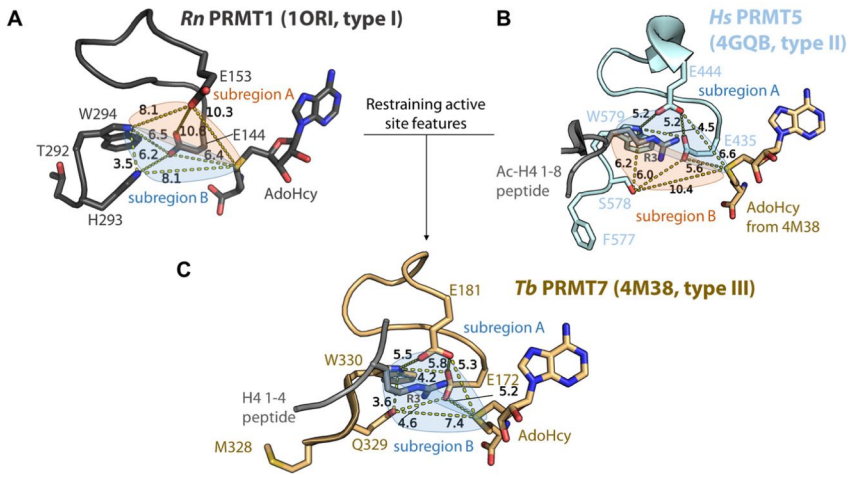

FIGURE 7. **PRMT active sites display distinct spatial architectures.** The active site (double E loop, THW loop, and AdoHcy) from *Rn*PRMT1 (1ORI, chain A; *dark gray*) (*A*), *Hs*PRMT5 (4GQB, chain A; *cyan*) (*B*), and *Tb*PRMT7 (4M38, chain A; *wheat*) (*C*) are shown. Crowded subregions of the active sites are highlighted in *light blue* and open subregions are highlighted in *orange*. *B* and *C*, substrate peptides co-crystallized with the enzyme are also shown. Distances between atoms are given in Ångströms and indicated by *yellow dashed lines*. Images were made using PyMOL (Schrödinger, LLC).

being produced with this peptide would be expected to occur at positions Arg-17 and Arg-19. These results indicate that the residue Met-48 may not be involved in mediating product specificity in mammalian PRMT1.

Discussion

Different methylarginine marks can be recognized by distinct reader proteins (17) and often behave as epigenetic switches, affecting the activation or silencing of certain genes (15, 16). Given the significance of ADMA and SDMA marks, it has become increasingly important to understand how product specificity arises to generate these residues. Having previously demonstrated the conversion of *Tb*PRMT7, a strictly MMA-producing type III enzyme, into a type I enzyme forming ADMA by mutation (25), we now present another *Tb*PRMT7 mutant that is capable of producing SDMA, exhibiting the product specificity of type II PRMTs (Fig. 2). Biochemical and mutational analyses of the enzyme's catalytic activity reveal that SDMA production occurs when it is presented with an already monomethylated substrate, demonstrating that this mutant of PRMT7, in contrast to the wild type, is able to recognize a monomethylated molecule as a substrate and carry out further methylation. In fact, the E181D/Q329A mutant enzyme binds H4(1–21) R3MMA with a higher affinity than the corresponding unmethylated peptide (Fig. 4). This observation illustrates that although the activity of the E181D/Q329A mutant is low, it still behaves, on the catalytic level, as a type II PRMT.

We also examined a mammalian PRMT1 mutant enzyme that was previously reported to produce SDMA along with its wild-type products, ADMA and MMA (24). We were unable to observe any symmetric dimethylation on histone H4 peptide substrates from this rat PRMT1 mutant enzyme (M48F) (Fig. 6). Coupled with our results from amino acid analysis of a homologous mutation in *Tb*PRMT7 (M75F; Table 1) and its mutation to alanine (M75A; Table 1) (25), our work did not confirm any role of Met-48 in affecting PRMT1 product specificity in the mammalian enzyme. It should be noted that the H4 peptide substrates used in our study differ from the GGRGGFGGRGGFGGRGGFG peptide used previously (24). Additionally, immunoblot analysis revealed that the reverse mutation in the PRMT5 enzymes of humans and *Caenorhabditis elegans*, where the corresponding wild-type residue is a phenylalanine (F327M and F379M, respectively) caused asymmetric dimethylation of human histone H4 (14). It would be interesting to examine these mutants with our more sensitive amino acid analysis techniques to determine any changes in product specificity more precisely.

Our previous mutagenesis results (25), coupled with those discussed here, highlight the major features of the PRMT active site, which may control mono- and dimethylation specificity. Conceptually, the active site of PRMTs, defined by the double E loop, the THW loop, and the AdoMet/AdoHcy cofactor, can be divided into two subregions, one of which is located between the two glutamate residues of the double E loop and above the substrate arginine (subregion A), while subregion B is adjacent to the THW loop and the region underneath the substrate arginine as displayed in Fig. 7. Our analysis reveals that the nature of these two subregions correlates well with, and therefore seems predictive of, product specificity in PRMTs. Specifically, type I PRMTs contain an open subregion A and a spatially restricted subregion B (Fig. 7*A*). The nature of these subregions in type II active sites is reversed with respect to type I PRMTs, with an open subregion B and a restricted subregion A (Fig. 7*B*). PRMT7's active site by contrast contains two restricted subregions, combining the restraining features of subregions A (type I) and B (type II) of the other two types of PRMTs (Fig. 7*C*). These spatial restrictions may be the key for PRMT7 to only monomethylate its substrates, thus classifying it as a type III PRMT enzyme.

The E181D mutation of *Tb*PRMT7 increases the space within subregion A of the active site by a single carbon-carbon

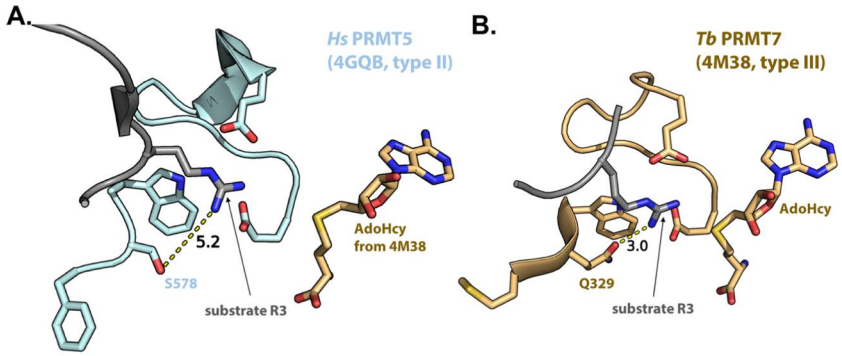

FIGURE 8. **THW loop of PRMT5 is further away from the substrate arginine than the THW loop of PRMT7.** *A,* active site of human PRMT5 (4GQB) is shown. *B,* active site of *Tb*PRMT7 (4M38) is shown. Distances between atoms are given in Ångströms and indicated by *yellow dashed lines*.

bond where the substrate arginine is stabilized. The distance between the glutamates of the double E loop, however, is not the essential factor in SDMA production because the glutamates of human PRMT5, the major SDMA producer in the cell, are actually closer together than even those in *Tb*PRMT7 (Fig. 7, *B* and *C*). The methylation type alteration can be largely attributed to the Q329A mutation, which, in combination with E181D, may result in the opening up of subregion B in the active site underneath the substrate arginine. It is important to note that the Q329A single mutant did not produce SDMA, suggesting that the THW loop may not be the sole contributor in determining type II methylation. Human PRMT5 has a serine residue in place of the corresponding glutamine residue in *Tb*PRMT7 that is located at a greater distance (5.2 Å *versus* 3.0 Å; Fig. 8) from the substrate arginine than the glutamine of *Tb*PRMT7 and is also pointed away from the active site (Fig. 7). In our *Tb*PRMT7 E181D/Q329A construct, the glutamine to alanine substitution removes an acetamide moiety in subregion B. This active-site alteration now allows for methylated arginines to bind more favorably and is better suited to accommodate a methylated nitrogen atom near the THW loop, allowing the other terminal nitrogen atom (positioned near the double E loop) to become methylated. A specific role of the THW loop in determining PRMT product specificity was first suggested in two recent reviews from Thompson and co-workers (2, 20).

In support of the importance of the THW loop in determining type II PRMT product specificity, the mutation of C431H in human PRMT9 shows a significant decrease in SDMA production relative to the wild-type enzyme (Fig. 5). Although no structure has been determined for this enzyme, the cysteine to histidine mutation introduces a bulkier moiety into the THW loop potentially contributing to further crowding in the active site, which in turn may prevent SDMA production. The concomitant marked increase in MMA production of the PRMT9 is consistent with a partially processive methylation mechanism, a characteristic of type I PRMTs (33).

Structural alignments of known type I, II, and III PRMTs show that the geometries of the active sites are highly conserved within each PRMT type (Fig. 9 and Table 2). Although our proposed model will benefit from further validation through structural studies of novel PRMTs and additional mutant enzymes, our results illustrate how small changes in the active site of PRMTs can markedly alter their catalytic specificity and thus aid in creating a spectrum of methylarginine species that may differentially mediate various biological pathways.

The emerging role of PRMTs in cancer (4, 5, 34, 35) has profoundly spurred the research into PRMT inhibitors (36). One of the major issues in this field, however, has been the promiscuity of many PRMT inhibitors derived from small molecule library screening (37). Approaches based on finding bisubstrate analogs that mimic the cofactor and the substrate arginine have the disadvantages of promiscuity and additionally, due to their highly charged nature, limited bioavailability precluding their administration as oral drugs (37). In light of such obstacles in the development of small molecule inhibitors of PRMTs involved in various diseases, it is our hope that our model will facilitate the rational design of specific and potent PRMT inhibitors by providing detailed insight into the distinct active-site architectures of the three types of PRMTs.

Experimental Procedures

Peptide Substrates—Histone H4(1–21) (Ac-SGRGKGGK-GLGKGGAKRHRKV) and histone H4(1–21) R3MMA (Ac-SGR(me)GKGGKGLGKGGAKRHRKV) peptides were kind gifts from Heather Rust (The Scripps Research Institute, Jupiter, FL) and Paul Thompson (University of Massachusetts Medical School, Worcester, MA). Peptides used for ITC analysis were purchased from AnaSpec.

*Protein Expression and Purification—Tb*PRMT7 wild-type and mutant enzymes were cloned, expressed, and purified as described previously (25). GST-PRMT9 wild-type, GST-PRMT9 C431H mutant, and GST-SF3B2(401–550) fragment were expressed and purified as described previously (28).

Human PRMT1 (*Hs*PRMT1) was expressed from a pET28b(+) vector with a short N-terminal His tag obtained from Dr. Paul Thompson (University of Massachusetts Medical School, Worcester, MA) (38). Rat PRMT1 (*Rn*PRMT1) M48F was expressed from a pET28b(+) vector obtained from Dr. Joan Hevel (Utah State University, Logan, UT) (24). Both constructs were expressed in *Escherichia coli* BL21(DE3) cells (Invitrogen) and grown in LB media con-

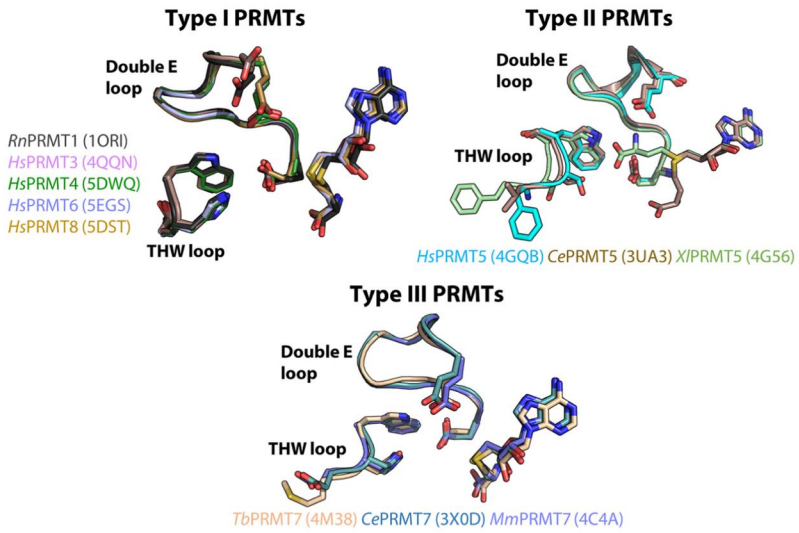

FIGURE 9. **Structural alignment of PRMT active sites.** Active sites of all three types of PRMTs are shown.

TABLE 2

Root mean square deviation (r.m.s.d.) values for structural alignments of the active-site double E loop, the THW loop, and AdoHcy made in PyMOL for type I, II, and III PRMTs from the indicated crystal structures

		r.m.s.d. (Å)	
	PRMTs	Cα	All atoms
Type I			
	*Rn*PRMT1 (1ORI)	0	0
	*Hs*PRMT3 (4QQN)	0.5	1.2
	*Hs*PRMT4 (5DWQ)	0.6	1.3
	*Hs*PRMT6 (5EGS)	0.7	1.2
	*Hs*PRMT8 (5DST)	0.6	1.1
Type II			
	*Hs*PRMT5 (4GQB)	0	0
	*Ce*PRMT5 (3UA3)	0.3	0.6
	*Xl*PRMT5 (4G56)	0.4	1.6
Type III			
	*Tb*PRMT7 (4M38)	0	0
	*Ce*PRMT7 (3X0D)	0.7	1.0
	*Mm*PRMT7 (4C4A)	0.7	1.1

taining kanamycin at 37 °C to an OD_{600} of ~0.6. Expression was induced with 1 mM isopropyl β-D-thiogalactoside (GoldBio) at 18 °C for 16 h. The cells were then harvested by centrifugation at 5,000 × *g* and 4 °C. The harvested cells were lysed using an EmulsiFlex cell homogenizer (Avestin) in 50 mM HEPES (pH 8.0), 300 mM NaCl, 0.5 mM phenylmethylsulfonyl fluoride (Sigma), and complete EDTA-free protease inhibitor mixture (Pierce). Lysed cells were centrifuged at 15,000 rpm for 50 min at 4 °C. The clarified lysate was loaded onto a 5-ml HisTrap HP Ni^{2+} column (GE Healthcare). The column was washed with 10 column volumes of the lysis buffer, including 50 mM imidazole-HCl (pH 8.0), and the protein was eluted with a 50–500 mM imidazole-HCl (pH 8.0) gradient. The eluted protein's purity was verified through SDS-PAGE analysis to be >95% (~40.6 kDa). The protein was then dialyzed against a storage buffer containing 50 mM HEPES (pH 8.0), 1 mM DTT, and 15% glycerol (v/v).

Isothermal Titration Calorimetry—ITC measurements were performed at 15 °C using a MicroCal auto-iTC200 calorimeter (MicroCal, LLC). Protein was incubated with 2-fold molar excess of AdoHcy for 1 h at room temperature. Protein and peptide samples were then extensively dialyzed against a buffer containing 20 mM HEPES (pH 7.5), 20 mM NaCl, and 0.5 mM tris(2-carboxyethyl)phosphine. 2 μl of 1–4 mM peptide was injected into 0.2 ml of 0.1–0.4 mM protein in the chamber every 150 s. Baseline-corrected data were analyzed with ORIGIN software.

Amino Acid Analysis of Protein and Peptide Substrates—In vitro methylation assays and amino acid analysis using the *Tb*PRMT7 wild-type and mutant enzymes were performed as described previously (25) in a buffer of 50 mM HEPES (pH 8.0), 10 mM NaCl, 1 mM DTT, and 5% glycerol in a final volume of 60 μl. Assays and amino acid analysis using human PRMT9 were also carried out as described previously (28, 29). For methylation assays with PRMT1, human and rat enzymes were used. The wild-type control was done with human PRMT1, and the mutant reactions were done with rat PRMT1 M48F. In both cases, 2.5 μg of PRMT1 and either 50 μM H4(1–21) or H4(1–21) R3MMA peptide were incubated at 37 °C for 3 h in a mixture containing 0.7 μM of *S*-adenosyl-L-[*methyl*-^{3}H]methionine ([*methyl*-^{3}H]AdoMet) (PerkinElmer Life Sciences; stock solution of 7 μM (78.2 Ci/mmol) in 10 mM H_2SO_4/EtOH (9:1, v/v)), 50 mM HEPES (pH 8.0), 10 mM NaCl, 1 mM DTT, and 5% glycerol in a final volume of 60 μl. Reactions were stopped, acid-hydrolyzed, and analyzed with cation exchange chromatography as described previously (25). Given the specific radioactivity of the [*methyl*-^{3}H]-AdoMet of 78.2 Ci/mmol and a counting efficiency of 50%, 1 fmol of methyl groups corresponds to 86 cpm.

Author Contributions—K. J., R. A. W., E. W. D., A. H., P. S., and S. G. C. planned the experiments. Experiments were performed by K. J., R. A. W., E. W. D., and A. H. K. J. and R. A. W. drafted the manuscript. K. J., R. A. W., E. W. D., A. H., P. S., and S. G. C. participated in the data analysis and interpretation, and K. J., R. A. W., E. W. D., A. H., P. S., and S. G. C. participated in manuscript revisions.

Acknowledgments—We thank H. Rust (The Scripps Research Institute) and P. Thompson (University of Massachusetts Medical School) for providing the H4(1–21) and H4(1–21) R3MMA peptides and the human His-PRMT1 plasmid; J. Hevel (Utah State University, Logan, UT) for providing the rat His-PRMT1 M48F plasmid; M. Dzialo (University of Leuven, Belgium) for help with amino acid analysis; G. Blobel (Rockefeller University) for support; D. Berman (Rockefeller University) for help with protein expression and purification; D. King (University of California at Berkeley) for mass spectrometry analysis; and the High Throughput Screening and Spectroscopy Resource Center at Rockefeller University.

References

1. Walsh, G., and Jefferis, R. (2006) Post-translational modifications in the context of therapeutic proteins. *Nat. Biotechnol.* **24,** 1241–1252
2. Fuhrmann, J., Clancy, K. W., and Thompson, P. R. (2015) Chemical biology of protein arginine modifications in epigenetic regulation. *Chem. Rev.* **115,** 5413–5461
3. Morales, Y., Cáceres, T., May, K., and Hevel, J. M. (2016) Biochemistry and regulation of the protein arginine methyltransferases (PRMTs). *Arch. Biochem. Biophys.* **590,** 138–152
4. Baldwin, R. M., Haghandish, N., Daneshmand, M., Amin, S., Paris, G., Falls, T. J., Bell, J. C., Islam, S., and Côté, J. (2015) Protein arginine methyltransferase 7 promotes breast cancer cell invasion through the induction of MMP9 expression. *Oncotarget.* **6,** 3013–3032
5. Yao, R., Jiang, H., Ma, Y., Wang, L., Wang, L., Du, J., Hou, P., Gao, Y., Zhao, L., Wang, G., Zhang, Y., Liu, D.-X., Huang, B., and Lu, J. (2014) PRMT7 induces epithelial-to-mesenchymal transition and promotes metastasis in breast cancer. *Cancer Res.* **74,** 5656–5667
6. Yang, Y., and Bedford, M. T. (2013) Protein arginine methyltransferases and cancer. *Nat. Rev. Cancer* **13,** 37–50
7. Karkhanis, V., Wang, L., Tae, S., Hu, Y. J., Imbalzano, A. N., and Sif, S. (2012) Protein arginine methyltransferase 7 regulates cellular response to DNA damage by methylating promoter histones H2A and H4 of the polymerase δ catalytic subunit gene, POLD1. *J. Biol. Chem.* **287,** 29801–29814
8. Wang, Y.-C., Peterson, S. E., and Loring, J. F. (2014) Protein post-translational modifications and regulation of pluripotency in human stem cells. *Cell Res.* **24,** 143–160
9. Lott, K., Zhu, L., Fisk, J. C., Tomasello, D. L., and Read, L. K. (2014) Functional interplay between protein arginine methyltransferases in *Trypanosoma brucei*. *Microbiologyopen* **3,** 595–609
10. Ferreira, T. R., Alves-Ferreira, E. V., Defina, T. P., Walrad, P., Papadopoulou, B., and Cruz, A. K. (2014) Altered expression of an RBP-associated arginine methyltransferase 7 in *Leishmania major* affects parasite infection. *Mol. Microbiol.* **94,** 1085–1102
11. Bedford, M. T., and Clarke, S. G. (2009) Protein arginine methylation in mammals: who, what, and why. *Mol. Cell* **33,** 1–13
12. Martens-Lobenhoffer, J., Bode-Böger, S. M., and Clement, B. (2016) First detection and quantification of *N*(δ)-monomethylarginine, a structural isomer of *N* (G)-monomethylarginine, in humans using MS(3). *Anal. Biochem.* **493,** 14–20
13. Wang, H., Huang, Z. Q., Xia, L., Feng, Q., Erdjument-Bromage, H., Strahl, B. D., Briggs, S. D., Allis, C. D., Wong, J., Tempst, P., and Zhang, Y. (2001) Methylation of histone H4 at arginine 3 facilitating transcriptional activation by nuclear hormone receptor. *Science* **293,** 853–857
14. Sun, L., Wang, M., Lv, Z., Yang, N., Liu, Y., Bao, S., Gong, W., and Xu, R.-M. (2011) Structural insights into protein arginine symmetric dimethylation by PRMT5. *Proc. Natl. Acad. Sci.* **108,** 20538–20543
15. Dhar, S. S., Lee, S.-H., Kan, P.-Y., Voigt, P., Ma, L., Shi, X., Reinberg, D., and Lee, M. G. (2012) Trans-tail regulation of MLL4-catalyzed H3K4 methylation by H4R3 symmetric dimethylation is mediated by a tandem PHD of MLL4. *Genes Dev.* **26,** 2749–2762
16. Migliori, V., Müller, J., Phalke, S., Low, D., Bezzi, M., Mok, W. C., Sahu, S. K., Gunaratne, J., Capasso, P., Bassi, C., Cecatiello, V., De Marco, A., Blackstock, W., Kuznetsov, V., Amati, B., *et al.* (2012) Symmetric dimethylation of H3R2 is a newly identified histone mark that supports euchromatin maintenance. *Nat. Struct. Mol. Biol.* **19,** 136–144
17. Gayatri, S., and Bedford, M. T. (2014) Readers of histone methylarginine marks. *Biochim. Biophys. Acta* **1839,** 702–710
18. Suárez-Calvet, M., Neumann, M., Arzberger, T., Abou-Ajram, C., Funk, E., Hartmann, H., Edbauer, D., Kremmer, E., Göbl, C., Resch, M., Bourgeois, B., Madl, T., Reber, S., Jutzi, D., Ruepp, M.-D., *et al.* (2016) Monomethylated and unmethylated FUS exhibit increased binding to Transportin and distinguish FTLD-FUS from ALS-FUS. *Acta Neuropathol.* **131,** 587–604
19. Dhar, S., Vemulapalli, V., Patananan, A. N., Huang, G. L., Di Lorenzo, A., Richard, S., Comb, M. J., Guo, A., Clarke, S. G., and Bedford, M. T. (2013) Loss of the major type I arginine methyltransferase PRMT1 causes substrate scavenging by other PRMTs. *Sci. Rep.* **3,** 1311
20. Fuhrmann, J., and Thompson, P. R. (2016) Protein arginine methylation and citrullination in epigenetic regulation. *ACS Chem. Biol.* **11,** 654–668
21. Schapira, M., and Ferreira de Freitas, R. (2014) Structural biology and chemistry of protein arginine methyltransferases. *Medchemcomm* **5,** 1779–1788
22. Cura, V., Troffer-Charlier, N., Wurtz, J. M., Bonnefond, L., and Cavarelli, J. (2014) Structural insight into arginine methylation by the mouse protein arginine methyltransferase 7: a zinc finger freezes the mimic of the dimeric state into a single active site. *Acta Crystallogr. D Biol. Crystallogr* **70,** 2401–2412
23. Hasegawa, M., Toma-Fukai, S., Kim, J. D., Fukamizu, A., and Shimizu, T. (2014) Protein arginine methyltransferase 7 has a novel homodimer-like structure formed by tandem repeats. *FEBS Lett.* **588,** 1942–1948
24. Gui, S., Gathiaka, S., Li, J., Qu, J., Acevedo, O., and Hevel, J. M. (2014) A remodeled protein arginine methyltransferase 1 (PRMT1) generates symmetric dimethylarginine. *J. Biol. Chem.* **289,** 9320–9327
25. Debler, E. W., Jain, K., Warmack, R. A., Feng, Y., Clarke, S. G., Blobel, G., and Stavropoulos, P. (2016) A glutamate/aspartate switch controls product specificity in a protein arginine methyltransferase. *Proc. Natl. Acad. Sci. U.S.A.* **113,** 2068–2073
26. Fisk, J. C., Sayegh, J., Zurita-Lopez, C., Menon, S., Presnyak, V., Clarke, S. G., and Read, L. K. (2009) A type III protein arginine methyltransferase from the protozoan parasite *Trypanosoma brucei*. *J. Biol. Chem.* **284,** 11590–11600
27. Wang, C., Zhu, Y., Caceres, T. B., Liu, L., Peng, J., Wang, J., Chen, J., Chen, X., Zhang, Z., Zuo, X., Gong, Q., Teng, M., Hevel, J. M., Wu, J., and Shi, Y. (2014) Structural determinants for the strict monomethylation activity by *Trypanosoma brucei* protein arginine methyltransferase 7. *Structure* **22,** 756–768
28. Hadjikyriacou, A., Yang, Y., Espejo, A., Bedford, M. T., and Clarke, S. G. (2015) Unique features of human protein arginine methyltransferase 9 (PRMT9) and its substrate RNA splicing factor SF3B2. *J. Biol. Chem.* **290,** 16723–16743
29. Yang, Y., Hadjikyriacou, A., Xia, Z., Gayatri, S., Kim, D., Zurita-Lopez, C., Kelly, R., Guo, A., Li, W., Clarke, S. G., and Bedford, M. T. (2015) PRMT9 is a type II methyltransferase that methylates the splicing factor SAP145. *Nat. Commun.* **6,** 6428
30. Feng, Y., Maity, R., Whitelegge, J. P., Hadjikyriacou, A., Li, Z., Zurita-Lopez, C., Al-Hadid, Q., Clark, A. T., Bedford, M. T., Masson, J. Y., and Clarke, S. G. (2013) Mammalian protein arginine methyltransferase 7 (PRMT7) specifically targets RXR sites in lysine- and arginine-rich regions. *J. Biol. Chem.* **288,** 37010–37025
31. Feng, Y., Xie, N., Jin, M., Stahley, M. R., Stivers, J. T., and Zheng, Y. G. (2011) A transient kinetic analysis of PRMT1 catalysis. *Biochemistry* **50,** 7033–7044
32. Huang, S., Litt, M., and Felsenfeld, G. (2005) Methylation of histone H4 by arginine methyltransferase PRMT1 is essential in vivo for many subsequent histone modifications. *Genes Dev.* **19,** 1885–1893
33. Wang, M., Xu, R.-M., and Thompson, P. R. (2013) Substrate specificity, processivity, and kinetic mechanism of protein arginine methyltransferase 5. *Biochemistry* **52,** 5430–5440
34. Bao, X., Zhao, S., Liu, T., Liu, Y., Liu, Y., and Yang, X. (2013) Overexpression of PRMT5 promotes tumor cell growth and is associated with poor

disease prognosis in epithelial ovarian cancer. *J. Histochem. Cytochem.* **61,** 206–217
35. Tarighat, S. S., Santhanam, R., Frankhouser, D., Radomska, H. S., Lai, H., Anghelina, M., Wang, H., Huang, X., Alinari, L., Walker, A., Caligiuri, M. A., Croce, C. M., Li, L., Garzon, R., Li, C., *et al.* (2016) The dual epigenetic role of PRMT5 in acute myeloid leukemia: gene activation and repression via histone arginine methylation. *Leukemia* **30,** 789–799
36. Schapira, M., and Arrowsmith, C. H. (2016) Methyltransferase inhibitors for modulation of the epigenome and beyond. *Curr. Opin. Chem. Biol.* **33,** 81–87
37. Hu, H., Qian, K., Ho, M.-C., and Zheng, Y. G. (2016) Small molecule inhibitors of protein arginine methyltransferases. *Expert Opin. Investig. Drugs.* **25,** 335–358
38. Zhang, X., and Cheng, X. (2003) Structure of the predominant protein arginine methyltransferase PRMT1 and analysis of its binding to substrate peptides. *Structure* **11,** 509–520
39. Zurita-Lopez, C. I., Sandberg, T., Kelly, R., and Clarke, S. G. (2012) Human protein arginine methyltransferase 7 (PRMT7) is a type III enzyme forming ω-N^G-monomethylated arginine residues. *J. Biol. Chem.* **287,** 7859–7870
40. Gottschling, H., and Freese, E. (1962) A tritium isotope effect on ion exchange chromatography. *Nature* **196,** 829–831

CHAPTER 8

Caenorhabditis elegans PRMT-7 and PRMT-9 Are Evolutionarily Conserved Protein Arginine Methyltransferases with Distinct Substrate Specificities

Caenorhabditis elegans PRMT-7 and PRMT-9 Are Evolutionarily Conserved Protein Arginine Methyltransferases with Distinct Substrate Specificities

Andrea Hadjikyriacou and Steven G. Clarke*

Department of Chemistry and Biochemistry and the Molecular Biology Institute, University of California, Los Angeles, 607 Charles E. Young Drive East, Los Angeles, California 90095-1569, United States

Supporting Information

ABSTRACT: *Caenorhabditis elegans* protein arginine methyltransferases PRMT-7 and PRMT-9 are two evolutionarily conserved enzymes, with distinct orthologs in plants, invertebrates, and vertebrates. Biochemical characterization of these two enzymes reveals that they share much in common with their mammalian orthologs. *C. elegans* PRMT-7 produces only monomethylarginine (MMA) and preferentially methylates R-X-R motifs in a broad collection of substrates, including human histone peptides and RG-rich peptides. In addition, the activity of the PRMT-7 enzyme is dependent on temperature, the presence of metal ions, and the reducing agent dithiothreitol. *C. elegans* PRMT-7 has a substrate specificity and a substrate preference different from those of mammalian PRMT7, and the available X-ray crystal structures of the PRMT7 orthologs show differences in active site architecture. *C. elegans* PRMT-9, on the other hand, produces symmetric dimethylarginine and MMA on SFTB-2, the conserved *C. elegans* ortholog of human RNA splicing factor SF3B2, indicating a possible role in the regulation of nematode splicing. In contrast to PRMT-7, *C. elegans* PRMT-9 appears to be biochemically indistinguishable from its human ortholog.

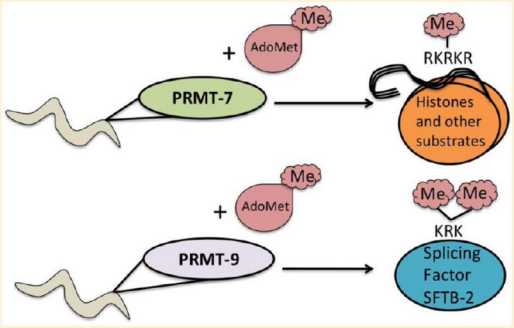

Protein arginine methylation is a posttranslational modification that is widely distributed in vertebrates, invertebrates, plants, and fungi.[1,2] Members of the mammalian protein arginine methyltransferase (PRMT) family modify arginine residues by introducing a methyl group onto the terminal guanidino groups, generating either exclusively monomethylarginine (MMA) (type III, PRMT7), MMA and symmetric dimethylarginine (SDMA) (type II, PRMT5 and PRMT9), or MMA and asymmetric dimethylarginine (ADMA) (type I, PRMT1−4, -6, and -8).[3,4] This family of enzymes has roles in the epigenetic regulation of transcription,[3] mRNA splicing,[5] DNA damage response,[6] carcinogenesis,[3,7,8] and signaling.[9] Many of these enzymes have multiple functions and roles, and changes in their expression have been implicated in tumorigenesis and disease.[3,4,7,8]

The majority of PRMTs have been well characterized, and their physiological substrates have been identified. PRMT7 and PRMT9, however, have received much less attention. While PRMT9 appears to have a major role in the regulation of alternative splicing,[5] for PRMT7 the situation is more complex. Recent studies have shown that PRMT7 is involved in preserving satellite cell regenerative capacity,[10] regulation of germinal center formation,[11] induction of the epithelial-to-mesenchymal transition,[12] and bone development,[13] in addition to roles in cancer such as the promotion of breast cancer metastasis through MMP9 expression.[14] However, it has not yet been possible to connect these phenomena to the specific enzymatic action of PRMT7. In addition, there is evidence that crosstalk of PRMT7 with other PRMTs can modify the epigenetic code. For instance, the knockdown of PRMT7 in mammalian cells has been shown to decrease the level of SDMA formation at arginine 3 in histone H2A and H4 in chromatin associated with specific genes[10,15,16] in spite of the fact that PRMT7 does not catalyze SDMA formation.[3,17,18] In addition, there is evidence of the association of increased levels of arginine 3 SDMA in histone H4 at specific genes with overexpression of PRMT7.[11] It thus appears that PRMT7 may function in conjunction with other PRMTs.

Because of the complexity of mammalian systems, PRMT7 from lower eukaryotes, including *Trypanosoma brucei*[19−22] and *Caenorhabditis elegans*,[23,24] has been studied. However, the trypanosome enzyme has a preference for RG-rich proteins such as RBP16,[19,21,22] while mammalian PRMT7 has a preference for R-X-R motifs in basic sequence contexts such as those found in histone H2B.[17,18] A crystal structure is available for *C. elegans* PRMT-7 that is similar to that determined for *Mus musculus* PRMT7, with both enzymes containing a single chain with two ancestrally duplicated

Received: March 28, 2017
Revised: April 20, 2017
Published: April 25, 2017

methyltransferase domains stabilized by a zinc ion.[24,25] We note that while the *T. brucei* ortholog is named PRMT7, its structure is divergent from those of the *C. elegans* and mouse enzymes, lacking the duplicated domain characteristic of plant, invertebrate, and vertebrate PRMT7 members.[1,2,19] A previous attempt to characterize *C. elegans* PRMT-7 (then named PRMT-2) *in vitro* was unsuccessful because it was enzymatically inactive under the conditions tested.[23] The authors of this same study[23] designated *C. elegans* PRMT-9 (then named PRMT-3) as a human PRMT7 ortholog, while more recent studies have shown it is more closely related to human PRMT9.[1,26]

Given the similarity of the *C. elegans* and mouse PRMT7 enzymes, and the difficulty of determining the mechanism of PRMT7 action in vertebrates, we sought to characterize the *C. elegans* ortholog. We have now been able to show that although the *C. elegans* enzyme is similar to the previously studied mammalian enzyme in its ability to form only MMA marks,[17,18,27] the nematode enzyme has distinct specificity for recognizing arginine residues in peptides and proteins, suggesting distinct functions.

Mammalian PRMT9 had also been challenging to characterize. None of the previously characterized PRMT methyl acceptors were recognized by human PRMT9.[26] However, it was possible to identify a complex with splicing factors SF3B2 and SF3B4 and to show that PRMT9 methylates SF3B2 to produce MMA and SDMA.[5,26] SF3B2 may be the only major substrate of this enzyme, and its modification appears to play a role in the regulation of alternative splicing.[5,26]

While *C. elegans* has no orthologs of mammalian PRMT2−4, -6, or -8, there is an ortholog of PRMT9.[1,2] In the previous study, this ortholog was shown to methylate recombinant histone H2A, producing only MMA.[23] Thus, we were interested in characterizing this *C. elegans* PRMT-9 to establish whether it plays a role similar to that of mammalian PRMT9. We now show that *C. elegans* PRMT-9 is a type II enzyme that produces MMA and SDMA, but it also appears to be highly specific for the *C. elegans* ortholog of the SF3B2 splicing factor, SFTB-2.

MATERIALS AND METHODS

Bacterial Protein Expression and Purification. *C. elegans* PRMT-7 cDNA and PRMT-9 cDNA were cloned into a pGEX-6P-1 plasmid[23] and were a kind gift from A. Fukamizu. The proteins were expressed in BL21 DE3 cells (Invitrogen); *C. elegans* GST-PRMT-7 and -9 enzymes were purified using the conditions described in ref 26, but with induction for 20 h at 18 °C using 0.13 mM isopropyl D-thiogalactopyranoside (IPTG) for GST-PRMT-7 and 1 mM IPTG for 20 h at 18 °C for both GST-PRMT-9 wild type and A391H mutant. The enzymes were purified as described and dialyzed overnight into 100 mM Tris-HCl and 100 mM NaCl (pH 7.5). *Homo sapiens* GST-PRMT7,[18] GST-PRMT9,[26] and GST-SF3B2[5,26] were expressed and purified as described previously. GST-GAR was expressed using 0.4 mM IPTG for 20 h at 18 °C and purified using a process similar to that used for the other proteins but was dialyzed into 50 mM HEPES, 120 mM NaCl, and 1 mM DTT (pH 8.0). The amino acid sequence for SFTB-2 (*C. elegans* SF3B2) was synthesized by GenScript, Inc., and cloned into a pGEX-6p-1 vector. GST-tagged SFTB-2 was purified using a process similar to that used for human SF3B2 and dialyzed overnight into 10 mM Na_2HPO_4, 2 mM KH_2PO_4, 137 mM NaCl, 2.7 mM KCl, and 1 mM DTT (pH 7.4).

Each of these plasmids encodes the full sequence of the *Schistosoma japonicum* glutathione *S*-transferase (UniProt entry P08515) followed by linker regions of SDLEVLFQGPLGSGIP (*C. elegans* PRMT-7), SDLEVLFQGPLGSPEFP (*C. elegans* PRMT-9), SDLQVLFQGPL (*C. elegans* SFTB-2), SDLVPRGSST (human PRMT7), and SDLVPRGS (GST-GAR) followed by the full amino acid sequences of either *C. elegans* PRMT-7 (UniProt entry Q9XW42), *C. elegans* PRMT-9 (UniProt entry O02325), human PRMT7 (UniProt entry Q9NVM4), human PRMT9 (UniProt entry Q6P2P2), *C. elegans* SFTB-2 (UniProt entry O16997), human SF3B2 (UniProt entry Q13435), or amino acids 1−145 of human fibrillarin (UniProt entry P22087), the latter of which has K2E and A145V substitutions. The GST-GAR fusion protein was previously erroneously reported to include human fibrillarin residues 1−148.[18,28] Purified proteins were analyzed via sodium dodecyl sulfate−polyacrylamide gel electrophoresis (SDS−PAGE) and then quantified using 10% trichloroacetic acid precipitation for a Lowry assay.

Peptide Synthesis. All H2B peptides used in these studies listed in Table S1 were synthesized by GenScript, Inc., and further validated by matrix-assisted laser desorption ionization time-of-flight mass spectrometry. Other peptides were gifts from their respective sources (see Table S1).

***In Vitro* Methylation Reactions.** Methylation reactions included 2 μg of enzyme and potential methyl-accepting protein substrate (5 μg) or peptide substrates at a final concentration of 12.5 μM. Mixtures were incubated at the indicated temperatures using a buffer of 50 mM potassium HEPES and 10 mM NaCl (pH 8.2) unless otherwise indicated and 0.7 μM *S*-adenosyl-L-[*methyl*-^{3}H]methionine {^{3}H-AdoMet, PerkinElmer Life Sciences, 82.7 Ci/mmol, 0.55 mCi/mL in 10 mM H_2SO_4/EtOH [9:1 (v/v)]} in a final reaction volume of 60 μL. Given a counting efficiency of 50%, 1 fmol of radiolabeled methyl groups corresponds to 91 cpm.

Amino Acid Analysis of Substrates Using High-Resolution Cation Exchange Chromatography. Reactions with peptide substrates were stopped by the addition of 3 μL of 25% trichloroacetic acid, and peptides were purified using OMIX C18 Zip-Tip pipet tips (Agilent Technologies). The reaction mixtures were then subjected to vacuum centrifugation to remove the Zip-Tip elution buffer consisting of H_2O and acetonitrile (50:50). Protein substrate reactions were stopped by the addition of an equal volume of 25% (w/v) trichloroacetic acid followed by centrifugation to give the protein pellet. Methylated peptides and proteins were subsequently acid hydrolyzed, mixed with nonradioactive methylated arginine derivatives, and separated and analyzed using high-resolution cation exchange chromatography as described in ref 5.

Detection of Methylated Substrates after SDS−PAGE. Protein substrate methylation reactions were stopped by the addition of 0.2 volume of 5× SDS sample loading buffer and run on a 12.6% polyacrylamide Tris-glycine gel. The gel was stained using Coomassie Blue, and after being destained overnight, gels were incubated in EN^{3}HANCE (PerkinElmer Life Sciences, catalog no. 6NE9701) autoradiography reagent, washed with water for 30 min, and then vacuum-dried. Dried gels were then placed in a cassette and exposed to autoradiography film (Denville Scientific, catalog no. E3012) at −80 °C for the amount of time indicated in the figure legends. Densitometry of the bands was performed using ImageJ.

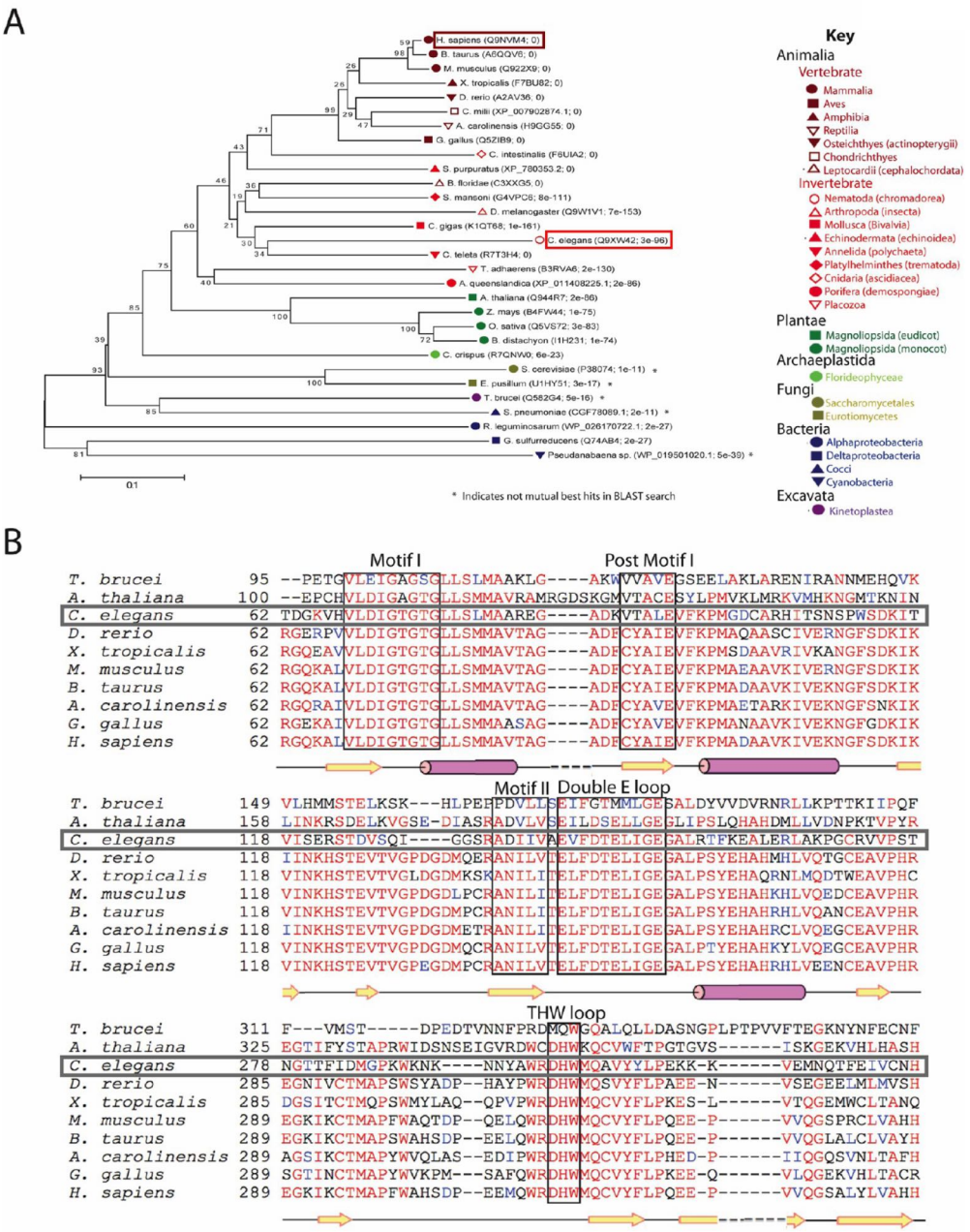

Figure 1. Evolutionary conservation of PRMT7 across the various kingdoms of life. (A) Phylogenetic tree based on human PRMT7. UniProt entries of representative orthologs from Animalia, Plantae, Archaeplastida, Fungi, Bacteria, and Excavata are shown with their *E* values based on a protein BLAST search against the human species.[29] The phylogenetic tree was constructed after amino acid sequences were aligned using MUSCLE in MEGA6 software as described in ref 26. Each ortholog sequence was then subjected to protein BLAST against the human protein database. All proteins were mutual best hits with the exception of those species marked with an asterisk. The number shown next to each branch is the percent of replicate trees with the same clustering in 500 bootstrap test replicates. The scale bar indicates the fraction of amino acid differences for each entry. *H. sapiens* PRMT7 is boxed in dark red, and *C. elegans* PRMT-7 is boxed in red. (B) Partial sequence alignment of the major motifs in PRMT7 orthologs across vertebrates, invertebrates, plants, and excavata (*T. brucei*) using the EMBL-EBI Clustal Omega Multiple Sequence Alignment software.[29] The major distinguishing motifs of protein arginine methyltransferases are boxed in black, including motif I, post motif I, motif II, the double E loop, and the THW loop. Red letters indicate identity and blue letters similar amino acid properties. The secondary structure is indicated on the bottom with β-strands colored yellow and α-helices colored magenta based on the structure of *M. musculus* PRMT7 (Protein Data Bank entry 4C4A[25]). The *C. elegans* PRMT-7 sequence is boxed in dark gray.

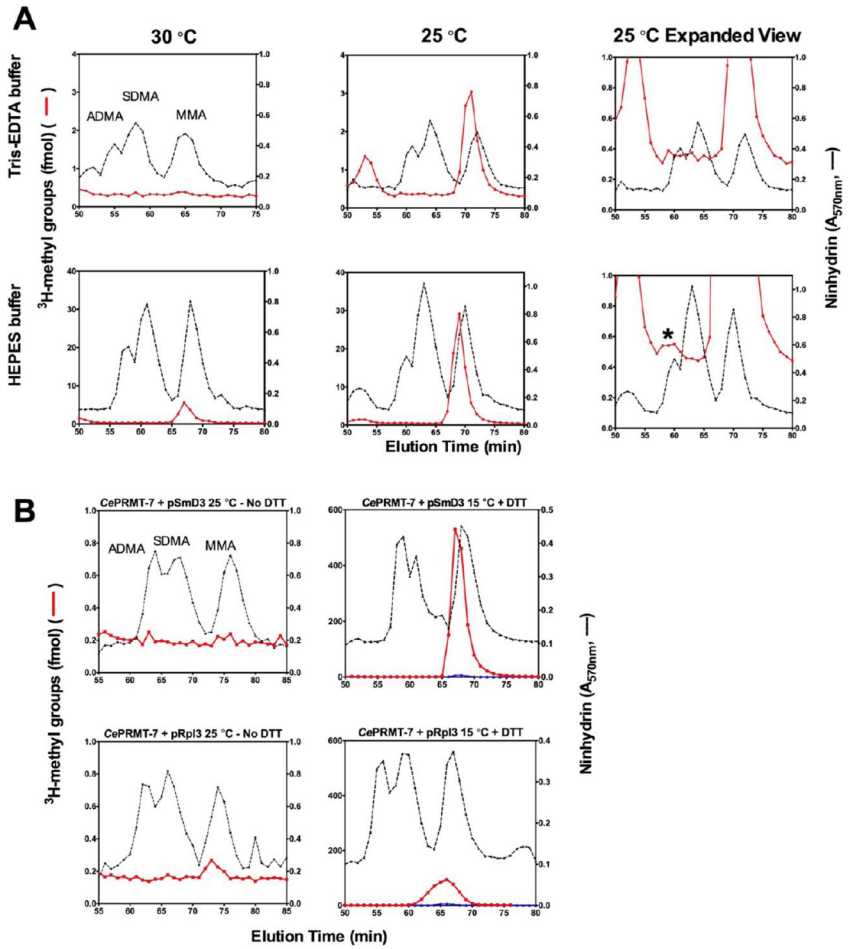

Figure 2. *C. elegans* PRMT-7 produces MMA, and its activity is dependent on temperature and metal ion. (A) Amino acid analysis of ^{3}H methylation reactions of *C. elegans* GST-PRMT-7 (2 μg) with GST-GAR (5 μg) after a 20 h reaction at 30 °C (left) or 25 °C (middle and right) in either Tris-EDTA buffer [100 mM Tris-HCl, 100 mM NaCl, and 2 mM EDTA (pH 8.0)] (top) or 50 mM potassium HEPES and 10 mM NaCl (pH 8.2) (bottom) as indicated in Materials and Methods. The final concentration of DTT in these reactions (from the GST-GAR preparation) was 0.16 mM. After trichloroacetic acid precipitation and acid hydrolysis, 1 μmol of each nonradiolabeled methylated arginine standard (ADMA, SDMA, and MMA) was added to the hydrolyzed pellet and amino acid analysis was performed as described in Materials and Methods. Dashed black lines indicate ninhydrin absorbance of the methylarginine standards with the peaks of ADMA, SDMA, and MMA identified using 50 μL of each fraction. Red lines indicate the elution of the radiolabeled methylated amino acids from the hydrolysates of the reactions. Radioactivity from 950 μL aliquots of each fraction is given as the average of three 5 min counting cycles using liquid scintillation counting. Radioactive methylated amino acids elute approximately 1 min before the nonradiolabeled standard because of the tritium isotope effect.[36] The right panels show an expanded view of the data from the middle columns at 25 °C to demonstrate that the enzyme produces MMA only under both buffer conditions. These reactions were replicated three independent times. The asterisk indicates the peak eluting prior to the position expected for ^{3}H-ADMA; this peak is not consistently observed in the replicates. (B) PRMT-7 enzyme activity is dependent on the presence of DTT. The enzyme was reacted with 12.5 μM pSmD3 (top) or pRpl3 (bottom) peptides at 25 °C in 50 mM potassium HEPES and 10 mM NaCl (pH 8.2) (left) or at 15 °C in the same buffer with the addition of 1 mM DTT. Results are presented as shown in panel A; the blue line in the right-hand panels indicates radioactivity for incubations to which no peptide substrate was added. These reactions were replicated twice with no DTT and once with DTT.

RESULTS

PRMT7 Is Widely Conserved in Vertebrates, Invertebrates, and Plants. The human PRMT7 sequence was analyzed by protein BLAST,[29] and the representative orthologs were compiled into a phylogenetic tree (Figure 1A). We found that the major PRMT structural motifs, including AdoMet-binding post motif I, the substrate-binding double E loop, and the THW loop, are well-conserved (Figure 1B). PRMT7 is widely distributed across vertebrates and invertebrates, including mollusks, insects, tunicates, and nematodes, as well as in higher plants (Figure 1A and ref 1). Significantly, the *C. elegans* ortholog is 32% identical to the human enzyme over the full polypeptide length and has an expected value of 3×10^{-96}. Fungi appear to lack a PRMT7 ortholog, with the closest relatives being more similar to PRMT1. Bacteria also seem to largely lack orthologs to PRMT7. The closest bacterial sequence homologues in *Streptococcus pneumoniae* and *Pseudanabaena* sp. are not mutual best hits to PRMT7, although the *Rhizobium leguminosarum* and *Geobacter sulfurreducens* species are most closely related to PRMT7. In addition,

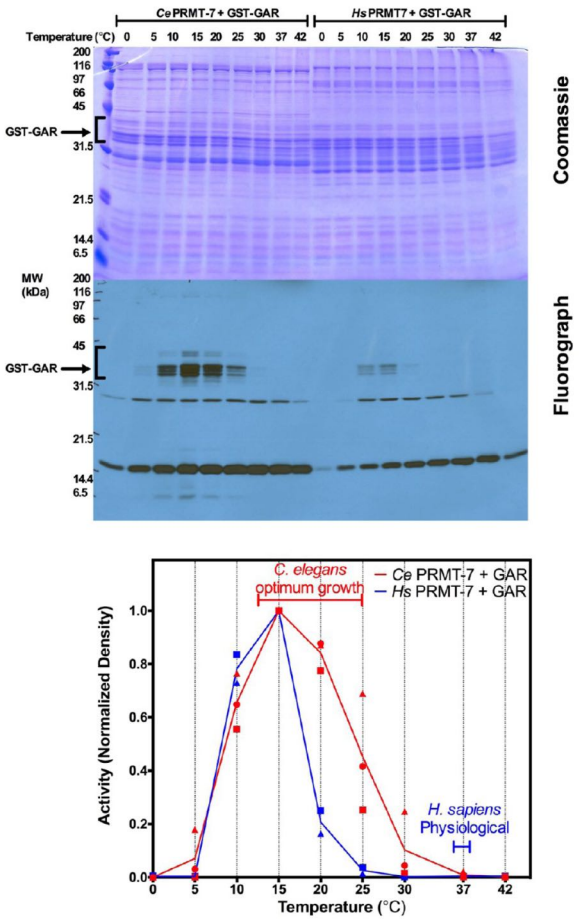

Figure 3. PRMT-7 has a temperature dependence consistent with *C. elegans* physiology. Methylation reaction mixtures consisting of 5 μg of GST-GAR substrate and 2 μg of enzyme (*C. elegans* GST-PRMT-7 or *H. sapiens* GST-PRMT7) were incubated for 20 h at the indicated temperatures in reaction buffer containing 50 mM potassium HEPES and 10 mM NaCl (pH 8.2) with 0.7 μM [*methyl*-^{3}H]AdoMet in a final reaction volume of 60 μL. The final concentration of DTT in these reactions (from the GST-GAR preparation) was 0.16 mM. Reactions were quenched by the addition of SDS sample loading buffer and polypeptides separated by 12.6% Tris-glycine SDS−PAGE followed by autoradiography as described in Materials and Methods. The dried gel was then exposed to Denville E3012 autoradiography film for 21 days at −80 °C. Molecular weight positions are shown from approximately 2 μg of unstained SDS−PAGE broad range marker (Bio-Rad, catalog no. 161-0317). This full experiment was independently replicated, and a further third replicate using only the *C. elegans* enzyme was also performed. Densitometry was performed using ImageJ on scanned images of the films and quantified as relative density and normalized to the highest peak of GST-GAR radioactivity in each individual film (*C. elegans*, red symbols; human, blue symbols; different symbols used to indicate each replicate experiment). Lines are drawn for the averaged normalized values. The optimal growth temperatures for *C. elegans*[31] and humans are indicated. Lower bands shown on the fluorography gel are nonspecific and not dependent on enzyme activity.

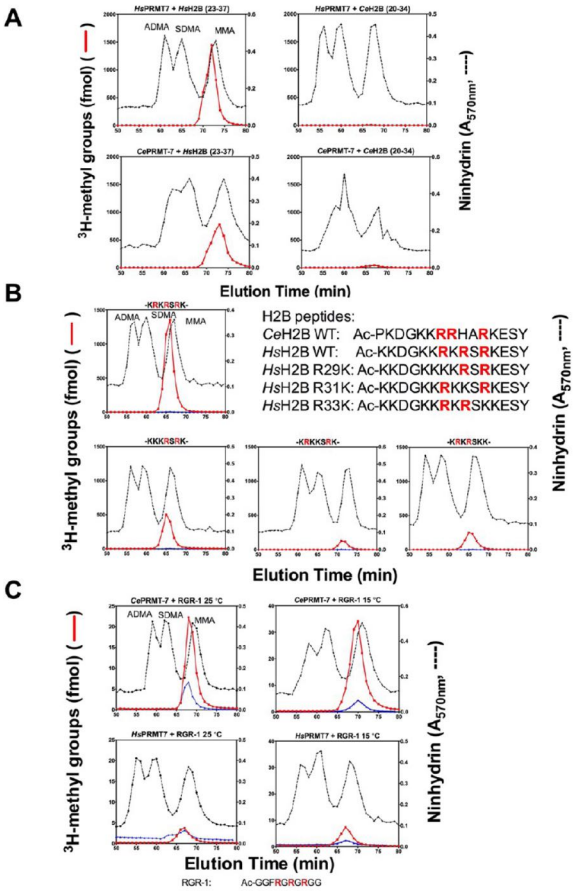

Figure 4. *C. elegans* PRMT-7 has an R-X-R substrate specificity similar to that of the human PRMT7 enzyme. (A) Amino acid analysis of reaction mixtures consisting of 2 μg of human GST-PRMT7 or *C. elegans* PRMT-7 enzymes, reacted with 12.5 μM synthetic human histone H2B (23−37) peptide[17,18] or a synthetic peptide containing the equivalent sequence from *C. elegans* histone H2B (20−34) at 15 °C as described in Materials and Methods, in 50 mM potassium HEPES buffer and 10 mM NaCl (pH 8.0) containing 1 mM DTT for 20 h. Reactions were repeated three times for human histone H2B (23−37) and twice for *C. elegans* H2B (20−34) at this temperature and also replicated at 25 °C once. (B) Amino acid analysis of reaction mixtures containing 2 μg of *C. elegans* GST-PRMT-7 enzyme reacted with 12.5 μM synthetic human histone H2B peptides (wild type, top; R29K, R31K, and R33K bottom) for 20 h, using the same conditions described above for panel A. These reactions were single replicates. (C) Amino acid analysis of reaction mixtures containing 2 μg of *C. elegans* or human PRMT-7/7 enzymes, reacted with 12.5 μM synthetic peptide RGR-1 (a sequence containing an R-X-R sequence where X = G) at 25 °C (left) or 15 °C (right), under the same reaction conditions as described for panel A. Reactions were replicated once, and the reaction of *C. elegans* with RGR-1 was replicated two additional times.

the type III (MMA forming) trypanosome *T. brucei* PRMT7[19,21] is most similar in sequence to human PRMT9 and is not a mutual best hit for human PRMT7. Importantly, *T. brucei* PRMT7 has a substrate specificity distinct from those of both human PRMT7 and PRMT9, preferring RG-rich proteins.[5,17−19,21,22,26]

The major conserved PRMT motifs are shown for selected species in Figure 1B. While all of the enzymes have similar motifs common to all seven β-strand methyltransferases (motif I, post motif I, and motif II), the *T. brucei* PRMT7 deviates significantly from the other proteins in the PRMT-specific

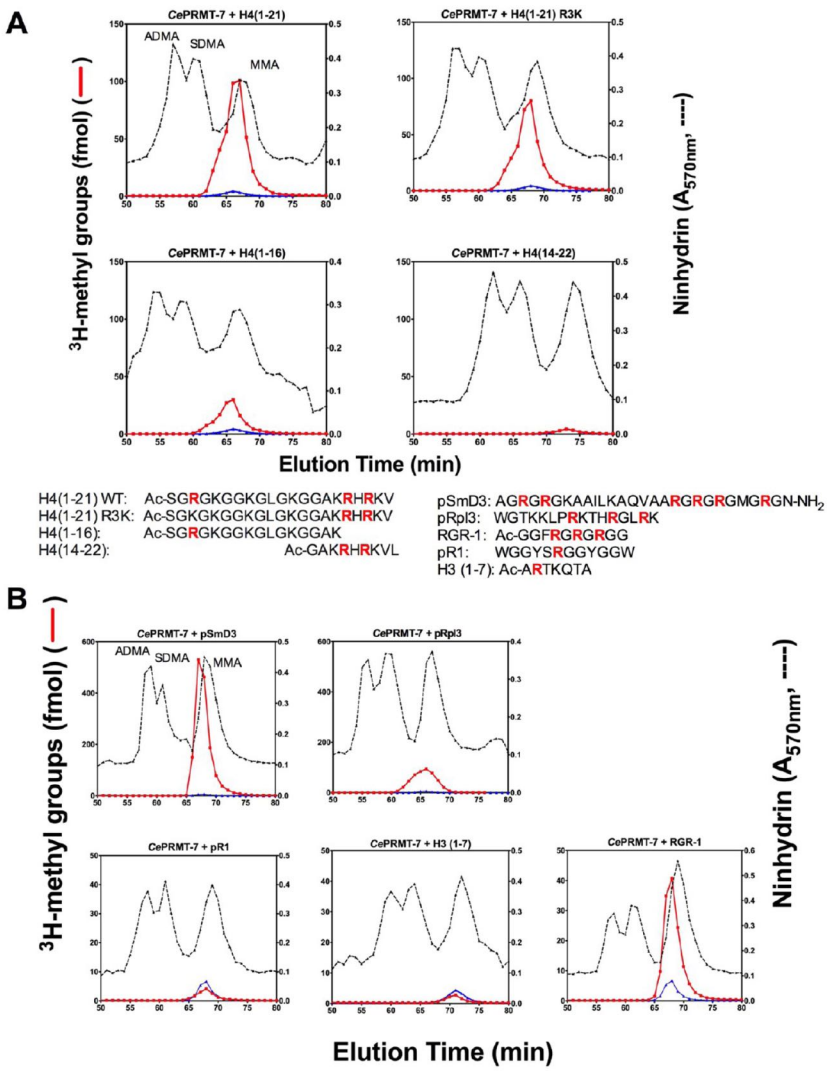

Figure 5. *C. elegans* PRMT-7 has a preference for R-X-R motifs in various peptide substrates. (A) *C. elegans* PRMT-7 (2 μg) was reacted with 12.5 μM various synthetic human histone H4 peptides (1−21 wild type, 1−21 R3K, 1−16 wild type, and 14−22) at 15 °C in 50 mM potassium HEPES and 10 mM NaCl (pH 8.0) with 1 mM DTT for 20 h. Amino acid analysis was performed as described above and in Materials and Methods. Reactions were replicated twice. (B) *C. elegans* PRMT-7 (2 μg) was reacted with various synthetic peptides [pSmD3, pRpl3, pR1, histone H3 (1−7), and RGR-1] at 12.5 μM under the conditions described for panel A. Reactions were single replicates. The reactions in the top panels for pSmD3 and pRpl3 are the same panels used in the right column of Figure 2B.

double E loop and the THW loop. When compared to the human PRMT7, the *C. elegans* protein has an identical DHW sequence in the THW loop as well as an identical double E loop with the exception of the replacement of a single leucine residue with a valine. These results indicate that PRMT7 is evolutionarily conserved with a marked presence in vertebrates, invertebrates, and plants, but not in lower organisms.

***C. elegans* PRMT-7 Produces Monomethylarginine.** When we assayed the *C. elegans* PRMT-7 methyltransferase activity under conditions used in the previous biochemical study[23] (30 °C with an EDTA-containing buffer), we also found no activity (Figure 2A, top left panel). However, when the incubation temperature is decreased to one more favorable for *C. elegans* growth (25 °C), some enzymatic activity producing MMA was seen (Figure 2A, top middle and right panels). When we switched to a buffer containing no metal ion chelator, some activity was seen at 30 °C (Figure 2A, bottom left panel) while much higher activity was seen at 25 °C (Figure 2A, bottom middle and right panel). Previous work had demonstrated the partial loss of activity of the mammalian PRMT7 enzyme with EDTA.[18] A zinc ion is present in a zinc finger motif in the mouse and *C. elegans* PRMT7/PRMT-7 structures located some distance from the active site, suggesting that it may play a role in stabilizing an active conformation of the enzyme.[24,25] Thus, it appears that EDTA may inhibit the activity by extracting this zinc ion. In addition, the *C. elegans* PRMT-7 enzyme activity appears to be dependent on the presence of the reducing agent dithiothreitol (DTT), as was previously observed with the mammalian enzyme.[27] *In vitro* methylation reaction mixtures with two synthetic peptides

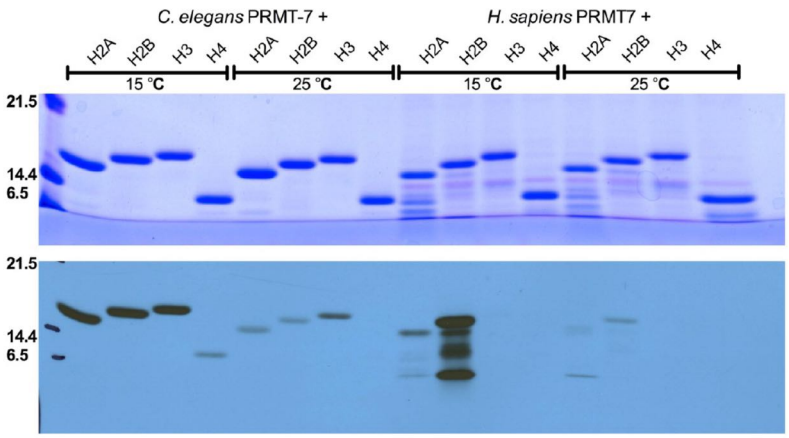

Figure 6. *C. elegans* PRMT-7 has a substrate specificity distinct from that of the mammalian ortholog for mammalian histones. Reaction mixtures consisting of 5 μg of substrate [recombinant human histones from New England BioLabs (H2A, M2502S; H2B, M2505S; H3.3, M2507S; H4, M2504S)] were reacted with 2 μg of *C. elegans* GST-PRMT-7 or human GST-PRMT7 at 15 or 25 °C as described in Materials and Methods. Reactions were stopped by the addition of sample loading buffer and polypeptides separated as described in Materials and Methods. The dried gel was then exposed to autoradiography film for 3 days at −80 °C. Molecular weight positions are shown from approximately 2 μg of unstained SDS−PAGE broad range marker as in Figure 3. The results shown here were replicated three times for *C. elegans* PRMT-7 and two times for human PRMT7. Radiolabeled bands migrating more rapidly than histone H2B in the lane with human PRMT7 appear to be proteolytic fragments.

containing R-X-R and similar sequences (pSmD3 and pRpl3) showed no activity at 25 °C without DTT (Figure 2B, left panels) but showed significant MMA-producing activity when DTT was added to the reaction buffer (Figure 2B, right panels) at 15 °C.

On the basis of reports that the expression level of PRMT7 can affect SDMA levels in mammalian histones,[11,12,15,16,30] we also asked if the active *C. elegans* PRMT-7 enzyme could catalyze dimethylation of arginine species. However, as shown in the expanded view of the amino acid analysis shown in Figure 2A (right panels), we find no dimethylated product consistent with SDMA or ADMA is formed under conditions where 0.4% of the MMA product would have been detected. Thus, *C. elegans* PRMT-7 produces only MMA and is thus a type III enzyme.

***C. elegans* PRMT-7 Is Most Active at or below Optimal Growth Temperatures.** In Figure 2, we noted the enzyme was much more active at 25 °C than at 30 °C. *C. elegans* is able to grow at a variety of temperatures ranging from 12 °C (slowest-growing) to 25 °C (fastest-growing), with most studies performed at 20 °C.[31] Continual incubation at >25 °C leads to sterility.[31,32] We thus performed *in vitro* methylation reactions with *C. elegans* PRMT-7 and GST-GAR over a wider range of temperatures, from 0 to 42 °C (Figure 3). After SDS−PAGE and fluorography, the methylation signal was quantified using densitometry and normalized. Fluorography revealed an activity maximum at 15 °C, with the enzyme still slightly active at the higher end of the physiological temperature range for *C. elegans* (20 and 25 °C). *In vitro* methylation reactions of human PRMT7 were performed as a comparison, and a similar but narrower dependence of activity on temperature is observed (Figure 3). The temperature dependence of the human enzyme observed here with a maximal activity at 15 °C and little or no activity at 37 °C is similar to what was reported previously.[18]

***C. elegans* PRMT-7 Recognizes a Wider Variety of Substrates Than Human PRMT7 Does.** Once reaction conditions were optimized for activity, we tested a variety of protein and peptide substrates to compare the methyl-accepting activity with peptide and protein substrates, including those recognized by human PRMT7. Because both human and mouse PRMT7 were shown to have a strong preference for R-X-R motifs flanked by basic residues in histone H2B peptides,[17,18] we decided to test these peptides with *C. elegans* PRMT-7. Amino acid analysis showed that *C. elegans* PRMT-7 can methylate synthetic human histone H2B peptides containing residues 23−37 (Figure 4A, bottom left panel). To determine whether the *C. elegans* enzyme better recognizes *C. elegans* amino acid sequences than human sequences, we performed the same experiment with the *C. elegans* histone H2B (20−34) peptide. Surprisingly, we found that the *C. elegans* enzyme recognized the human peptide better than the *C. elegans* peptide (Figure 4A, bottom). We compared this activity to that of human PRMT7 with the human peptide and the *C. elegans* peptide (Figure 4A, top panel) and found that the human enzyme did not methylate the *C. elegans* H2B peptide sequence. These results suggest that, at least *in vitro*, histone H2B may not be a major substrate of PRMT-7 in *C. elegans*.

Because *C. elegans* PRMT-7 was able to methylate the human histone H2B peptide, we then tested our collection of single R-to-K mutants of this peptide (Figure 4B). When it was reacted with the wild-type H2B peptide, we see similar results as in Figure 4A, but the removal of a single arginine from the peptide greatly decreased the activity (Figure 4B, bottom panels). The histone H2B R29K peptide reduced methylation counts to a level that was ∼40% of that of the wild-type peptide sequence. The R31K and R33K mutant peptides further decreased the activity to ∼10 and ∼22%, respectively, signifying the importance of arginine residues in a sequential R-X-R motif. Because our data showed that PRMT-7 prefers an R-X-R motif in histone H2B, we tested another synthetic peptide containing an R-X-R sequence, where X is a glycine, a sequence found in many GAR motif proteins. We tested the *C. elegans* and human enzymes with this RGR-1 peptide at 25 and 15 °C and found that the *C. elegans* enzyme weakly methylated this peptide at both temperatures (Figure 4C, top row), while the human

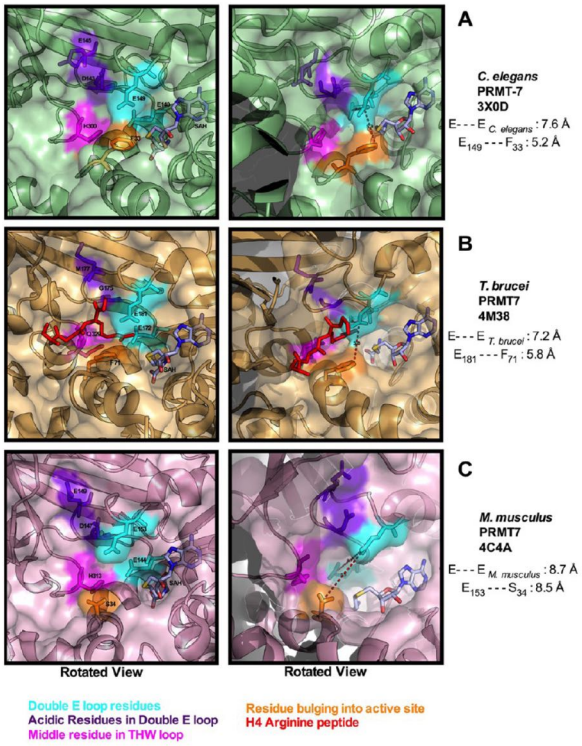

Figure 7. Active site architecture of *C. elegans*, trypanosome, and mammalian PRMT7s. (A) Pymol surface and cartoon representation of the active site of *C. elegans* PRMT-7 (Protein Data Bank entry 3X0D[24]). Flanking glutamate double E loop residues are colored cyan (E140 and E149); internal loop acidic residues are colored purple (D143 and E145), and a THW loop residue is colored magenta (H300). The residue colored orange (F33) protrudes from a helix to form a cavity with E149. The distance from the side chain carboxyl carbon of E140 to the side chain carboxyl carbon of E149 is 7.6 Å, and the distance from the side chain carboxyl carbon of E149 to the closest side chain carbon atom in F33 is 5.2 Å. *S*-Adenosylhomocysteine (SAH) is shown in CPK coloring. (B) Pymol surface and cartoon representation of the active site of *T. brucei* PRMT7 (Protein Data Bank entry 4M38[20]), highlighting residues corresponding to those shown in panel A. Flanking double E loop residues E172 and E181 are colored cyan; G175 and M177 (residues corresponding to D143 and E145, respectively, in *C. elegans*) are colored purple, and the Q329 THW loop residue is colored magenta. The residue colored orange (F71) corresponds to F33 in the *C. elegans* structure and also protrudes from a helix to form a cavity with E181. The distances between the flanking double E residues and E181 and F71 are given as in panel A. The arginine 3 residue of the cocrystallized histone H4 peptide is colored red. (C) Pymol surface and cartoon representation of the active site of *M. musculus* PRMT7 (Protein Data Bank entry 4C4A[25]), highlighting residues corresponding to those shown in panels A and B. The distances between the flanking double E residues and E153 and S34 are given as in panels A and B. We note that the S34 side chain oxygen is shown in two conformations.

PRMT7 enzyme showed much less activity (Figure 4C, bottom row), indicating a slightly broader specificity for the *C. elegans* enzyme.

Once we saw the differences in substrate specificity of the *C. elegans* PRMT-7 enzyme when compared to that of the previously characterized human enzyme, we tested it against another panel of synthetic peptides with various sequences containing pairs of arginine residues in R-X-R motifs as well as single-arginine sequences. Upon incubation with synthetic histone H4 peptides (1−21 wild type, 1−21 R3K, 1−16, and 14−22), we saw greatly reduced activity when the R-X-R sequence at the C-terminus of the peptide was removed (Figure 5A). This peptide contained the sequence of the *C. elegans* histone, one identical to that of the human peptide. The histone H4 (1−21) R3K peptide gave just a slight decrease in methylation activity [20% decrease (Figure 5A, top right panel)], but removal of the last five residues in the peptide of residues 1−16 caused an almost 70% decrease in activity (Figure 5A, bottom left panel). This signified that the PRMT-7 enzyme primarily methylates the R-X-R sequence but could also recognize and methylate a single arginine. Reacting the enzyme with a small peptide containing only the R-X-R sequence of H4 (14−22) yielded almost no activity, indicating there might be a secondary site of contact and binding for the peptide to be correctly situated in the active site (Figure 5A, bottom right panel).

Other peptides containing R-G-R and peptides containing a single arginine residue were reacted with the *C. elegans* enzyme (Figure 5B). In a longer peptide sequence containing two pairs of R-G-R sequences [pSmD3 (Figure 5B, top left panel)], we saw very high methylation activity. In a reaction mixture with pRpl3 peptide (Figure 5B, top middle panel) that contains three more widely spaced arginine residues, we see an activity that is almost double that of that seen with the RGR-1 peptide (Figure 5B, bottom right panel). *C. elegans* PRMT-7 was not able to methylate smaller peptides, such as pR1 (containing only one R flanked by G) or a peptide containing the first seven residues from histone H3 (Figure 5B, bottom panels).

We then tested full-length histones as substrates of both the human and *C. elegans* PRMT7 enzymes. We methylated recombinant human histone proteins at either 15 or 25 °C and separated the polypeptides via SDS−PAGE. At both temperatures, we found that the *C. elegans* PRMT-7 enzyme was active in methylating histones H2A, H2B, and H3, but only weakly methylated H4 (Figure 6). This was a surprising result because the enzyme could methylate H4 peptides (Figure 5A). We note that the sequence of histone H4 in humans and *C. elegans* is identical with the exception of one residue in the central domain. Human PRMT7, on the other hand, was very specific for histone H2B as noted previously,[17] indicating a distinct difference in substrate specificity between the two enzymes.

Crystal Structures of PRMT7 Orthologs Unveil a Distinct Pocket in the Active Site Potentially Contributing to Substrate Specificity. Although the characterized mammalian, trypanosome, and *C. elegans* PRMT7 homologues all produce MMA, there are significant differences in their substrate specificity (this study and refs 18 and 22). We therefore examined the active site architecture of the available PRMT7 crystal structures of each of these enzymes. The substrate arginine residue is generally bound between the two glutamate residues in the double E loop.[3,4,22] The distance between the side chain carboxyls of the two glutamates in the double E loop is relatively similar in the *C. elegans* and *T. brucei* enzymes (7.6 and 7.2 Å, respectively), compared to a larger distance (8.7 Å) in the *M. musculus* enzyme (Figure 7). In addition, in PRMT7 from *C. elegans* and *T. brucei*, there is a phenylalanine residue that protrudes into the active site (F33 and F71) and may limit the size of a methyl-accepting sequence. The distance between the side chain carboxyl carbon

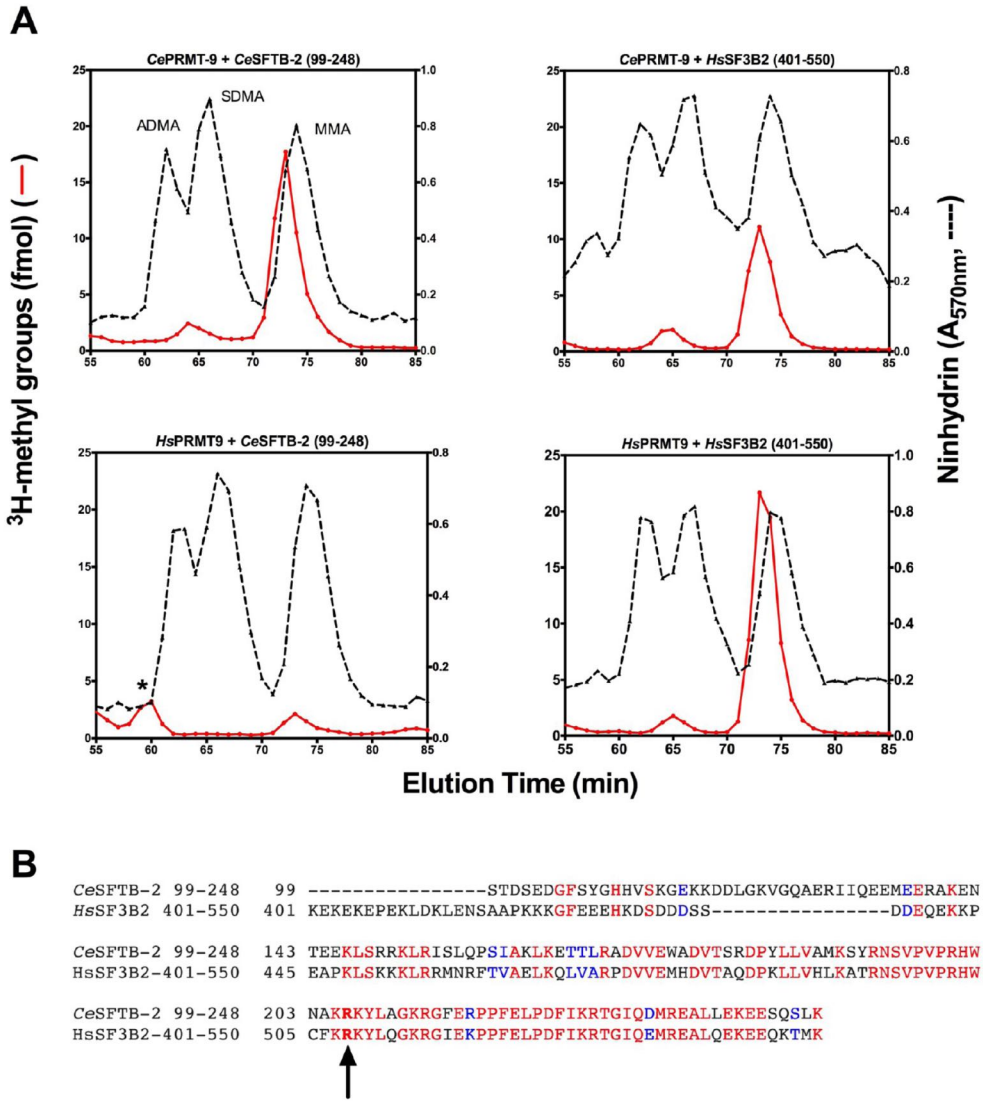

Figure 8. *C. elegans* PRMT-9 symmetrically dimethylates SFTB-2, the *C. elegans* ortholog of the mammalian SF3B2. (A) Amino acid analysis was performed as described in the legend of Figure 2 on methylation reaction mixtures consisting of 5 μg of substrate (*C. elegans* GST-tagged SFTB-2 fragment 99−248 or *H. sapiens* GST-tagged SF3B2 fragment 401−550) and approximately 2 μg of enzyme (*C. elegans* GST-tagged PRMT-9 enzyme or *H. sapiens* GST-tagged PRMT9 enzyme) that were incubated for 20 h at 25 °C (nematode enzyme) or 37 °C (human enzyme) in a reaction buffer consisting of 50 mM potassium HEPES and 10 mM NaCl (pH 8.2) with a final concentration of 0.7 μM [*methyl*-^{3}H]AdoMet in a volume of 60 μL. The reactions were quenched by the addition of a final trichloroacetic acid concentration of 12.5% and mixtures acid-hydrolyzed as described in Materials and Methods. The asterisk indicates a radioactive peak eluting prior to the expected position of ^{3}H-ADMA. The experiment was replicated twice. (B) Sequence alignment of *C. elegans* SFTB-2 (UniProt entry O16997) residues 99−248 and human SF3B2 (UniProt entry Q13435, bottom). Red letters indicate identity, and blue letters indicate similar amino acid properties. The bolded R and black arrow indicate the methylation site for the enzyme.

of the second glutamate residue of the double E loop and the closest side chain carbon of the phenylalanine residue is 5.2 and 5.8 Å in *C. elegans* and *T. brucei*, respectively (Figure 7A,B). However, the corresponding residue in *M. musculus* PRMT7 is a serine residue whose β-carbon is much farther (8.5 Å) from the glutamate residue (Figure 7C), potentially creating a pocket that could accommodate arginine residues flanked by residues with bulkier side chains such as lysine residues. We also note that the two acidic residues in the interior of the double E loop (colored purple in Figure 7) are more exposed to the surface in *M. musculus* (Figure 7C) than the corresponding residues in the *C. elegans* or *T. brucei* enzymes. These results provide insight into the broader substrate specificity of the non-mammalian PRMTs.

The *C. elegans* PRMT-9 Enzyme Methylates RNA Splicing Factor SFTB-2/SF3B2 and Forms SDMA. We previously showed a phylogenetic tree demonstrating a *C. elegans* ortholog of PRMT9 present in higher organisms;[26] this ortholog was originally named PRMT-3 but is now designated PRMT-9.[1,23,26] In addition, *C. elegans* also contains an ortholog

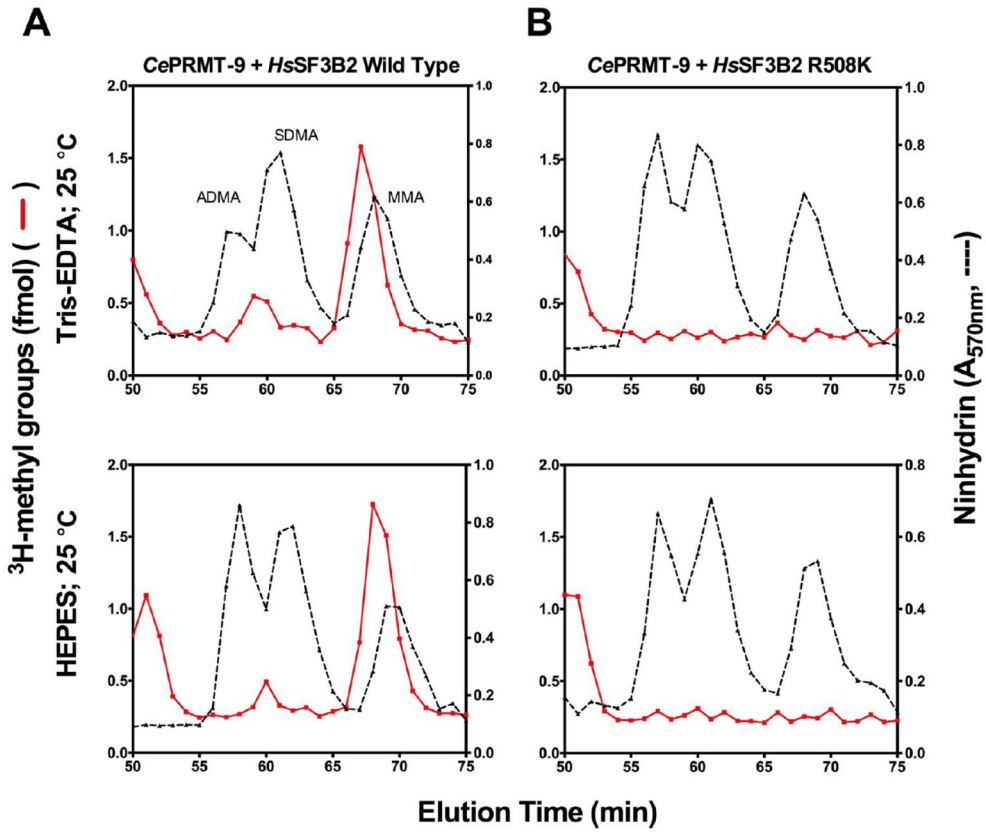

Figure 9. *C. elegans* PRMT-9 methylates SF3B2 at the same R508 site that is methylated by the mammalian PRMT9 enzyme. (A) Amino acid analysis of a methylation reaction mixture consisting of 2 μg of *C. elegans* GST-PRMT-9 enzyme with 5 μg of human GST-SF3B2 (401−550) wild type at 25 °C for 20 h in either 100 mM Tris-EDTA buffer (pH 8.0) (top) or 50 mM potassium HEPES and 10 mM NaCl (pH 8.2) (bottom). Reactions were quenched by the addition of a final trichloroacetic acid concentration of 12.5% and mixtures acid-hydrolyzed as described above. Reactions were duplicated twice. (B) Methylation reactions of *C. elegans* PRMT-9 reacted with the human GST-SF3B2 (401−550) R508K mutant fragment, under the same reaction conditions described for panel A at 25 °C for 20 h. Reactions were duplicated twice.

of mammalian splicing factor SF3B2, now designated SFTB-2. SF3B2 is the only identified substrate of mammalian PRMT9.[5,26] To determine if *C. elegans* PRMT-9 plays a similar physiological role by methylating SFTB-2, we analyzed the products of both human and *C. elegans* PRMT-9 enzymes with the methylatable fragment F3 of both splicing factors, corresponding to human residues 401−550 and *C. elegans* residues 99−248 (Figure 8A). When the *C. elegans* enzyme was incubated with the *C. elegans* SFTB-2 and mammalian SF3B2 fragments, we detected both MMA and SDMA formation (Figure 8A, top panels). In a control experiment, we also detected MMA and SDMA formation with the human enzyme and substrate (Figure 8A, bottom right panel). However, when we reacted the human enzyme with the *C. elegans* SFTB-2 polypeptide, we found only a small MMA peak; no SDMA was detected (Figure 8A, bottom left panel). SF3B2 and SFTB-2 are similar in sequence in the conserved region surrounding the R508 methylation site in the human protein[5,26] but diverge in the N-terminal region (Figure 8B).

To ask if the *C. elegans* enzyme was specific for the same site, we reacted *C. elegans* PRMT-9 with the wild type and R508K mutant of the human SF3B2 fragment (Figure 9). We observed that methylation was abolished in the fragment with the R508K mutation (Figure 10B, top and bottom right panels), as compared to the case for the wild-type SF3B2 fragment (Figure 10A, top and bottom left panels), suggesting that the mammalian and *C. elegans* enzymes share the same strict specificity for this arginine residue in the splicing factor.

C. elegans PRMT-9 Does Not Recognize Non-SFTB-2/SF3B2 Substrates. Because most PRMTs recognize a variety of substrates, we tested multiple known substrates with the *C. elegans* enzyme, including GST-GAR, RNA binding protein Rbp16, and recombinant histones H2A and H2B (Figure 10). Amino acid analysis of reactions using the same conditions as described by Takahashi et al.,[23] the first study to detect MMA activity with this PRMT-9 enzyme, showed that it did not appreciably methylate these substrates (Figure 10A, top right panel). We did, however, observe a very low MMA activity upon the methylation of recombinant histone H2A, consistent with the previous result.[23] We also analyzed these reaction mixtures, along with corresponding mixtures with the human PRMT9 enzyme, using SDS−PAGE fluorography, and observed that both PRMT9 enzymes methylated only their corresponding SF3B2 substrate fragments (Figure 10B).

Temperature Dependence of _C. elegans_ PRMT-9. We next compared the activity at various temperatures of both the human and nematode PRMT9 enzymes with the human SF3B2 substrate using SDS−PAGE fluorographic analysis (Figure 11).

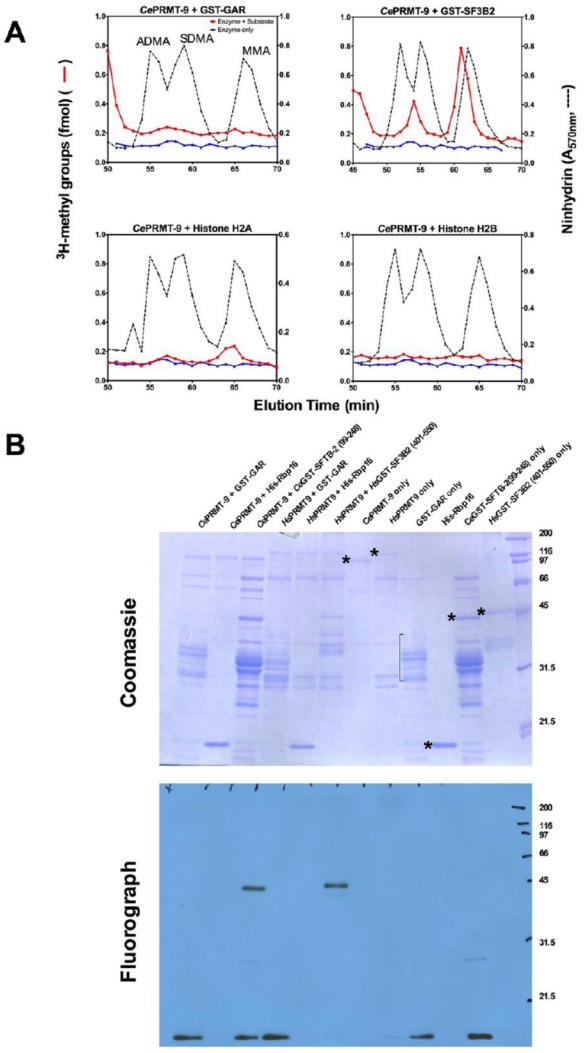

Figure 10. Substrate specificity of *C. elegans* PRMT-9. (A) Methylation reactions for amino acid analysis were set up using 2 μg of *C. elegans* PRMT-9 with 5 μg of various substrates [GST-GAR, top left; GST-SF3B2 (401−550), top right; recombinant human histone H2A, bottom left; recombinant human histone H2B, bottom right], in 100 mM Tris-EDTA buffer (pH 8.0) for 6 h at 30 °C, under conditions defined by Takahashi et al.[23] These reactions using these conditions were single replicates. (B) *In vitro* methylation reaction mixtures consisting of 2 μg of *C. elegans* PRMT-9 or human PRMT9 enzyme were reacted with 5 μg of substrate [GST-GAR, His-Rbp16, or GST-SFTB-2 (*C. elegans* fragment 99−248) or GST-SF3B2 (human fragment 401−550)] for 20 h at 25 °C (*C. elegans*) or 37 °C (human) in 50 mM potassium HEPES, 10 mM NaCl, and 1 mM DTT (pH 8.2) with 0.7 μM [*methyl*-^{3}H]AdoMet. Sample loading buffer was added to stop the reactions, and polypeptides were separated using SDS−PAGE, using the same methods described in the legend of Figure 3. The gel was then dried and exposed to film for 7 days at −80 °C. The Coomassie-stained gel is shown in the top panel, and the fluorographic exposure is shown in the bottom panel. The molecular weight standards are shown as described in the legend of Figure 3. This experiment was replicated independently using amino acid analysis.

We found that the *C. elegans* enzyme is active at the physiological growing temperatures for the nematode,[31] while the human enzyme is most active at the body's expected physiological temperature of 37 °C.[26] These PRMT9 enzymes are active over a range of temperatures wider than that of the PRMT7 enzymes analyzed in Figure 3.

THW Loop Residues Are Responsible for the SDMA Forming Ability of *C. elegans* PRMT-9. The central residue in the conserved THW loop has been shown to play a role in the formation of MMA and SDMA in *T. brucei* PRMT7 and in human PRMT9.[23] Specifically, mutating the central cysteine residue in the human PRMT9 THW motif to histidine greatly enhanced the ability of the enzyme to form MMA and weakened its ability to form SDMA.[22] Making the same mutation in the *C. elegans* PRMT-9 enzyme, converting the alanine residue in the central position of the THW loop to a histidine residue, resulted in the loss of SDMA formation and reduced the extent of MMA formation (Figure 12). The inverse H300A mutation made in the *C. elegans* PRMT-7 enzyme resulted in the loss of activity (data not shown). Interestingly, additional DTT added to the reaction mixtures, for the wild-type and A391H mutant enzymes (blue line in all panels), enhanced the formation of MMA but did not affect the formation of SDMA (Figure 12).

■ DISCUSSION

While many different physiological roles have been described for PRMT7,[10−16,30] endogenous *in vivo* substrates have yet to be identified. PRMT7 is widely distributed across vertebrates, invertebrates, and plants. Fungi such as *Saccharomyces cerevisiae* and *Endocarpon pusillum* do not contain a PRMT7 ortholog, as their top BLAST hits match well with the major PRMT1 ortholog (Figure 1). Other studies have not found corresponding orthologs in *S. cerevisiae* or *Schizosaccharomyces pombe*.[1] What was most surprising is our identification of potential bacterial PRMT7 orthologs from *R. leguminosarum* and *G. sulfurreducens* that were mutual best hits to human PRMT7. Methylation of arginine residues has never been observed in bacteria, and no PRMT genes have been previously reported in bacteria. These prospective bacterial orthologs lack an apparent THW loop and do not contain the ancestrally duplicated C-terminal domain, much like the *T. brucei* ortholog of PRMT7. *G. sulfurreducens* does contain the characteristic TPR motifs of human PRMT9, yet the closest human hit when analyzed with protein BLAST is PRMT7. Further work needs to be done to confirm if these potential enzymes actually methylate arginine residues. Presumably, the retention of PRMT7 in higher organisms reflects its specific cellular roles, including the limitation of its activity to monomethylation, its substrate specificity, and its potential for regulation and crosstalk with other modifying enzymes.

Optimizing reaction conditions for the *C. elegans* PRMT-7 enzyme, such as lowering the reaction temperature, removing metal ion chelators, and adding reducing agents such as DTT, proved to be essential for determining its substrate preference and methylation activity. While the optimal temperature for the activity of *C. elegans* PRMT-7 falls clearly in the physiological range of this organism, the human PRMT7 enzyme also demonstrates a similar temperature preference range where it is much more active than it is at 37 °C. This is an unusual property for a human enzyme and may be important for its activity in regions of localized hypothermia such as in lung tissue exposed to cold air or in the extremities. It would be interesting to correlate the function of PRMT7 with the expression of cold-inducible RNA binding proteins CIRP and

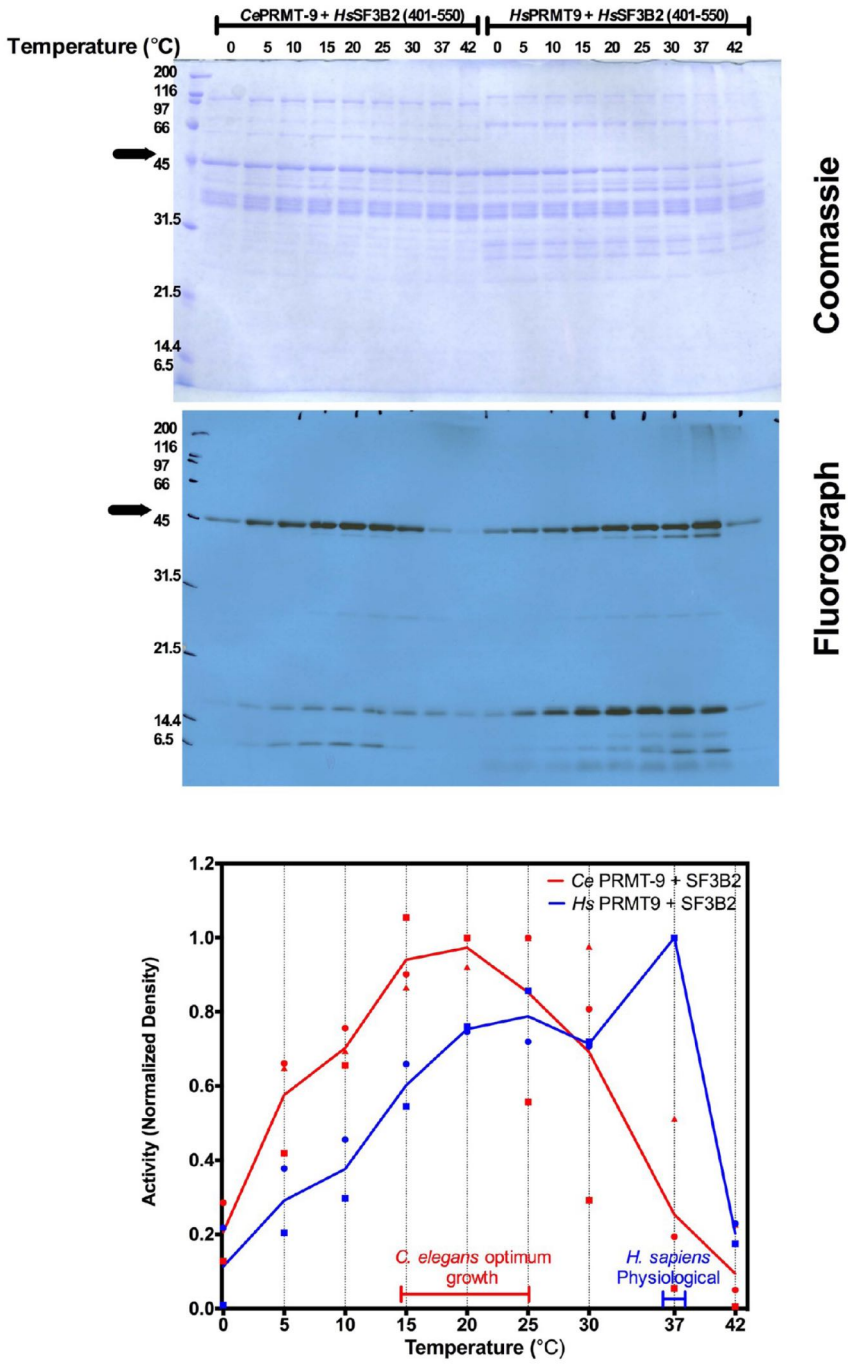

Figure 11. Temperature dependence of *C. elegans* PRMT-9. Methylation reaction mixtures consisting of 5 μg of substrate (*H. sapiens* GST-tagged SF3B2 fragment 401−550) were reacted with 2 μg of enzyme (both *C. elegans* and *H. sapiens* PRMT9 enzymes) at the various temperatures indicated for 20 h in 50 mM potassium HEPES and 10 mM NaCl (pH 8.2) with 0.7 μM [*methyl*-^{3}H]AdoMet in a final reaction volume of 60 μL. Reactions were quenched by the addition of sample loading buffer, and proteins were separated using SDS−PAGE using the same methods described in the legend of Figure 3. The gel was dried and exposed to autoradiography film for 21 days at −80 °C. A Coomassie gel (top) and fluorograph (bottom) are shown. Molecular weight positions are shown from approximately 2 μg of unstained SDS−PAGE broad range marker as described in the legend of Figure 3. This experiment was replicated independently, and a third replicate using the *C. elegans* PRMT-9 enzyme was performed. The bottom panel indicates the densitometry of the bands comparing the methylation activity of the *C. elegans* enzyme to that of the human enzyme. Densitometry was performed using ImageJ on the scanned images of the films and quantified as described in the legend of Figure 3 (*C. elegans*, red symbols; human, blue symbols). A solid line is drawn for the average of the normalized values of the replicates. The optimal growth temperatures for *C. elegans*[31] and humans are indicated.

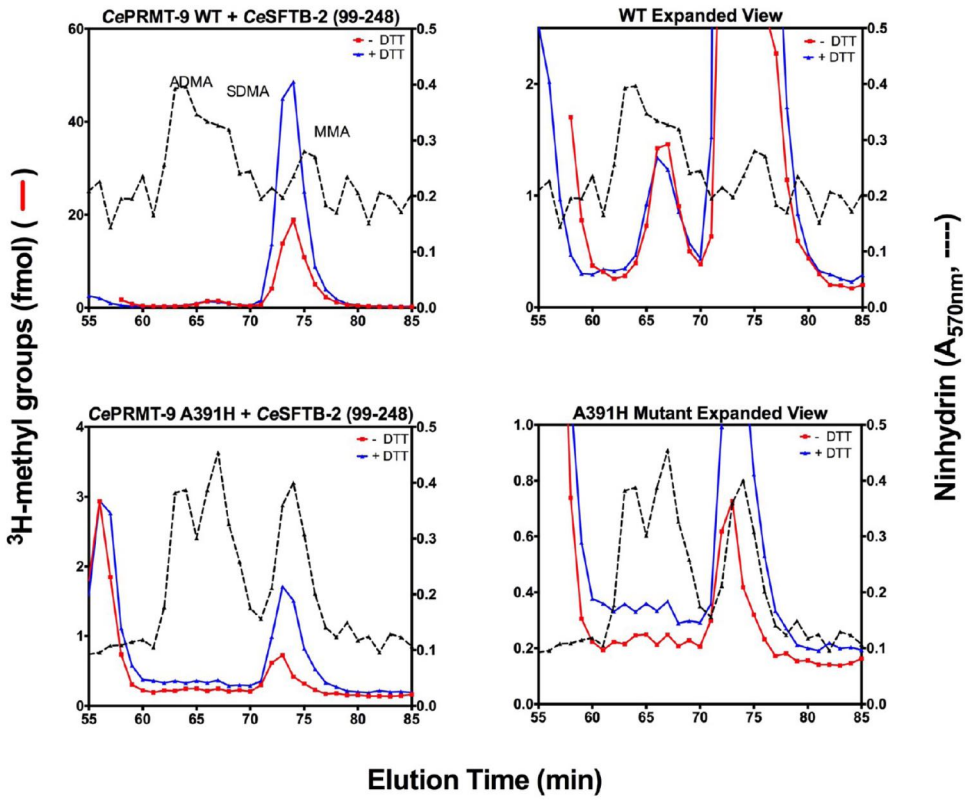

Figure 12. *C. elegans* PRMT-9 THW loop residues are important for conferring SDMA specificity and a small DTT effect. (A) *C. elegans* PRMT-9 enzyme (2 μg) wild type (top) or THW loop mutant A391H (bottom) was reacted with approximately 5 μg of *C. elegans* SFTB-2 for 20 h at 25 °C in the reaction buffer containing 50 mM potassium HEPES and 10 mM NaCl (pH 8.0) with (blue line) or without (red line) 1 mM DTT, as indicated. Mutation of THW loop residue A391 to the conserved histidine residue abolishes the SDMA activity, producing only MMA, consistent with previous work with the human enzyme PRMT9 C431H mutant.[22] These reactions were single replicates.

RBM3, both of which are known to be methylated at arginine residues.[33] Alternatively, the small amount of activity of human PRMT7 at 37 °C may be sufficient for its function, or there may be other proteins or small molecules present in human cells that allow for enhanced activity at normal body temperature.

We show here that *C. elegans* PRMT-7 methylates human histone H2B peptides, prime *in vitro* substrates for the human PRMT7 enzyme, but less methylation of the corresponding *C. elegans* H2B peptide was seen (Figure 4A). This result suggests that histone H2B may not be a major physiological substrate for *C. elegans* PRMT-7. It has been shown in proteomic studies that there is divergence in conservation of methylation sites across various organisms,[34] indicating the methylation sites can differ across different species and organisms.

Our results also indicate the importance of multiple arginine residues in an R-X-R motif for recognition by both *C. elegans* PRMT-7 and human PRMT7. However, the *C. elegans* enzyme does not appear to have a strong preference for adjacent basic residues and methylated substrates with adjacent glycine residues such as pSmD3. Peptides with single arginine residues were generally not substrates, but a histone H4 1−16 peptide containing a single arginine residue was weakly methylated by *C. elegans* PRMT-7. It appears that the length of the peptide, the positioning of arginine residues, and the nature of adjacent and distant residues play a role in substrate specificity.

Comparison of the activity of the human and *C. elegans* PRMT7s on intact human recombinant histones confirms the specificity of the human enzyme for H2B.[17] However, we observe here that *C. elegans* PRMT-7 methylates all of the histone proteins, with the exception of only weakly methylating histone H4 (Figure 6). This broader substrate methylation leads us to believe that its physiological substrates, while not identified yet, could potentially be different from and more numerous than those of its mammalian ortholog.

To further probe the substrate specificity of these enzymes, we examined the active site architectures of *C. elegans*,[24] *T. brucei*,[20] and *M. musculus* PRMT7.[25] Surface modeling of their crystal structures reveals differences that may relate to their activities. As discussed in Results, the distances between the two terminal glutamates in the double E loop were closer together in the *C. elegans* and *T. brucei* structures than in the mouse structure. In addition, there are differences in residues, in particular a phenylalanine (*C. elegans* or *T. brucei*) or serine (mouse) residue that comes in contact with the second glutamate of the double E loop. These structural differences may explain why we see such distinct substrate specificity among the various orthologs of PRMT7, indicating that the enzyme may have evolved to have different functions and substrates among different organisms. Further work needs to be done to confirm the importance of these residues in conferring substrate specificity.

C. elegans also has a PRMT-9 ortholog that has been conserved from invertebrates to mammals with a potentially similar physiological function. We show here that the *C. elegans* PRMT-9 enzyme produces SDMA and MMA on the splicing factor SF3B2 ortholog in *C. elegans*, SFTB-2. Additionally, we found that the enzyme methylates the same R508 residue on SF3B2 as the human enzyme, suggesting that PRMT-9 may also play a regulatory role in nematode alternative RNA splicing. It will now be important to directly examine the effect of methylation of SFTB-2 on the regulation of splicing in *C. elegans*, a process that has been shown to be similar to human splicing mechanisms.[35]

■ ASSOCIATED CONTENT

Supporting Information

The Supporting Information is available free of charge on the ACS Publications website at DOI: 10.1021/acs.biochem.7b00283.

Peptide sequences used in the text (Table S1) (PDF)

Accession Codes

C. elegans PRMT-7 (UniProt entry Q9XW42), *C. elegans* PRMT-9 (UniProt entry O02325), human PRMT7 (UniProt entry Q9NVM4), human PRMT9 (UniProt entry Q6P2P2), *C. elegans* SFTB-2 (UniProt entry O16997), human SF3B2 (UniProt entry Q13435), and amino acids 1−145 of human fibrillarin (UniProt entry P22087).

■ AUTHOR INFORMATION

Corresponding Author

*Department of Chemistry and Biochemistry and Molecular Biology Institute, University of California, Los Angeles, 607 Charles E. Young Dr. E., Los Angeles, CA 90095-1569. Telephone: 310-825-8754. E-mail: clarke@mbi.ucla.edu.

ORCID

Andrea Hadjikyriacou: 0000-0002-3420-367X

Steven G. Clarke: 0000-0002-7303-6632

Author Contributions

A.H. and S.G.C. conceived the project and wrote the manuscript. A.H. performed the experiments.

Funding

This work was supported, in whole or in part, by National Institutes of Health Grants GM026020 (to S.G.C.) and GM007185, a Ruth L. Kirschstein National Research Service Award (to A.H.), funds from the Elizabeth and Thomas Plott Chair in Gerontology of the UCLA Longevity Center (to S.G.C.), funds from a UCLA Dissertation Year Fellowship (to A.H.), and a UCLA Faculty Research Award (to S.G.C.).

Notes

The authors declare no competing financial interest.

■ ACKNOWLEDGMENTS

The authors thank Alexander Patananan (University of California, Los Angeles) for his advice on *C. elegans* biology and Akiyoshi Fukamizu (University of Tsukuba, Tsukuba, Japan) for providing the cDNA clones of *C. elegans* GST-PRMT-7 and GST-PRMT-9. The authors also thank Adam Frankel (University of British Columbia, Vancouver, BC) for the R1 peptide and Mark T. Bedford (M. D. Anderson Cancer Center, Houston, TX) for the GST-SF3B2 plasmid. The authors also thank members of the Clarke laboratory, in particular Jonathan Lowenson, Kanishk Jain, and Rebeccah Warmack, for useful comments on the manuscript.

■ ABBREVIATIONS

PRMT, protein arginine methyltransferase; MMA, ω-N^G-monomethylarginine; ADMA, ω-N^G,N^G-asymmetric dimethylarginine; SDMA, ω-N^G,N'^G-symmetric dimethylarginine; AdoMet, *S*-adenosyl-L-methionine; [*methyl*-^{3}H]AdoMet, *S*-adenosyl[*methyl*-^{3}H]-L-methionine; GAR, glycine- and arginine-rich domain of human fibrillarin.

■ REFERENCES

(1) Wang, Y., Wang, J., Chen, C., Chen, Y., and Li, C. (2015) A novel BLAST-Based Relative Distance (BBRD) method can effectively group members of protein arginine methyltransferases and suggest their evolutionary relationship. *Mol. Phylogenet. Evol. 84*, 101−111.

(2) Wang, Y. C., and Li, C. (2012) Evolutionarily conserved protein arginine methyltransferases in non-mammalian animal systems. *FEBS J. 279*, 932−945.

(3) Fuhrmann, J., Clancy, K. W., and Thompson, P. R. (2015) Chemical biology of protein arginine modifications in epigenetic regulation. *Chem. Rev. 115*, 5413−5461.

(4) Bedford, M. T., and Clarke, S. G. (2009) Protein arginine methylation in mammals: Who, what, and why. *Mol. Cell 33*, 1−13.

(5) Yang, Y., Hadjikyriacou, A., Xia, Z., Gayatri, S., Kim, D., Zurita-Lopez, C., Kelly, R., Guo, A., Li, W., Clarke, S. G., and Bedford, M. T. (2015) PRMT9 is a Type II methyltransferase that methylates the splicing factor SAP145. *Nat. Commun. 6*, 6428.

(6) Auclair, Y., and Richard, S. (2013) The role of arginine methylation in the DNA damage response. *DNA Repair 12*, 459−465.

(7) Yang, Y., and Bedford, M. T. (2013) Protein arginine methyltransferases and cancer. *Nat. Rev. Cancer 13*, 37−50.

(8) Baldwin, R. M., Morettin, A., and Côté, J. (2014) Role of PRMTs in cancer: Could minor isoforms be leaving a mark? *World Journal of Biological Chemistry 5*, 115−29.

(9) Likhite, N., Jackson, C. A., Liang, M., Krzyzanowski, M. C., Lei, P., Wood, J. F., Birkaya, B., Michaels, K. L., Andreadis, S. T., Clark, S. D., Yu, M. C., and Ferkey, D. M. (2015) The protein arginine methyltransferase PRMT5 promotes D2-like dopamine receptor signaling. *Sci. Signaling 8*, ra115.

(10) Blanc, R. S., Vogel, G., Chen, T., Crist, C., and Richard, S. (2016) PRMT7 preserves satellite cell regenerative capacity. *Cell Rep. 14*, 1528−1539.

(11) Ying, Z., Mei, M., Zhang, P., Liu, C., He, H., Gao, F., and Bao, S. (2015) Histone arginine methylation by PRMT7 controls germinal center formation via regulating Bcl6 transcription. *J. Immunol. 195*, 1538−47.

(12) Yao, R., Jiang, H., Ma, Y., Wang, L., Wang, L., Du, J., Hou, P., Gao, Y., Zhao, L., Wang, G., Zhang, Y., Liu, D. X., Huang, B., and Lu, J. (2014) PRMT7 induces epithelial-to-mesenchymal transition and promotes metastasis in breast cancer. *Cancer Res. 74*, 5656−5667.

(13) Kernohan, K. D., McBride, A., Xi, Y., Martin, N., Schwartzentruber, J., Dyment, D. A., Majewski, J., Blaser, S., Care4Rare Canada Consortium, Boycott, K. M., and Chitayat, D. (2017) Loss of the arginine methyltranserase PRMT7 causes syndromic intellectual disability with microcephaly and brachydactyly. *Clin. Genet. 91*, 708−716.

(14) Baldwin, R. M., Haghandish, N., Daneshmand, M., Amin, S., Paris, G., Falls, T. J., Bell, J. C., Islam, S., and Côté, J. (2015) Protein arginine methyltransferase 7 promotes breast cancer cell invasion through the induction of MMP9 expression. *Oncotarget 6*, 3013−3032.

(15) Karkhanis, V., Wang, L., Tae, S., Hu, Y. J., Imbalzano, A. N., and Sif, S. (2012) Protein arginine methyltransferase 7 regulates cellular response to DNA damage by methylating promoter histones H2A and H4 of the polymerase δ catalytic subunit gene, POLD1. *J. Biol. Chem. 287*, 29801−29814.

(16) Dhar, S. S., Lee, S. H., Kan, P. Y., Voigt, P., Ma, L., Shi, X., Reinberg, D., and Lee, M. G. (2012) Trans-tail regulation of MLL4-

catalyzed H3K4 methylation by H4R3 symmetric dimethylation is mediated by a tandem PHD of MLL4. *Genes Dev. 26*, 2749−2762.
(17) Feng, Y., Maity, R., Whitelegge, J. P., Hadjikyriacou, A., Li, Z., Zurita-Lopez, C., Al-Hadid, Q., Clark, A. T., Bedford, M. T., Masson, J. Y., and Clarke, S. G. (2013) Mammalian protein arginine methyltransferase 7 (PRMT7) specifically targets RXR sites in lysine- and arginine-rich regions. *J. Biol. Chem. 288*, 37010−37025.
(18) Feng, Y., Hadjikyriacou, A., and Clarke, S. G. (2014) Substrate specificity of human protein arginine methyltransferase 7 (PRMT7) - The importance of acidic residues in the double E loop. *J. Biol. Chem. 289*, 32604−32616.
(19) Fisk, J. C., Sayegh, J., Zurita-Lopez, C., Menon, S., Presnyak, V., Clarke, S. G., and Read, L. K. (2009) A type III protein arginine methyltransferase from the protozoan parasite *Trypanosoma brucei*. *J. Biol. Chem. 284*, 11590−11600.
(20) Wang, C., Zhu, Y., Caceres, T. B., Liu, L., Peng, J., Wang, J., Chen, J., Chen, X., Zhang, Z., Zuo, X., Gong, Q., Teng, M., Hevel, J. M., Wu, J., and Shi, Y. (2014) Structural determinants for the strict monomethylation activity by *Trypanosoma brucei* protein arginine methyltransferase 7. *Structure 22*, 756−768.
(21) Debler, E. W., Jain, K., Warmack, R. A., Feng, Y., Clarke, S. G., Blobel, G., and Stavropoulos, P. (2016) A glutamate/aspartate switch controls product specificity in a protein arginine methyltransferase. *Proc. Natl. Acad. Sci. U. S. A. 113*, 2068−2073.
(22) Jain, K., Warmack, R. A., Debler, E. W., Hadjikyriacou, A., Stavropoulos, P., and Clarke, S. G. (2016) Protein arginine methyltransferase product specificity is mediated by distinct active-site architectures. *J. Biol. Chem. 291*, 18299−18308.
(23) Takahashi, Y., Daitoku, H., Yokoyama, A., Nakayama, K., Kim, J.-D., and Fukamizu, A. (2011) The *C. elegans* PRMT-3 possesses a type III protein arginine methyltransferase activity. *J. Recept. Signal Transduction Res. 31*, 168−172.
(24) Hasegawa, M., Toma-Fukai, S., Kim, J. D., Fukamizu, A., and Shimizu, T. (2014) Protein arginine methyltransferase 7 has a novel homodimer-like structure formed by tandem repeats. *FEBS Lett. 588*, 1942−1948.
(25) Cura, V., Troffer-Charlier, N., Wurtz, J.-M., Bonnefond, L., and Cavarelli, J. (2014) Structural insight into arginine methylation by the mouse protein arginine methyltransferase 7: a zinc finger freezes the mimic of the dimeric state into a single active site. *Acta Crystallogr., Sect. D: Biol. Crystallogr. 70*, 2401−2412.
(26) Hadjikyriacou, A., Yang, Y., Espejo, A., Bedford, M. T., and Clarke, S. G. (2015) Unique features of human protein arginine methyltransferase 9 (PRMT9) and its substrate RNA splicing factor SF3B2. *J. Biol. Chem. 290*, 16723−16743.
(27) Zurita-Lopez, C. I., Sandberg, T., Kelly, R., and Clarke, S. G. (2012) Human protein arginine methyltransferase 7 (PRMT7) is a type III enzyme forming ω-N^G-monomethylated arginine residues. *J. Biol. Chem. 287*, 7859−7870.
(28) Tang, J., Gary, J. D., Clarke, S., and Herschman, H. R. (1998) PRMT 3, a type I protein arginine *N*-methyltransferase that differs from PRMT1 in its oligomerization, subcellular localization, substrate specificity, and regulation. *J. Biol. Chem. 273*, 16935−16945.
(29) McWilliam, H., Li, W., Uludag, M., Squizzato, S., Park, Y. M., Buso, N., Cowley, A. P., and Lopez, R. (2013) Analysis tool web services from the EMBL-EBI. *Nucleic Acids Res. 41*, W597−W600.
(30) Jelinic, P., Stehle, J. C., and Shaw, P. (2006) The testis-specific factor CTCFL cooperates with the protein methyltransferase PRMT7 in H19 imprinting control region methylation. *PLoS Biol. 4*, e355.
(31) Corsi, A. K., Wightman, B., and Chalfie, M. (2015) A transparent window into biology: A primer on *Caenorhabditis elegans*. In *Worm Book Genetics* (De Stasio, E. A., Ed.) pp 387−407, Worm Book.
(32) Petrella, L. N. (2014) Natural variants of *C. elegans* demonstrate defects in both sperm function and oogenesis at elevated temperatures. *PLoS One 9*, e112377.
(33) LLeonart, M. E. (2010) A new generation of proto-oncogenes: Cold-inducible RNA binding proteins. *Biochim. Biophys. Acta, Rev. Cancer 1805*, 43−52.
(34) Larsen, S. C., Sylvestersen, K. B., Mund, A., Lyon, D., Mullari, M., Madsen, M. V., Daniel, J. A., Jensen, L. J., and Nielsen, M. L. (2016) Proteome-wide analysis of arginine monomethylation reveals widespread occurrence in human cells. *Sci. Signaling 9*, rs9.
(35) Gracida, X., Norris, A. D., and Calarco, J. A. (2016) Regulation of tissue-specific alternative splicing: *C. elegans* as a model system. In *Advances in Experimental Medicine and Biology*, pp 229−261, Springer International Publishing Switzerland, Cambridge, MA.
(36) Gottschling, H., and Freese, E. (1962) Tritium isotope effect on ion exchange chromatography. *Nature 196*, 829−831.

CHAPTER 9

PRMT7 Methylation of Age-Modified Histone H2B Containing an Isoaspartyl Residue at Position 25

PRMT7 Methylation of Age-Modified Histone H2B Containing an Isoaspartyl Residue at Position 25

Andrea Hadjikyriacou, Anuj Chhabra, and Steven Clarke

ABSTRACT

Protein arginine methylation is involved in several cellular processes, and is especially important in the regulation of transcription through the modification of histone tails. Methylation reactions can function with acetylation and phosphorylation reactions in crosstalk pathways to affect the types of proteins that are recruited to activate or repress transcription. While the histone tails are heavily modified by enzymatic reactions, there is also evidence that the histones can be subjected to non-enzymatic reactions that occur spontaneously in the aging process. One such process is the conversion of asparagine and aspartic acid residues to isomerized and racemized species. Previous studies have shown that the accumulation of isoaspartyl damage affecting aspartic acid-25 on histone H2B can lead to autoimmune responses, such as those seen in lupus erythematosus. In addition, other work has shown the presence of a D-isoaspartyl residue at active chromatin loci, suggesting the possibility that cells may respond to isoaspartyl damage regulatory pathways. Our previous work has also shown that human PRMT7 preferentially methylates histone H2B in RXR motifs in a basic residue-rich region that is known to interact with DNA and is in close proximity to the aspartic acid-25 residue. In this study, we examined the effect of L- and D-isoaspartyl damage on the ability of PRMT7 to methylate histone H2B peptides. We also looked at the ability of PRMT7 to methylate histones purified from nucleosomes from brain tissue of protein-L-isoaspartate *O*-methyltransferase (*Pcmt1*) knockout mice. In addition, we probed for other potential substrates by testing PRMT7 with

fragments from the intracellular loops of dopamine receptor proteins that contain basic rich regions consisting of RXR motifs.

INTRODUCTION

Protein arginine methylation is a common posttranslational modification that is associated with regulation of gene expression through the covalent modification of histone tails (1, 2). Depending on the type of modification deposited on histone tail residues (methylation, phosphorylation, acetylation), various reader proteins are recruited, and can turn transcription machinery on or off (2). The type of methyl marks deposited affect transcription; for example, asymmetric dimethylarginine (ADMA) is commonly associated with transcriptional activation, whereas symmetric dimethylarginine (SDMA) can lead to repression; the role of monomethylarginine (MMA) on the status of transcription has not yet been uncovered (1).

The family of protein arginine methyltransferases (PRMTs) can methylate in three patterns: producing MMA only (PRMT7 only), or going on to a second step and dimethylating arginine residues (ADMA – type I enzymes PRMT1-4, 6, 8; SDMA – type II enzymes, PRMT5, 9). Most of the PRMTs in this family have been well characterized, and physiological substrates have been identified. PRMT7's physiological substrate(s) and role(s), on the other hand, remain largely unknown. While biological roles of PRMT7 have been suggested, including functions in the regulation of muscle stem cell regeneration (3) and in breast cancer cell invasion through induction of the epithelial-to-mesenchymal (EMT) transition (4), there has been no biochemical *in vivo* evidence implicating methylation activity of PRMT7 as the cause and effect of these functions.

Previous work (5–7) has shown that a very good *in vitro* substrate for PRMT7 is human histone H2B, as it prefers a RXR motif in a basic-rich sequence context and such a motif is found in residues 29-33 in this histone. While no *in vivo* evidence of this modification from mammalian purified histones has been yet found, it may be possible that this modification is tissue or gene specific, with PRMT7 methylating histones only at specific gene loci. Recent studies (8, 9) have shown evidence that histone H2B containing isoaspartyl damage at the position of aspartic acid-25 can contribute to the autoimmune response, especially in systemic lupus erythematosus (8), and evidence for the presence of such damaged histone H2B at the loci of active chromatin (9). In addition, X-ray and electron cryomicroscopy (cryo-EM) structures available of nucleosomes for both human and *Xenopus laevis* show the portions of the histone H2B tail protruding and interacting with the nucleosome wrapped DNA (10, 11). The inaccessibility of arginine residues 29, 31, and 33 due to their interaction and binding to the DNA was pointed out previously from these structures, as were the difficulties in detecting *in vivo* methylation of these residues due to the nature of the sequence and cleavage by traditional digestion methods for mass spectrometry approaches (5). While the aspartic acid 25 residue was not seen in the human structure, this residue was present in the *X. laevis* structure at a distance of 2.7 Å from its protein backbone carboxyl to the DNA. We note that the downstream sequence recognized by PRMT7 is slightly different in the amphibian and mammalian histones (KRRKTR in *X. laevis* and KRKRSR in humans). We thus hypothesized that the presence of an isoaspartyl residue at position 25 of histone H2B may cause a kink in the peptide backbone and displace the residues from interacting with the DNA, subsequently affecting the methylation capabilities of PRMT7.

Because it is clear that PRMT7 prefers basic-rich regions in RXR motifs (5–7), we also tested the activity of PRMT7 on fragments of the intracellular loops of the dopamine D2 receptor in humans and DOP-3 in the nematode *Caenorhabditis elegans*, which were shown to be substrates for PRMT5 (12). These fragments contain conserved sequences of arginine repeats and were of great interest for potential methylation and regulation by PRMT7.

MATERIALS AND METHODS

Protein Purification—Human recombinant GST-tagged PRMT7 was expressed and purified as described in (6). *C. elegans* GST-PRMT-7 was expressed and purified as described in (7). GST-tagged dopamine receptor fragment plasmids were a generous gift from the Ferkey lab (12). Plasmids for both GST-D2 (211-232) and GST-DOP-3 (202-232) were transformed into BL21 DE3 *E. coli* cells, and expressed using 0.5 mM isopropyl D-thiogalactopyranoside (IPTG, Gold Bio, catalog no. 12481C25) at 18 °C for 16 h. Cells were then harvested and proteins purified using a slurry of glutathione Sepharose 4B resin (GE Healthcare, catalog no. 17-0756-01) and dialyzed into buffer containing 50 mM Tris-Cl, 120 mM NaCl, pH 7.5. His-PCMT1 was purified as described in (13, 14) and was a gift from Rebeccah Warmack in the Clarke laboratory.

Histone purification from mouse nucleosomes—Histones from wild type and *Pcmt1*$^{-/-}$ mice were purified using the protocol adapted from (9). In short, freshly excised mouse brains from either wild type or *Pcmt1*$^{-/-}$ mice that were 51 days old were placed immediately into a glass homogenization tube along with the addition 9 volumes of homogenization buffer (5 mM potassium HEPES, pH 7.6, 0.5 mM EDTA, 10% (w/v) sucrose, and 1/100 dilution of mammalian protease inhibitor (cOmplete, Roche Applied Science, catalog no. 11697498001)) at

4 °C. These samples were then subsequently homogenized using a Teflon pestle rotating at 310 rpm. The homogenates were centrifuged at 800 x g for 30 min, and the nuclear pellet fraction was passaged 20 times through a 25-gauge needle. The passaged sample was then spun again at 3,000 x g for 10 min and then resuspended in 0.4 N H_2SO_4 with gentle rotation for 1 h at 4 °C. The suspension was then centrifuged at 14,000 x g (High Speed Spin, HS) for 10 min, and the supernatant was precipitated with a final concentration of 25% (w/v) trichloroacetic acid (TCA), followed by another HS spin. The nucleosome pellets were washed with cold acetone, and subjected to another HS spin, where the supernatant was removed and pellets air-dried for 20 min. The nucleosome pellets were resuspended in 10 mM sodium phosphate buffer, pH 7.4. Protein concentration was approximated by estimating the amount of Coomassie stain on the polypeptide band compared to that on known amounts of standard proteins after SDS-PAGE.

Assay to detect isoaspartyl methylation—To measure the number of labile methyl groups formed due to isoaspartyl methyl ester formation, we subjected our peptides and substrates to a base labile volatility assay, as described in (14). In brief, approximately 100 pmol of peptide substrate were reacted with 5 µg of recombinant His-PCMT1 enzyme and a final concentration of 9.6 µM *S*-adenosyl-L-[*methyl*-^{3}H]methionine ([^{3}H]AdoMet, Perkin Elmer Life Sciences, 82.7 Ci/mmol, 0.55 mCi/ml in 10 mM H_2SO_4/EtOH (9:1, v/v) (diluted hot and cold to 400 µM, with a specific activity of 55 cpm/pmol AdoMet), in a buffer containing 135 mM Bis-Tris at pH 6.4 in a final volume of 100 µl. The reactions were incubated for the time indicated in the figure legends at 37 °C and quenched by the addition of 10 µl of 2 M sodium hydroxide. 100 µl of this mixture was then spotted onto filter paper placed in the neck of scintillation vials containing 5 mL of scintillation fluid (RPI Safety-Solve, Research Products International, catalog no. 111177). Vials

were tightly capped and incubated at room temperature for 2 h, after which the filter paper was carefully removed and vials were counted via liquid scintillation counting (three 5-min counting cycles) to determine the labile methyl groups transferred. Background was subtracted and the cpm value determined was converted to pmol [^{3}H]-methyl groups transferred per pmol substrate using the specific activity of the diluted AdoMet as 55 cpm/pmol AdoMet.

In vitro methylation reactions—Reactions were set up by the addition of approximately 2 µg of GST-PRMT7 enzyme, a final concentration of 12.5 µM for peptide substrates (or as indicated in the figure legends), 0.7 µM final concentration [^{3}H]AdoMet, reaction buffer containing 50 mM potassium HEPES, 10 mM NaCl, pH 8.0, 1 mM DTT (unless otherwise indicated) in a final reaction volume of 60 µl. Reactions were incubated for 20 h at 15 °C (or as indicated in legend). If a protein substrate was used, reactions were quenched by the addition of equal volume 25% TCA, washed with acetone, and acid hydrolyzed; if the substrate was a peptide, reactions were terminated by the lowering of reaction pH by the addition of 3 µl of 25% TCA and purified using OMIX C18 Zip-Tips (Agilent Technologies). The reactions were then vacuum centrifuged to remove the elution buffer of 1:1 H_2O:acetonitrile. The reactions were then acid hydrolyzed as described: reactions were hydrolyzed after the addition of 50 µl of 6 N hydrochloric acid in a chamber consisting of an acidic environment under vacuum and high heat (110 °C) for 20 h. After hydrolysis, reactions were subject to vacuum centrifugation to remove excess acid.

Amino acid analysis of methylated peptides and proteins—Methylated arginine species were analyzed via high-resolution cation exchange chromatography as described previously (15). In short, *in vitro* methylation reactions were separated on high-resolution cation exchange resin

after the addition of nonradiolabeled standards, and 1 minute 1 mL fractions were collected and analyzed. 50 µl of each fraction was used to determine the elution position of the methylated arginine standards, and 950 µl was combined with 8 mL of liquid scintillation fluid and counted on a Beckman Liquid Scintillation counter LS6500. Liquid scintillation counting gives a counting efficiency of about 50%, so that 1 fmol of radiolabeled methyl groups corresponds to 91 cpm. Each vial was counted for three 5-min cycles.

Detection of methylated substrates after SDS-PAGE/fluorography—In vitro methylation reactions that were to be separated on SDS-PAGE were quenched by the addition of 5x SDS-loading buffer, and entire mixture was loaded on a 12% Resolving Bis-Tris Polyacrylamide SDS-PAGE gel, pH 6.4 in MOPS (3-Morpholinopropane-1-sulfonic acid) buffer. Gels were then Coomassie Blue stained for 1 h, and destained overnight. After 1 h water wash, gels were treated with EN^{3}HANCE (Perkin Elmer Life Sciences, catalog no. 6NE9701) buffer for 1 h, and then washed with water for 30 min before vacuum drying. The dried gels were then exposed to autoradiography film (Denville Scientific, catalog no. E3012) for the specified time at -80 °C.

RESULTS

Arginine residues methylated by PRMT7 on histone H2B (23-37) fragment interact with DNA in intact nucleosomes—Since we were able to previously show that human PRMT7 produces MMA on substrates containing RXR motifs in a basic sequence, in particular a peptide of histone H2B tail that is close to the histone core, we studied the X-ray crystal structures and cryo-EM structures of the *X. laevis* and human nucleosomes at resolution of 1.9 and 4.5 Å respectively (10, 11). The *X. laevis* structure shows the position of arginine residues that are methylated on histone

H2B by PRMT7 *in vitro* and the aspartic acid on the histone tail in close contact with the DNA (Fig. 1A, B). The aspartic acid 25 is in close contact with the DNA, where its protein backbone carboxyl is within hydrogen bonding distance to the DNA (2.7 and 3.2 Å; Fig. 1A, C). In addition, the arginine residues are also in close contact with the DNA backbone, and each arginine residue (R29, R30, and R33) is within hydrogen bonding distance (Fig. 1 D-F). Comparably, we are able to see the position of the three arginine residues (R29, R31, and R33) from the human histone H2B similarly positioned, in close contact with the DNA (Fig. 2). Each of these residues is found in a position nearby or interacting with the DNA. We see that the R29 terminal nitrogen atom of the guanidino group comes within 5.3 Å of the DNA (Fig. 2C), while R31 and R33 terminal nitrogen atoms are within hydrogen bonding distance of the DNA backbone and bases (Fig. 2D, E). These interaction distances are interesting as the residue that is closest to the DNA, R31, is also the most "important" or "required" residue in the motif for PRMT7 to methylate the basic-rich H2B sequence (6, 7).

PRMT7 methylation of H2B peptides is affected by isoaspartyl residues in the 25 position—To test our hypothesis that isoaspartyl damage of histone H2B can affect PRMT7 methylation of the R29/R31/R33 sequence, we tested different peptides of this sequence, one containing an L-isoaspartyl residue in the D25 position (Fig. 3A peptide 3) or a D-isoaspartyl residue in the corresponding D25 position (Fig. 3A peptide 5). We confirmed the presence of the L-isoaspartyl residue using a base labile assay, and saw increased volatile methyl groups transferred with the L-isoaspartyl containing peptide (Fig. 3B). We did not see any base labile activity with the D-isoaspartyl containing peptide as expected, as PCMT1 does not recognize the D-iso conformation. Once we confirmed the presence of the isoaspartyl residue on the peptide, we then

tested the *in vitro* methylation activity of PRMT7 on these peptides using amino acid analysis (Fig. 3C). We observed the production of MMA with each of these peptides, and no dimethyl arginine product was formed. When we normalized the total counts of the MMA peak from the amino acid analysis to correct for the difference in peptide concentration using an HPLC fluorometer based assay for amino acid analysis, we saw that the L-isoaspartyl containing peptide (peptide 3) was a better substrate of PRMT7 than its corresponding wild type peptide (peptide 2) (Fig. 3D). The normalized counts for the peptide containing the D-isoaspartyl residue (peptide 4) did not have a difference from its corresponding wild type peptide (peptide 5) (Fig. 3D). Thus, it seems the presence of an L-isoaspartyl residue in the 25 position of this peptide may enhance the methylation activity.

Histone H2B (23-37) aged peptide confirms methylation activity of PRMT7 is affected by presence of isoaspartyl residue in 25 position—Since we were able to show that PRMT7 methylation activities on isoaspartyl containing peptides were affected (Fig. 3), we wanted to confirm this result by aging the histone H2B (23-37) peptide. We aged the peptide and generated isoaspartyl residues by incubating the peptide at 55 °C for 42 days. We then confirmed the isoaspartyl-formation by base labile assay, and we saw increased volatile methyl groups transferred with the aged peptide (Fig. 4A). We then confirmed the methylation activity by incubating the aged and unaged peptide with GST-PRMT7, and did amino acid analysis. In Fig. 4B, right panel, PRMT7 has a higher activity on the aged H2B (23-37) peptide containing L-isoaspartyl residues than the unaged peptide.

Histones from Pcmt1$^{-/-}$ mouse nucleosomes contain elevated levels of isoaspartyl residues—Since the structures of nucleosomes indicate that the residues of interest are interacting with the DNA, and we saw that PRMT7 methylation activity on isoaspartyl containing peptides was affected, we wanted to see if PRMT7 could methylate histones from intact nucleosomes and if the activity would be affected by the isoaspartyl residues. To test this, we purified histones from wild type and *Pcmt1*$^{-/-}$ mouse brain (Fig. 5A). We further verified the presence of isoaspartyl residues with the base labile assay, and saw significantly higher volatile methyl groups with the *Pcmt1*$^{-/-}$ histones, as expected (Fig. 5B). Lastly, we tested PRMT7 methylation activity on the histones in *in vitro* methylation assays, and detected the activity via SDS-PAGE fluorography (Fig. 5C). The reactions were incubated for 1 h or 20 h, to see if methylation activity is affected by time or degradation, and included recombinant histone H2B as a control, as PRMT7 methylates histone H2B protein (6, 7). We saw that there was not much increase in methylation of the *Pcmt1*$^{-/-}$ nucleosomes in the size range where we expect the histones to be. This could potentially be due to the histones already being fully methylated *in vivo*. More work needs to be done to examine methylation of intact nucleosomes.

Human PRMT7 does not methylate RXR sequences in dopamine receptor proteins, but C. elegans PRMT-7 prefers the substrate—Since our previous work showed that PRMT7 preferentially methylates RXR motifs in a basic context (5, 6), we were rather interested when a report showed that human PRMT5 methylated a fragment of an intracellular loop of the human dopamine receptor protein D2 and the *C. elegans* ortholog DOP-3 (12). These receptor fragments contain sequences of RXR in a basic-rich region (Fig. 6A). In *in vitro* methylation reactions, PRMT7 activity was tested with and without DTT (Fig. 6B) with both human GST-D2 fragment

and *C. elegans* GST-DOP-3 fragment. As PRMT7 activity is dependent on DTT, it was interesting that the activity was low on both of the receptor fragments (Fig. 6B), but it seemed to have more of a preference for the DOP-3 fragment, which contains different residues in between the Arg residues (Fig. 6A). Since the DOP-3 fragment was preferred by human PRMT7, we wondered if the *C. elegans* PRMT-7 would also methylate this fragment, as it has a similar RXR substrate preference (7). It was very interesting that *C. elegans* PRMT-7 more readily methylated both of the dopamine receptor fragments, with an obvious preference for its own DOP-3 fragment (Fig. 6C).

DISCUSSION

Although the physiological substrates of human PRMT7 have yet to be uncovered, our previous work has shown that histone H2B is a rather good *in vitro* substrate (5–7), methylating Arg29, Arg31, and Arg33 residues that are found in a basic-rich, RXR context. While there is no *in vivo* evidence as of yet of methylation on histone H2B on these sites, it is possible that these modifications may be tissue/life stage specific, or perhaps affected by the presence of other modifications. Since it has been established in the literature that crosstalk between modifications on histone tails is a common phenomenon (16), we approached the question of whether it is possible there is also crosstalk with isoaspartyl damage and the placement of methylation marks on histones. Previous work has shown evidence for autoimmune responses to isoaspartyl damage in histone H2B in systemic lupus erythematosus (8), as well as for the enrichment of D-isoaspartyl variant of H2B at active chromatin (9).

Recent X-ray and cryo-EM structures (10, 11) of *X. laevis* and human nucleosomes show that the arginine residues methylated by PRMT7 *in vitro* interact with the DNA that is wrapped

around the reconstituted nucleosome core (Fig. 1 and 2). In addition, in the *X. laevis* structures, we are able to see the proximity of the aspartic acid residue to the DNA, further strengthening our hypothesis that an isoaspartyl residue will affect the positioning of these residues in contact with the DNA. We hypothesized that the presence of an isoaspartyl residue on D25 can potentially create a kink in the histone tail, causing the arginine residues that preferentially are embedded/interact with the DNA, to be more exposed and open to methylation by PRMT7.

We found that PRMT7 activity on H2B peptides was affected by the presence of isoaspartyl residues (Fig. 3 and 4), and that there was even a difference between the L-isoaspartyl versus D-isoaspartyl containing H2B peptides (Fig. 3). It would be interesting to further explore whether methylation of H2B is more prevalent in disease models such as autoimmunity and systemic lupus erythematosus (8), or if it has the potential to be a regulatory modification of gene expression along with the D-isoaspartyl damage (9).

It would also be of interest to further probe for the ability of PRMT7 to methylate purified mouse nucleosomes that have accumulated isoaspartyl damage, in hopes of verifying our proposed mechanism that PRMT7 methylates the histone H2B tail after aging or damage. It would be useful to perform mass spectrometric studies to confirm the presence of the isoaspartyl residue is on histone H2B Asp25 and verify this damage is not accumulated damage elsewhere on the histones. Further work will look into the reconstitution of the nucleosome core with the addition of aged and unaged histone H2B; this would tell us a lot about PRMT7's preference. It may also be possible that there is tissue specific PRMT7 methylation of the histones, as we see increased expression in high throughput studies (17). PRMT7 may function as a point of regulation for only a few specific loci or tissues where it is expressed or needed.

FOOTNOTES

This work was supported in full or in part by National Institutes of Health Grants GM026020 to S.G.C., and GM007185, a Ruth L. Kirschstein National Research Service award to A.H. In addition, funds from the Elizabeth and Thomas Plott Chair in Gerontology of the UCLA Longevity Center (to S.G.C) and a UCLA Dissertation Year Fellowship to A.H.

Abbreviations used are: PRMT, protein arginine methyltransferase; MMA, ω-N^G-monomethylarginine; ADMA, ω-N^G,N^G-asymmetric dimethylarginine; SDMA, ω-N^G,N'^G-symmetric dimethylarginine; AdoMet, *S*-adenosyl-L-methionine; [^{3}H]AdoMet, *S*-adenosyl-[*methyl*-^{3}H]-L-methionine; TCA, trichloroacetic acid; Cryo-EM, cryoelectron microscopy, OPA, *o*-phthalaldehyde

ACKNOWLEDGEMENTS

The authors would like to thank the Mamula and Aswad labs for their generous gifts of the isoaspartyl-containing H2B peptides, as well as the Ferkey labs for the GST-tagged dopamine receptor fragment plasmids. The authors would also like to thank Rebeccah Warmack for advice and use of purified His-PCMT1 protein, as well as Dr. Jonathan Lowenson, for advice along the way and for the harvesting of mouse brains for nucleosome purification.

FIGURES AND LEGENDS

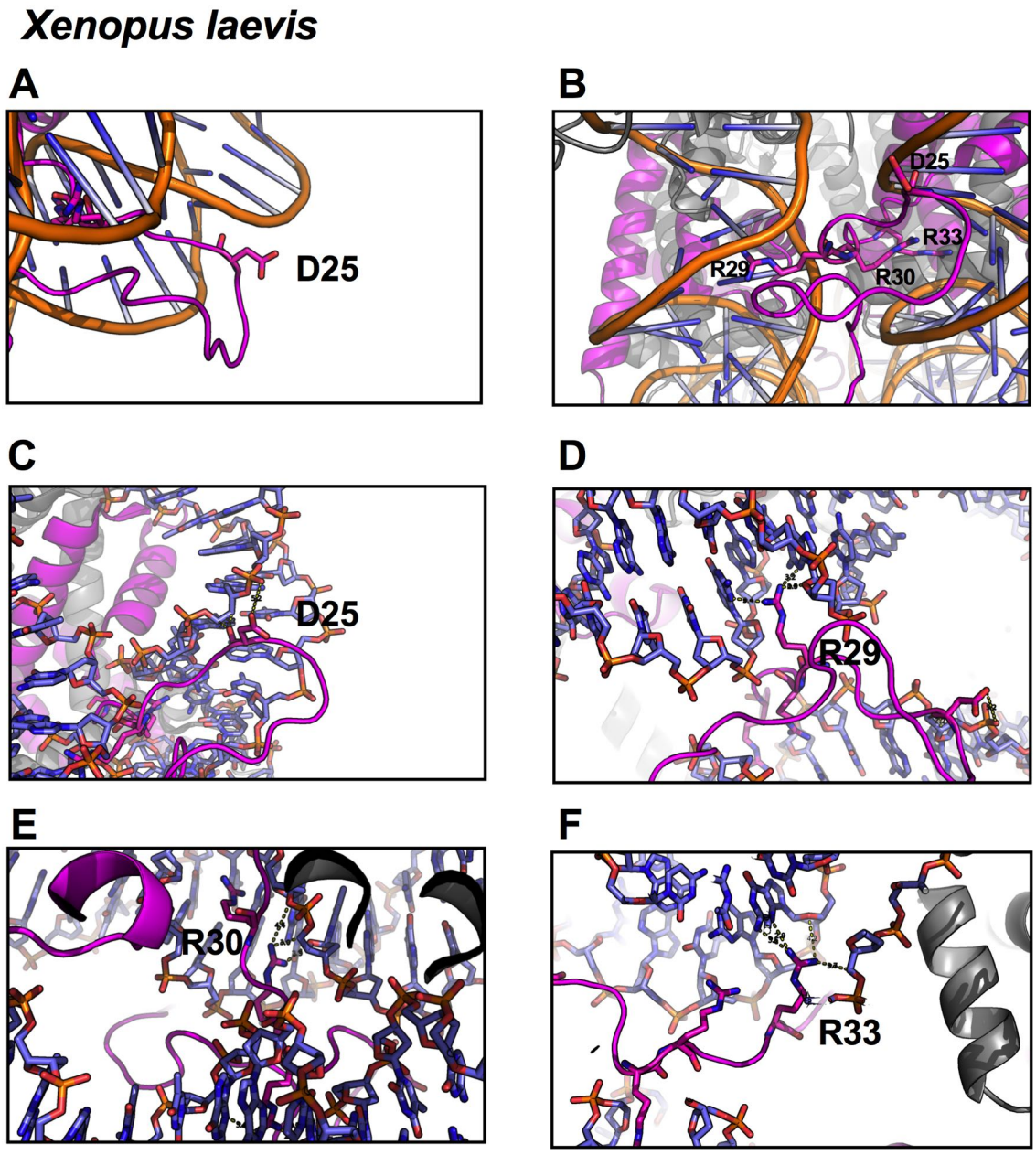

FIGURE 1. X-ray crystal structure of *X. laevis* histone H2B in complex with DNA, showing aspartic acid and arginine residues of interest. Pymol representation of histone H2B and DNA from an X-ray crystal structure (PDB: 1KX5) (11). A. View of histone H2B (magenta) with

aspartic acid residue D25 shown as a stick with red oxygen atoms. The DNA helix backbone is colored orange with blue-gray lines representing the bases. B. A rotated view of histone H2B with the arginine residues R29, R30, R33 and aspartic acid D25 shown as sticks, with blue nitrogen atoms and red oxygen atoms. DNA helix backbone is shown in same colors as in A and other histone proteins are colored gray. C. Interactions of aspartic acid 25 with DNA backbone, with atoms shown in CPK colors. The closest contact of aspartic acid with the DNA is from the carboxyl oxygen from the protein backbone, at distances of 2.7 and 3.2 Å, and a further contact of the side chain with DNA of 5.2 Å. D-F. The closest contacts of the two omega nitrogens of R29 is 2.5, 3.2 and 3.4 Å with the bases. The closest contacts of the two omega nitrogens of R30 is 2.9, 3.0, and 4.4 Å with the DNA backbone and bases. The closest contacts of the two omega nitrogens of R33 are 2.9, 3.5, 3.7 and 4.2 Å from the DNA backbone and bases.

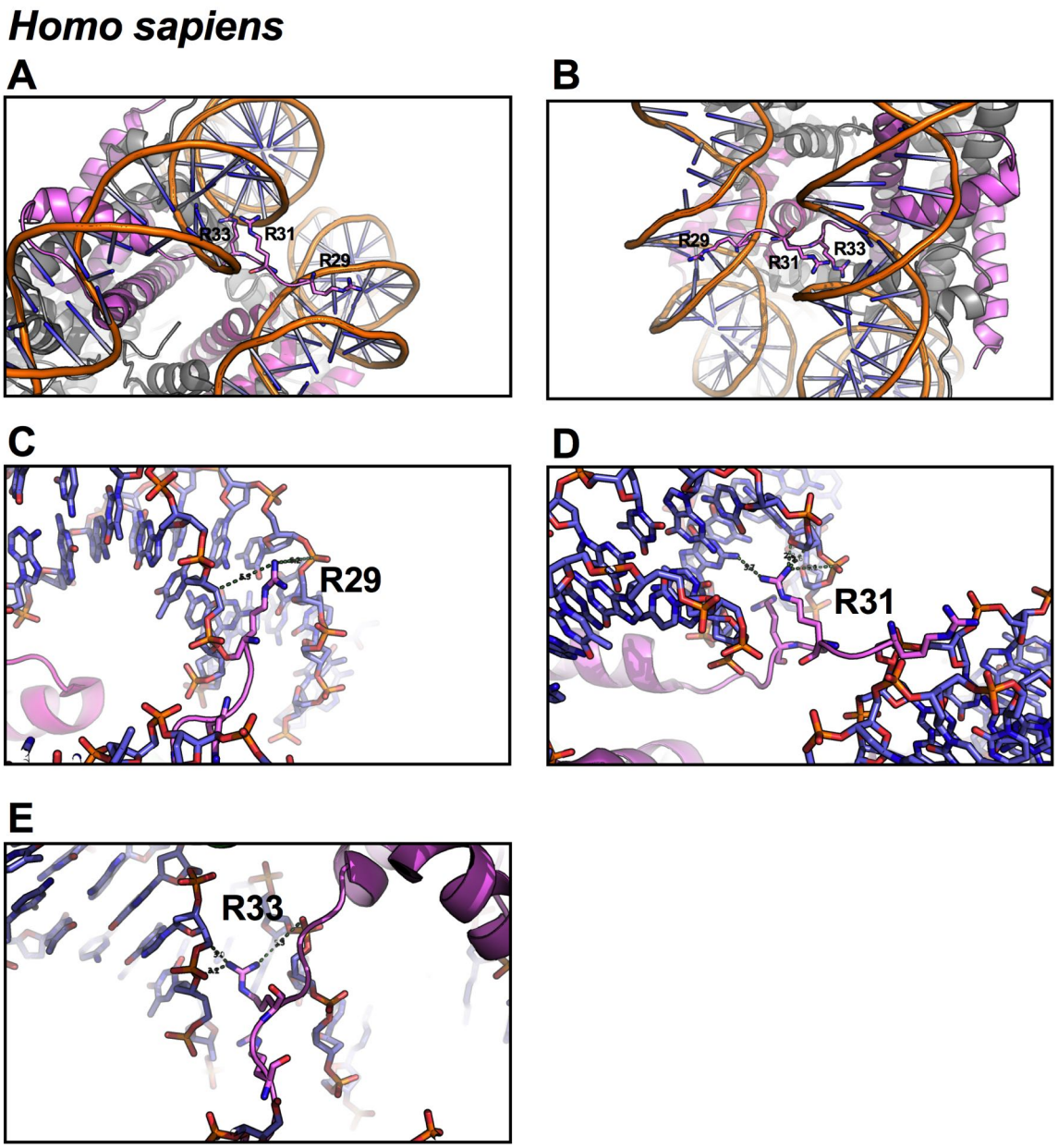

FIGURE 2. Electron cryomicroscopy structure of human histone H2B in complex with DNA shows arginine residues of interest interacting with DNA. Pymol representations are shown of histone H2B and DNA from a modified nucleosome cyro-EM structure (PDB: 5KGF) (10). (A-B). Two views of histone H2B (magenta), with arginine residues R29, R31 and R33 shown as sticks with blue nitrogen atoms. The DNA helix backbone is colored in orange with the bases represented by grayish blue lines. Other histone proteins are colored in gray. (C-E).

Interactions of histone H2B R29/R31/R33 with the DNA, with atoms shown as stick figures in CPK colors. The closest contacts of one omega-nitrogen atom of R29 with the DNA backbone are 5.3 and 6.2 Å. The closest contacts of the two omega-nitrogen atoms of R31 with the DNA backbone and bases are 2.6, 2.8 and 3.7 Å. The closest contacts of the two omega-nitrogen atoms of R33 with the DNA backbone are 3.0, 3.1, and 5.3 Å.

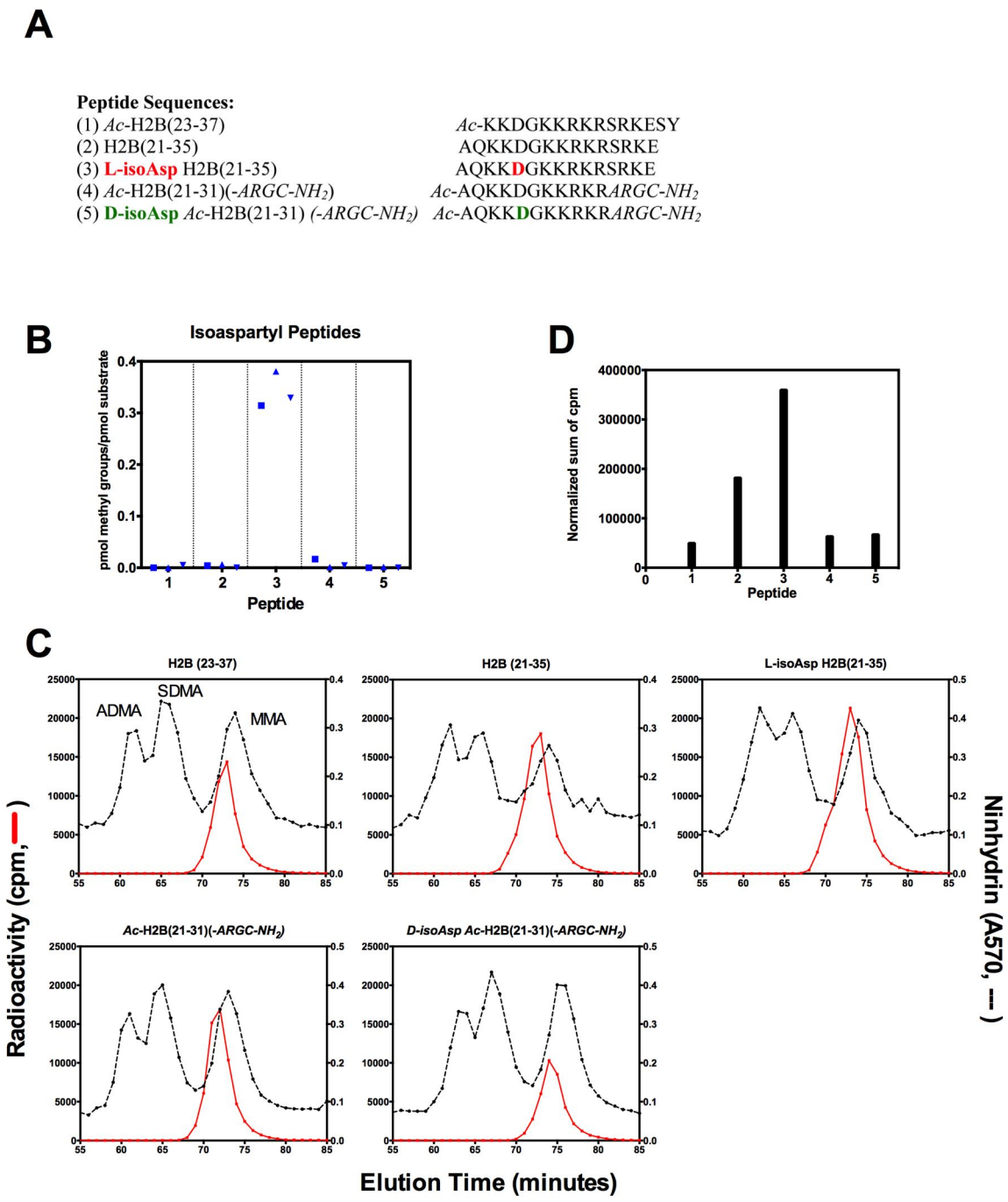

FIGURE 3. The presence of an isoaspartyl residue affects methylation activity of human PRMT7 on synthetic peptides. A. Alignment of sequences of peptides used in this study. Peptide 1 was described in Chapters 3 and 4 (5, 6); Peptides 2 and 3 were described in Doyle et al. (8); Peptides 4 and 5 were described in Qin et al. (9). The L-isoaspartyl residue shown in red,

the D-isoaspartyl residue is shown in green. B. PCMT1 assay to identify L-isoaspartyl residues as described in the "Materials and Methods" section. Here, we incubated peptides for 1h in triplicate and each point is represented here as different shapes. C. Cation exchange analysis of methylated amino acids from hydrolysates of *in vitro* methylation reactions were done with a nominal 12.5 µM final concentration of peptide, with 2 µg of GST-PRMT7 enzyme as described in "Materials and Methods," in a reaction buffer of 50 mM potassium HEPES, 10 mM NaCl, pH 8.0, containing 1 mM DTT for 22 h at 15 °C. Reactions were quenched by the addition of 3 µl of 25% TCA, peptides were purified using OMIX C18 Zip-Tip pipette tips, acid hydrolyzed and analyzed by cation exchange chromatography as described in "Materials and Methods." D. Radioactivity in the MMA peak from the experiments shown in Panel C were normalized for the small differences in the peptide concentration used. The counts of the peak for MMA were added up, and normalized to the calculated relative concentration of each peptide as determined by a reverse phase HPLC *o*-phthalaldehyde (OPA) amino acid analysis as described in Hadjikyriacou et al. (18). The HPLC elution gradient was optimized for the separation of the amino acids found in these specific peptides. We measured the relative concentrations of the aspartic acid, glutamic acid, and serine OPA derivatives and normalized the fluorescence of the amino acids of each peptide to the value for peptide 1. In short, 1000 pmol of each peptide (as determined by weight) was acid hydrolyzed, dried, and brought up in 10 µl. Amino acids were separated on a ZORBAX Eclipse AAA analytical 4.6 x 150 mm 5 micron reverse phase HPLC column using a gradient consisting of 50 mM sodium acetate pH 5.4 and a buffer consisting of 80% methanol : 20% 50 mM sodium acetate pH 5.4. The total MMA peak counts were multiplied by a factor equal to the average OPA fluorescence of a group of Asp, Glu and Ser amino acids in the peptide 1 hydrolysate divided by the average OPA fluorescence of the same

amino acids in peptides 2-5, respectively. Normalized total counts (cpm) for the MMA peak plotted in panel D are as follows: Peptide 1, 49,825 cpm; Peptide 2, 182,006 cpm; Peptide 3, 359,847 cpm; Peptide 4, 63,463 cpm; and Peptide 5, 67,169 cpm.

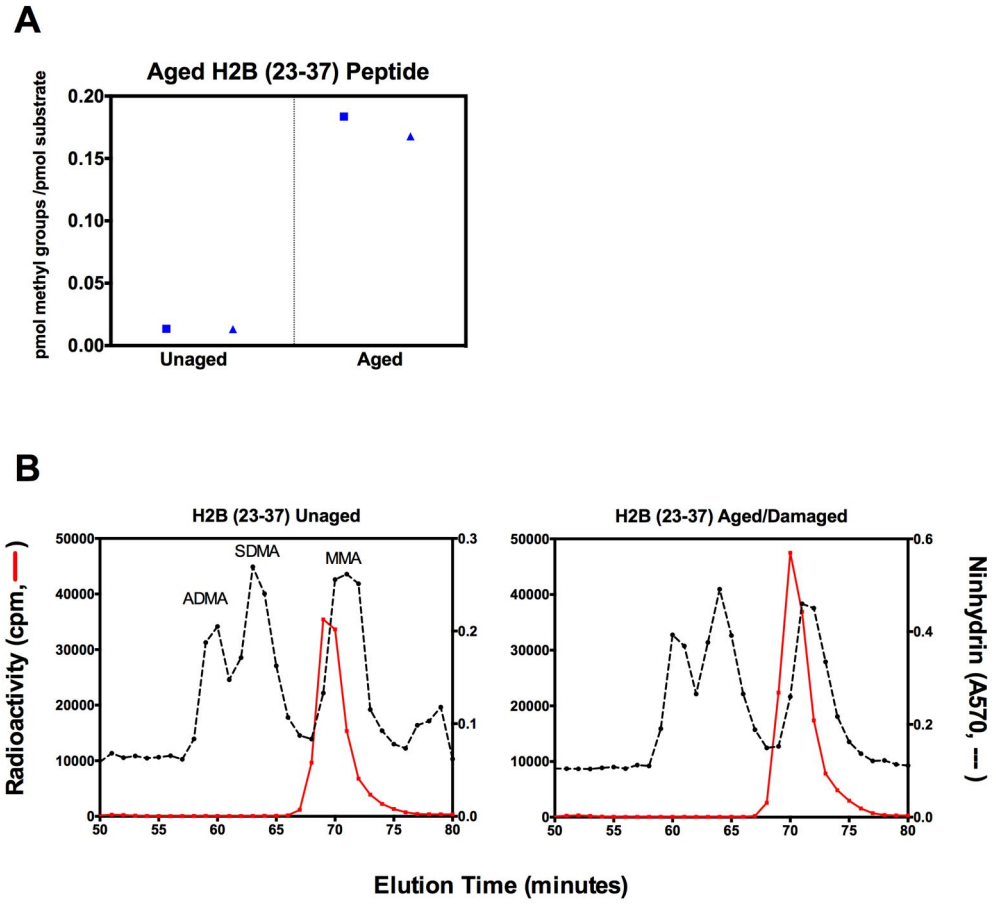

FIGURE 4. L-isoaspartyl damage on synthetic histone H2B peptide affects methylation activity. A. Synthetic histone H2B peptides consisting of residues 23-37 were aged at 55 °C for 42 days to form isoaspartyl residues. L-isoaspartyl residue assay on aged and unaged histone H2B peptides was done as described in "Materials and Methods" with duplicate incubations for 2 h. Each point is representative of the replicate. B. Amino acid analysis of reactions with 2 µg of GST-PRMT7 reacted with 12.5 µM of unaged or aged H2B (23-37) peptide, in the same reaction

conditions described in Figure 2 and “Materials and Methods.” Reactions were incubated at 15 °C for 20 h, quenched and zip-tipped as described above, and methylated arginine derivatives separated on high resolution cation exchange chromatography. The total sum of counts of the MMA peak for the unaged peptide was approximately 110,000 cpm, whereas the aged/damaged peptide sum was approximately 145,000 cpm.

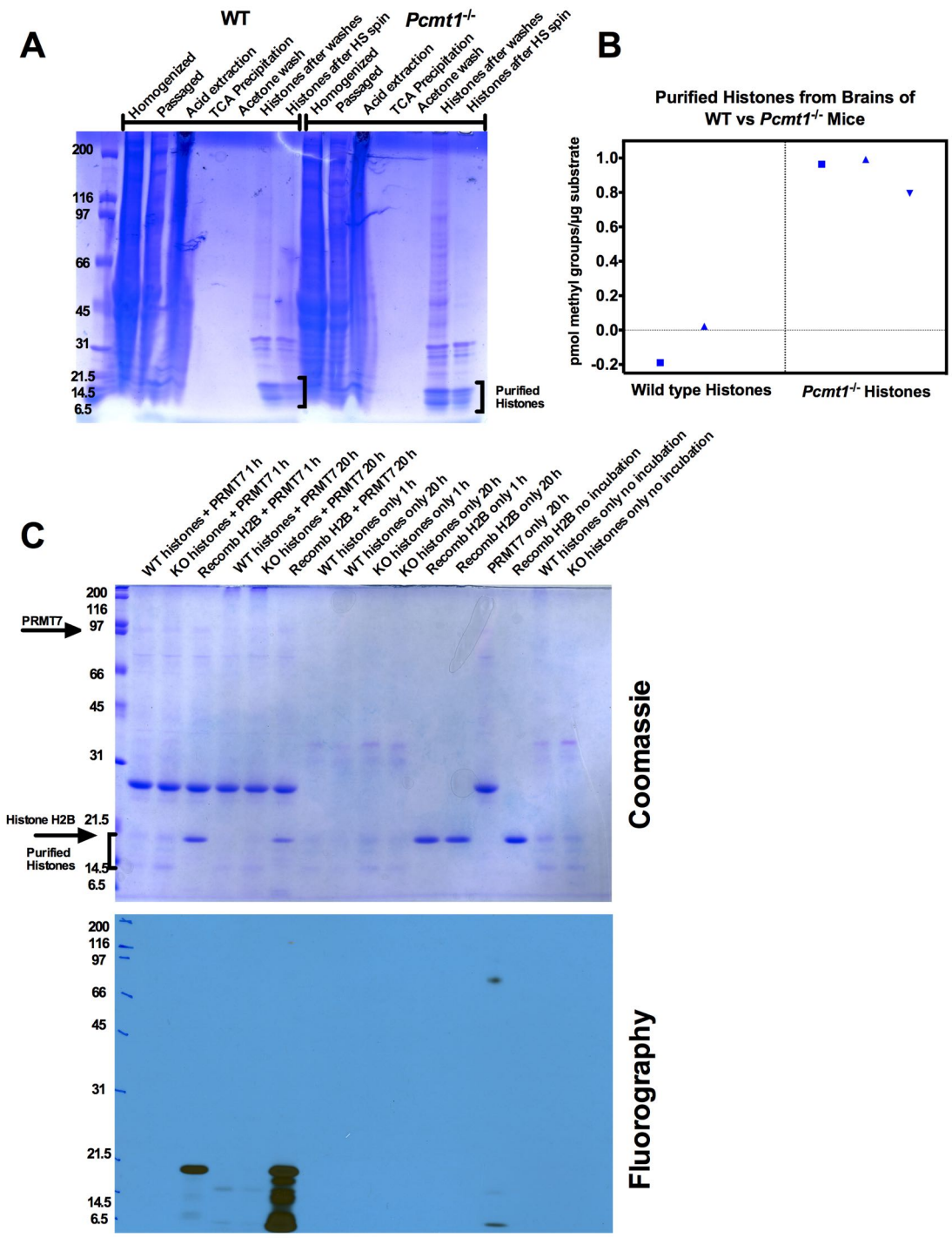

FIGURE 5. Histones purified from *Pcmt1*$^{-/-}$ mouse nucleosomes accumulate isoaspartyl damage and are methylated by PRMT7. A. Coomassie Blue stain of histones purified from mouse nucleosomes from wild type (WT) and *Pcmt1*$^{-/-}$ mouse brain tissue, as described in

"Materials and Methods", on a 4-20% Bis-Tris gel (Genscript, Inc., M42015). In each lane, 30 µl was loaded of each purification step as labeled for both the wild type and *Pcmt1*$^{-/-}$ knock out, including the brain homogenate, homogenate after needle passage (passage), acid extraction, TCA precipitation, acetone wash, histones after washes, and histones after high speed (HS) spin. Bracket indicates location of histones on migration on SDS-PAGE. Molecular weight standards are indicated from 2 µg of a Broad Range ladder (BioRad, Cat. No. 161-0317). B. Assay for L-isoaspartyl residues comparing wild type and *Pcmt1*$^{-/-}$ purified histones. In short, 5 µg of His-PCMT1 enzyme was reacted with approximately 6.25 µg of histones purified from nucleosomes in the same buffer and conditions as described in "Materials and Methods" and in Figure 2, and incubated for 2 h at 37 °C. Reactions were done in duplicate for wild type and triplicate for *Pcmt1*$^{-/-}$, and the background radioactivity was subtracted. Data is represented as pmol [^{3}H]-methyl groups transferred per µg substrate and replicate points are shown. C. Methylation of purified histones was assayed using *in vitro* methylation reactions that consisted of approximately 6.25 µg of purified histones, 2 µg GST-PRMT7, 0.7 µM [^{3}H]AdoMet in 50 mM potassium HEPES buffer, 10 mM NaCl, pH 8.0, 1 mM DTT in a final volume of 60 µl at 15 °C for 20 h. Reactions were then loaded and proteins separated on a 12% Bis-Tris gel, and prepared for fluorography as described in "Materials and Methods." Dried gel was exposed to film for 14 days at -80 °C. Experiment was replicated once. Arrows indicate purified full length PRMT7 and recombinant histone H2B, and bracket indicates purified histones from nucleosomes.

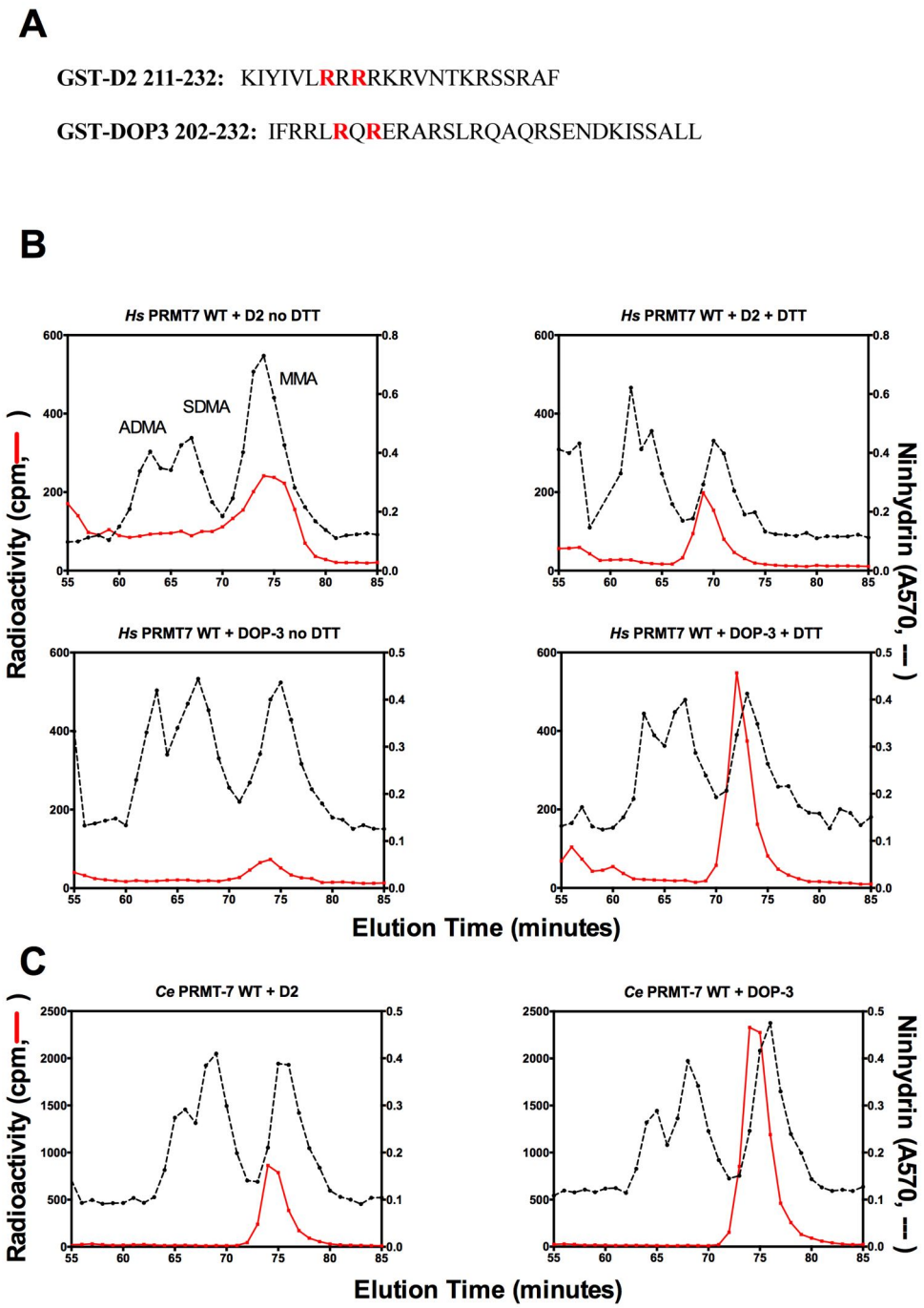

FIGURE 6. Intracellular loops of dopamine receptors are relatively poor substrates for human PRMT7 but are better substrates for *C. elegans* PRMT-7. A. Sequences of GST-tagged peptides of intracellular loop of dopamine receptors human D2 (UniProt ID: P14416, amino acids 211-232) and *C. elegans* DOP-3 (UniProt ID: Q6RYS9, amino acids 202-232) (12).

Two arginine residues in RXR motif methylated by PRMT5 in Likhite et al. (12) are shown in red. B. Amino acid analysis of *in vitro* methylation reactions consisting of 5 µg of GST-tagged substrate and 2 µg of enzyme, in a methylation buffer as described above, 50 mM potassium HEPES, 10 mM NaCl, pH 8.0, with the addition of 1 mM DTT or no DTT (as indicated in panels). Reactions with no DTT were incubated at 25 °C for 20 h, and reactions with DTT were incubated at 15 °C for 20 h. C. Amino acid analysis of *in vitro* methylation reactions of 5 µg of GST- tagged dopamine receptor (D2 or DOP-3) with 2 µg of *C. elegans* GST-PRMT-7 enzyme, under the same reaction conditions described above, at 15 °C for 20 h, with 1 mM DTT.

REFERENCES

1. Fuhrmann, J., Clancy, K. W., and Thompson, P. R. (2015) Chemical Biology of Protein Arginine Modifications in Epigenetic Regulation. *Chem. Rev.* **115**, 5413–5461
2. Blanc, R. S., and phane Richard, S. (2017) Arginine Methylation: The Coming of Age. *Mol. Cell*. **65**, 8–24
3. Blanc, R. S., Vogel, G., Chen, T., Crist, C., and Richard, S. (2016) PRMT7 Preserves Satellite Cell Regenerative Capacity. *Cell Rep.* **14**, 1528–1539
4. Baldwin, R. M., Haghandish, N., Daneshmand, M., Paris, G., Falls, T. J., Bell, J. C., Islam, S., and Côté, J. (2014) Protein arginine methyltransferase 7 promotes breast cancer cell invasion through the induction of MMP9 expression. *Oncotarget*. **6**, 3013–3032
5. Feng, Y., Maity, R., Whitelegge, J. P., Hadjikyriacou, A., Li, Z., Zurita-Lopez, C., Al-Hadid, Q., Clark, A. T., Bedford, M. T., Masson, J. Y., and Clarke, S. G. (2013) Mammalian Protein Arginine Methyltransferase 7 (PRMT7) Specifically Targets RXR Sites in Lysine- and Arginine-rich Regions. *J. Biol. Chem.* **288**, 37010–37025
6. Feng, Y., Hadjikyriacou, A., and Clarke, S. G. (2014) Substrate Specificity of Human Protein Arginine Methyltransferase 7 (PRMT7) - The importance of acidic residues in the double E loop. *J. Biol. Chem.* **289**, 32604–32616
7. Hadjikyriacou, A., and Clarke, S. G. (2017) Caenorhabditis elegans PRMT-7 and PRMT-9 Are Evolutionarily Conserved Protein Arginine Methyltransferases with Distinct Substrate Specificities. *Biochemistry*. 10.1021/acs.biochem.7b00283
8. Doyle, H. A., Aswad, D. W., and Mamula, M. J. (2013) Autoimmunity to isomerized histone H2B in systemic lupus erythematosus. *Autoimmunity*. **46**, 6–13
9. Qin, Z., Zhu, J. X., and Aswad, D. W. (2015) The D-isoAsp-25 variant of histone H2B is

highly enriched in active chromatin: potential role in the regulation of gene expression? *Amino Acids*. 10.1007/s00726-015-2140-9

10. Wilson, M. D., Benlekbir, S., Fradet-Turcotte, A., Sherker, A., Julien, J.-P., McEwan, A., Noordermeer, S. M., Sicheri, F., Rubinstein, J. L., and Durocher, D. (2016) The structural basis of modified nucleosome recognition by 53BP1. *Nature*. **536**, 100–103
11. Davey, C. A., Sargent, D. F., Luger, K., Maeder, A. W., and Richmond, T. J. (2002) Solvent mediated interactions in the structure of the nucleosome core particle at 1.9 Å resolution. *J. Mol. Biol.* **319**, 1097–1113
12. Likhite, N., Jackson, C. A., Liang, M., Krzyzanowski, M. C., Lei, P., Wood, J. F., Birkaya, B., Michaels, K. L., Andreadis, S. T., Clark, S. D., Yu, M. C., and Ferkey, D. M. (2015) The protein arginine methyltransferase PRMT5 promotes D2-like dopamine receptor signaling. *Sci. Signal.* **8**, 1–10
13. Patananan, A. N., Capri, J., Whitelegge, J. P., and Clarke, S. G. (2014) Non-repair pathways for minimizing protein isoaspartyl damage in the yeast Saccharomyces cerevisiae. *J. Biol. Chem.* **289**, 16936–16953
14. Warmack, R. A., Mansilla, E., Goya, R. G., and Clarke, S. G. (2016) Racemized and Isomerized Proteins in Aging Rat Teeth and Eye Lens. *Rejuvenation Res.* **19**, 309–317
15. Yang, Y., Hadjikyriacou, A., Xia, Z., Gayatri, S., Kim, D., Zurita-Lopez, C., Kelly, R., Guo, A., Li, W., Clarke, S. G., and Bedford, M. T. (2015) PRMT9 is a Type II methyltransferase that methylates the splicing factor SAP145. *Nat. Commun.* 10.1038/ncomms7428
16. Molina-Serrano, D., Schiza, V., and Kirmizis, A. (2013) Cross-talk among epigenetic modifications: lessons from histone arginine methylation. *Biochem. Soc. Trans.* **41**, 751–9

17. Uhlén, M., Fagerberg, L., Hallström, B. M., Lindskog, C., Oksvold, P., Mardinoglu, A., Sivertsson, Å., Kampf, C., Sjöstedt, E., Asplund, A., Olsson, I., Edlund, K., Lundberg, E., Navani, S., Szigyarto, C. A., Odeberg, J., Djureinovic, D., Takanen, J. O., Hober, S., Alm, T., Edqvist, P., Berling, H., Tegel, H., Mulder, J., Rockberg, J., Nilsson, P., Schwenk, J. M., Hamsten, M., Feilitzen, K. Von, Forsberg, M., Persson, L., Johansson, F., Zwahlen, M., Heijne, G. Von, Nielsen, J., and Pontén, F. (2015) Tissue-based map of the human proteome. *Science (80-.).* 10.1126/science.1260419

18. Hadjikyriacou, A., Yang, Y., Espejo, A., Bedford, M. T., and Clarke, S. G. (2015) Unique Features of Human Protein Arginine Methyltransferase 9 (PRMT9) and Its Substrate RNA Splicing Factor SF3B2. *J. Biol. Chem.* **290**, 16723–16743

CHAPTER 10

Future Goals and Perspectives

My thesis work has extensively biochemically characterized the activity types of two members of the protein arginine methyltransferase family, PRMT7 and PRMT9. Previous work had identified the PRMT7 enzyme and its activity type, but PRMT9 had remained an elusive enzyme, as no activity had been previously detected with any of the substrates tested. Crucial routes I took to characterize these enzymes included the optimization of the reaction conditions, as I found that temperature and reducing agents in the buffer are very important, in addition to using various methods to identify potential physiological substrates. Within the last few years, progress in the PRMT field has greatly accelerated, uncovering physiological roles of the more minor PRMTs in mammals as well as PRMTs in lower organisms like nematodes. Generation of PRMT knockout organisms like mice and worms have provided a wealth of information as far as phenotypes and give significant clues to potential physiological roles that can be further explored. The results presented in this dissertation provide a strong biochemical foundation for PRMT7 and PRMT9 for which further biological and physiological studies can be based. I will now address my thoughts and suggestions for further topics to be studied to advance the characterization and uncovering the physiological roles of these enzymes in the PRMT field.

What is the physiological substrate(s) and role of PRMT7? Is PRMT7 a lone wolf, or does it interact with a slew of proteins?

In Chapters 3, 4, 8 and 9, significant work has been done to characterize the PRMT7 enzyme activity and I attempted to determine the physiological substrate by testing other usual PRMT substrates. The best *in vitro* substrate thus far has been histone H2B, however it has not been possible yet to show that this is a physiological substrate *in vivo.* In addition, it is not clear whether PRMT7 may work as a part of a complex *in vivo*. To address these concerns and to

identify the physiological substrate, the enzyme needs to be expressed and purified after generation of a stable cell line in mammalian cells. Previous lab members have tried transient induction and purification from mammalian cells, with no evidence found for potential partner proteins associated with PRMT7. In addition, collaborators have tried biotinylation assays, where any surrounding or interacting proteins would be biotinylated using a system in which the biotinylation enzyme BirA was coexpressed with the enzyme in hopes to biotinylate/tag any potential interacting cofactors or substrate proteins; this proved to not be successful and would have to be optimized. The interactions between PRMT7 and any cofactors may be transient, which may make it difficult to capture. Additionally, PRMT7 seems to be highly expressed in certain tissues, such as in the endocrine, immune system, liver, lung, gastrointestinal and reproductive tissues (1). Furthermore, expression studies show PRMT7 is localized to the nucleoplasm (1), indicating potential important roles in modifying nucleosome machinery. These factors are very important to consider when studying PRMT7, and may make a difference when identifying potential substrates and cofactors. Other lab mates and collaborators have attempted to identify substrates using tissues from PRMT7 knock out mice, but this has proven to be more difficult than expected. It may be helpful to use RNAseq analysis to see what processes and systems are affected when PRMT7 is depleted, similarly to what was done in Chapter 5 for PRMT9 affecting alternative splicing events.

What is the physiological substrate(s) of Caenorhabditis elegans enzymes PRMT-7 and PRMT-9?

My work in Chapter 8 biochemically characterizes the *C. elegans* orthologs PRMT-7 and PRMT-9, and while they are conserved, they seem to have different functions. In this chapter I

showed that *C. elegans* PRMT-7 has a broader substrate preference than its mammalian ortholog, while *C. elegans* PRMT-9 seems to be indistinguishable from the human enzyme. Whether PRMT-9 methylation of the splicing factor in *C. elegans* plays a role on modulating alternative splicing like we have seen with human PRMT9 (Chapter 5; (2)) still needs to be investigated. Further work exploring and identifying the physiological substrate(s) for PRMT-7 and PRMT-9 in *C. elegans* could implicate potential new roles for the mammalian enzymes. What we learn from these future studies identifying new substrates can tell us more about these enzymes' evolutionary conservation and divergence.

Does an intact nucleosome containing isoaspartyl damage get methylated by PRMT7?

My preliminary work in Chapter 9 shows that PRMT7 methylates a synthetic peptide of histone H2B with an isoaspartyl residue close to the RXR motif. It would be rather interesting to age intact histone H2B proteins, reconstitute the nucleosome, and see if there are differences in methylation of the unaged versus aged nucleosome. In addition, it would be interesting to determine the extent of isoaspartyl formation on endogenous histones, and see if we can detect this modification *in vivo*.

Does the PRMT9 C431H substitution occur physiologically in disease models, and does the mutation generating primarily MMA affect the recruitment of SMN?

In Chapters 5 and 6 of this dissertation, I identified the activity type and substrate of mammalian PRMT9 and also delved into the biochemical characterization of this enzyme, uncovering what makes it unique from the other enzymes in the family. These discoveries were crucial, as they uncovered the role of PRMT9 in the cell as specific and specialized to affecting

alternative splicing. In Chapter 7, along with mutations in the *T. brucei* PRMT7, I uncovered a specific mutation in human PRMT9 (mutation of Cys to His in the THW loop) that made the enzyme much more able to methylate its substrate, and also only produced MMA. Since we showed in Chapter 5 that PRMT9 activity and methylation was necessary for the correct assembly of spliceosomal subunits and the regulation of alternative splicing, it would be interesting to see if the production of MMA only affects the recruitment of SMN, a methylarginine reader protein and mediator of spliceosomal assembly. This could potentially be a system that cancer cells hijack, in order to destroy the correct assembly of the spliceosome, and ultimately, correct splicing and production of functional genes and proteins. It would be particularly interesting to look at various disease alleles and see if this specific mutation is common in certain diseases and cancers.

Does loss of PRMT9 in mammals lead to any significant phenotype? Does PRMT9 have any other roles or substrates in mammals, and are there any other substrates in C. elegans?

Our collaborators at MD Anderson have been able to successfully produce PRMT9 knockdown HeLa cells, but we have not seen a knockout organism. A PRMT9 knockout mouse would be very useful in determining any explicit phenotypes and aid in discovery of any other potential substrates by *in vitro* tissue analysis. We have preliminarily tested PRMT-9 knockdown in the nematode *C. elegans* using siRNA, but no significant phenotypes were detected. It would be useful to use CRISPR-cas9 to delete the gene and study any explicit phenotypes, as well as using a lysate of these knock out worms to do *in vitro* methylation assays for any other possible substrates. A PRMT9 knockout organism can provide a wealth of information on any other potential roles and substrate of the enzyme.

Do the TPR motifs in PRMT9 play a role in protein scaffolding? Is there a regulatory role in correct substrate binding and positioning?

PRMT9 contains three tetratricopeptide repeats (TPR) at its N-terminus (2–4). My work in Chapters 5 and 6 showed that an intact, full-length protein containing the TPR motif was necessary for methyltransferase activity and binding of the substrate SF3B2. TPR motif is a degenerate sequence consisting of 34 amino acids in a repeat that gives a helix-turn-helix structural motif, and is usually found in 3-16 repeats in natural proteins, with the most common amount of repeats being 3 (5). A wide range of proteins contain TPR motifs and have varying functions, for example, in cell cycle control, transcription, protein transport, splicing, and chaperones (6). Determination of the co-crystal structure of PRMT9 with SF3B2 would tell much about the interaction of the substrate with the enzyme, and could potentially give information on other potential interacting proteins.

REFERENCES

1. Uhlén, M., Fagerberg, L., Hallström, B. M., Lindskog, C., Oksvold, P., Mardinoglu, A., Sivertsson, Å., Kampf, C., Sjöstedt, E., Asplund, A., Olsson, I., Edlund, K., Lundberg, E., Navani, S., Szigyarto, C. A., Odeberg, J., Djureinovic, D., Takanen, J. O., Hober, S., Alm, T., Edqvist, P., Berling, H., Tegel, H., Mulder, J., Rockberg, J., Nilsson, P., Schwenk, J. M., Hamsten, M., Feilitzen, K. Von, Forsberg, M., Persson, L., Johansson, F., Zwahlen, M., Heijne, G. Von, Nielsen, J., and Pontén, F. (2015) Tissue-based map of the human proteome. *Science (80-.).* 10.1126/science.1260419
2. Yang, Y., Hadjikyriacou, A., Xia, Z., Gayatri, S., Kim, D., Zurita-Lopez, C., Kelly, R., Guo, A., Li, W., Clarke, S. G., and Bedford, M. T. (2015) PRMT9 is a Type II methyltransferase that methylates the splicing factor SAP145. *Nat. Commun.* 10.1038/ncomms7428
3. Hadjikyriacou, A., Yang, Y., Espejo, A., Bedford, M. T., and Clarke, S. G. (2015) Unique Features of Human Protein Arginine Methyltransferase 9 (PRMT9) and Its Substrate RNA Splicing Factor SF3B2. *J. Biol. Chem.* **290**, 16723–16743
4. Bedford, M. T., and Clarke, S. G. (2009) Protein Arginine Methylation in Mammals : Who, What, and Why. *Mol. Cell*. **33**, 1–13
5. Grove, T. Z., Cortajarena, A. L., and Regan, L. (2008) Ligand binding by repeat proteins: natural and designed. *Curr. Opin. Struct. Biol.* **18**, 507–515
6. Blatch, G. L., and Lässle, M. (1999) The tetratricopeptide repeat: a structural motif mediating protein-protein interactions. *Bioessays*. **21**, 932–9